ASSESSING NEW METHODS FOR MEASURING FOREST UNDERSTOREY VEGETATION USING TERRESTRIAL LASER SCANNING

JOSEPH RYDING, BSc. MSc.

Thesis submitted to the University of Nottingham for the Degree of Doctor of Philosophy

October, 2016

Abstract

Forest structure is the complex 3D arrangement of all components within the forest architecture. This includes stems, foliage, branches (the components of trees) but also includes non-tree components such as understorey shrubs and herbs. Understanding the structural components of forests is critical when considering forest ecosystems. The structure of a forest can affect functional and compositional characteristics such as productivity and species richness with structure being an important factor influencing animal-habitat associations. Structural characteristics of forests include the size distribution and spatial organisation of trees, and the horizontal and vertical density of objects within the understorey.

Trees are the dominant feature of any forest, but the understorey is also very important when considering forest characteristics. Examining the links between the spatial distribution of understorey material and ecological parameters, such as diversity and productivity, has an important role in ecological studies.

There are multiple field survey techniques that can be applied when collecting data for a forest survey. For a technique to be an effective survey tool it should be readily quantifiable, repeatable, cost-effective, easily assessed, ecologically meaningful and where possible not contain observer bias. Traditional methods of forest survey are very common as they offer reliable, low cost estimations of forest structural parameters such as diameter, height and understorey cover.

Recent developments within 3D data collection using terrestrial laser scanning (TLS) have allowed foresters and ecologists to reproduce the structural parameters collected during traditional forest surveys. These developments have shown the usefulness of 3D data collection in assessing forest structure, but have focused on replicating existing forest metrics rather than developing new ones. For TLS to reach its full potential within the field of forest ecology, new metrics and indices need to be developed specifically for laser scan analysis.

This study developed and tested new methods of forest survey, concentrating on understorey vegetation, using commercially available TLS. Results showed that

these new techniques can provide novel structural assessments of the understorey layers of forests for use in forest ecology surveys, not available through traditional methods.

Using a new index describing the vertical component of forest understorey, it was shown how the relationship between deer browsing and forest structure can be identified through feature extraction from laser scanning. The method developed required minimal manual processing and was applied to large data sets. The structural changes between high and low deer density sites were also observed through the creation of an understorey density profile. This method, specifically targeted at the lower layers of the understorey, successfully identified structural change at the decimetre level. Using microtopography estimates from understorey point clouds it was shown how understorey complexity corresponded with vegetation surfaces extracted through TLS. This suggests that correlation between understorey structure (and therefore habitat type) and the microtopography of vegetation surfaces may be used for detailed assessment of understorey structural characteristics utilising TLS.

In addition to the development of novel analysis methods, new techniques for acquiring TLS data of forest understorey were examined. The use of a standardised methodology for temporal surveying, utilising a common digital terrain model and fixed ground control, as developed here, provides a framework from which further data can be acquired. This approach offers a relatively quick, efficient, non-destructive assessment of temporal change within forests. A novel method of forest survey utilising handheld mobile laser scanning (HMLS) was also tested, showing its potential to complement static TLS surveying by providing increased survey coverage and allowing point cloud processing to be considered for areas which are otherwise difficult to access.

For Jenny and the two unknowns...

who have become Lily and Marlowe.

Acknowledgements

I would like to express my sincere gratitude to my supervisors, Dr. Martin Smith, Dr. Markus Eichhorn and Dr. Craig Hancock, for their support, guidance and friendship during the planning, analysis and writing of this thesis. I greatly appreciate all of the time and effort they have put into my supervision over the last years. Without their efforts I would not have been able to finish this work. Extra special thanks is given to Markus, who as well as providing guidance covering all aspects of forest ecology and survey, provided a place to rest and eat in Nottingham when I was visiting. I hope the friendships built during this time of study will last for many years.

I would also like to thank those staff at the University of Nottingham who have assisted me during these studies. This includes Lukasz Bonenburg for all of his help in the field trials at Kirton Wood and Nicholas Kokkas for support with software licencing and access to the university computers. Special thanks also go to Thierry Hoy for all of his help during the WoodMAD trials, for pulling the survey cart through miles of woodland and for making four weeks living in a bed and breakfast bearable and even enjoyable.

Thanks also to Emily Williams for her advice and guidance when using the ZEB1 handheld mobile laser scanner. Without Emily the section on handheld laser scanning in forest would not have been possible.

Finally, I would like to thank my wife, family and friends for putting up with laser and tree talk for over five years. Their support and encouragement and constant reminders that I need to finish (Barbara), have helped me through to this point and it is much appreciated. A special mention is given to my twin daughters Marlowe and Lily, who have only been around for the final few months of this work, but whose arrival has reminded me why I wanted to study for a Ph.D. in the first place.

Declaration

I declare that the thesis is the result of my own work which has been undertaken during my period of registration for this degree at The University of Nottingham.

Contents

[1]Parts of this sub-section have been modified from Ryding et al. (2015)

[2]This chapter has been modified from Ryding et al. (2015)

List of Abbreviations

ALS aerial laser scanning.

ANOVA analysis of variance.

BTO British Trust for Ornithology.

CRS coordinate reference system.

DBH diameter at breast height.

Defra Department for Environment, Food and Rural Affairs.

DEM digital elevation models.

DTM digital terrain model.

DWEL Dual-Wavelength Echidna Lidar.

EVI Echidna Validation Instrument.

FHD foliage height diversity.

GME Geospatial Modelling Environment.

GNSS Global Navigation Satellite System.

HMLS handheld mobile laser scanning.

ICP iterative closest point.

IMU inertial measuring unit.

InSAR Interferometric SAR.

KDE kernel density estimation.

LAI leaf area index.

PAI plant area index.

PCL point cloud library.

RANSAC Random Sample Consensus.

REDD + reduced emissions from deforestation and forest degradation.

SALCA Salford Advanced Laser Canopy Analyser.

SAR Synthetic Aperture Radar.

TIN triangulated irregular network.

TLS terrestrial laser scanning.

UDP understorey density profile.

VNVI vertical to non-vertical index.

WoodMAD woodland management and deer.

Chapter 1

Introduction

1.1 Background and motivation

Forests are highly complex structures that are critically important across multiple ecosystems and are fundamental to our understanding of how global, regional and local ecological processes work. At the present time forests account for roughly 40% of Earth's ice-free landmass and play a significant role in the biogeochemical processes that regulate the exchanges between terrestrial ecosystems and the atmosphere (Gonzalez et al., 2010). In addition to this forests contain over 80% of Earth's terrestrial species (Aerts and Honnay, 2011) and as such are hugely important not only for environmental reasons but also for human economic ones.

With the continuing decrease of forest habitats and resultant loss of biodiversity that has been occurring in recent decades (Butchart et al., 2010; Aerts and Honnay, 2011) the importance of understanding the complex structure of forests has become ever more important. Particular interest has been shown in forest management practices and how human behaviour can affect forest interactions and processes (Thompson et al., 2014). The importance of forests for maintaining global biodiversity can be seen in the commitment of governments and organisations to initiatives aimed at sustainable management of forest ecosystems (Grayson and Maynard, 1997) and the accepted understanding that, through better management practices, forest habitats and ecosystems can be maintained (Maginnis and Sayer, 2013).

As the dangers associated with increased CO_2 in the atmosphere brought on by the burning of fossil fuels are realised, the importance of forests as a global carbon sink and their potential for carbon sequestration has also come to the fore (Pan et al., 2011). This can be seen with the proposed introduction of climate change mitigation strategies such as reduced emissions from deforestation and forest degradation (REDD +) where carbon credits will be provided to developing countries for the reduction of carbon emissions from deforestation and for the enhancement of forest stocks (Thompson et al., 2014). Pimentel et al. (1997) estimated the 'damage avoided' through carbon sequestration by forests to be $135 billion per year.

Understanding that forests are of critical importance to global biodiversity and that they also have a role in mitigating increasing carbon levels in the atmosphere highlights the importance of surveying, analysing and understanding forest systems. Through improvements to existing survey methods and the introduction of new ones, there is the potential to increase our ability to model how the complex functions of forests operate at global, regional and local levels. From this it may be possible to enhance the development of sustainable forest management practices that deliver increased biodiversity whilst also allowing for improved carbon mitigation. Examples of the development of such practices include the German forest management policy where mono-specific forests are converted into mixed stands that are species rich, producing forests that are environmentally and economically more beneficial (Kenk and Guehne, 2001).

To deliver improvements to forest management practice, forest structure and how it relates to ecosystem functions needs to be examined. Forest structure is the complex 3D arrangement of all components within the forest architecture. This includes stems, foliage, branches (the components of trees) but also includes non-tree components such as understorey shrubs, herbs and epiphytes (plants that grow on trees).

Whilst trees are the dominant feature of forests, non-tree components such as understorey vegetation play an important role within forest ecosystems. Interactions within the understorey can determine which plants will occupy the higher strata of forests (overstorey composition) (Gilliam, 2007) and although the understorey may contain less biomass than tree components, the high turn over of understorey biomass (annual change) affects belowground processes such as decomposition and soil nutrients (Nilsson and Wardle, 2005).

Despite the importance of understorey communities to forest ecosystems, the majority of forest surveys concentrate on the measurement of tree parameters such as height and diameter, with Gonzalez et al. (2013) highlighting a lack of research covering understorey vegetation. Hart and Chen (2006) state that even though boreal forest understorey is the most diverse component of boreal communities, it is the least understood. The importance of understanding all components of forests, including the understorey, within a 3D framework is therefore crucial when considering the function of forests and how they interact with the environment.

The manipulation of geospatial data within a 3D framework such as a point cloud (a set of data points representing the external surface of an object) or surface model is a common method for the extraction and analysis of structural components within multiple industries and research fields. These include construction and civil engineering (Soni et al., 2014), design processing (Cabaleiro et al., 2014), the entertainment industry (Mihalyi et al., 2015), geoscience (Hartzell et al., 2014) and medicine (Welsh et al., 2014). The application of similar analysis and modelling methodologies across multiple disciplines, combined with the recent reduction in cost of graphics hardware, has allowed for a rapid increase in the use of these processes. As a result of this rapid uptake, 3D modelling and feature extraction are now considered fundamental processing techniques across a range of independent fields.

Forest science has not been excluded from this rapid expansion of 3D data analysis, with the modelling and extraction of features from forest point clouds being a goal of forestry research over the last twenty years (Wulder et al., 2012). With the advent of the first aerial laser scanning (ALS) systems in the 1990s (Ackermann, 1999; Wehr and Lohr, 1999), early tests showed the suitability of this technology for the determination of digital elevation models (DEM) over forested regions (Kraus and Pfeifer, 1998; Axelsson, 2000). From these initial studies on surface modelling the extraction of forest structural parameters from aerial data sets soon followed.

Current techniques for the 3D processing of data from forest surveys are dominated by aerial systems operating above the canopy at regional scales. These ALS surveys have increased the ability to collect forest inventory data over large areas with substantial cost savings (Hyyppä et al., 2012), but there is still a need for permanent sample plots within forest sites for the calibration of aerial acquired data (Hopkinson et al., 2013; Liang and Hyyppä, 2013; Hauglin et al., 2014). In addition to the calibration of aerial data sets, there is also a need to understand how forests operate across a range of scales beneath the canopy, such as when examining understory microhabitats (Baraloto and Couteron, 2010) or assessing understory structural diversity (Thomas et al., 1999; Barbier et al., 2008). It is in these areas that ground-based survey techniques can play a pivotal role.

Through the collection of point cloud data from beneath the canopy, terrestrial laser scanning (TLS) systems have the ability not only to replicate existing forest structural indices, but also allow for the development of new ones (Kint et al., 2003; Pommerening, 2006). The potential of TLS for forest surveys can be seen in the development and testing of bespoke laser scanning instruments solely for the purpose of ground-based forest surveying. Examples of these bespoke lasers scanning systems include the Echidna Validation Instrument (EVI) (Jupp et al., 2009), Salford Advanced Laser Canopy Analyser (SALCA) (Gaulton et al., 2010) and Dual-Wavelength Echidna Lidar (DWEL) (Douglas et al., 2012).

Newnham et al. (2015) suggested that for TLS to reach its full potential it requires a re-think of vegetation surveys and their application across a wide range of disciplines. For TLS to develop into the proven forest survey tool that ALS has, it is suggested that all aspects of the survey process need to be re-examined, from the collection of data to the processing and analysis of data, from a forest ecology viewpoint.

This study aimed to assess the use of commercially available TLS instruments for the purpose of characterising the structural properties of forest understorey. The study can be considered as two different trial types examining: (1) novel understorey feature extraction techniques using point cloud data sets (vertical component, vertical density and horizontal cover); and (2) novel understorey data collection and measurement techniques (temporal surveys and handheld mobile laser scanning). The examination of handheld mobile laser scanning (HMLS) in Chapter 8 of this thesis is modified from Ryding et al. (2015).

Data used in this study for the development of new feature extraction techniques were collected as part of a British Trust for Ornithology (BTO) project examining the effects of changes in woodland structure on bird populations as a result of deer browsing. Data were collected from lowland, broad-leaved woods across England and Wales. For this reason the techniques developed were specifically targeted at extracting metrics used to assess the effects of deer browsing in the UK. However, although directed at deer browsing, these techniques also have the potential to be used as new measurement tools providing information on understorey structure of relevance to general interest areas such as habitat mapping, forest history, fire impact and threats.

Furthermore, although tested using data collected from temperate, broad-leaved woods, the feature extraction techniques and data collection methods also have potential to be used across different forest types (such as boreal and tropical forest) where there is a need to understand the role of understorey across multiple forest ecosystems (Nilsson and Wardle, 2005).

The requirements for this study were driven by the need to effectively examine understorey structure, beyond the levels commonly used in ecological surveys. The BTO highlighted decimetre resolution of the understorey as being an improvement over traditional analysis methods (Fuller et al., 2014) where understorey vegetation is typically divided into coarse height bands. For this reason processing was completed at 1 cm resolution, although lower resolution may well be sufficient for other applications such as when examining the impact of fire on understorey structure. Vegetation surfaces used for cover estimates in Chapter 6 were created at a lower resolution of 5 cm which reduced the processing time from 48 hours to 1 hour. In practice, researchers may need to consider the trade-off between time and resolution, particularly for time-sensitive applications.

1.2 Aims and objectives

The main aim of this study was to assess the application of commercially available TLS instruments for the estimation of forest structural attributes used to assess understorey vegetation, beyond those currently extracted from ALS and TLS surveys.

It was proposed that through combining geospatial analysis and feature extraction techniques, forest understorey metrics of importance to ecologists could be examined at a finer spatial scale than is currently available. Using this analysis method the novel assessment of forest understorey structural attributes not currently collected may also be possible.

Through the collection of TLS data from forest sites with varying deer density levels, combined with the knowledge that high deer density can lead to the suppression of recruitment and the simplification of forest structure at low levels, it was proposed that deer density could be used as a proxy for structural change within the understorey.

In order to meet this main aim, a number of subsidiary aims were set that are covered in each of the subsequent chapters of this report. The subsidiary aims were set to address the questions:

- (1) What are the traditional methods of conducting surveys within forests? and (2) how have developments within remote sensing been used to extract forest structural parameters used in ecological studies?

- (1) Can TLS be used to extract the vertical components of the understorey layers of forests effectively, with minimal manual processing, from large data sets? and (2) to what extent does point occlusion affect the extraction of the vertical component using TLS?

- (1) Can TLS be used for the estimation of the vertical distribution of herbaceous layer vegetation? and (2) can heterogeneity of the horizontal distribution of vegetation layers within plot sites be assessed using TLS?

- (1) Can TLS be used for the estimation of the horizontal distribution of understorey vegetation cover within forest plots? and (2) are any novel understorey measurements available?

- (1) Can TLS be used to measure temporal change within the understorey for applications in forest ecology? (2) if so, what are the requirements for understorey temporal surveying (work flows)? and (3) are any novel temporal assessments available?

- (1) Can TLS measurements of forests be replicated using HMLS? (2) does the use of HMLS provide any advantages in practical ease over TLS or field survey methods? (3) are any novel measurements available? and (4) what are the remaining challenges for the application of HMLS in forest monitoring?

To achieve these aims a number of objectives were set:

- develop knowledge and understanding of current and historic forest survey methods and limitations,

- develop a method for TLS surveys, directed at the understorey, within forest sites,

- develop a method for the extraction of structural components from point cloud data sets from which different forest understorey structural types may be identified,

- develop a method for the estimation of vertical density within forest point cloud data sets collected at low levels,

- develop a method for the estimation of understorey cover from point cloud data sets,

- develop a method and best practice guidelines for performing understorey temporal surveys using TLS, and
- develop a method, with a list of current limitations, for the acquisition of forest survey data using a handheld mobile laser scanner.

1.3 Thesis overview

Following the introduction, Chapter 2 provides a review of the extraction of forest structural attributes through surveying. This examines the current methods for the measurement of forest structure including the components of forest structure and common measurement techniques. An overview of the current status of TLS for extracting forest structural parameters is also given. The geospatial manipulation of forest data is examined through descriptions of the current methods for the extraction of forest features from point cloud data sets. Chapter 3 details survey methods and instrumentation. This chapter describes the survey methodology and motivation for the different trial sites and data sets used in the study. Descriptions of the laser scan instruments used and their basic operating principles are also provided. Chapter 4 examines the identification of the vertical component within forests from TLS. This chapter introduces a novel method for the classification of point returns based on vertical alignment from which correlation can be seen between the vertical component of forest and deer browsing levels. Chapter 5 introduces a method for the estimation of the vertical density within the herbaceous layer through TLS. The analysis described here examines the use of the MacArthur-Horn transformation to account for the presence of laser scan point occlusion, building on methods currently used when studying the canopy from ALS acquired data sets. Chapter 6 introduces a new approach to understorey cover assessment using TLS. A novel analysis method combining processing techniques from geomorphology allowing for the creation of microtopographic surfaces describing understorey vegetation type is also presented. Chapter 7 highlights the use of TLS for assessment of temporal change within forests. The metrics developed in previous chapters are tested against temporal data sets to assess their application for change monitoring. Suggested best practice guidelines for performing TLS temporal surveys examining understorey vegetation are also presented. Chapter 8 outlines the use of handheld mobile laser scanning (HMLS) for forest surveys. This chapter describes a new technique for the collection of point cloud data from a HMLS and its potential for forest surveying. A trial site was surveyed using both a handheld and static instrument with the trial examining the accuracy of the two systems and the potential benefits of using a handheld approach for forest surveying.

Chapter 2

Review of methods for extracting forest structural attributes

2.1 Introduction

With forests being one of the most valuable sources of natural resources throughout human history, the importance of trying to quantify a forest's potential has been understood for centuries. From timber reserves in the ancient Mediterranean (Meiggs et al., 1982) to the development of forestry legislation in renaissance Venice (Appuhn, 2000) and the birth of modern governmental forestry institutes in the nineteenth century (Östlund et al., 1997; LaBau, 2007), accurate forest survey information has been a goal of consecutive generations, albeit for different political and economic reasons.

The first forest surveys were simple timber inventories allowing for the value of a forest to be assessed. Detailed survey designs were only implemented in the 1940s (Frayer and Furnival, 1999) and this can be thought of as the birth of the modern forest survey. Advances in the field then saw forest surveys using aerial photographs being introduced in the 1950s (Bickford, 1952). Finally, in the latter half of the 20th and early 21st centuries, forest surveys embraced new technologies with the introduction of satellite and aerial remote sensing providing global and regional forest data sets and ground based remote sensing systems providing a local perspective (Suárez et al., 2005; Bienert et al., 2006b).

Within the forest science community there is a distinction between forestry surveys and forest ecology surveys. Whilst both are concerned with the measurement of forest structural attributes from which further properties can be assessed, the final purpose differs. Forestry surveys are primarily aimed at the estimation of timber, or more recently carbon stocks, within a given forest and can be thought of as broadly describing a forest in human economic terms. A forest ecology survey differs in that the purpose is to describe a forest in an ecological sphere, such as through the assessment of biodiversity. Although both disciplines share common methodologies and there is overlap between them, there is also a clear difference in the aims of both of these survey types.

Alongside common forestry parameters such as tree diameter, stem density and tree height, forest ecology surveys commonly collect additional structural parameters associated with non-tree features such as ground cover type, area of ground cover and foliage density. Forest ecology surveys are still primarily conducted using traditional estimation methods such as callipers, tape measures, cover boards and clinometers, although modern technologies such as laser-relascopes have become more common in recent years (McElhinny et al., 2005; Newton, 2007).

Whatever the method or purpose, the goal of forestry and forest ecology surveying has always been to provide detailed information on the structural properties of forests. These structural properties can then be used in further estimations of forest parameters, an example being allometric relationships (the quantitative relationship between key dimensions and other attributes) linking the diameter of tree trunks measured at 1.3 m above ground, this measurement is known as diameter at breast height (DBH), to biomass (Zianis and Mencuccini, 2004). In this way field measurements of only a select number of attributes can be used to build a more detailed overview of the forest.

The aim of this chapter is to address the questions: (1) what are the traditional methods of conducting surveys within forests? and (2) how have developments within remote sensing been used to extract forest structural parameters for ecological studies?

2.2 Measuring forest structure

Within the field of forest ecology there are multiple characteristics that can be used to measure rates of ecological processes and identify microhabitats present within a forest ecosystem. These include functional characteristics such as productivity, or compositional characteristics like species richness, succession and relative abundance (Dale and Beyeler, 2001). It is the structural characteristics however, such as size distribution and spatial organisation of trees, that are considered the most crucial parameters for the assessment of forest processes and habitats (Kint et al., 2008). Reasons for this include: (1) forest structure is directly related to the habitats of many different animal and plant species and is therefore convenient as an indicator of biodiversity; (2) forest structure is a direct economic measure (e.g. wood production); and (3) structural attributes can act as surrogates for functional and compositional characteristics. When considering the practical assessment of forest ecosystems, perhaps the most fundamental reason for the use of structural parameters is that they are often easier to measure than compositional or functional characteristics (Lindenmayer et al., 2000).

Forests are highly complex, three-dimensional environments and their structural characteristics can be considered at various hierarchical scales. From the landscape scale (kilometres) to the micro-structure of individual branches (decimetres), structural parameters are used to assess habitats and processes present across all spatial scales of the forest ecosystem. The critical hierarchy can be considered as the stand scale (a specific area uniform in species composition, typically at the 0.1 to 1.0 ha scale), as it is here that the horizontal and vertical positioning of woody structure and foliage combine to create micro-climatic conditions within the canopy and understorey (Kuuluvainen et al., 1996).

Tree height and DBH are examples of well-established forest structural parameters that constitute important measures when assessing a forest ecosystem. The vertical arrangement of foliage, or foliage height diversity (FHD), is also often used when describing forest structure (Wood et al., 2012). A traditional forest survey may collect a selection of structural parameters such as tree height and DBH, but it is unlikely that data on all available structural parameters will be collected as this would be too time-consuming.

There are multiple field survey techniques that can be applied when collecting data for a forest survey. For a technique to be an effective survey tool it should be readily quantifiable, repeatable, cost-effective, easily assessed, ecologically meaningful and where possible not contain observer bias (West, 2009).

Traditional field survey techniques for the measurement of forest structural parameters include callipers or measuring tape when estimating tree diameter, clinometers when estimating tree height and cover boards when estimating FHD. These field survey techniques have been widely applied over many years as they meet the criteria of being repeatable, cost-effective, easily assessed and provide measures that are ecologically important.

With advances in technology over the previous decade a number of new methods for the estimation of forest structural parameters have been tested. These include, but are not limited to: lidar (Popescu et al., 2011), imaging spectroscopy (Kalacska et al., 2007), Synthetic Aperture Radar (SAR) and Interferometric SAR (InSAR) (Hyde et al., 2007). Of these new technologies, lidar has been shown to provide the required resolution in all three spatial dimensions needed by ecologists and foresters for the successful extraction of structural parameters (Seidel et al., 2011b).

The use of aerial laser scanning (ALS) and terrestrial laser scanning (TLS) for the measurement of fundamental parameters of structure (DBH, position, etc.) has been assessed in multiple studies (see Section 2.2.3). Up to this point studies have focused on the canopy layer of forests with comparatively few dedicated to the understorey and ground-level (Figure 2.1). It is the extraction of previously difficult to estimate characteristics, such as those beneath the canopy, that offers new and potentially exciting developments within the field. Lichti et al. (2002) provide an overview of the fundamentals of lidar operation, systems and applications. Vauhkonen et al. (2014) provides a full description of the current status of ALS for forest surveys. Liang et al. (2016) and Newnham et al. (2015) provide accounts of the current status of TLS in forestry.

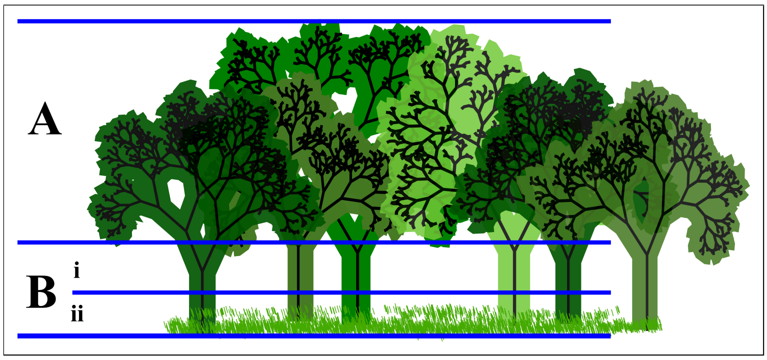

Figure 2.1: Overview of forest layers:
(A) canopy (Bi) understorey
(Bii) understorey: forest floor

2.2.1 The components of forest structure

A number of different forest attributes are measured by foresters and ecologists to help characterise structure within forest stands. The structural attributes of forest are listed in Table 2.1, grouped into the forest elements that they are used to describe (Figure 2.2).

Table 2.1: Forest structure: attributes used in characterisation (modified from McElhinny et al., 2005)

Element	Attribute
Tree diameter	Tree DBH DBH distribution DBH diversity Standard deviation of DBH
Tree height	Height of overstorey Standard deviation of tree height Horizontal variation in height
Tree spacing	Trees per hectare Nearest neighbour indices
Foliage	Foliage height diversity Number of strata Foliage density within different strata
Canopy cover	Canopy cover Gap size classes Average gap size
Understorey vegetation	Shrub cover Shrub height Total cover of understorey Saplings per hectare

Within the literature on forest surveys, tree diameter is a fundamental measure used for estimation of tree size and can be considered the most important parameter when characterising forest structure. The diameter of a tree is typically taken as the diameter at a height of 1.3 m above the ground surface (DBH). The use of DBH is generally quantified through measures of the mean DBH or converted to basal area estimates within a plot. Another common value used within the literature is the number of trees above a given diameter, known as

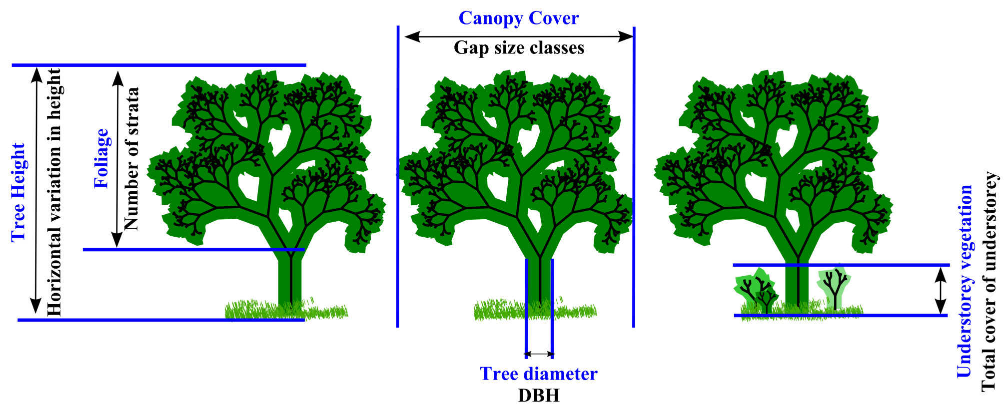

Figure 2.2: Overview of forest structure: elements (blue) and attributes (black)

the threshold diameter. Frequency distribution of DBH is also used. The mean DBH of a plot site is directly linked to the basal area of the plot, which is also related to stand volume and biomass (West, 2009). Tree diameter also has economic importance in that it may be indicative of the worth of a tree. Variation in diameter may also reflect competition within the stand and how trees grow in relation to surrounding stems (Velázquez et al., 2016). Multiple studies have also shown the relationships between tree diameter and tree height, with the measurement of diameter being an established proxy for the structural attributes associated with height (Buongiorno et al., 1994).

Tree height can be considered at the single tree level (such as when estimating from DBH measurements), or across a stand (such as when estimating height of the overstorey from remote sensing). Like diameter, height is an important attribute when assessing forests, as variation in height can be an indicator of other important factors such as age ranges and habitat diversity. Height can also be used as an indicator of total wood volumes. Measuring the tallest trees within a forest stand can also be used for the assessment of forest productive capacity, an important measure when assessing how rapidly trees will grow (West, 2009).

The number of trees per hectare is a simple measure of the spacing of trees within a plot that has been used to assess successional stages (how forests develop over time) within forest (Spies and Franklin, 1991). Further descriptions include spacing variation and clustering which can be used when assessing forest processes like competition and regeneration (Svensson and Jeglum, 2001).

Foliage is an important measure when describing forest structure with the vertical arrangement of foliage (FHD) showing strong correlation with avian diversity (Tanabe et al., 2001; Lesak et al., 2011). This is interpreted as increased FHD causing an increase in niche space for birds (Müller et al., 2010). McElhinny et al. (2005) notes however, that FHD is an ambiguous measure when assessing forest structure as there is no established method for its measurement and that a more straightforward approach is to characterise structure using canopy cover.

Canopy cover is a useful structural attribute to measure as it varies during stand development and has been used as a component of forest structural indices (Franklin et al., 2002). Canopy gaps are also indicative of changes in canopy cover with the distribution of gaps being used to assess succession (Ziegler, 2000). However, the usefulness of canopy cover as a structural attribute is limited by the relative difficulty in its estimation, with the literature showing predominance toward diameter and height measurements.

Understorey vegetation contains a number of measures that can be used to describe structure. Spies and Franklin (1991) list these as being: (1) cover of the herbaceous layer; (2) density of shade tolerant saplings; (3) cover of deciduous shrubs; (4) density of sub-canopy saplings; and (5) cover of all understorey vegetation. Although understorey characteristics have been shown to influence biodiversity within forests (Van Den Meersschaut, Vandekerkhove, et al., 2000), the influence of canopy conditions on the understorey has meant the majority of studies to date have focused on the canopy.

2.2.2 Common forest measurement techniques

Multiple field survey techniques for the measurement of forest structural parameters have been developed. These techniques can be broadly classified into direct or indirect methods. Direct measurement involves contact between the measured feature and the surveyor such as when measuring stem diameter with a tape. Indirect measurement is the estimation of parameters without contact, such as in the case of hemispherical photography of the canopy.

A further classification of survey method is destructive and non-destructive. Destructive surveys require the target to be collected and removed from the plot site such as litter traps for measuring leaf area index (LAI) or felling of trees for measurement of total biomass. Non-destructive methods do not involve removal of material from the survey site.

An overview of the common methods for the estimation of forest structural parameters can be seen in Table 2.2.

Common forest survey techniques utilise simple equipment for direct measurement, such as measuring tape and height poles. These techniques have been popular choices for foresters and ecologists over the last century due to their low cost and ease of use. The development of optical instruments for survey work allowed indirect assessment of forest structural parameters to be made. Instruments used include cameras and relascopes which are also relatively cheap and easy to use. With the introduction of optical devices came the creation of new forest indices extracted from data collected through optical surveys, showing how developments in technology have fed advances within the field.

In recent decades laser equipment has been developed that replicates many of the direct and optical survey techniques in use. Examples include the laser point quadrat and the laser relascope. These instruments are very useful tools (although come at increased cost compared to optical devices) but have been designed to replicate existing measuring techniques, not for the creation of new ones.

2.2.3 The current status of TLS for forest surveys

The uptake of TLS for forest surveys has not been as rapid as for ALS and although early trials showed promise, the technique has not yet replaced manual measurement methods for plot-scale surveys (Newnham et al., 2015). The technique has however, been used in multiple trials for the estimation of a range of forest parameters. An overview of studies examining the measurement of forest structure using TLS can be seen in Table 2.3.

Table 2.2: Overview of traditional methods for the estimation of forest structural parameters

Technique	Parameter	Method	Comments
Diameter tape	diameter	direct	measurements taken to 1 mm
Dendrometer bands	diameter	direct	for short term repeated measurements of stem growth to nearest 0.25 mm
Callipers	diameter	direct	measures circular diameter
Relascope	diameter basal area tree height	indirect	used for preliminary assessment of timber. Less accurate than callipers or tape for diameter estimation
Measuring pole	tree height	direct	measure to about 8 m
Clinometer	tree height	indirect	accuracy commonly not better than 0.5 m
Litter trap	leaf area	direct	time consuming
Hemispherical photography	leaf area	indirect	can underestimate leaf area in dense canopies
Spherical densiometer	canopy cover	indirect	can contain user bias
Point quadrat	foliage density	indirect	easy to carry out, can underestimate density
Cover board	vegetation density	indirect	easy to carry out, can underestimate density
Sward stick	vegetation height	direct	no significant bias

Table 2.3: Forest structure: elements measured using TLS

Element	Reference
Tree diameter	Hopkinson et al. (2004), Thies and Spiecker (2004), Bienert et al. (2006a), Bienert et al. (2007), Huang et al. (2011), Pueschel et al. (2013), Pueschel et al. (2013), Olofsson et al. (2014)
Tree height	Hopkinson et al. (2004), Bienert et al. (2006a), García et al. (2011), Huang et al. (2011), Olofsson et al. (2014),
Tree spacing	Hopkinson et al. (2004), Watt and Donoghue (2005), Liang and Hyyppä (2013)
Foliage	Hosoi and Omasa (2006), Jupp et al. (2009), Zhao et al. (2011)
Canopy cover	García et al. (2011), Zhao et al. (2011), Seidel et al. (2012b), Hopkinson et al. (2013), Danson et al. (2014)
Gap fraction	Danson et al. (2007), Cifuentes et al. (2014)
Understorey vegetation	Seidel et al. (2012a), Srinivasan et al. (2014)
Woody structure	Méndez et al. (2014), Boudon et al. (2014)
Leaf modelling	Magney et al. (2014), Béland et al. (2014b)

2.3 Methods for the extraction of features from point cloud data sets

The output from TLS surveys, using commonly available laser scanning instruments, is a point cloud holding object information in the form of a Cartesian coordinate (x, y, z) describing a position in 3D space. With modern TLS collecting returns at up to 9.76 x 10^5 per second, a point cloud describing a forest plot can easily contain millions of individual data points (Ryding et al., 2015). From this point cloud it is then necessary to extract the desired information from which forest structural parameters can be estimated.

Current extraction methods used for the estimation of forest structural parameters from point clouds can be characterised by three approaches: (1) geometric modelling; (2) voxel based extraction; and (3) texture analysis. An overview of these approaches is given as the required extraction method will determine survey specifications and the final available outputs from the analysis.

Currently there are a limited number of software packages that are specifically designed for the extraction of structural parameters from forest point clouds. The software for forestry applications include Treemetrics (TreeMetrics, 2014) and LiForest (Forest, 2014) which are principally used for the extraction of timber volumes from point clouds collected in managed forest. At the present time there are no commercial software primarily aimed at the field of forest ecology.

2.3.1 Geometric modelling

Geometric modelling (also known as surface fitting) involves the creation of surfaces from points and is commonly used to create accurate models for distance/volumetric measurements such as in civil engineering projects (Tang et al., 2010), reverse engineering in manufacturing (Durupt et al., 2008) and geological analysis (Buckley et al., 2008). The technique was first used within forest studies to extract DBH estimations through shape recognition and circle fitting on horizontal slices across point clouds (Simonse et al., 2003; Bienert et al., 2006a; Bienert et al., 2006b; Bienert et al., 2007; Maas et al., 2008). These initial studies highlighted the potential of TLS for the extraction of dendrometric parameters and made it possible for the automated analysis of point cloud data sets (Dassot et al., 2011).

The use of this method at different heights within the understorey and canopy has been used to create stem profiles from which trees can be modelled from the base to the lower reaches of the crown (Henning and Radtke, 2006a) (Figure 2.3). Recent research has built on these studies to show how complete trees can be reconstructed and modelled for total above ground volume estimates (Hackenberg et al., 2014). This estimation of woody content has multiple applications from biomass estimations (Yu et al., 2013; Raumonen et al., 2013) to orchard modelling (Méndez et al., 2014).

In addition to the estimation of woody structure, surface modelling has been used to estimate canopy attributes such as crown leaf area index (Moorthy et al., 2008) and crown volumes (Fernández-Sarría et al., 2013a) from beneath the canopy. Fernández-Sarría et al. (2013a) highlights two methods for canopy volume estimation: (1) a total canopy volume calculated as a convex-hull formed from the point cloud; and (2) a volume accretion combining sections taken through the canopy and modelled individually.

(a) Point cloud (b) Modelled stem

Figure 2.3: Example showing modelling of (a) point cloud data into (b) stem profile using Leica Cyclone processing software. The stem profile was generated manually using subsections of data used to model cylinders which were then combined into a single profile.

Through the use of automation in combination with modelling, point cloud data sets can be used to extract forest indices through bespoke software and processing. Hackenberg et al. (2014) present a semi-automated approach to stem modelling (tree extraction and tree pre-processing were performed manually) with outputs of stem parameters including: (1) tree height; (2) total above ground volume; (3) stem volume; (4) DBH; (5) branch volume; and (6) crown space occupation. In addition to traditional dendrometric parameters, Metz et al. (2013) showed how using convex-hull modelling of tree crown shape could be used to improve the precision of models relating competition and growth within the canopy.

Raumonen et al. (2013) presents the automatic extraction of precision tree models from laser scan data using surface modelling. In this work it states that the advantages of such a modelling procedure is that it is comprehensive, precise, compact, automatic and fast. Until very recently this was not possible due to constraints (computer memory and processing time) with modelling large data sets.

Common detection approaches for the production of accurate surface models from point clouds include the Hough transform method and the Random Sample Consensus (RANSAC) algorithm. Weber et al. (2010) provides a description of surface reconstruction methods from point clouds.

2.3.2 Voxel based extraction

Voxel based extraction of features is when point cloud data sets are converted into a 3D grid (voxel space) from which resultant grid properties can be extracted. This form of analysis has been an important processing and extraction tool across many fields within 3D data processing in recent years. Examples from across different industries include Lehtomäki et al. (2016) using voxel geometry for the processing of road and street environment point clouds and Maturana and Scherer (2015) examining the detection of potentially obscured objects from lidar data sets relevant to autonomous vehicles.

Voxel based analysis has also been used for the extraction of multiple forest structural parameters using TLS including the assessment of 3D forest canopy structure (Henning and Radtke, 2006b), leaf area distribution (Béland et al., 2014a), volume estimations (Hosoi et al., 2013) and biomass calculation (Fernández-Sarría et al., 2013b). Voxel based extraction takes more computational time than geometric modelling (Fernández-Sarría et al., 2013a; Pathak et al., 2009) and results can be affected by the defined voxel size and also sampling setup (Cifuentes et al., 2014; Béland et al., 2014a). However, benefits of voxel based extraction include attribute analysis of both geometry and neighbourhood relationships (Brolly et al., 2013). An example of this being how voxel based analysis may be used to extract surface features from a point cloud (geometry), but it can also provide details of the point counts within the voxels describing that surface (neighbourhood analysis) and therefore can be used to assess point relationships such as clustering.

The extraction of forest structural parameters through voxel based extraction involves the conversion of point cloud data sets into voxel-based 3D models (Figure 2.4). This allows for the description of the scanned environment at the resolution of the voxel element size. The limits of the point cloud and the individual voxel size define the overall voxel space (Schilling et al., 2011). Through the use of a fixed 3D grid each of the point returns within the point cloud can be assigned to a voxel. The conversion of point returns into voxel space can be achieved through use of the following equations:

$$vX = int\left(\frac{X - X_{min}}{\Delta vX}\right) \tag{2.1}$$

$$vY = int\left(\frac{Y - Y_{min}}{\Delta vY}\right) \tag{2.2}$$

$$vZ = int\left(\frac{Z - Z_{min}}{\Delta vZ}\right) \tag{2.3}$$

where (vX, vY, vZ) are the given voxel coordinates, int describes a function of rounding to the nearest integer, (X, Y, Z) are the point return coordinates, $(X_{min}, Y_{min}, Z_{min})$ are the minimum limits of the point returns and $(\Delta vX, \Delta vY, \Delta vZ)$ are the dimensions for the voxel element (Hosoi and Omasa, 2006). Voxel grids can then be assigned values to describe the number of point returns contained within them.

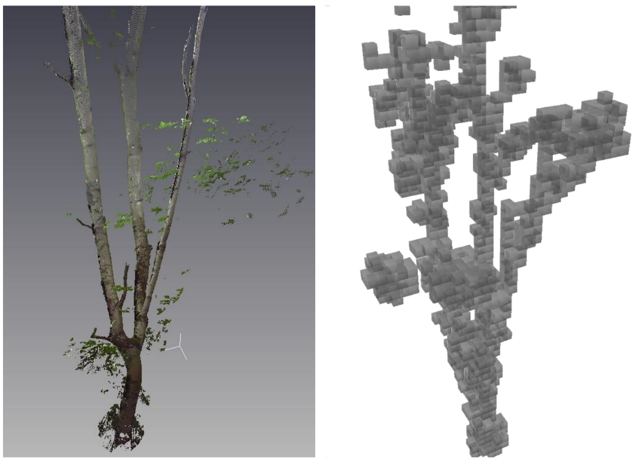

(a) Point cloud (b) Voxel space

Figure 2.4: Example showing conversion of (a) point cloud data into (b) 3D voxel space using ESRI Arcmap software. Each voxel represents a 1 cm^3 where a point return has been identified.

In addition to the point returns held within the point cloud dataset, the use of ray-tracing within 3D voxel space allows additional geospatial data to be extracted from the survey (McDaniel et al., 2012). This includes: (1) voxels with no returns but that have beams passing through them - empty space; (2) voxels with no returns due to shadowing by objects - occlusion; and (3) voxels with no returns due to no information - unknown. Using these distinctions, voxels can be classified into different types (Figure 2.5).

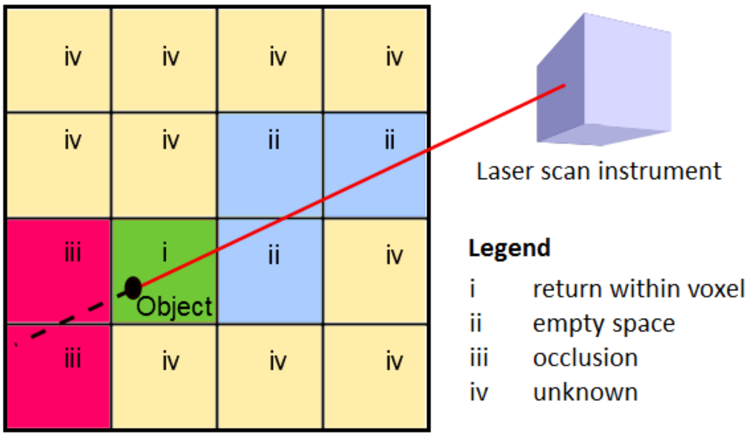

Figure 2.5: Example of how voxel analysis can be used to classify voxel space into different types using ray tracing. This can be used to highlight areas of potential point occlusion or empty space.

With the 3D voxel space defined and values assigned to individual voxels it is also possible to determine attributes for each individual voxel. Attributes can be divided into statistical or point distribution types. Statistical attributes are those such as number of returns and number of penetrations. Point distribution attributes are those such as the central point, spread of return points within voxel and standard deviation of the location of returns within a voxel (Bienert et al., 2010).

2.3.3 Texture analysis

Texture analysis is the examination of surfaces from remotely sensed data. This type of analysis has been used within a range of applications including monitoring of coastal erosion (Rosser et al., 2005; Royán et al., 2014), assessing pavement surface characteristics (Bitelli et al., 2012) and for studying inscribed stone surfaces in archaeology (Spring and Peters, 2014).

Within the forest ecology literature texture analysis from point clouds is limited when compared to geometric modelling and voxel based extraction. The identification of tree species, which is a fundamental aspect of forest inventory surveys (Dufrêne and Legendre, 1997), has been attempted using texture analysis from lidar, although current research shows significant differences between field surveys and extraction of species from point clouds (Dassot et al., 2011). Full waveform analysis of ALS data sets for species identification has also been tested, with results showing the potential of this technique (Vaughn et al., 2012), although work is still ongoing.

The application of species identification from TLS, however, has seen limited success using texture analysis. Othmani et al. (2014) recently outlined a method where geometric texture was used to estimate roughness measures from which species could be classified correctly in approximately 88% of trees surveyed, but further studies are needed.

2.4 Discussion

2.4.1 What are the traditional methods of conducting surveys within forests?

The importance of forest surveys has been known for many years with the result that there are multiple different methods for the estimation of forest structural parameters. Traditional methods are still very common as they offer reliable, low cost estimations.

Traditional field survey techniques offer direct measurement of forest structural parameters such as using callipers or measuring tape when estimating tree diameter, clinometers when estimating tree height and cover boards when estimating FHD. The development of optical instruments for survey work has allowed indirect assessment of forest structural parameters. With the introduction of optical devices came the creation of new forest indices extracted from data collected through optical surveys, showing how developments in technology have fed advances within the field.

In recent decades laser equipment has been developed that replicates many of the direct and optical survey techniques in use. These laser instruments are very useful tools but have been designed to replicate existing measuring techniques, not for the creation of new ones.

2.4.2 How have developments within remote sensing been used to extract forest structural parameters used in ecological studies?

Modern technological advances in ALS have brought great improvements to the field of forestry in recent years, most notably the ability to collect regional forest survey data that can be used for national forest inventory surveys at a greatly reduced cost than was previously possible. Ground based TLS, however, has not shown the same levels of uptake within the forestry or forest ecology communities, although it is suggested the potential is there.

What TLS systems provide is a very accurate, reliable, repeatable method for the collection of dense point cloud information. At the present time forest ecology research using TLS has primarily followed the replication of existing metrics. As Newnham et al. (2015) notes, perhaps for TLS to reach its full potential it is not the replication of existing metrics that should be investigated, but rather the identification of new ones.

Multiple studies have shown that TLS can be used to replicate traditional dendrometric parameters such as DBH and tree height, but if used for these applications the outputs still rely on allometric relationships for the detailed estimation of biomass or total wood volume. Using TLS for the direct estimation of volume removes the need for allometric relationships and has the potential for more accurate estimations.

If it is agreed that TLS has not reached its potential within the forestry community for timber estimations and forest inventory surveys, then it should also be accepted that it has barely registered within the forest ecology community. If the research published within the field of TLS within forest surveying is viewed as a whole, forest ecology applications are a minor component.

Those studies that have tested TLS for ecological surveys have commented on its potential (Eitel et al., 2013; Davies and Asner, 2014; McMahon et al., 2015), but again, these studies have tended to replicate existing metrics rather than explore new ones. The aim of the present study was to assess TLS for estimating existing metrics used within forest ecology, but also to examine new metrics and indices currently unavailable to the forest ecologist. As it is the new metrics and indices, only available through the collection of detailed 3D information, that may allow TLS to reach its potential.

This study aims to build on previous research and describes new metrics and indices for examining the forest understorey that may be extracted using TLS.

This will be detailed in a number of different trials in the following chapters. The next chapter outlines the survey specifications and instrumentation used for the trials within this study and will provide a grounding and best practice guidelines for any future TLS surveys within forest plots that are concerned with understorey vegetation.

Chapter 3

Survey methodology and instrumentation

3.1 Introduction

The design and implementation of a terrestrial laser scanning (TLS) survey in a forest is of particular importance given the relationship between survey setup and the final point cloud accuracy. Soudarissanane et al. (2011) present an examination of the factors that influence the quality of laser scan results with instrument mechanism, atmospheric conditions, object surface properties and scan geometry being the four factors that have the largest impact on quality of the final point cloud.

Given that TLS forest surveys are performed in varying atmospheric conditions (seasonal variations, weather, variable light), collect returns from multiple object surface types (stems, dry foliage, wet foliage, deadwood, etc.) and are performed within a complex environment (uneven terrain, poor line-of-sight), forests present a challenge for the successful collection of any accurate laser scan data.

There have been many previous studies examining the most effective application of TLS within forests to make sure the survey output provides the required coverage and accuracy (Bienert et al., 2006a; Pueschel et al., 2013; Pueschel, 2013; Cifuentes et al., 2014; Seidel et al., 2015). Using these studies, combined with knowledge and experience gained in earlier trials as part of a masters thesis (Ryding, 2009), a best practice approach to TLS surveying in forests has been developed that was used in the trials outlined here. This best practice approach can be considered when examining the understorey using the instruments described.

Multiple TLS surveys were conducted as part of this study with each having been designed and implemented to help answer a particular research objective. To reach these objectives 57 forest point clouds have been analysed with 475 individual laser scan setups utilising both static TLS and handheld mobile laser scanning (HMLS) technology.

The first laser scan data set collected as part of this study provided 20,000 m^2 of filtered, registered survey data. Such a large data set was possible as it was collected as part of a Department for Environment, Food and Rural Affairs (Defra) intensive study examining the effects of changing woodland structure on bird populations in the UK caused by deer. This is referred to as the woodland management and deer (WoodMAD) data set. Although funded by Defra, this project was managed by the British Trust for Ornithology (BTO).

A second laser scan data set was also used for the trials that utilised a previously constructed ecological survey plot. This allowed for the detailed examination and comparison of survey methods through allowing replicable surveys to be designed and carried out over a period of time.

Collecting laser scan data may not be enough on its own to provide a detailed, accurate point cloud. In most cases single point clouds need some level of post-processing to provide a final point cloud that can be used for analysis. Some companies (such as GeoSlam) provide on-line data processing whereby the data collected is uploaded to a server and returned as a complete point cloud (Ryding et al., 2015). It is much more common however, for data processing to be completed in-house using instrument specific software. Processing methods outlined in this study utilised both in-house and on-line data processing.

This chapter describes the instruments, test sites, survey designs and basic data processing work flows for all of the trials outlined in the study. The work flows described, including the novel use of HMLS, and can be used as a suggested best practice guideline for any future TLS forest surveys examining the understorey. In addition, more detailed, trial-specific processing methods have been outlined in following chapters where necessary.

3.2 Instrumentation

A variety of different TLS types including time-of-flight, phase-based, single return and multiple return are commercially available and they provide distinct advantages and disadvantages when considering collecting laser scan data within a forest. Fröhlich and Mettenleiter (2004) and Pfeifer and Briese (2007) provide a description of the different measurement and system configurations available.

Calders et al. (2014) discussed the advantages of multiple return scanners over single return instruments in forest surveys, with multiple return scanners providing increased sampling at greater distance. However, there is an increased cost associated with multiple return instruments however, with the majority of commercially operated systems using a single return mechanism.

Two commercially available laser scan instruments were used during the trials in this study: (1) the FARO focus 3D which is a standard survey grade TLS instrument; and (2) the ZEB1 which is a HMLS, a recent development within the field of ground-based laser scanning. Both instruments are at the lower end of the cost scale for commercially available equipment.

Although cost was not the sole reason for choosing these instruments, economic practicalities were considered when selecting the laser scan instruments to be used. The aim of the trials outlined here was to assess TLS for forest ecology surveys examining understorey vegetation. If a scanner provides excellent output, but is not commercially available or is only available at a high cost, this will impact on the likelihood of the method being adopted as a regular survey tool, irrespective of the success of the survey method. As with many aspects of forest survey there is always a trade-off between desired results and practicality.

3.2.1 The FARO Focus 3D

Static TLS data were acquired using a FARO Focus 3D (FARO Technologies Inc., Lake Marry, USA) instrument. The instrument uses an infrared beam operating at wavelength 1550 nm. The scanner is a phase-based, single (first) return scanning instrument. Full technical details can be found in Appendix A.

The FARO Focus 3D is a commercially available TLS instrument that has been designed for use in architecture or civil engineering projects. It is lightweight (5.2 kg) and small (24 x 20 x 10 cm) making it more appropriate for forest surveying than some of the larger instruments currently available. The instrument has a working range of up to 120 m and a maximum point collection of 9.76 x 10^5 per second. For each point return XYZ coordinates and a reflectance value (intensity of returning beam) are given. Using the internal colour camera RGB values for each return can also be acquired.

The FARO Focus 3D instrument has also shown its potential for forest surveying in multiple previous trials (Dassot et al., 2011; Othmani et al., 2013; Seidel et al., 2015).

3.2.2 The ZEB1[1]

HMLS data were acquired using a ZEB1 (GeoSlam Ltd., Bingham, UK) instrument. This novel system uses an infrared beam operating at 950 nm and has primarily been used in mining and building surveys, with Ryding et al. (2015) introducing the instrument for use in forests. Technical details can be found in Appendix A.

Instead of using a Global Navigation Satellite System (GNSS) within the navigation module, as is common within many MLS (Guan et al., 2015), the ZEB1 makes use of a technology taken from the robotics community, simultaneous localisation and mapping (SLAM). The concept of SLAM is that a robot can be placed in an unknown environment and has the ability to create a map and then navigate to a particular destination. An introduction to the science can be read in Durrant-Whyte and Bailey (2006) and Bailey and Durrant-Whyte (2006). The mapping module of such technology forms the basis for use within the ZEB1. The fact that the ZEB1 is lightweight (0.7 kg) and has no reliance on GNSS makes it an ideal data capture method for inaccessible areas such as under tree canopies and indoors (Thomson et al., 2013). James and Quinton (2014) identified the significant advantages of the ZEB1 for the rapid survey of complex topography, with expected survey times being 40 times quicker than with a static TLS instrument. In the same study it was also concluded that even with the limitations in data density and accuracy shown in the ZEB1 system, its usefulness in difficult environments would make it a highly practical survey solution.

The ZEB1 consists of a 2D laser scanner and low-cost inertial measuring unit (IMU), both of which are positioned on top of a spring which has been designed to have the resonant frequency of the average human gait (Bosse et al., 2012). As the user carries the ZEB1 through the environment, the scanner head rocks back and forth creating a 3D field of measurement with data being captured at the speed of movement. The algorithm used to calculate the position of the scanner head uses a moving time window of the trajectory data. As new data is added the algorithm uses a linearised model to minimise the error in the IMU measurements along with minimising the correspondences between the 3D

[1] Parts of this sub-section have been modified from Ryding et al. (2015)

point cloud data for the respective time segment. The correspondences for the 3D point cloud are minimised using a technique similar to the iterative closest point algorithm (Besl and McKay, 1992), but instead of solving for one rigid transformation the solution is solving for a continuous trajectory (Bosse et al., 2012). The final smoothed trajectory is used to compute the coordinates for the full 3D point cloud. The ZEB1 converges on the best solution when the scanned area contains many unique features which can be identifiable in consecutive rocks of the scanner and when swath paths are less then 30 m apart.

The ZEB1 instrument works best where there is an enclosed survey environment (such as indoors) and where the surfaces are static (James and Quinton, 2014). Enclosed outdoor environments such as under tree canopies are therefore sources of both static surfaces (large stems) and irregular surfaces (foliage, small stems and understory), creating a challenging and potentially uncertain survey environment.

3.3 Study sites

3.3.1 WoodMAD

Previous studies have shown that deer can influence the structure, composition and ecosystem processes in forest sites where deer browsing is common (White, 2012). The structural changes brought about by deer browsing can then have a detrimental effect on the preferred habitat of songbirds such as Blackcap, Common Nightingale, Garden Warbler, Common Chiffchaff and Willow Warbler (Gill and Fuller, 2007) and also greatly reduce tree regeneration, shrub cover and plant reproduction (Frerker et al., 2014).

Previous studies examining the effects of deer browsing on forest structure have used multiple methods of assessment. These include: cover boards to estimate foliage density (Gill and Fuller, 2007); DBH measurements used to calculate tree density (White, 2012); and understorey biomass collection to estimate the resources sustaining deer populations (Saout et al., 2014). All of these studies confirm that high levels of deer browsing reduce the low level growth seen within forests. White (2012) showed that in forest where deer density is high, trees were failing to regenerate due to saplings being removed through browsing. The same study also highlighted how browsing patterns can influence structure, with high deer density limiting recruitment into the sub-canopy layers and having the effect of leaving the forest in a relatively open state.

Through the collection of TLS data from forest sites with varying deer density levels, combined with the knowledge that high deer density can lead to the suppression of recruitment and the simplification of forest structure at low levels, it was proposed that the extraction of forest structural parameters from TLS data could be tested against expected structural properties brought about by deer browsing.

As part of this project 40 intensive monitoring sites across the UK were chosen as test plots for TLS. These test plots were chosen to cover two distinct deer density groups: high and low deer density. Deer density was assessed by the BTO using distance sampling (Buckland et al., 2000), and from observations of deer at night using thermal imaging (Gill et al., 1997).

In addition to deer density, plots were also grouped into those which were managed and unmanaged, allowing for assessment based on management practice, with management practice for each site provided by the BTO.

Whilst deer density can affect woodland structure, there is no guarantee that deer levels will be directly indicative of the structural properties of a forest (i.e. deer may be present but not browse, or an open forest can be caused by other factors such as disease). Limitations to this data set include the use of high and low deer density sites that exhibit structural properties not associated with their deer browsing levels.

The survey sites used in this study are also all of the same type (lowland, broadleaved woodland) meaning the relevance of the developed feature extraction and data collection techniques may need examining in other UK forest types, such as upland woods, pinewoods and wet woodlands. The relevance to boreal and tropical forests will also need to be examined.

All laser scan data were collected in June 2012 with an average of two surveys being carried out each day, dependent on distance between forest sites. The BTO provided stand details within designated woodland sites for each of the 40 laser scan plot sites.

Location details, transect coordinates, transect bearing and plot maps for the WoodMAD data set can be found in Appendix B.

3.3.2 Kirton Wood

Kirton Wood SSSI (GB grid ref: SK 707684), is a 46 ha semi-natural ash and wych elm woodland managed by Nottinghamshire Wildlife Trust (Figure 3.1).

Kirton Wood has been left to develop largely undisturbed since the 1930s and as a consequence there is a uniformity of size of trees. Shrub communities include field maple, hawthorn and hazel. Dense ground flora is also present throughout, dominated by bramble, honeysuckle, goosegrass and dog's mercury.

Within Kirton Wood an ecological survey area has previously been constructed to allow continuing scientific studies at the site. The survey area measures 50 m by 50 m and contains 25 subplots (10 x 10 m).

The survey area within Kirton wood is a complex forest site with poor access and limited tracks. The site offers difficult conditions for TLS, as opposed to the relatively open, easily accessible plantation sites commonly used for testing TLS for forestry applications. The site therefore poses a rigorous test for laser scanning in an environment common to ecological studies.

3.4 Survey design

3.4.1 Static TLS survey

Multiple previous studies have examined the most effective use of static TLS for forest measurement (Bienert et al., 2006a; Pueschel et al., 2013; Pueschel, 2013; Cifuentes et al., 2014; Seidel et al., 2015). From these previous studies, forest TLS surveys can be considered in three categories: (1) single scan; (2) multiple scan; and (3) multiple-single scan.

The single scan method is where a TLS instrument is positioned in the centre of the area of interest and collects return information covering a full 360° in the horizontal. This method allows for quick surveys but the final point cloud will only contain point returns for surfaces in direct line of sight of a single scan setup. The multiple scan method requires the scanning instrument to be moved to different scan setup locations from where individual point clouds are acquired. This method uses post-processing to merge the individual scans together (known as scan registration) to produce a final point cloud. This method has the advantage of producing larger final point clouds, but does involve increased levels of processing and requires a method for the accurate registration of individual scans. Registration is commonly performed through the use of survey scan targets, although the use of these does increase survey time and can introduce matching errors into the final point cloud. The multiple-single scan method uses multiple scans but with the analysis of the data performed on each individually, not as a single, registered point cloud.

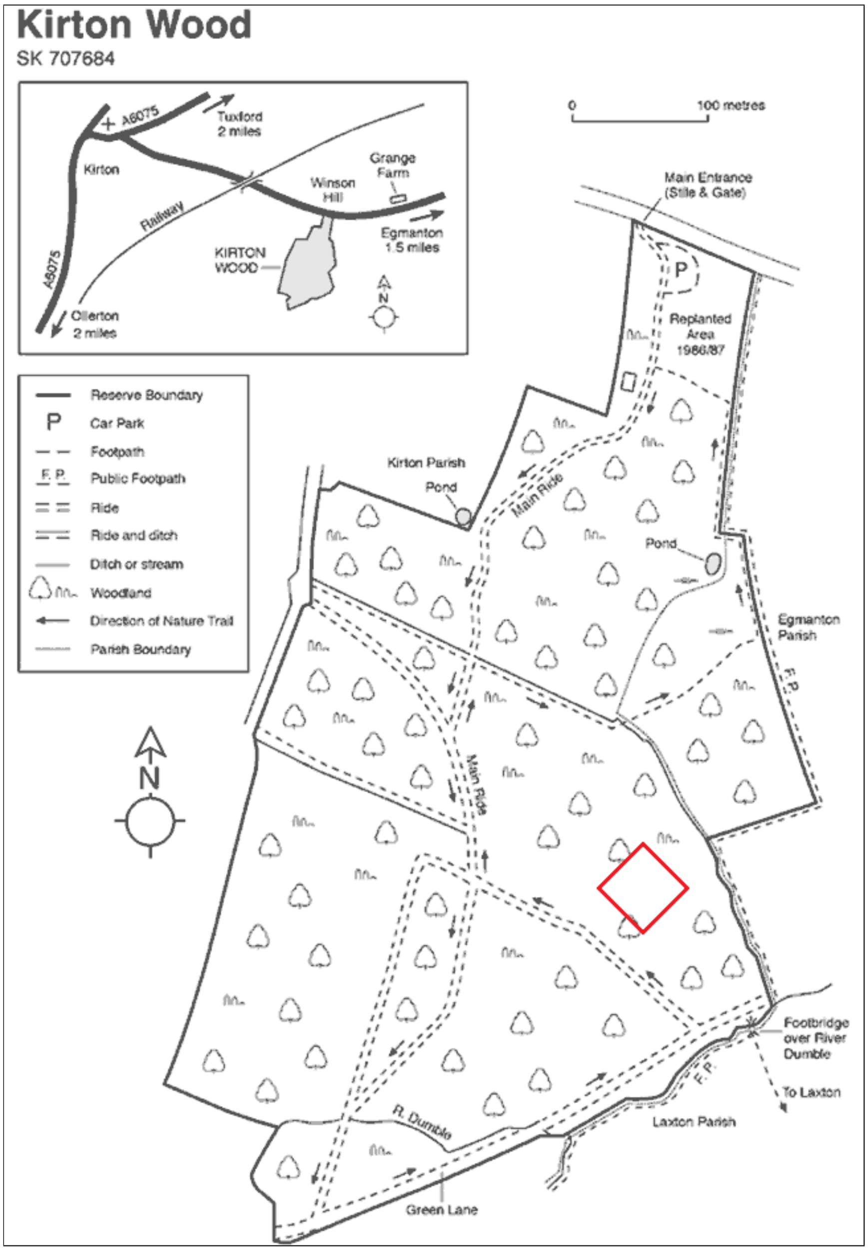

Figure 3.1: Reserve map of Kirton Wood with test site location marked as red square (map provided by Nottinghamshire Wildlife Trust)

Pueschel et al. (2013) showed how for surveys in forests, accuracy of stem detection and volume estimates improves when using the multiple scan method. For the trials outlined in this study all surveys were carried out using the multiple scan method.

FARO Focus 3D data was collected at each survey location with a spatial resolution of 7.67 mm at 10 m. The scans covered a field of view 360° in the horizontal and 305° in the vertical with full colour panoramic photographs obtained using the instrument's internal camera, time permitting. Higher resolutions were possible, but the chosen value allowed fast surveys that met the required data resolution for the WoodMAD project (less than 10 mm at 13 m). The scanner height varied with each site depending on ground vegetation, with a height close to 1.3 m maintained where possible.

3.4.1.1 WoodMAD survey

The coordinates of the start point for each laser scan survey was selected before the site was visited. The range of easting and northing coordinates within each site were found and a single location identified by randomly selecting one easting and one northing. This made sure that survey areas were not chosen for ease of access. Each laser scan survey plot had dimensions of 10 m by 50 m. The transect direction was determined on site by throwing a marker flag in the air, the direction it landed was the direction of transect.

Within each survey, 11 individual instrument positions were used, combined with a minimum of 9 targets to register the scans. If there was poor line of site between scan setups and targets (often seen in sites with dense understorey), further targets were used to make sure registration was successful. Scanner setup and target locations were chosen to maximise field of view between scans. A survey setup plan (based on experience from earlier trials) can be seen in Figure 3.2, highlighting ideal locations for targets and scanners.

Each transect area was marked with twine and flags to ensure trampling was kept to a minimum and survey targets could be positioned at optimum locations for scan overlap (Figure 3.3).

3.4.1.2 Kirton wood survey

The laser scan surveys carried out at the Kirton Wood trial site followed the same principles as used for the WoodMAD data collection including the use of the multiple scan method, with the instrument positioned outside each area of

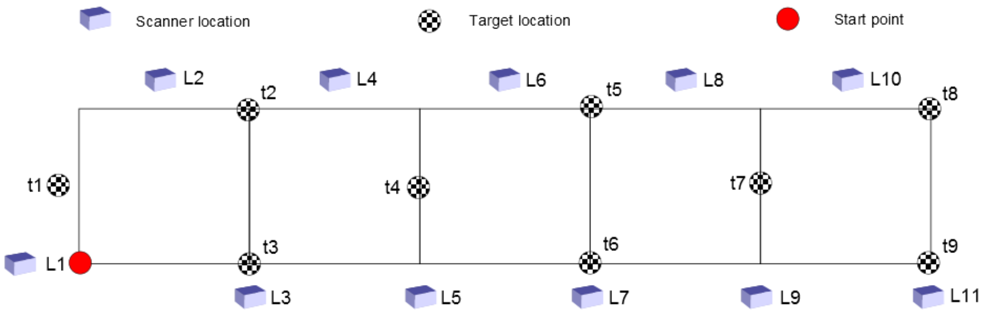

Figure 3.2: Survey design showing setup (L) and target (t) locations.

(a) Marking out transect

(b) Setting up targets

(c) Scan instrument and targets

(d) Pre-survey checks

Figure 3.3: Photographs of forest laser scan survey procedure where each site was first marked using string and flags (a). Targets were then positioned at the optimum location (b), before scanner setup (c) and final checks (d).

interest and a scanner height of 1.3 m used where possible.

At each subplot location three scans were obtained using the FARO Focus 3D. Two large target spheres (Ø 0.1 m) were used for registration and also for geo-referencing during temporal survey analysis (Chapter 7.4.3). Five smaller registration spheres (Ø 0.0725 m) were used to produce the known points needed for point cloud registration. At each subplot a single target sphere was placed in the centre of the area of interest with the second positioned 1.5 m outside the subplot. The smaller registration spheres were distributed evenly outside the subplot (but close to the boundary) to give line-of-sight to the scanner positions and to maintain good geometric spread allowing for a more stable point cloud registration. An idealised survey plan can be seen in figure 3.4.

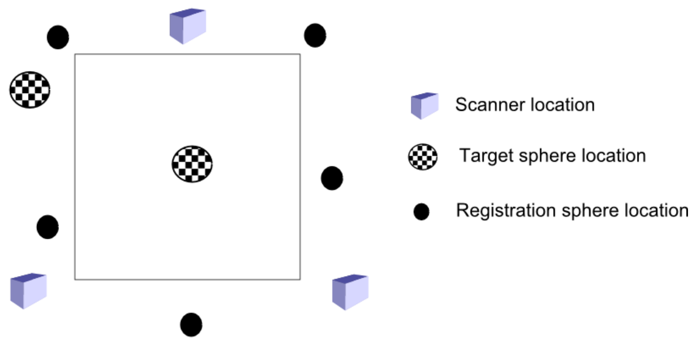

Figure 3.4: Trial subplot survey design showing idealised setup and target locations used at Kirton Wood.

3.4.2 HMLS survey

The range of the ZEB1 handheld scanner (as noted by the manufacturer) is approximately 15 m when working outdoors. This equates to a maximum swath distance of 30 m when designing a survey plan. With the reduction in line-of-sight that is commonly encountered in forest, this maximum swath distance may not provide adequate coverage due to occlusion caused by stems and branches. Maximising the coverage whilst minimising survey time is a goal of survey design and should allow for the most cost-effective use of the ZEB1 instrument.

All surveys started and ended at the same point allowing for a closed loop of survey data. This followed the manufacturer's guidelines for reducing errors in the final registration. A steady walking speed was maintained throughout each survey with the rocking of the scanner head being kept constant. This made sure a similar density of points was collected with each rock of the scanner.

ZEB1 data was acquired with the user slowly walking across the plot site with

Figure 3.5: Zeb1 handheld mobile laser scanner in operation for forest mapping

the instrument remaining at breast height throughout (Figure 3.5).

3.5 Scan registration

Scan registration is the process by which individual laser scans are combined to provide a single point cloud where all points are within the same coordinate reference system (CRS). Bornaz et al. (2003) provide a description of the process of scan registration.

In the WoodMAD and Kirton wood surveys outlined above, registration was performed using static, spherical targets that remained as fixed points between adjacent scans. Although the use of scan targets is time-consuming they do provide accurate registration results. Other methods for scan registration are available for static TLS surveys but these commonly require planar surfaces which are used as fixed points instead (Ripperda and Brenner, 2005). As planar surfaces are not common within a forest, it was decided that fixed targets would offer a practical solution for accurate scan registration.

All registration using the FARO Focus 3D data was performed in FARO Scene software (Pueschel et al., 2013). This is proprietary software developed by FARO for the main purpose of scan registration. The software has a grading mechanism for registration whereby the relative locations of scan targets used during registration are compared in adjacent scans. If the quality criterion are not met (maximum of 15 mm baseline errors between target centroids) the software will not allow registration to take place. In this way a minimum accuracy requirement for all of the FARO Focus 3D data was applied.

All scan data acquired using the ZEB1 HMLS were registered remotely using the GeoSlam servers. Data were uploaded to the server and registration performed at a rate of 1:1 meaning a 15 minute survey would take 15 minutes to register. Once registered, data were available to download from the server as a complete point cloud.

3.6 Data processing

All laser scan data used in this trial were subject to some form of filtering before the final point cloud was exported. Filters are commonly used to detect multiple erroneous scan points as part of a standard laser scan survey. Erroneous points are commonly caused by ambient radiation (atmospheric radiation with the same wavelength as the lidar instrument that is identified as a likely point return) and surface multi-path (when a point return is reflected from two surfaces before hitting the sensor) and can be detected as outliers within the main point cloud data set. A description of the detection, cause and methods for the successful removal of point cloud outliers is given by Sotoodeh (2006).

To avoid the inclusion of likely outliers within a final point cloud FARO Scene applies two default filters that remove points considered to be isolated (stray points) and those with a weak return strength (dark points). In a similar way the on-line point cloud processing used by GeoSlam for the ZEB1 applies filters to make sure only valid point returns (as set by manufacturers parameters) are exported in the final point cloud delivery.

In addition to the standard filters applied by the registration software, point cloud decimation was carried out to a level of 1 cm^3. Decimation is the structured re-sampling of point cloud data to produce a single return per voxel unit. Through processing the point cloud in this way the varied point resolution seen across the plot site, which is a result of the scanning geometry and data acquisition method (Soudarissanane et al., 2011), can be removed. This allows multiple surveys to be assessed for point returns within the same spatial framework (i.e. a single return for each 1 cm^3 voxel). Decimation of point clouds often also results in reduced processing times, as a consequence of the decreased quantity of data.

Using centimetre decimation resulted in considerably shortened processing time (by a factor of ten) and it was felt that this processing advantage was greater than having millimetric modelling accuracy. As with many aspects of forest ecology surveys a trade off between speed and accuracy was made.

Furthermore, with the complexity of forests combined with the dynamics of surveying outdoors (the effects of foliage movement due to wind, ambient solar radiation increasing laser return noise and the presence of variable reflective surfaces), it is questionable if millimetric accuracy is even possible in a TLS forest survey. Pirotti et al. (2013) found that a tree stem modelling accuracy of 1 cm could be achieved through TLS in ideal survey conditions and with limited undergrowth present, but these conditions are uncommon.

3.6.1 Correction to ground height

In addition to filtering and decimating the point cloud data sets, all data were transformed from a scanner-centric vertical datum (how TLS measure height) to one referencing ground surface. In this way all of the heights extracted from the forest point clouds were consistent with traditional methods of forest ecology surveys that use the ground surface as the vertical datum.

To achieve height above ground the first step was to create a digital terrain model (DTM) from the point cloud data. This follows previous studies examining TLS for forest surveys. Ashcroft et al. (2014) used the lowest point as recorded by the scanner for each vertical grid to determine ground level following the method outlined by Henning and Radtke (2006b). This method can be used to accurately assess terrain, but Ashcroft et al. (2014) showed that dense understorey can prevent beams reaching the ground surface and so overestimate the height of the ground. The accuracy of the method also relies on the size of the grid used to assess lowest point, with larger grids (5 m x 5 m) reducing the chance of dense vegetation blocking the ground (causing height over-estimation), but also increasing the likelihood that small-scale variations in ground surface would be 'smoothed-over'.

In this trial DTM creation used a two stage process. A coarse surface model was first created using horizontal grids of 3 m x 3 m. The lowest point in each grid was then assigned as the ground surface and a triangulated irregular network (TIN) created to describe the forest plot. TINs are vector based representations of surfaces (based on a network of non-overlapping triangles, in this case created using Delaunay triangulation) providing a variable distribution of points accurately describing terrain. All heights from the scanner were then corrected to this TIN surface. Following this a horizontal grid of 0.5 m was used to created a DTM from the adjusted point cloud from which a second adjusted point cloud was produced. The difference between the coarse DTM adjusted point cloud and the second, finer DTM was then examined manually for each site. Where the finer DTM showed an increase in ground surface (over 5 cm) compared to the coarse terrain model, this highlighted areas of potential over-estimation in ground surface held within the finer-scale DTM. These areas were then visually assessed and if dense vegetation was found, the lowest point as described by the coarse DTM was used. In this way fine-scale terrain features within the 0.5 m terrain model were maintained, whilst over-estimations of ground surface caused by dense vegetation were highlighted and removed.

3.6.2 Development of scripts

After the initial registration of point clouds using instrument specific software, all processing was completed using Python scripting developed for this trial. The Python scripts utilised multiple libraries including Point Cloud Library, Arcpy and the Geospatial Modelling Environment.

3.7 Discussion

The survey procedures presented here were designed specifically for the trials outlined in this study and were carried out in lowland broad-leaved woodlands of the UK. Trials were completed using a medium range (125 m) phase-based instrument. The methods outlined represent a best practice guideline for the assessment of understorey vegetation for this specific woodland type and scanning instrument as they are based on a considerable amount of experience.

Forests pose a particular difficulty for TLS surveying due to their complicated structure, difficult terrain and limited line-of-site. This is true of UK lowland broad-leaved forest, but also of many different forest types globally. Although the new methods presented here were designed for a specific forest type, the application of these methods across different forests should be possible. One example is how changes in understorey vegetation density and stem density between broad-leaved forest and boreal forest may result in a different optimal distance between survey setups (grids of 10 m by 10 m outlined in Figure 3.2), however, the overall survey design should stay the same.

There are also limitations to the FARO Focus 3D when considering its use for forest surveying. As the FARO instrument uses a phase-based mechanism there is an increase in the amount of 'noise' (stray points) seen in resultant point clouds when compared against a time of flight instrument. These stray points are caused by ambient solar radiation and can increase when there is bright sunshine or when scanning towards the sky. For this reason phase-based instruments may not provide the detail necessary when surveying the canopy from the ground. Phase-based instruments also typically have decreased range compared to time of flight instruments, something that may impact their effectiveness when working in open forests or examining tall canopy (over 20 metres).

The novel use of a HMLS instrument for forest surveying brings its own consideration when planning a survey. Target spheres are not used in this method, considerably reducing the time needed for a survey, but to make sure coverage is maintained in the area of interest, thorough survey planning and 'walking tracks' should be designed before surveying begins. The design of these tracks will be discussed more in Chapter 8.

Using the survey method outlined here for the WoodMAD data set, the following chapter will explore a new structural attribute extracted from TLS data sets through the creation of a vertical to non-vertical index.

Chapter 4

Developing a new method for estimating the vertical component of forest understorey using terrestrial laser scanning

4.1 Introduction

Structural data collected beneath the forest canopy is used by ecologists to help develop effective management and conservation strategies, with habitat structure an influence on animal-habitat associations (Hunter, 1999; Davies and Asner, 2014; Bergner et al., 2015). Due to the difficulty in collecting data on the 3D structural characteristics of forest using traditional ecological survey techniques, forest ecological surveys have traditionally focused on 2D mapping of stem locations (e.g. Eichhorn, 2010) from which further spatial patterns, such as stem clustering, can be calculated (Freeman and Ford, 2002).

The development of techniques for automating the extraction of features from point cloud data, with classification based on geometric properties, is an important topic within remote sensing, photogrammetry and robotics. From the extraction of building structures (Vanegas et al., 2012) to the detection of objects (Serna and Marcotegui, 2013) and the identification of curbstones or road markings (Guan et al., 2014), point cloud interpretation based on geometric classification is a research field that is rapidly growing. Weinmann et al. (2015) provides a detailed description of recent developments.

Previous studies have shown how terrestrial laser scanning (TLS) data can be used to extract canopy structure through estimation of gap fraction (Cifuentes et al., 2014), leaf area index (LAI) (Moorthy et al., 2008) and canopy heights (Olofsson et al., 2014). Less dominant is work focused on how TLS can be used to assess the rates of processes operating within forest systems, the distribution of microhabitats within them or the interactions between biotic and abiotic components (Ashcroft et al., 2014).

Separately, Michel et al. (2008) successfully used vegetation density estimations obtained through TLS data to link the structure of forest to the nesting habits of two bird species; Yang et al. (2013b) combined thermal imaging with TLS in forests for the study of bat flight behaviour; McMahon et al. (2015) showed how a portable canopy lidar could be used to evaluate the relationship between management history and canopy structure across several UK woodlands; and Seidel et al. (2015) used TLS to determine attributes of tree growing space and neighbourhood structure within forests. These studies highlighted the potential for TLS in the measurement of 3D ecosystem structure, although currently this potential has yet to be realised (Eitel et al., 2013).

Of the research currently published on TLS within forests (Chapter 2), the majority of studies have primarily tried to improve existing allometric relations, such as those concerned with biomass estimations (Seidel et al., 2012a). In comparison, there are very few published studies showing the development of new measures or indices for use within forest ecology surveys, an area where TLS may be used to improve the collection of 3D ecological data and provide alternative analysis methods when considering geospatial relationships within forest.

Previous research has examined the detailed extraction of features and parameters using the accurate 3D modelling of individual trees (Hackenberg et al., 2014; Boudon et al., 2014; Calders et al., 2015) providing precise estimates of biomass and tree structure. These methods offer improvements in estimation accuracy over the use of allometric relationships to determine biomass, although the methods can be labour intensive and time-consuming as they require individual trees to be isolated from point cloud data sets.

With 40 individual point clouds covering 20,000 m^2, the WoodMAD data set posed difficulties in processing and feature extraction in that the methods developed had to be fully automated and relatively quick. The detailed assessment of individual tree 3D properties (using methods where each tree would require manual extraction from the data set) did not represent a realistic approach to extracting information over such a large data set. For efficiency and consistency the work flow requirements were that the final outputs should be relevant to forest ecologists, but also be produced with minimal manual processing and relatively computationally light (e.g. a single plot could be processed on a standard desktop computer in hours).

For TLS to reach its potential within forest ecology, all aspects of the survey process need to be re-examined. Developing feature extraction methods for components that can be used as surrogates for functional or compositional characteristics would provide further advantages to the use of TLS for forest ecology surveys. If traditional forest ecology surveys are dominated by those attributes that are relatively easy to collect, have ecological meaning and are repeatable (such as the collection of DBH using tape), TLS feature extraction should concentrate on those attributes that are difficult to collect using traditional methods, but that are also ecologically important.

When assessing which geometric structures to extract from TLS surveys of forests, how those structures affect further ecological attributes, such as the availability of food, the provision of shelter or the availability of cover, should guide the selection (i.e. how ecologically meaningful are they). This poses the question, which geometric properties of forests have the most importance when examining ecological attributes?

Tews et al. (2004) reviewed multiple publications between 1960-2003 and concluded that the majority of studies found a positive correlation between habitat heterogeneity and species diversity. While Zellweger et al. (2016) showed that estimates of vegetation structure improved predictions of bird and butterfly species richness, with vegetation diversity associated with light availability, food resources and shelter. Huang et al. (2014) also outlined the importance of estimating 3D forest structure when predicting avian diversity, with height heterogeneity an important supplement for habitat characterisation and richness models of forest bird species. Whereas Muiruri et al. (2015) showed how bird forage and predation rates were affected by tree species diversity at different spatial scales within forests. These studies show the importance of spatial analyses within forests and highlight how increasing the understanding of forest structure can help improve the understanding of animal-habitat associations. Using TLS to estimate vegetation heterogeneity, combined with targeted feature extraction, has the potential to play a pivotal role when considering how structural attributes affect composition and species diversity within forests.

There are multiple definitions of forest with a general definition being an area of land dominated by trees or other woody vegetation. The Oxford Dictionary (2016) provides a secondary definition of a forest as 'a large number or dense mass of vertical or tangled objects, i.e. a forest of high-rise apartments'. This definition, although not ecological meaningful, does highlight that the vertical arrangement of objects is important when considering the idea of a forest.

As trees are the dominant feature of forests the geometry of tree stems (and more specifically their vertical component), and how this relates to other geometric features within forests, has been suggested as a useful surrogate for the heterogeneity of vegetation within forests.

The potential application of the vertical component to assess forest vegetation can be seen when comparing different forest types. Firstly, a monoculture forest in a relatively open state used for timber harvesting (with access for vehicles and very little understorey), is expected to be dominated by the stems of trees growing vertically and with few other geometric properties. This scenario can be considered as exhibiting vertical dominance indicative of vegetation homogeneity. Secondly, an old growth forest showing high levels of heterogeneity, species richness and with dense understorey would be expected to show dominance of non-vertical components. The stems of the trees would still contain vertical geometry, but understorey vegetation, branches, foliage and other growth would be expected to contain multiple other geometric features contributing to the structural composition. In this case it is expected that the dominance of the non-vertical component would be indicative of vegetation heterogeneity.

A comparison of forest type in relation to vertical component is shown in Figure 4.1, where two forest types are expected to exhibit different proportions of vertical component.

Through using estimates of the vertical and non-vertical component, TLS surveys may provide additional information on the compositional and functional characteristics of forests not collected during traditional forest ecology surveys. The metrics extracted may include the total value of the vertical component and also values for the vertical component within distinct height bands. Figure 4.2 outlines how different forest types could be expected to exhibit unique levels of vertical component with height, depending on their structural and compositional characteristics.

Measurement gaps within point clouds (point occlusion) are a source of potential

(a) Expected vertical dominance. (b) Expected non-vertical dominance

Figure 4.1: Forests dominated by tree stems (such as monoculture forests) are expected to show vertical dominance (a). Mixed forests exhibiting increased levels of ground vegetation are not expected to exhibiting vertical structural dominance (b).

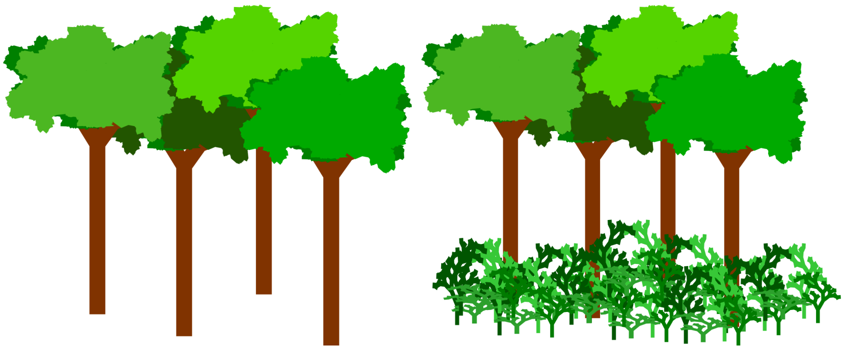

(a) Monoculture forest with no understorey vegetation.

(b) Monoculture forest with understorey vegetation.

(c) Mixed forest with high levels of understorey vegetation.

Figure 4.2: Monoculture forests with no understorey vegetation (a) would be expected to show uniform levels of vertical dominance up to the start of the canopy. Monoculture forests with understorey vegetation (b) would be expected to show variation in structural component with height. Mixed forests with high levels of understorey vegetation (c) would be expected to show uniform levels of non-vertical dominance.

error whenever using TLS in forests (Bienert et al., 2006a). Multiple scans help to mitigate some of these errors (Cifuentes et al., 2014), but in a complicated environment such as a forest, occlusion is likely to be present within any final data set. It was noted by Béland et al. (2014a) that few studies have investigated occlusion effects in TLS surveys of forest and that this remains a major challenge. It is expected therefore, that occlusion will affect the success of any method for the extraction of vertical component from forests.

The aims of this study were to address the questions: (1) Can TLS be used to extract the vertical components of the understorey layers of forests effectively, with minimal manual data processing, from large data sets? and (2) to what extent does point occlusion affect the extraction of the vertical component using TLS?

To achieve these aims, an objective was set to develop a method for the extraction of vertical features from forest point cloud data sets, using automation where possible and without time-consuming data processing. The effect of point occlusion on this method was also considered.

It was expected that when extracting vertical features from forest plots, those with high deer density would show a dominance of vertical (stem) material at low levels in the forest. This is due to the fact that smaller saplings and understorey growth would be removed through deer browsing. In contrast, forests with low deer density were expected to show an increase in non-vertical material where saplings and understorey growth can expand unimpeded by deer browsing habits.

4.2 Methods

To fulfil the trial objective a forest structural index derived from estimates of vertical and non-vertical components was created. The structural index was then tested against forest sites with known levels of deer browsing. Through the collection of TLS data from forest sites with varying deer density levels, combined with the knowledge that high deer density can lead to the suppression of recruitment and the simplification of forest structure at low levels (White, 2012), the extraction of vertical components using TLS was tested.

This trial tested extraction techniques using classification of points based on their vertical alignment within voxel space. It was expected that through the gridding and voxelisation of data sets an assessment of individual points based on their neighbourhood relationships could be made. Using this method, each point within a forest data set was assigned an attribute of either vertical or non-vertical.

To assess the influence of occlusion at varying heights, point return counts and voxel occupancy were compared across different height bands for surveyed data sets (expected to contain occlusion) and simulated data sets (no occlusions present). Using simulated data allowed for an 'ideal' point cloud to be produced that could be used to model how point return numbers and voxel occupancy changes across different forest layers (understorey vegetation through to canopy). It was expected that the difference between modelled data and surveyed data may highlight areas where occlusion was having an adverse affect on the collection of point returns.

4.2.1 Site descriptions

Three of the data sets collected from the WoodMAD survey plots were used in this study for developing and testing work flows for the creation of a structural index. The three forest point clouds were chosen to represent forests with identifiable management practices (managed, unmanaged) and deer density (high, low). Plot details and characteristics for these three sites are listed in Table 4.1. Data from all 40 BTO test sites were used once the analysis work flow had been developed.

Table 4.1: Site descriptions provided by British Trust for Ornithology

	Ampfield Wood	Fridd Mathrafal	West Blean and Thornden Wood
Management	managed	managed	unmanaged
Stand details	oak 50 yrs	oak, hawthorn	mature oak, hazel
Deer density	high	low	low
Area	Weald	Welsh Marches	Kent
Date of survey	08/06/2012	27/06/2012	14/06/2012
Easting (BNG)	439678	311638	614275
Northing (BNG)	124506	310858	164133

Photographs showing the three survey test sites can be seen in Figure 4.3. The plot view photographs were taken at a height of c. 1.5 m above the ground and show a horizontal view through the site. The ground view photographs were taken at a height of c. 1.0 m above the ground and show a representative area of ground cover within the site.

(a) Ampfield: plot view

(b) Ampfield: ground view

(c) Ffridd Mathrafal: plot view

(d) Ffridd Mathrafal: ground view

(e) West Blean and Thornden: plot view

(f) West Blean and Thornden: ground view

Figure 4.3: Photographs of woodland plot sites showing horizontal view through transect and ground cover view.

4.2.2 Laser scan data collection and preparation

The field survey point clouds processed for this trial were all collected, filtered and registered using the procedures outlined in Chapter 3. See Figure 4.4 (a, b, c) for point cloud visualisation.

4.2.3 Simulated data sets

In addition to field data collected as part of the WoodMAD project, forest point cloud data sets were simulated to allow analysis and testing of the developed measures on data sets with known structural properties. A Python script was developed to construct multiple simulations of the size and complexity required (within constraints), mimicking stems, foliage and unordered ground-level growth (Figure 4.4 (d, e, f)).

The Python script randomly positioned a point within the plot area (the area was 10 m x 30 m), this was taken as the centroid of the stem. A height and maximum radius for the stem was then randomly chosen from between a minimum and maximum value. The min/max values for stem radius and height were changed with each iteration of the script to give different forest properties within the simulation (i.e. tall thin trees, short wide trees or a combination). A minimum stem radius was then randomly selected from between 1/3 and 2/3 of the maximum stem radius, with the maximum radius describing the stem at ground level and the minimum radius describing the top of the stem. The tree height and min/max radius were then used to calculate the radius at 1 cm increments (height bands) from 0 m up to the top of the stem. The script then created points to describe a circle (the stem surface) within each 1 cm height band with point spacing <1 cm. Using this method multiple circles were positioned on top of each other to describe a tapering stem.

Each tree stem within a plot was then assigned a tree type (apple, mango, rubber or walnut). Using tree canopy geometry data provided by Sinoquet et al. (2009) the simulation then built a canopy model for each stem. The canopy model included area and orientation information for each leaf contained within the tree canopy geometry data set. The process was then repeated to create multiple stem/canopy models used for testing.

With stems and foliage randomly positioned within each simulated plot site the final task was the introduction of understorey vegetation. To achieve this, points were randomly distributed within the lower levels of each plot up to a randomly chosen maximum understorey height. This process did not replicate the structure of understorey vegetation, but it did provide unordered point returns indicative of the non-vertical component that would allow the work flow for extraction of vertical component to be tested.

To make sure the simulated and surveyed data sets contained similar point density, all simulated data sets were decimated to 1 cm^3 as described in Chapter 3.

Although the simulated data sets were not representative of real forest (they lack any branching structure) they allowed for the simple simulation of laser point returns with height. All leaf and stem surfaces within the simulation data sets were modelled, something that is not possible in a forest survey due to laser occlusion.

In addition to x,y,z coordinates the simulation script also assigned each point an attribute to define its type; vertical for stem points, and non-vertical for canopy/ground-level points. Using this attribute the structural characteristics of each simulated forest plot could be determined.

4.2.4 Data processing: development of structural index

A graphical representation of the initial steps of the processing work flow can be seen in Figure 4.5. The first stage in data processing was to sub-divide the point cloud data set into 10 cm vertical zones for analysis (referred to as height bands). This was performed using a Python script that split forest point clouds based on their height about ground (z value). Zoning was used to examine vertical structural characteristics at the 10 cm scale and to isolate defined structural regions such as ground cover and understorey. Zoning also allowed for smaller sections of point returns to be analysed at a single time, this had the effect of reducing the computational requirements and therefore increasing processing speeds.

A height band depth of 10 cm was chosen after discussions with the BTO as part of the initial WoodMAD survey design. BTO ecologists identified decimetre analysis as an improvement on existing methods and as allowing detailed examination of vertical structure, particularly with reference to bird nesting patterns. Height bands of 1 metre would be quicker to process than 10 cm bands, but the identification of change in vertical structure would be much coarser and less applicable to examining habitat changes within the understorey, with the maximum height of understorey occurring between 0.5 m and 2 m above the ground (Gilliam, 2007).

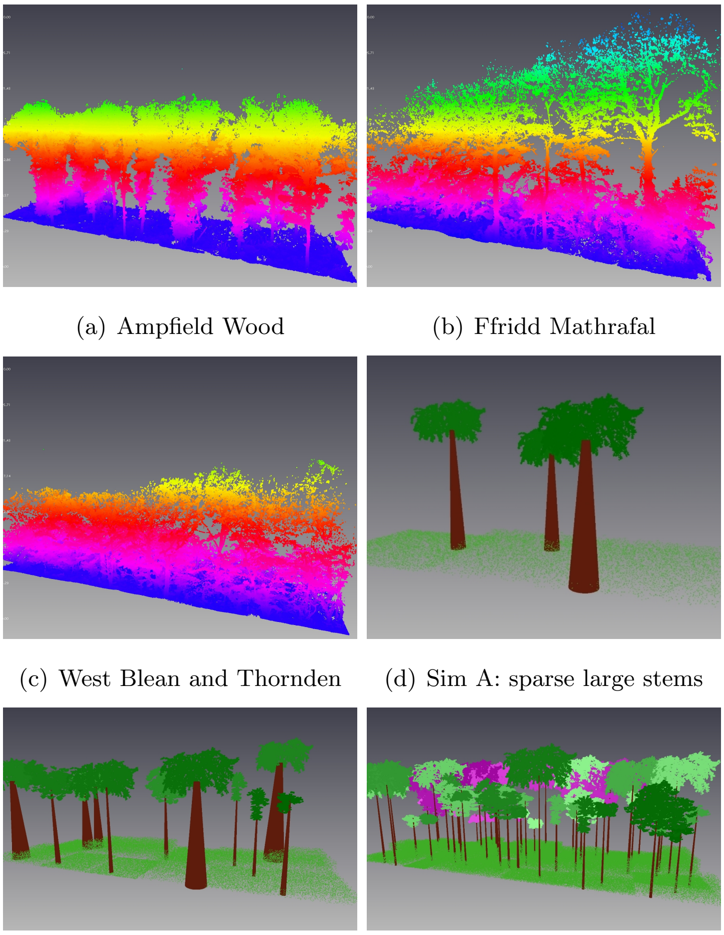

(a) Ampfield Wood (b) Ffridd Mathrafal

(c) West Blean and Thornden (d) Sim A: sparse large stems

(e) Sim B: moderate mixed stems (f) Sim C: dense thin stems

Figure 4.4: Showing visualisation of forest point cloud data sets used for testing of methods, these include three trial sites (coloured by height) and three simulated forest point clouds representing forest with different structural properties. All forest sites are 10 m x 50 m in area. simulations are 10 m x 30 m.

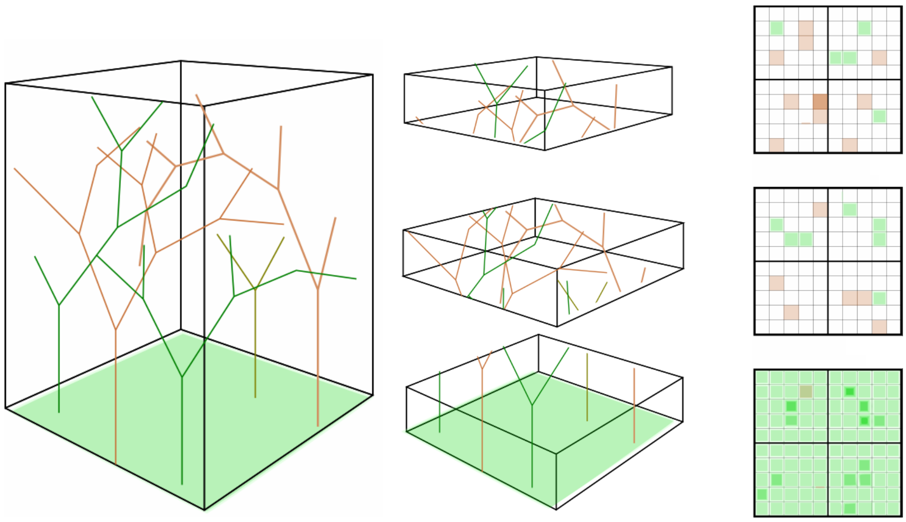

(a) Complete point cloud (b) Vertical slicing (c) Point density calculation

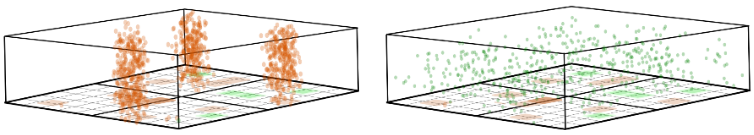

(d) Extracted vertical component (e) Extracted non-vertical component

Figure 4.5: Point cloud data processing work flow figures showing steps taken using Python scripts for automation. The processing follows sub-figures a - e: (a) initial point cloud; (b) slicing of point cloud into vertical height bands; (c) the creation of point density values for each 10 cm height band; (d, e) the extraction of the vertical and non-vertical component based on point density values.

The next stage of data processing was point density analysis to detect potential vertical components. Working on each height band separately, every point was assessed individually and the density of vertical points (referred to as point density) within a defined search area (described by a rectangular prism covering 2 cm x 2 cm in the horizontal and 10 cm in the vertical) calculated. With decimation being carried out at 1 cm^3 the horizontal distance of 2 cm allowed for a 1 cm search either side of the point. Each point return was then assigned its point density as a fourth attribute, with the final output being a text file with the format of the original file (x,y,z,pd). In this way height band point clouds could be visualised and coloured based on their vertical point density.

The assessment of scan returns based on point density was used as point density values can be indicative of vertical features when used in combination with small search areas and restricted height bands (see Figure 4.6). A stem which is vertical will provide point returns in each of the vertically adjacent voxels within the point cloud. Figure 4.6a shows this as five voxels containing stem returns. A stem growing off-vertical will provide returns in vertically adjacent voxels, depending on how close to the vertical it is growing. Figure 4.6b shows this as three voxels containing stem returns. A stem growing horizontally will provide few vertically adjacent voxels within the point cloud, depending on the diameter of the stem. Figure 4.6c shows this as a single voxel containing stem returns. The point density value can therefore be representative of the vertical structure within each search area.

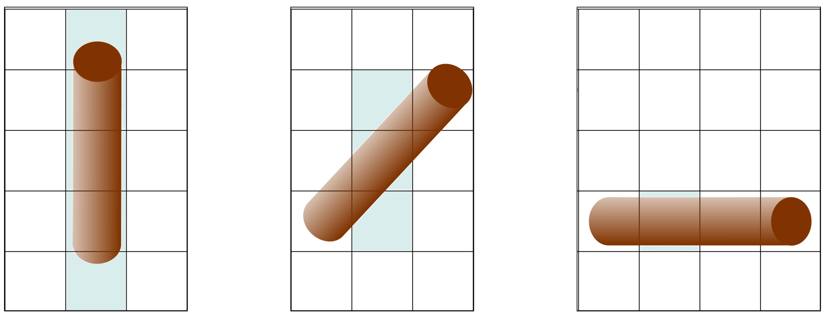

(a) vertical (b) 45° (c) horizontal

Figure 4.6: Showing examples of vertical alignment within voxel space. Shaded grid squares show voxels with point returns inside for: (a) vertical objects - shown as five filled voxels; (b) objects at 45° - shown as three filled voxels; and (c) horizontal objects - shown as one filled voxel.

The determination of the initial sub-classification of returns based on point density was an important step in the creation of a vertical to non-vertical index. If the cut-off point between vertical and non-vertical was too low, the result would show bias toward non-vertical classification. Too high and the bias would be toward vertical classification.

With the data processing parameters used here (of 10 cm in the vertical), a point density value of 10 would mean partners in all neighbouring vertical voxels and therefore a high likelihood of being a vertical component. In comparison, a point density value of 1 would mean it was isolated from the neighbouring vertical voxels and therefore had a high likelihood of being a non-vertical component. Figure 4.7 shows a forest point cloud with point returns coloured by their vertical point density value.

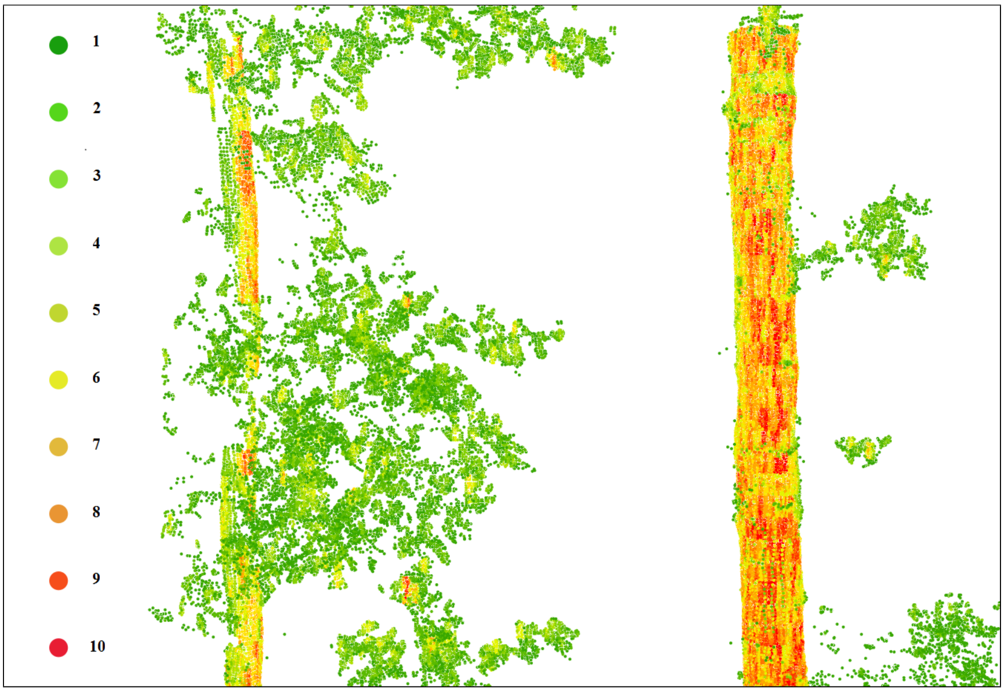

Figure 4.7: Forest point cloud coloured with point density values. the colour ramp goes from low point density (green) to high point density (red).

A selection of cut-off points were chosen and tested for their suitability across the three test data sets. After examining the resultant point clouds a cut-off point of 4.0 was chosen to be indicative of vertical structure. The selection of a cut-off point was a manual, iterative process whereby each of the three test sites were examined and the most appropriate value found through visual inspection. The cut-off point does not identify points that are confirmed as vertical structure. Instead, the cut-off should be seen as the most appropriate point density value from which vertical structural analysis can be performed. Some point returns from foliage material may be classified as vertical and vertical stem material may be classified as non-vertical. The overall classification cut-off was selected to best represent where foliage is classified as non-vertical and stem material as vertical. Figure 4.8 shows a side view section through the Ampfield Wood data set where the effect of different point density cut-off values can be seen.

Using the three trial sites, during work flow testing it was found that classification based solely on vertical point density produced a bias towards non-vertical material. This was especially apparent on the surfaces of stems where areas of low point returns (caused by shadowing) were incorrectly classified as non-vertical (less than four returns within a voxel column).

Knowing that vertical components are clustered (such as on the surface of a stem), it was proposed that by using cluster analysis on the initial vertical classification, the assignment of vertical attribute could be refined.

With all point returns classified as vertical or non-vertical through vertical point density analysis, the next stage of the analysis was to perform a kernel density estimation (KDE) for each height band. A KDE was used to estimate the spatial distribution of vertical component across each height band. The KDE was performed through ESRI Arcpy utilising the Spatial Analyst toolset. Using this process a k-density raster grid was created that described the density of the vertical component within each height band. The grid values within each raster held the relative density of the vertical component for each 1 cm^2 grid square. The values for each raster grid were then applied to the original point data set. Any points falling within a raster grid of greater than 750 (the fixed units of the software being events per m^2) were classified as vertical component (see Figure 4.9). The value of 750 was chosen through an iterative process of manual, visual inspection.

The KDE step worked by classifying point returns as vertical, based on the proximity of other vertical points, therefore helping to mitigate the occlusion effects caused by branches, stems and foliage which may cause point density values to fall below the cut-off point.

The next step in vertical and non-vertical analysis was the calculation of a vertical to non-vertical index (VNVI):

$$vnvi = \left(\frac{F_{count}}{T_{count}}\right) - \left(\frac{S_{count}}{T_{count}}\right) \tag{4.1}$$

where F_{count} is the count of non-vertical returns, S_{count} is the count of vertical returns and T_{count} is the total count of point returns. A value of -1 indicates complete vertical dominance, a value of $+1$ complete non-vertical dominance. A single stem growing in an open plot would be expected to give VNVI of near -1 (complete vertical dominance).

(a) Point density values greater than or equal to 1.

(b) Point density values greater than or equal to 2.

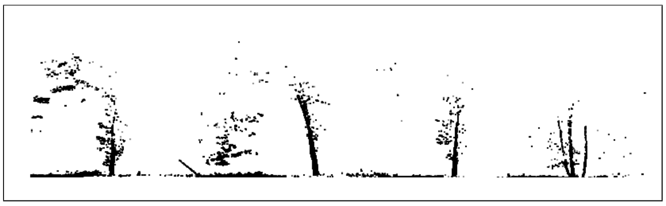

(c) Point density values greater than or equal to 4.

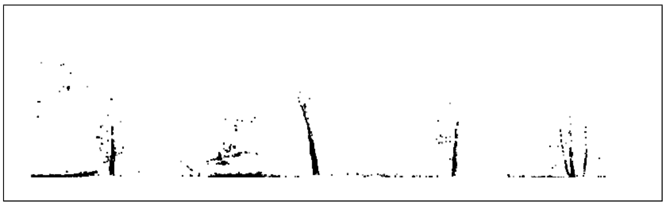

(d) Point density values greater than or equal to 6.

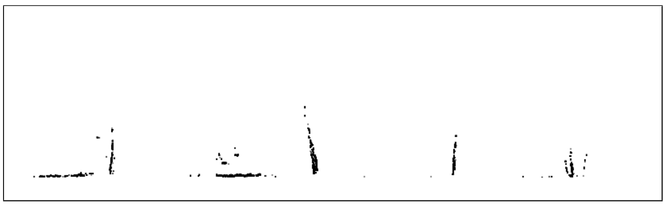

(e) Point density values greater than or equal to 8.

Figure 4.8: Ampfield Wood side view (30 m section showing full vertical profile), highlighting how different point density values can be used to isolate point returns based on vertical structure.

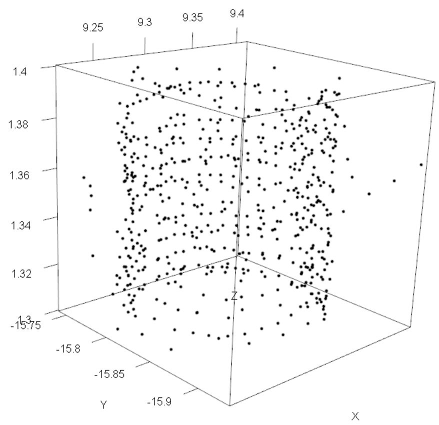

(a) All points describing the stem

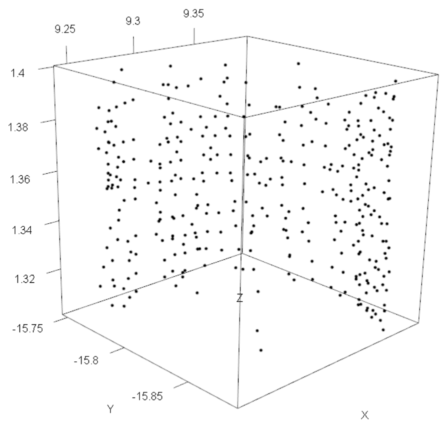

(b) Only points classified as vertical through point density analysis

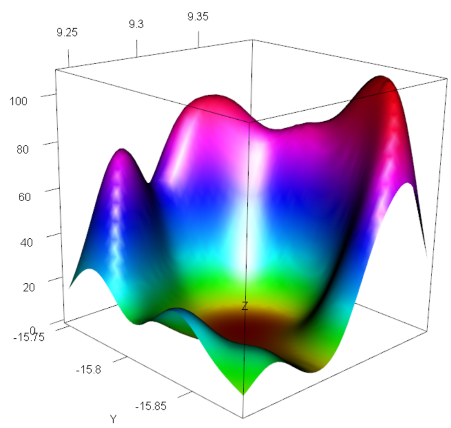

(c) K density surface created from vertical points

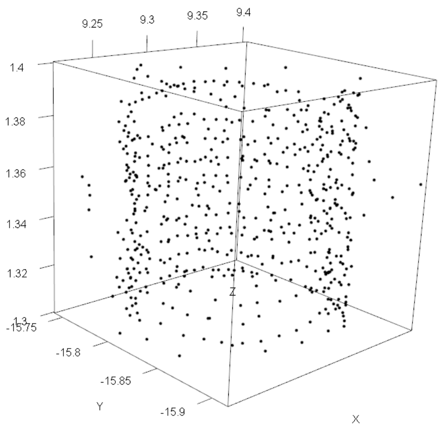

(d) All points classified as vertical through combined point density and kernel density analysis

Figure 4.9: Initial raw point cloud data (a) is used to create a point density value used for vertical classification, resulting in a point cloud containing only vertical points (b). This data is used to create a k-density surface (c) that describes the likely positioning of vertical component within a height band. This surface is used to assign a further vertical attribute based on a combined point density and k-density approach (d).

Although the VNVI describes the vertical component, spatial distribution of vertical component is also an important factor when examining forest structural properties in relation to further ecologcial attributes. Assessment of spatial distribution may also highlight plots where complicated structure may adversely affect the creation of the VNVI.

Two forests may provide similar values for the vertical component, but this does not mean they would have similar ecological attributes. A forest may exhibit vertical dominance through the presence of large, single, tree stems such as in a managed plantation forest. Whereas, a second forest may exhibit vertical dominance through the presence of multiple smaller stems growing in clusters such as in an Ash coppice forest (where stems are felled to allow multiple shoots to grow from the same stump). Both may show the same levels of vertical dominance, but it is the secondary values for spatial distribution of vertical component that would be indicative of the presence of coppice. An example of the expected relevance of spatial distribution can be seen in Figure 4.10.

(a) decreased cluster count. (b) increased cluster count due to coppice.

Figure 4.10: Spatial distribution within vertical component provides further information of stand structural attributes relevant to forest ecology. Both plots shown are expected to exhibit dominance of vertical component, with (a) decreased vertical cluster count and (b) exhibiting increased vertical cluster count due to presence of coppice.

The spatial distribution of point returns within each forest plot was assessed using the clustering of vertical returns. This was carried out using the following steps: (1) isolation of vertical point clusters; (2) calculation of cluster centroids; (3) calculation of cluster radii; and (4) neighbour analysis on clusters.

The isolation of vertical point clusters was performed using the point cloud library (PCL) (Aldoma et al., 2012). The Euclidean Cluster Extraction module was used to identify clusters within individual height bands from which clustered points were extracted. A cut-off point of 5 cm was used to define points within a cluster. The PCL module uses 3D clustering so it was felt that the 10 cm vertical thickness of each height band would not influence the effectiveness of the method as points would be analysed across both the horizontal and vertical. With clusters isolated, the centroid and radius of each cluster were determined. This was performed using the Standard Distance tool from the Spatial Statistics library of Arcpy.

Using the centroid coordinate from each cluster, distances between clusters were calculated using point distance processing. This was carried out using the Geospatial Modelling Environment (GME) (Beyer, 2012) which utilises R within a geospatial framework. From these analyses the mean distance between clusters of vertical component and the mean radius of these clusters could be determined for each height band.

A full work flow for the creation of a VNVI and cluster analysis can be seen in Figure 4.11.

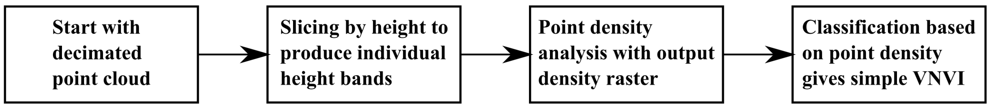

(a) Step 1: initial classification based on point density

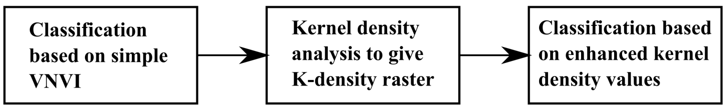

(b) Step 2: classification based on density analysis

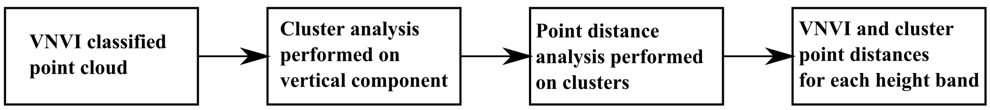

(c) Step 3: nearest neighbour analysis on clustered regions

Figure 4.11: Point cloud processing workflow diagram

To assess the likely affect of occlusion within the data set a voxel based assessment similar to Béland et al. (2014a) was used. In this method the data set was gridded using 10 cm^3 and 1 m^3 voxels (referred to as the target voxels) and two metrics were calculated for each height band: (1) percentage of target voxels within each height band that were occupied; and (2) the mean point returns per target voxel, within those voxels where returns were present. Using these metrics it was possible to assess how the penetration rate of the target voxels changed with height.

The 1 m^3 voxels allowed the general distribution of material within the site to be assessed and provided information on the extent of the area being surveyed. It would be unlikely that shadowing would block out all laser returns from a 1 m^3 volume so using the percentage of voxels with point returns inside was expected be indicative of the spatial extent of material within the site, regardless of shadowing. An example being how the lower levels of the understorey were expected to show high levels of 1 m^3 voxels with point returns, as this area was expected to contain increased material giving rise to point returns. The canopy would also be expected to show high levels of voxel penetration using 1 m^3 volumes, although this may be reduced if there were dense lower levels of foliage causing point occlusion within the upper parts of the canopy.

Mean point return counts within the 10 cm^3 voxels were used to assess occlusion on the distribution of point returns within height bands and provided information on how point return numbers changed with distance from the laser scanner. Only target voxels with returns inside were used, from which the mean point count within was determined. It was expected that the mean point return counts within voxels would be affected by forest structure with areas of forest containing stem objects expected to provide more returns than those ares of foliage (due to stems providing a surface where dense returns would be created). The mean return count within the 10 cm^3 target voxels was expected to decrease with distance from the scanner location due to increased shadowing caused by branches, stems and foliage. If no occlusion was present mean return count was expected to remain roughly constant within zones such as the understorey and canopy.

A voxel based estimation method (where point returns are counted inside a set target voxel) was chosen as this does not require entry and exit points (ray tracing) from voxels to scanner location for individual laser pulses. This reduces the computational requirements and time taken to perform analysis considerably. With 11 scanner locations and plot sites of 10 x 50 m it was felt that ray tracing for every point return would be too time-consuming to consider.

4.2.5 Analysis

Analysis was performed across the complete WoodMAD data set covering 40 survey sites.

The VNVI mean and standard deviation for each plot site were determined using the VNVI values from height bands 50-190 cm above ground surface (referred to as zone A) and for height bands 200-990 cm (referred to as zone B). Splitting the analysis into two distinct height bands allowed assessment of the technique when considering zones where deer browsing was expected to be present (zone A) and then further into the canopy (zone B). Data from 0 cm up to 40 cm were removed from analysis for this trial as it was expected to show increased levels of occlusion due to the presence of ground surface growth such as grass, ferns and bramble. The limit of zone A was set at 190 cm as the study was assessing the use of TLS for extraction of structural properties related to deer browsing. Deer browsing was not expected to influence foliage/stem ratios above 2 m.

The original survey data were collected at a resolution of 7.67 mm at 10 m. This represents a resolution of 10 mm at 13 m. As the data were decimated to 1 cm^3 allowing voxel unit assessment, any point returns collected at a distance of more than 13 m from the scanning instrument would show point spacing greater than the decimation level (therefore adjacent voxels would not be expected to contain returns). For this reason a maximum height of 10 m was used as a cut-off point in zone B to make sure all data comparisons using voxel spacing were compared against data sets where the point spacing was less than the voxel decimation.

Clustering estimations on vertical point returns were assessed using the mean and standard deviation of the nearest neighbour and the mean and standard deviation of the cluster diameter. Cluster counts and nearest neighbour distances were calculated across zones A and B.

Profiles generated from the number of points classified as vertical were also used as an independent test for the effectiveness of the method for extracting VNVI. As all forests contain vertical component the total count of point returns classified as vertical was not expected to change for high and low deer density sites. It was the proportion of vertical material within a forest (at different height bands) that was expected to change. An example being how two stems of the same size, one with foliage and one without, would be expected to provide the same number of points describing the vertical component (stem surface). The difference in the stems would only be apparent when considering the proportion of vertical to non-vertical material.

In addition to profiles using points classified as vertical, profiles using total return counts for different deer densities and management practices were also generated. It was expected that total point returns would be indicative of material present within a forest height band, but would not be useful when estimating the structural differences between high and low deer density sites as geometric properties are not taken into account. An example being how a coppice woodland with no foliage would be expected to provide a high point count due to the presence of multiple stems. A non-coppice forest with high levels of understorey vegetation and foliage would also be expected to provide a high number of point returns. It was expected therefore, that point count on its own would not provide a distinction between forests with different structural properties.

The total point return profiles acted as a further independent test that any differences showing in VNVI between high and low deer density sites were due to structural changes within the forests rather than raw point count differences.

All analysis schemes were assessed against the known characteristics for each site (deer density and management practice).

4.3 Results

All results are for analysis across the complete set of 40 woodland plot sites. Expanded results tables can be found in appendix C.1.

4.3.1 Vertical to non-vertical index

The VNVI extracted within zone A followed expectations that deer density would show a positive relationship with VNVI. Across all height bands within zone A the mean VNVI were lower for high deer density sites compared against low deer density sites (Figure 4.12). This is indicative of high deer density sites having a decrease in the amount of non-vertical component when compared against low deer density sites. Looking at the mean VNVI values the difference between mean VNVI values of high/low deer density sites was greatest at a height of 100 cm above the ground where the difference was approximately 0.6, or 30% of total VNVI.

There is a slight increase in the mean VNVI across height bands when considering managed plots against unmanaged plots, although the difference is not as clear as for high/low deer density, with the maximum difference between means across height bands being approximately 0.1, or 5% of total VNVI.

Of the forest sites analysed within zone A, 21 show a negative mean VNVI with 19 exhibiting positive mean values. The woodland sites exhibiting a negative mean VNVI comprised 16 high deer density sites and 5 low deer density sites. Those sites exhibiting a positive mean VNVI comprised 15 low deer density sites and 4 high deer density sites. These results show that high deer density sites are more likely to provide negative VNVI values compared with low deer density sites, representing a tendency toward vertical dominance within the 50 cm to

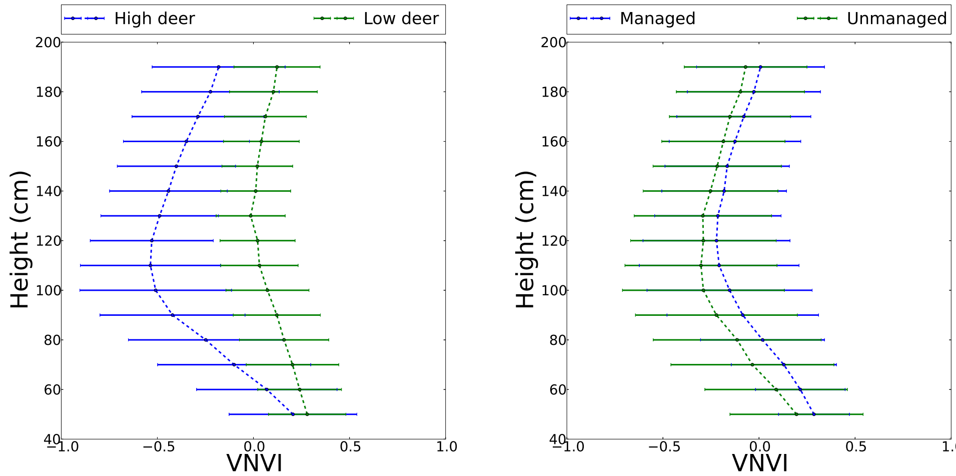

(a) deer density

(b) management

Figure 4.12: VNVI comparison for zone A showing mean and standard deviation of VNVI within height bands for high/low deer density and managed/unmanaged forest plots.

190 cm height band where deer densities are high.

Within zone B, 3 sites show a negative mean VNVI with 37 exhibiting positive mean values. The woodland sites exhibiting a negative mean VNVI comprised 2 high deer density sites and 1 low deer density sites. Those sites exhibiting a positive mean VNVI comprised 18 low deer density sites and 19 high deer density sites. These results show that from 200 cm up to 990 cm there is a tendency toward positive VNVI values, representative of dominance of non-vertical components, within both high and low deer density plots.

Overall VNVI results (min, max and mean) for high/low and manged/unmanaged sites are shown in Table 4.2. It was seen that deer density had a more pronounced affect on the VNVI values than management practice, with management practice causing no clear difference between the resultant VNVI values. This suggests that management practice may not be a contributor to changes within vertical structure.

Within zone A high/low deer sites showed a difference in the mean of VNVI of 0.395 and managed/unmanaged showed a difference in the mean of VNVI of 0.096. Within zone B high/low deer sites showed a difference in the mean of VNVI of 0.152 and managed/unmanaged showed a difference in the mean of VNVI of 0.003.

Full results for each plot site within zone A can be found in Tables 4.3 and 4.4, grouped by deer density. From this it was seen that Wyre NNR 01 showed

Table 4.2: Overall VNVI values across different deer density sites shows that high deer density sites produce decreased VNVI values (min/max/mean) compared to low deer density sites.

zone	deer/management	overall VNVI values		
		min	max	mean
A	high deer	-0.646	0.269	-0.296
	low deer	-0.065	0.347	0.099
	managed	-0.323	0.343	-0.053
	unmanaged	-0.391	0.270	-0.149
B	high deer	-0.191	0.703	0.371
	low deer	0.090	0.823	0.533
	managed	-0.002	0.745	0.450
	unmanaged	-0.103	0.783	0.453

the largest tendency toward vertical dominance with a mean VNVI of -0.73. Ffridd Mathrafal 02 showed the largest tendency toward non-vertical dominance with a mean VNVI of 0.32. The standard deviation of VNVI for individual plots showed that Wyre NNR 03 contained the highest variation of VNVI between vertical height bands (standard deviation of 0.62). In comparison, Ellenden Wood showed the lowest variation of VNVI between vertical height bands (standard deviation of 0.04).

Table 4.3: VNVI values for each plot site across high deer density sites within height band 50-190 cm.

plot	VNVI values				
	min	max	mean	std	variance
Ampfield03	-0.62	0.38	-0.23	0.29	0.086
Ampfield04	-0.83	0.52	-0.23	0.38	0.147
Bentley03	-0.72	0.38	-0.24	0.33	0.112
Bentley04	-0.85	0.08	-0.48	0.31	0.093
Blackmoor	-0.45	0.22	-0.09	0.22	0.050
Haughwood	-0.18	0.64	0.12	0.26	0.069
Hound01	-0.50	-0.02	-0.33	0.15	0.023
Hound03	-0.92	-0.27	-0.69	0.18	0.031
Hound05	-0.25	0.44	0.01	0.19	0.038
Kingswood01	-0.21	0.40	0.17	0.22	0.047
Kingswood10	-0.58	0.28	-0.06	0.31	0.098
Langley02	-0.66	-0.10	-0.40	0.20	0.042
Langley05	-0.69	-0.01	-0.41	0.20	0.041
LeaPagets03	-0.65	0.20	-0.31	0.27	0.074
Romers	-0.09	0.50	0.13	0.21	0.045
WyreMain01	-0.98	0.25	-0.70	0.40	0.158
WyreMain03	-0.90	0.35	-0.40	0.33	0.108
WyreMain04	-0.86	0.02	-0.51	0.33	0.112
WyreNNR01	-0.97	0.55	-0.73	0.43	0.186
WyreNNR03	-0.99	0.57	-0.54	0.62	0.387

The mean and standard deviation of VNVI within height bands across zone

Table 4.4: VNVI values for each plot site across low deer density sites within height band 50-190 cm.

plot	VNVI values				
	min	max	mean	std	variance
BigForest03	-0.18	0.43	0.08	0.17	0.028
BleanHomestall01	-0.28	0.26	-0.15	0.14	0.020
BleanHomestall04	-0.01	0.24	0.08	0.08	0.006
BleanHomestall06	-0.26	0.36	-0.06	0.17	0.028
EastBlean01	0.11	0.29	0.18	0.05	0.002
EastBlean03	-0.15	0.36	0.02	0.15	0.023
Eastridge01	0.10	0.46	0.26	0.11	0.012
Eastridge05	0.04	0.33	0.14	0.10	0.009
Ellenden	-0.54	-0.37	-0.44	0.04	0.002
FfriddMathrafal02	0.17	0.48	0.32	0.10	0.010
FfriddMathrafal04	0.09	0.56	0.31	0.17	0.027
GwernDdu01	-0.37	0.41	-0.05	0.29	0.083
GwernDdu04	0.10	0.51	0.25	0.13	0.016
PoleLees02	-0.06	0.52	0.24	0.22	0.047
PoleLees05	-0.03	0.57	0.23	0.22	0.046
SpoutFigyn	-0.16	0.32	-0.02	0.14	0.020
WestBlean01	0.07	0.39	0.18	0.09	0.007
WestBlean02	-0.00	0.31	0.12	0.10	0.010
WestBlean03	-0.05	0.23	0.10	0.08	0.007
WestBlean04	0.11	0.28	0.17	0.05	0.002

B are shown in Figure 4.13. Results for plot sites within zone B (minimum, maximum, mean and standard deviation of VNVI) can be found in Appendix C. For both deer density and management practice there is a increase of VNVI with height within zone B, indicative of a movement toward non-vertical dominance within the point cloud. High deer density sites show a reduction in the mean of VNVI when compared against low deer density sites, with the difference in VNVI remaining approximately 0.1 across zone B. No obvious difference can be observed between VNVI for managed/unmanaged sites within zone B.

The number of point returns classified as vertical for high/low deer density sites can be seen in Figure 4.14. It was seen that the mean was similar across all height bands within both zones of analysis.

Total return counts can be seen in Figure 4.15. It was seen that total return counts were similar with height across high/low deer density sites. This follows expectations that total return count may not be indicative of vertical structural change and that variations in VNVI are not caused by variations in total return count.

VNVI profiles for high/low deer density sites are shown in Figure 4.16. It was seen that high deer density plots show higher variations within VNVI than low

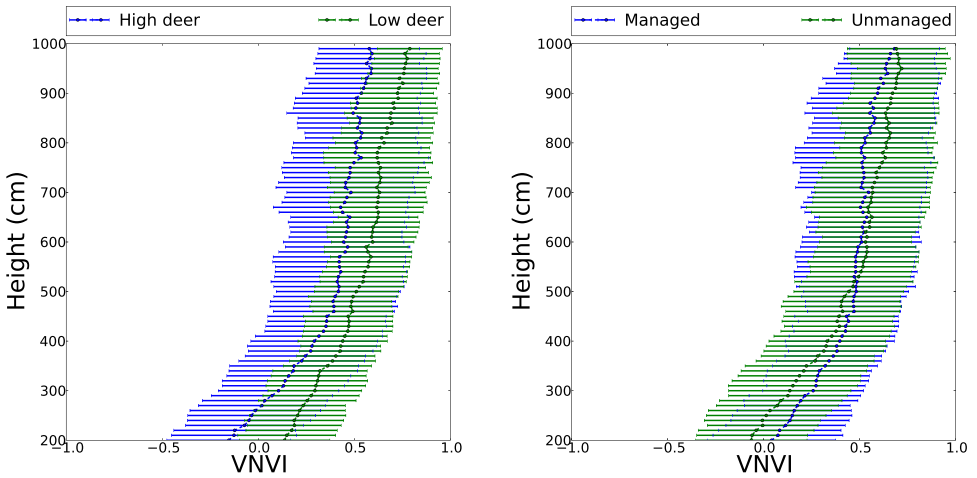

(a) deer density (b) management

Figure 4.13: VNVI comparison for 200 cm to 1000 cm above ground showing mean and standard deviation of VNVI within height bands for high/low deer density and managed/unmanaged forest plots.

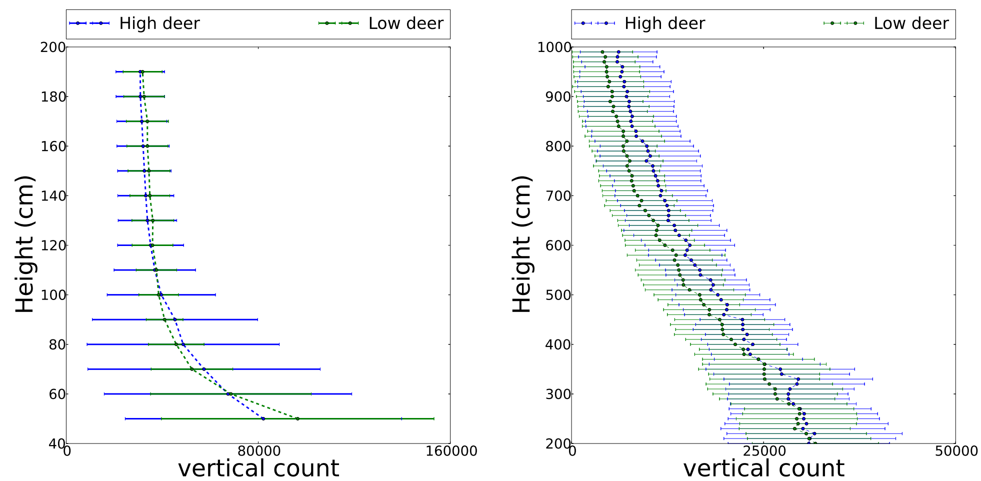

(a) zone A (b) zone B

Figure 4.14: Mean and standard deviation of the number of point returns classified as vertical across high and low deer density sites. Results are for zone A (a) and zone B (b). The mean vertical component count values are similar for both high and low deer density sites across both zones of analysis

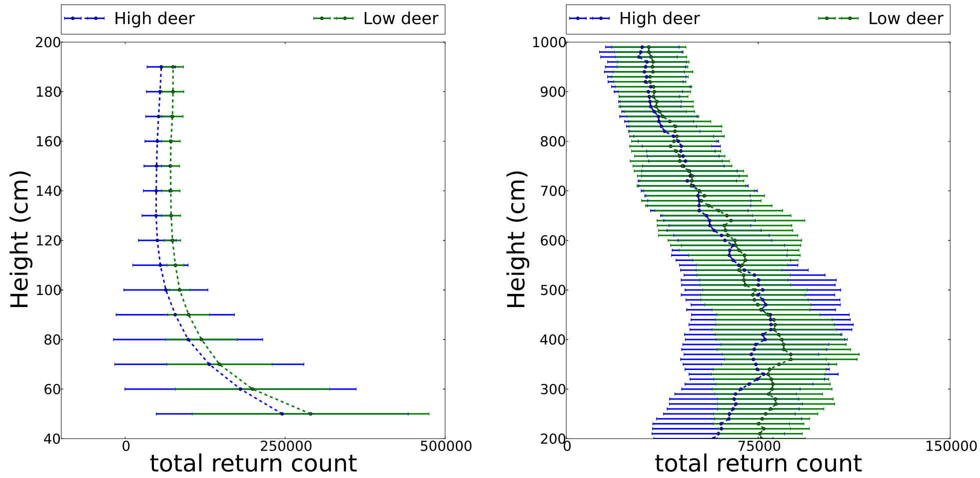

(a) zone A (b) zone B

Figure 4.15: Mean and standard deviation of total return count across high and low deer density sites for zone A (a) and zone B (b). The mean total return count values are similar for both high and low deer density sites.

deer density plots. This is visible in the VNVI profiles and also in the overall standard deviation of VNVI across zone A (Table 4.2). Overall standard deviations of VNVI for high/low deer density sites are 0.293 and 0.129 respectively. In comparison, the overall standard deviations of VNVI within managed/unmanaged plots are similar with values of 0.206 and 0.216 respectively. VNVI profiles for managed/unmanaged sites can be found in appendix C.1.

Results showing VNVI profiles for the simulated data sets can be seen in Figure 4.17. The raw data shows the true VNVI profile as determined through point types (foliage or stem) when building the simulation. The processed data shows the VNVI as extracted through the automated process. The results using simulated data show a tendency to underestimate VNVI which equates to a bias toward classification of vertical component. It was seen that even with this bias however, the automated process was successful in distinguishing between zones of vertical and non-vertical dominance.

4.3.2 Vertical clusters and nearest neighbour distance

Overall results for vertical cluster count across zones A and B can be seen in Table 4.5. Mean and standard deviation of vertical cluster count across height bands within zone A for high/low deer and unmanaged/managed sites can be seen in Figure 4.18.

The results for zone A show mean cluster counts of 62 and 97 for high and low

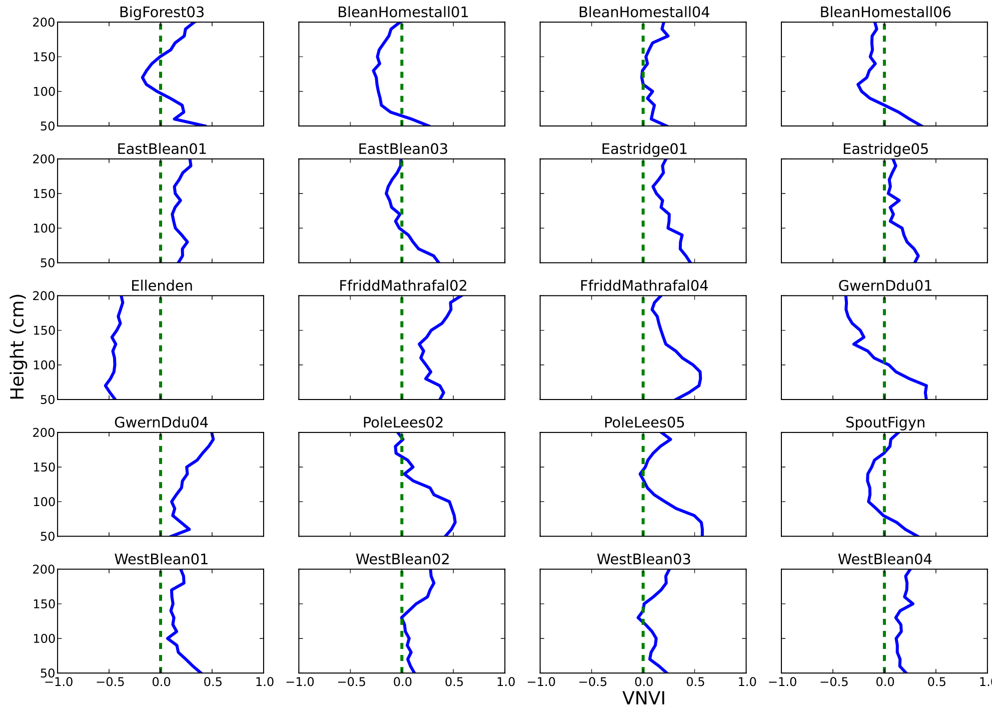

(a) high deer density

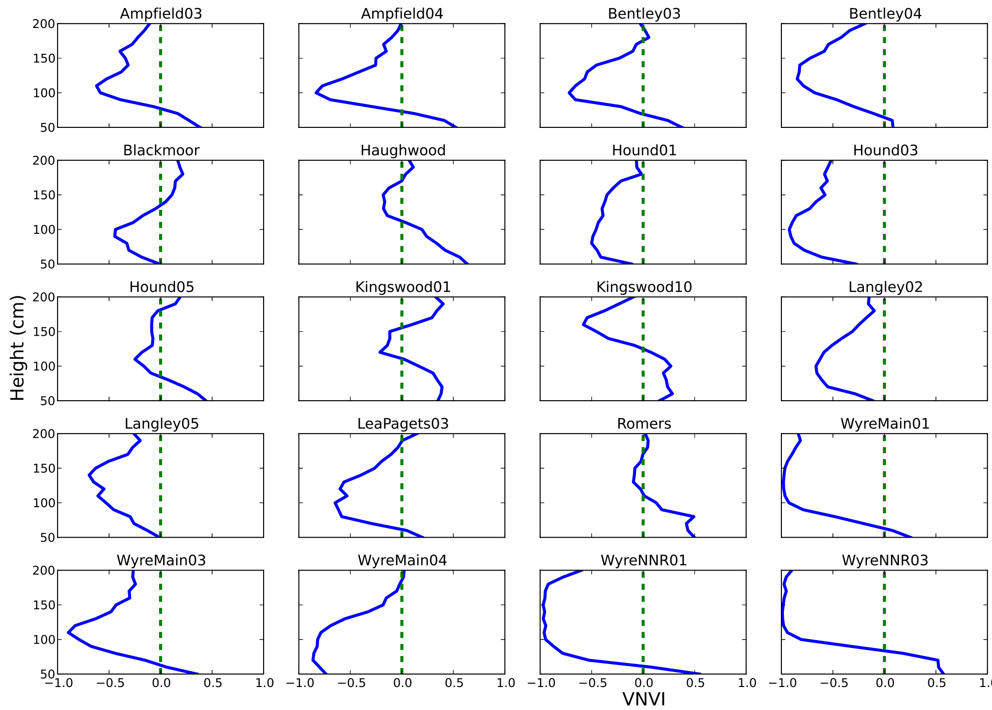

(b) low deer density

Figure 4.16: VNVI profiles across zone A with sub-figures divided into high (a) and low (b) deer density.

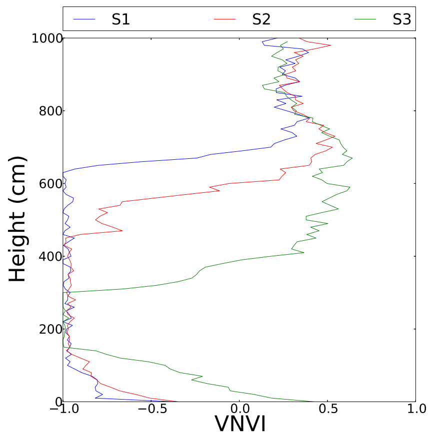

(a) Processed data

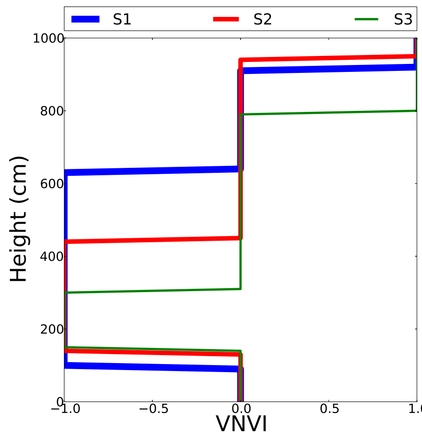

(b) Raw data

Figure 4.17: Simulated data sets (S1, S2, S3) with VNVI profiles as extracted from the automated process (a) and directly from the point attributes describing stem and foliage (b). The automated process successfully identifies change within vertical component, but does show a bias toward classification of vertical component in areas of understorey and canopy material.

deer density sites respectively, with a difference in the mean of approximately 30 seen across the vertical height bands (Figure 4.18a). Across zone B the cluster counts for high/low deer density sites reduces to 38 and 45 respectively. If clusters of vertical component are taken as surrogates for stems, this suggests a reduction in the number of stems seen within high deer density sites across both zones, with the largest reduction apparent within zone A.

The results for managed/unmanaged sites show less variation with the mean cluster count being 72 and 88 respectively across zone A. This reduces to 36 and 48 respectively for zone B.

Table 4.5: Overall values for vertical cluster count across all height bands in each zone, split into deer density and management practice.

zone	deer/management	overall cluster count values		
		min	max	mean
A	high deer	54	92	62
	low deer	84	118	97
	managed	59	105	72
	unmanaged	77	105	88
B	high deer	20	59	38
	low deer	20	87	45
	managed	19	59	36
	unmanaged	19	87	48

Overall results for nearest neighbour distances across zones A and B can be seen in Table 4.6. Mean and standard deviation of nearest neighbour distances across

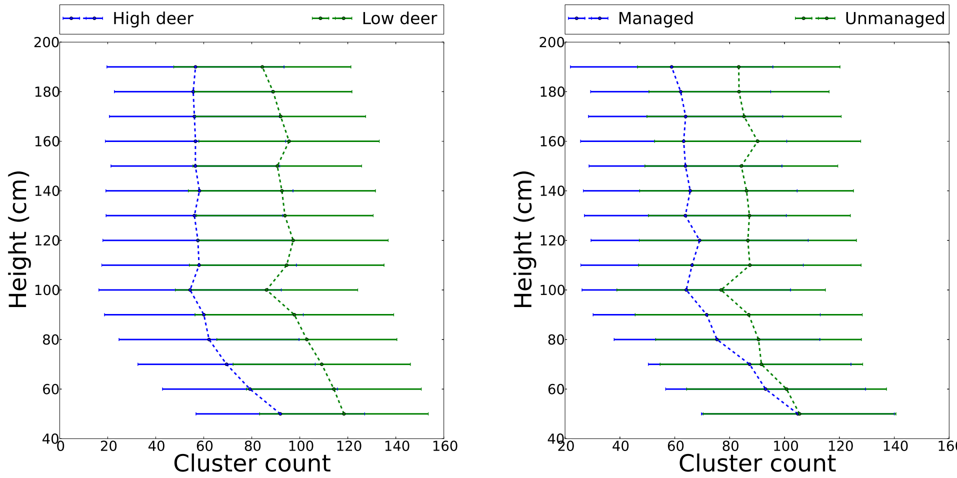

(a) deer density (b) management

Figure 4.18: Mean and standard deviations of vertical cluster count within height bands (zone A) for high/low deer density and managed/unmanaged forest plots.

height bands within zone A for high/low deer and unmanaged/managed sites can be seen in Figure 4.19.

The results for zone A show mean nearest neighbour distances of 1.60 m and 1.07 m for high and low deer density sites respectively, with a mean difference of approximately 0.5 m seen across the vertical height bands (Figure 4.19a). Across zone B the mean nearest neighbour distances for high/low deer density sites increase to 1.98 m and 1.96 m respectively. If mean nearest neighbour distances are taken as a surrogate for nearest distance between stems, then the results suggest stems are generally closer together in sites with low deer density. This is to be expected as the total number of vertical clusters increases in low deer density sites (Table 4.5), resulting in more stems per plot site with the consequence that the distance between clusters would be expected to decrease.

Table 4.6: Overall values for nearest neighbour distance across all height bands in each zone, split into deer density and management practice.

zone	deer/management	overall nearest neighbour distance (m)		
		min	max	mean
A	high deer	1.11	1.87	1.60
	low deer	0.94	1.18	1.07
	managed	1.02	1.53	1.37
	unmanaged	1.04	1.47	1.30
B	high deer	1.51	4.03	1.98
	low deer	1.16	5.41	1.96
	managed	1.41	5.06	2.10
	unmanaged	1.36	4.23	1.84

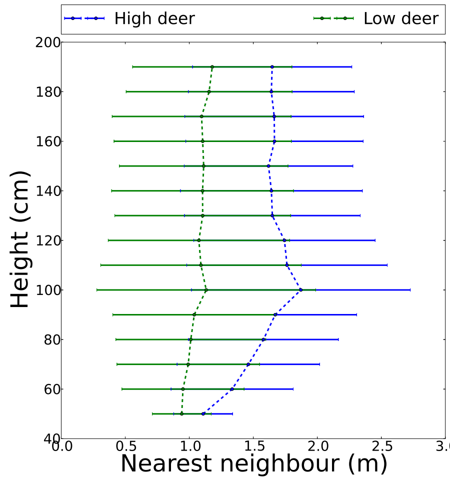

(a) deer density

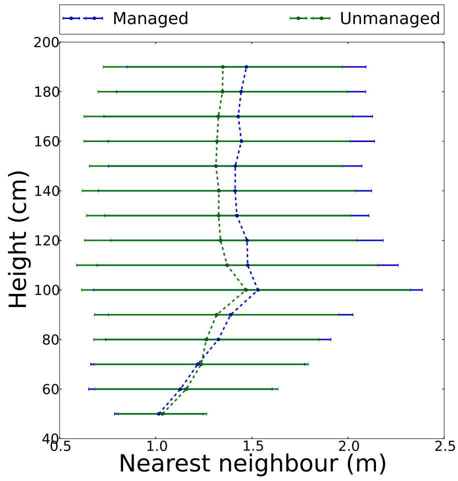

(b) management

Figure 4.19: Mean and standard deviations of nearest neighbour distance within height bands (zone A) for high/low deer density and managed/unmanaged forest plots.

The mean cluster count and nearest neighbour distance for individual plot sites (grouped into high/low deer density) can be seen in Table 4.7. From these results it was seen that the largest cluster count was at Ellenden Wood (188) and the lowest cluster count was at Wyre NNR 01 (23). The largest distance to nearest neighbour was seen at Bentley 03 (2.82 m) and the shortest distance to nearest neighbour at Ellenden Wood (0.68 m)

Height profiles showing the results for vertical cluster count and nearest neighbour distance from the simulated data sets can be seen in Figure 4.20. The results show that the automated extraction method successfully identified the individual stems from each of the simulated data sets as individual clusters within the understorey layers. This corresponded to 3 stems in simulation one, 11 stems in simulation two and 48 stems in simulation three. Where the canopy started the cluster count increased and did not match the actual number of stems. This was due to canopy material being incorrectly classified as vertical component and therefore leading to an increase in the subsequent cluster count.

The automated method also successfully extracted nearest neighbour distances, with distance to nearest neighbour remaining relatively constant up to the lower canopy. A stepped decrease in mean nearest neighbour distance of approximately 75 cm was seen in simulation two at a height of approximately 1 m. Within the canopy nearest neighbour distances fell across all three simulated data sets, this corresponds to the increase in cluster count seen and is a consequence of dense canopy material being incorrectly classified as vertical component.

Table 4.7: Mean vertical cluster count and mean nearest neighbour distance for each plot calculated across all height bands within zone A, presented grouped into high/low deer density sites.

high deer density			low deer density		
plot	mean cluster count	mean nearest neighbour distance (m)	plot	mean cluster count	mean nearest neighbour distance (m)
Ampfield03	48	1.62	BigForest03	105	1.02
Ampfield04	36	2.08	BleanHomestall01	132	0.92
Bentley03	28	2.82	BleanHomestall04	111	0.98
Bentley04	32	2.12	BleanHomestall06	97	0.95
Blackmoor	57	1.15	EastBlean01	122	0.80
Haughwood	46	1.30	EastBlean03	121	1.08
Hound01	150	0.81	Eastridge01	90	1.15
Hound03	37	2.17	Eastridge05	97	1.09
Hound05	48	1.38	Ellenden	188	0.68
Kingswood01	47	1.60	FfriddMathrafal02	92	1.02
Kingswood10	105	1.06	FfriddMathrafal04	66	1.35
Langley02	63	1.19	GwernDdu01	62	1.35
Langley05	89	1.25	GwernDdu04	92	1.02
LeaPagets03	76	1.04	PoleLees02	49	1.55
Romers	107	0.94	PoleLees05	77	1.09
WyreMain01	43	2.18	SpoutFigyn	72	1.31
WyreMain03	39	1.31	WestBlean01	70	1.21
WyreMain04	123	1.08	WestBlean02	108	0.96
WyreNNR01	23	2.45	WestBlean03	101	0.97
WyreNNR03	42	2.54	WestBlean04	93	0.98

4.3.3 Point occlusion

Results for the assessment of the effects of occlusion with height can be seen in Figures 4.21 and 4.22.

Using the 1 m^3 voxels the results from the simulated data sets (Figure 4.21a) show 100% voxel occupancy at ground level (this is expected as the ground should provide 100% coverage) with a drop to between 5 and 18% occupancy at 1 to 2 m above the ground. This represents the understorey zone where only stem material is present. Where the canopy begins in each simulation, the voxel occupancy increases in response to foliage material present.

In comparison, the data from high/low deer density sites (Figure 4.21b) show voxel occupancy of approximately 80% at ground level. This then drops to between 10 and 25% occupancy at 1 m above the ground before rising again to between 20 and 30% occupancy at a height of 4 m. For both high and low deer desnity sites the maximum voxel occupancy (not including ground level) is seen

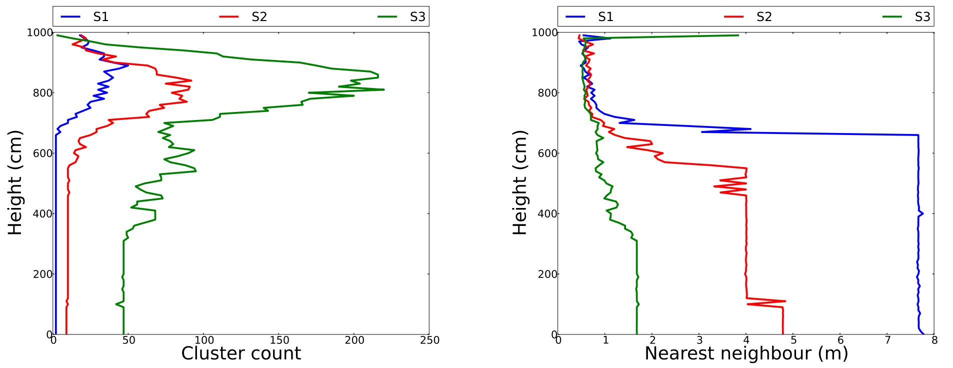

(a) Vertical cluster count (b) Vertical clusters nearest neighbour

Figure 4.20: Simulated data sets show how vertical component cluster count and nearest neighbour assessment can be used to extract forest spatial attributes, beneath the canopy. Simulation 1 (S1) comprised three large stems approximately 8 m apart with very low understorey vegetation. Simulation 2 (S2) comprised 11 mixed diameter stems approximately 4 m apart with low understorey vegetation. Simulation 3 (S3) comprised 48 densely packed, small diameter stems with increased levels of understorey vegetation.

at 4 m above the ground. From 4 m upwards voxel occupancy drops.

These results show a similar distribution of voxel occupancy for the simulated and surveyed data sets, up to a height of approximately 4 m. Above this height the simulated data sets show an increase in voxel occupancy up into the canopy. In contrast the surveyed data sets show a decrease in voxel occupancy, even though it would be expected that material volumes would actually be increasing due to the presence of increased branches and foliage within the canopy.

With the 10 cm^3 voxel analysis the simulated data sets show a relationship between mean point returns per target voxel and vegetation layer (Figure 4.22a). Here it was seen that ground level layers with stems and random points provide a low mean point return per voxel. In the height bands where only stems are present, the mean point return per voxel increases, indicative of the high density of points describing the surface of each stem. Where the canopy begins, mean point returns per voxel falls due to an increase in the number of voxels with foliage point returns and a less dense distribution of points. This follows expectations that with no shadowing within a point cloud, the density of returns within a voxel will be related to the components present within the forest.

The surveyed data sets (Figure 4.22b) from high deer sites show an increase in mean point returns per voxel at a height of approximately 1 m above the ground, this is similar to the increase observed in the simulated data sets when ground level growth gave way to height bands with only stem material. At 2 m above the ground both high and low deer density sites show a steady decrease in mean point returns per voxel from approximately 30% at 2 m to approximately 25% at 10 m, with very little variation observed.

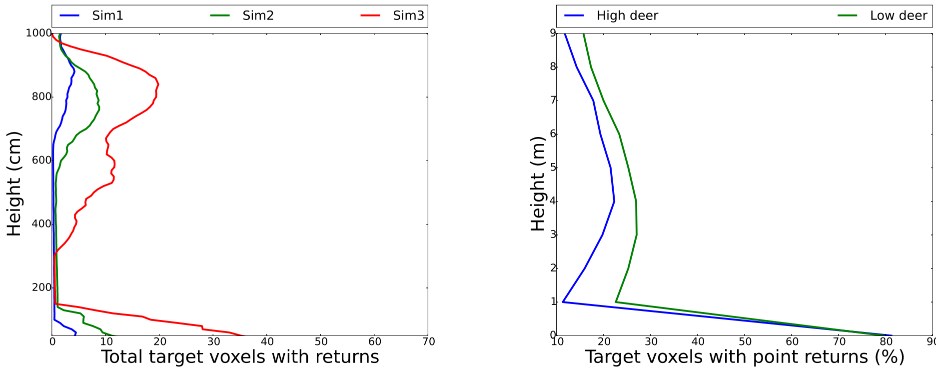

(a) Simulated data sets (b) High and low deer density sites

Figure 4.21: The area within each height band with 1 m^3 voxels providing point returns offers an assessment of occlusion levels within the data set. The simulated data (a) show 100% coverage at ground level and then peaks again within the canopy. The high/low deer density sites show 80 % coverage at ground level, but voxel penetration rates then peak at 4 m above the ground, with penetration rates falling into the canopy.

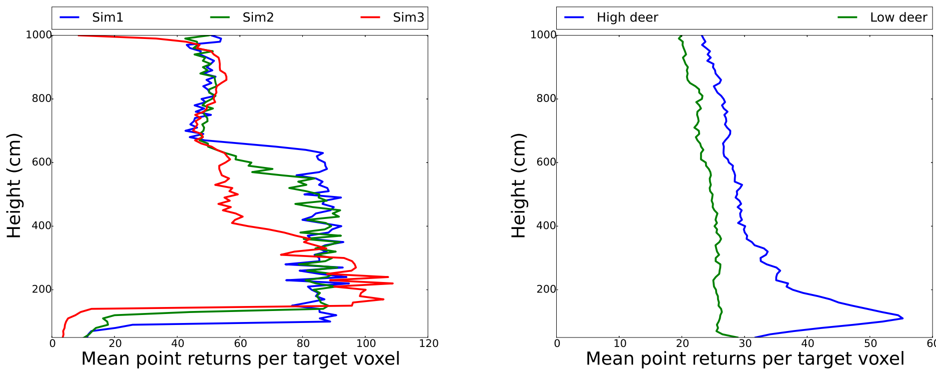

(a) Simulated data sets (b) High and low deer density sites

Figure 4.22: The mean count within each 10 cm^3 voxel containing a return provides information on the distribution of returns within height bands.

4.4 Discussion

4.4.1 Can TLS be used to extract the vertical components of the understorey layers of forests effectively, with minimal manual processing, from large data sets?

Using the methods developed for VNVI extraction, TLS was used to successfully extract the vertical components of forest plots. The method presented here required minimal manual data processing and was applied to large data sets.

Differences in vertical to non-vertical index extracted through TLS were seen within results grouped by deer density. Where deer browsing levels were high, non-vertical material was reduced and where deer browsing was low, non-vertical material was increased in the understorey. The results also show that vertical component and total point returns remain similar regardless of deer density. This suggests that the presence of deer in forests results in a reduction in the amount of non-vertical material, rather than an increase in the total amount of vertical material. If vertical and non-vertical components are taken as surrogates for stem and foliage material, the results follow expectations, and previous studies i.e. White (2012), that deer browsing can lead to reduced understorey growth in forests.

Using this method allowed for identification of patterns within the vertical structure of forests related to deer browsing for 10 cm height bands. The differences in VNVI between high and low deer density sites were most evident from approximately 60 cm to 160 cm above the ground. This offers an improvement over existing studies examining deer browsing by allowing the effects of deer browsing to be assessed to 10 cm (an example being how the largest difference in VNVI between high/low deer density plots was found to be at 100 cm). Boulanger et al. (2015) used four vegetation height bands (up to 50 cm, shrubs 50 cm to 2 m, shrubs over 2 m and trees) to assess the effects of deer browsing meaning change could only be assessed between these layers, not within them. Rooney and Waller (2003) used a single height band of 30-200 cm and counted numbers of sugar maple twigs within this layer to assess the effect of browsing. Again, this method only provided information on a single height band 170 cm deep. These methods are proven and understandable, as surveying stems in 10 cm height bands using traditional methods would be very time-consuming, but it does highlight the additional analysis benefits that using TLS combined with extraction of VNVI can bring to a forest survey.

Although VNVI is not a direct indicator of deer presence (multiple processes can lead to the same structural properties), the results support the use of TLS derived point clouds for the extraction of forest structural properties for use in forest ecology studies. This trial has highlighted the possible use of VNVI to detect structural differences in forest plots related to vertical component.

With the TLS derived point clouds from the WoodMAD project showing a link between VNVI and deer browsing levels, it is suggested that VNVI may provide information on additional habitat-animal associations, such as how fine scale structural changes (such as those seen across 10 cm height bands) may affect the availability of food or shelter within distinct vertical layers of a forest. This would allow analysis of forest plots beyond that currently undertaken during traditional forest ecology surveys.

An example is how the variation of VNVI within vertical height bands between 0.5 m and 2.0 m may be indicative of the homogeneity of vertical structure. Those plots where the standard deviation of VNVI is low would suggest that relative levels of stem and foliage remain similar with height. Alternatively, a high value for standard deviation of VNVI may identify plots where foliage and stem levels vary within the vertical layers, indicative of structural heterogeneity. This has the potential to offer a novel approach to forest surveying through allowing the structural attributes (and therefore heterogeneity) of a forest plot to be assessed in 10 cm layers. This provides improvements over existing methods for the estimation of heterogeneity where it is common to use just 4 strata (<1 m, 1-3 m, 3-10 m, 10-20 m and ≥ 20 m) from which heterogeneity of vertical component is assessed, e.g. Larrieu et al. (2015).

The relationship between standard deviation of VNVI and vertical structure can be seen in the results for Ellenden and Wyre NNR 03, where the standard deviation of VNVI within zone A was 0.04 and 0.62 respectively. This difference in standard deviation suggests sites where the heterogeneity of vertical structure is different. Looking at Figure 4.23 this can be seen in the plot photographs where Wyre NNR 03 contains an increased amount of lower level growth compared to Ellended wood, causing an increase in the standard deviation across the vertical height bands. This difference is also seen in the VNVI profiles for zone A (Figure 4.16), where Wyre NNR 03 shows a very large decrease in VNVI from approximately 75 cm to 100 cm. In comparison the Ellenden profile shows a near constant VNVI value from 50 cm up to 200 cm.

This interpretation of point cloud derived structural parameters has the potential to be used to improve the understanding of relationships between forest

(a) Ellenden Wood (b) Wyre NNR 03

Figure 4.23: Showing plots where the mean of VNVI and variance of VNVI are (a) -0.44 and 0.00 - indicating dominance of vertical structure that is homogeneous within the vertical and (b) -0.54 and 0.39 indicating dominance of vertical structure but variation within the vertical layers

structural attributes and ecosystem functions. Using the previous example, the VNVI method highlighted a sudden structural change between 75 cm and 100 cm within Wyre NNR 03. This identified a 25 cm layer where vertical structural change occurred, i.e. the transition from height bands containing both understorey vegetation and stems, to height bands where only stem material was present. This structural change may indicate a zone of change where the ability of animals to forage or shelter is altered.

Latifi et al. (2015) examined the use of ALS for estimating canopy and understorey density within vertical layers, but found that results were dependent on forest type as forests with thick canopies blocked returns from the understorey. Using a TLS based method to estimate understorey components allows for detailed point return information to be collected beneath the canopy, reducing the effect of shadowing (compared to aerial systems) when examining understorey vegetation.

In addition to the ability of the VNVI method to determine the dominance of either vertical or non-vertical material, using cluster extraction of vertical components allows for the assessment of the horizontal density of vertical component through extraction of vertical cluster counts and nearest neighbour distances. Using Ellenden and Wyre NNR 3 as examples (Figure 4.23), the mean cluster counts are 188 and 42 and the mean nearest neighbour distances are 0.68 m and 2.54 m, respectively. Looking at the combined results for plot sites (VNVI, cluster count, nearest neighbour distance) allows for a thorough assessment of how the vertical and non-vertical components of forests combine to create unique habitats. From the results of the VNVI method the vertical properties for each woodland describe its spatial relationships beyond those commonly collected in traditional forest ecology surveys.

An advantage of the VNVI analysis technique over point cloud extraction methods requiring detailed 3D processing (Liang et al. (2016) lists these techniques and notes they are challenging to perform due to complicated modelling requirements), is through its ability to provide a near-automated approach to point cloud assessment. This allowed it to be successfully applied to the 40 Wood-MAD sites without the need for time-consuming manual editing of data. This novel approach to TLS forest data analysis is an effective method of forest structural extraction that can be used to process large-scale point clouds comprised of hundreds of millions of point returns.

4.4.2 To what extent does point occlusion affect the extraction of vertical component?

Occlusion effects within the point cloud data sets were highlighted in patterns seen in the voxel occupancy and the mean point returns per target voxel. Although point returns within the 1 m^3 target voxel were recorded up to a height of 10 m, the height band showing the maximmum number of voxels with returns was 4 m (not including ground level). With no occlusion effects present it would be expected that point return numbers would increase in the canopy due to an increase in branch and foliage material (the canopy being the forest layer containing the most material). This is represented simplistically in the simulation data sets where the maximum number of voxels with returns was seen in the canopy.

These results support the conclusions drawn by Béland et al. (2014a), that although laser hits are returned from the canopy layer when using ground based laser scanning, occlusion plays a significant role in restricting data collection. With the maximum voxel returns being identified at a height of 4 m above ground, all data above this level must be considered to contain increased levels of occlusion.

Occlusion is important when considering the application of a VNVI method for forest ecology as increased shadowing within a point cloud reduces the number of point returns. This can be seen in the results for total return count (Figure 4.15) where total point return count falls above 4 m, even though it would be expected to increase due to more material within the canopy. This reduction in point returns above 4 m means that there will be less likelihood of finding

4 point returns within vertical columns in each height band (the cut-off point used during analysis). A reduction in vertical alignment will then result in a bias towards classification as non-vertical material. This can be seen in Figure 4.13 where VNVI moves towards non-vertical dominance throughout zone B.

Vertical material would be expected to decrease within the canopy as stems give way to branches and foliage in the upper layers, but as the point returns are also reduced it is difficult to trust the VNVI values at increased height.

In order to mitigate occlusion effects the VNVI method should only be used for selected height bands. The appropriate height bands will vary with forest structural properties, but for this trial height bands below 4 m showed reduced occlusion effects across all 40 sites and therefore VNVI was considered to be reliable below this height. As occlusion rates will change depending on forest type, the application of VNVI will vary with forest type.

Using the developed VNVI method offers a new approach to examining forest structure through the extraction of vertical and non-vertical component for distinct height bands. The total amount of vegetation and its density is also of critical importance when considering forest and it is the analysis of vertical density through use of TLS data collection that will be examined in the following chapter.

Chapter 5

The estimation of vertical density within the herbaceous layer through terrestrial laser scanning

5.1 Introduction

Understanding the lower layers of forests is critical when considering forest ecosystems as it is an important feature affecting regeneration, nutrient cycling and biodiversity (Simonson et al., 2014). Waterman et al. (1995) refers to these lower layers as the herbaceous layer and understorey, but they are also known as the regeneration layer. These layers are also a critical habitat for multiple animals including birds and mammals (Holmes and Sherry, 2001; Litvaitis, 2001; MacFaden and Capen, 2002). The estimation of vegetation density within the herbaceous layer across woodland sites, therefore, has the potential to improve our understanding of how understorey components influence forest processes and functions (Nilsson and Wardle, 2005). Gonzalez et al. (2013) identified a lack of research covering understorey vegetation, with the suggestion that productivity within the understorey could be comparable to that of trees.

The two main components of understorey are the vertical and horizontal distributions of vegetation (Nudds, 1977). Traditional methods for the estimation of understorey vegetation include the sward stick and rising plate to measure sward height (Murphy et al., 1995; Stewart et al., 2001), cover boards to measure vertical structure (Nudds, 1977) and quadrats to measure ground vegetation (Sakai and Ohsawa, 1994). The sward stick and cover board methods are quick and easy to complete and can be used as input into biomass estimations across woodland sites (West, 2009). The quadrat method can provide detailed information on understorey vegetation. Bonham (2013) provides a detailed description of the different methods for the measurement of terrestrial vegetation.

Aerial laser scanning (ALS) has been used in multiple studies to assess various components of forest understorey. These include applications of ALS for forest fuels assessment (Gajardo et al., 2014), predicting the occurrence of understorey plant species relevant to bear forage (Nijland et al., 2014) and estimating understorey vegetation through variations in leaf area density profiles (Bouvier et al., 2015). White et al. (2012) used remote sensing data to detect changes in the forest floor habitat after severe ice storms in northeast North America damaged the canopy of up to 12% of the trees in Southern Quebec. These studies show the effectiveness of the method for large scale regional surveys, but the resolution of the results obtained through ALS are at the landscape to regional scale, rather than the micro (single tree) or macro (stand) habitat scales. For this reason it is limited in its usefulness for detailed analysis at local geospatial scales. In addition, the accuracy of results can be reduced by dense canopy (Singh et al., 2015) meaning that ALS may not be suitable for all forest types.

Although terrestrial laser scanning (TLS) allows for more detailed analysis at micro/macro scales than ALS, the trials of TLS for the analysis of understorey vegetation have so far been limited. Ashcroft et al. (2014) created forest density profiles (primarily aimed at the canopy) from TLS data that showed TLS provided less variation in estimates compared to observer results. The Ashcroft et al. (2014) trial used 25 cm bins for analysing point return data. Using this resolution it was found that the method could not be used accurately near the ground or in areas where the ground surface was uneven, as it was not possible to reliably distinguish the ground surface in these areas. It was concluded that TLS has the potential to improve existing studies through producing results with less subjectivity than where users directly estimate cover.

Multiple ecological studies have shown the importance of examining fine-scale structure for the assessment of forest communities (Pearman, 2002; Burton et al., 2011; Burton et al., 2014) with factors regulating species diversity operating at different spatial scales (Reich et al., 2012; Schertzer et al., 2015). The measurement and analysis of micro-scale structural properties across understorey and ground-level vegetation is therefore an important goal for ecological studies. It is here that TLS offers the potential for novel measurements currently unavailable using traditional survey methods.

In addition to the vertical structural properties of forests, the horizontal changes in structural characteristics within forest plots (known as horizontal heterogeneity) are a fundamental measure recorded during ecological surveys. Franklin and Van Pelt (2004) provides a description of horizontal heterogeneity and how it is linked to the successional stages of forests. Here it was shown that old growth forests are characterised by heterogeneity within the spatial distribution of structures, with the irregular horizontal distribution of layers being an important dimension of spatial complexity within old growth forests. In comparison, young stands show a uniformity (homogeneity) within the horizontal spatial distribution of structures.

The aim of this study was to address the questions: (1) Can TLS be used for the estimation of the vertical distribution of herbaceous layer vegetation? and (2) can heterogeneity of the horizontal distribution of vegetation layers within plot sites be assessed using TLS.

It was expected that high deer density sites would show a horizontal and vertical homogeneity in the spatial distribution of objects due to less material being present in the understorey. Conversely, low deer density sites were expected to show a more complex structure resulting in vertical and horizontal heterogeneity of understorey objects.

5.2 Methods

Studies have shown that the presence of deer fundamentally affects the communities of understorey vegetation (Suzuki et al., 2013). Using TLS data collected during the WoodMAD trials, vertical density profiles created from TLS data were tested against known deer densities (see Chapter 3 for details of the WoodMAD project). Using multiple understorey density profiles at each plot site the vertical and horizontal heterogeneity of material was then assessed.

The final output from a TLS survey is a point cloud describing laser hits (referred to as point returns) within the survey area. Seidel et al. (2011a) present a method for the non-destructive estimation of tree biomass where the relationship between dry weight of the tree (obtained through a harvest approach) and the total number of point returns was established. In this way point return numbers were directly linked to biomass. Using a similar approach, in this study the amount of material within the understorey (density profile) was estimated from the number of point returns collected by the laser scanning instrument.

5.2.1 Site description and data collection

All data were collected as part of the WoodMAD project examining the effect of deer browsing on woodland bird habitats. Full details of the sites can be found in Chapter 3 and Appendix A.

All TLS data were collected in June 2012 using a FARO Focus 3D TLS instrument.

5.2.2 Data preparation

All laser scan data were registered, filtered and decimated using voxel based extraction to a level of 1 cm^3, see Chapter 3 for full details.

5.2.3 Development of an understorey density profile

To evaluate the use of TLS for the assessment of understorey vegetation density within woodland plots, an understorey density profile was generated from point cloud data sets at each forest site. Through the creation of a density profile, assessments and comparisons could be made across different woodland types. A graphical overview of the method can be seen in Figure 5.1.

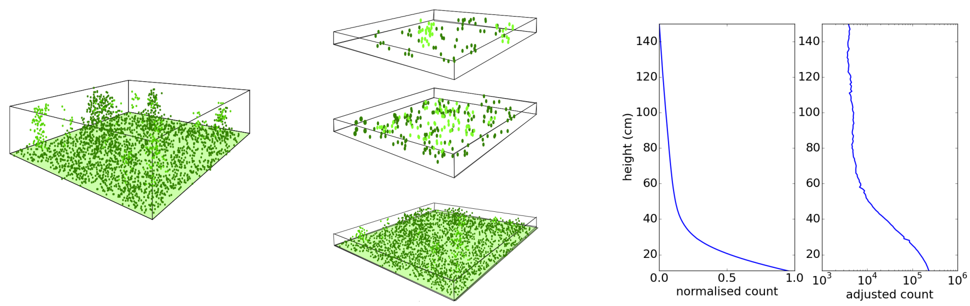

(a) all data (b) slice extraction. (c) normalised and adjusted profiles.

Figure 5.1: Graphical work flow outlining the main steps in the creation of an understorey density profile from forest point cloud data set: (a) Point cloud data from ground to 1.5 m including total point count; (b) slicing of the point cloud in 1 cm height bands; and (C) normalising of point count by dividing each height band count with the total point count for 10-150 cm before calculation of adjusted point count.

With the expectation that vegetation would increase close to the ground due to low level growth such as grasses, brambles and saplings, occlusion was expected to limit the usefulness of a direct point return count to determine the density of objects (vegetation) towards the ground surface.

Occlusion errors close to the ground within point clouds were mitigated through a process based on the MacArthur-Horn transformation (MacArthur and Horn, 1969). Building on the work of Lefsky et al. (1999), Harding et al. (2001) adjusted the MacArthur-Horn transformation and described a method that can be used to derive a canopy height profile from airborne laser altimeter data. Understorey analysis methods using TLS have also used this profiling technique for estimating vegetation metrics that focus on the canopy (Sumida et al., 2009; McMahon et al., 2015). Palace et al. (2015) showed that the transformation is equivalent to:

$$PAI(h) = -ln(1 - cover(h)) \tag{5.1}$$

where $cover(h)$ is the fraction of ground that is obscured by vegetation below height, h, and $PAI(h)$ is the plant area index above h. These outputs are given as area per unit ground surface area.

For the creation of a density profile a single point return was taken as a 'filled' 1 cm^3 voxel representing an object within the understorey. The number of objects within a height band was then used to assess vegetation density.

Data were used from 10 cm up to a height of 1.5 m above the ground as this covers the limit of the herbaceous layer (Gilliam, 2014) and 1.5 m is also close to the approximate height of the scanner, so where occlusion was expected to be at a minimum. Point return data from below 10 cm were excluded to avoid any errors within the creation of the DTM that might mean that in certain areas (such as where topography was complicated) the ground surface itself was contributing to the point return count.

In previous uses of the MacArthur-Horn transformation to estimate plant area index, the transformation is applied to correct for occlusion within the canopy brought about by dense understorey, this can be thought of as an upward facing correction that is used to estimate the area behind objects causing occlusion. Using data from scanner height to ground to examine the density of understorey vegetation uses the same principle (i.e. that dense vegetation will cause occlusion to occur behind objects), but for a downward facing correction. Also, instead of using the transformation to provide an estimate of area per unit ground area, it was used here to provide an estimate of filled voxels per unit ground area, where the unit ground area was 1 cm^2. The equation is equivalent to:

$$\text{adjusted point returns}(h) = -ln(1 - \text{point count}(h)) \tag{5.2}$$

where point count (h) is the number of filled voxels from 150 cm to height band, (h), and adjusted point returns(h) is the point count adjusted for occlusion at depth h. Using this equation the adjusted point return value should not be viewed as a direct metric for the 'true' point return count corrected for occlusion, but rather as an indicator of point return count (density of objects) accounting for occlusion with distance from the scanner.

Point cloud data was first sliced into 1 cm height bands to extract point returns on their z coordinates. The total point return count was then found for each 1 cm height band. From this a cumulative point return count, working from 1.5 m down to 10 cm, was calculated for each height band with the lowest height band (10 cm) containing a sum of all the point returns.

The cumulative return count for each height band was then normalised by dividing by the total point return count, hence giving the 10 cm height band a value of 1. This provided an understorey point return distribution to near ground level. Using the MacArthur-Horn transformation with the return count within each height band and the normalised cumulative return count as inputs, a cumulative adjusted point return count for each height band was calculated.

The adjusted point count for each individual height band was the difference in cumulative adjusted count between adjacent height bands. Once this had been calculated an offset between the original point count and the adjusted point count for each height band was found.

To test the ability of the method to assess heterogeneity five sub-sections (10 m by 10 m) from each plot site were extracted along a central transect running the length of the plot site. A density profile was then created for each sub-section (Figure 5.2).

5.2.4 Analysis

For each plot site a single density profile for the entire data set (to assess overall vertical heterogeneity of structure) and five sub-sections of data (used to assess horizontal heterogeneity of structure) were created.

The data were divided into six analysis zones to allow different layers within the understorey to be examined: (a) 10-25 cm; (b) 26-50 cm; (c) 51-75 cm; (d)

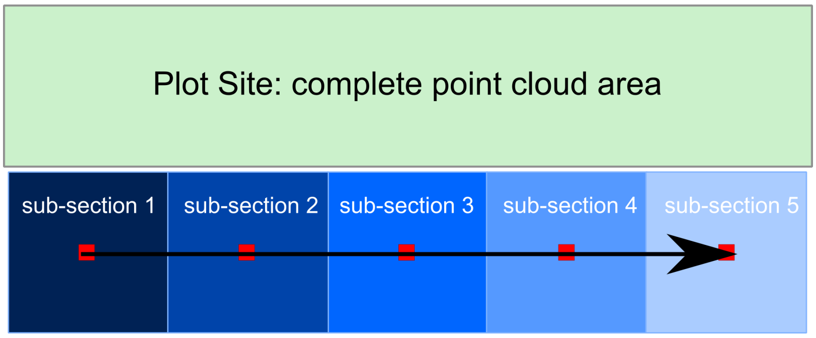

Figure 5.2: Showing location of sub-sections of data within point cloud extent, used to assess understorey density heterogeneity.

76-100 cm; (e) 101-125 cm; and (f) 126-150 cm. The adjusted point returns for each 1 cm height band in each analysis zone were found. From these the mean and standard deviation of returns within each analysis zone were calculated. Analysis zones of 25 cm were chosen as this provided coarse zones of assessment as used in other studies (i.e Ashcroft et al. (2014)), but still allowed for a finer scale assessment at the 1 cm level.

The Mann-Whitney U test (McKnight and Najab, 2010) was used to assess if the distributions of mean adjusted point return values within zones of analysis differed significantly between high and low deer density sites.

Vertical heterogeneity was assessed within plot sites using the mean adjusted point return count within analysis zones. Horizontal heterogeneity of density was assessed using the standard deviation of mean adjusted point returns within sub-sections.

5.3 Results

5.3.1 Understorey density profiles

Using the mean adjusted return count within analysis zones (overall results presented in Table 5.1) it was found that the adjusted count varied significantly (see Table 5.2 for Mann-Whitney U test results) between high and low deer density sites across analysis zones C-F (51-150 cm) where a decrease in return count was observed in high deer density sites. In comparison, no significant difference was found across analysis zones A and B (10-50 cm) for high and low deer density sites. Looking at the finer scale results based on 1 cm height bands (Figure 5.3), it was found that the difference in mean adjusted point count becomes significant (between high and low deer sites) at a height of 57 cm.

Table 5.1: Mean of adjusted returns for different deer density plots across vertical analysis zones. Values are mean returns per cm.

deer density	mean adjusted returns within vertical height bands (cm)					
	10-25	26-50	51-75	76-100	101-125	126-150
High	97,127	31,704	9,604	4,992	4,296	4,820
Low	94,964	29,235	13,584	8,808	7,345	7,035

Table 5.2: Results for the Mann-Whitney U test examining mean weighted return count within analysis zones show that zones A and B do not have a significant difference in mean returns between high and low deer density sites, whereas zones C-F do show a significant difference.

analysis zone	U	P	significant
A	194	>0.05	no
B	145	>0.05	no
C	66	<0.05	yes
D	61	<0.05	yes
E	75	<0.05	yes
F	105	<0.05	yes

The mean of adjusted returns for each vertical height band classified by deer density can be seen in Tables 5.3 and 5.4.

The understorey density profiles for all plots can be seen in Figures 5.4 and 5.5. Using these in combination with the mean adjusted returns within analysis zones (Tables 5.3 and 5.4) allowed changes within the adjusted return count across vertical zones (within each data set) to be identified. These changes in return count represent a change in object detection within the point cloud and may be used to identify structural changes within understorey vegetation present within the forest plots at different heights above the ground.

Looking at the individual plot site results it was seen that the maximum/minimum adjusted returns within height band A were found at Gwern Ddu 01 (218,976) and Ellenden (22,836), respectively. This shows Gwern Ddu containing approximately 9 times as many adjusted point returns as Ellenden from 10-25 cm height. Plot photos for these sites are shown in Figure 5.6 highlighting the difference in ground level material.

The difference between Gwern Ddu 01 and Ellenden can also be seen in the understorey density profile for each site (Figure 5.5), where Gwern Ddu 01 shows a sudden change in gradient of slope within the profile at a height of approximately 60 cm. In comparison the profile for Ellenden shows a much more stable gradient of slope from 150-10cm, representative of less structural change (homogeneity of

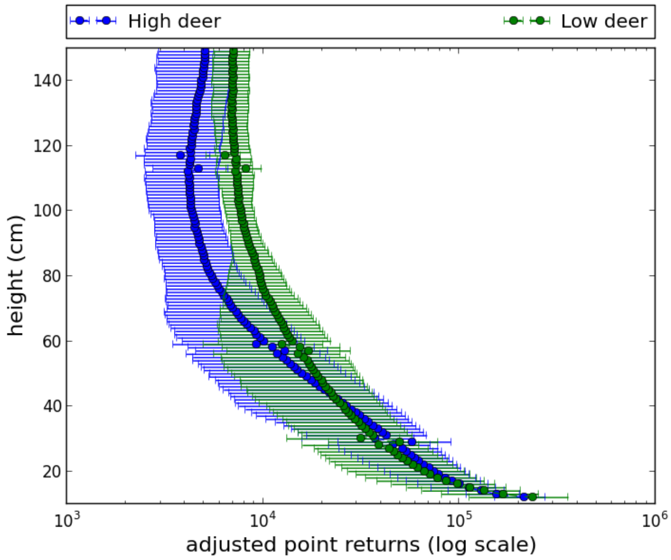

Figure 5.3: Mean and standard deviation for adjusted point returns within 1 cm height bands for high and low deer density sites.

Table 5.3: The mean adjusted returns per 1 cm vertical layers, calculated across analysis zones for each plot. Results shown are for high deer density sites.

plot site	height bands (cm).					
	10-25	26-50	51-75	76-100	101-125	126-150
Ampfield03	131,062	28,450	8,979	3,791	3,335	4,533
Ampfield04	114,205	38,010	7,362	3,053	3,553	4,335
Bentley03	104,915	24,631	6,460	3,094	2,587	3,067
Bentley04	83,809	13,348	4,798	2,743	2,222	2,390
Blackmoor	94,010	15,552	6,395	4,910	5,771	7,183
Haughwood	103,609	30,583	8,582	4,863	3,522	3,755
Hound01	102,337	23,620	8,574	8,096	7,793	7,790
Hound03	46,030	7,871	3,265	2,797	2,824	3,008
Hound05	98,539	51,182	15,310	5,205	4,242	4,439
Kingswood01	90,538	66,595	28,206	8,029	2,932	4,599
Kingswood10	150,843	48,947	19,291	8,461	6,184	8,172
Langley02	41,081	15,489	7,769	5,851	5,609	6,036
Langley05	53,116	13,339	8,632	6,687	5,801	5,771
LeaPagets03	82,799	20,688	8,396	4,981	4,709	4,916
Romers	119,383	60,968	11,711	7,260	6,888	7,081
WyreMain01	168,866	46,540	5,993	3,407	3,240	3,219
WyreMain03	92,984	19,141	7,212	4,003	3,211	3,448
WyreMain04	39,579	10,290	7,652	7,126	6,987	8,277
WyreNNR01	125,105	24,574	3,373	2,268	2,183	2,142
WyreNNR03	99,735	74,260	14,128	3,207	2,326	2,234

Table 5.4: The mean adjusted returns per 1 cm vertical layers, calculated across analysis zones for each plot. Results shown are for low deer density sites.

plot site	height bands (cm).					
	10-25	26-50	51-75	76-100	101-125	126-150
BigForest03	173,380	33,725	10,830	7,558	6,568	6,479
BleanHomestall01	98,891	22,995	9,642	8,089	7,300	7,023
BleanHomestall04	75,080	23,953	11,526	8,883	7,654	7,348
BleanHomestall06	66,303	25,383	9,849	7,406	6,838	6,937
EastBlean01	35,871	10,795	8,370	8,677	8,073	9,289
EastBlean03	117,161	34,539	16,416	10,800	9,588	8,118
Eastridge01	92,661	34,123	13,847	10,479	9,724	8,308
Eastridge05	169,827	53,536	18,442	10,720	9,277	9,011
Ellenden	22,836	10,322	8,447	7,920	7,889	7,926
FfriddMathrafal02	125,876	32,191	14,114	8,134	7,191	6,499
FfriddMathrafal04	103,060	69,384	30,213	11,187	6,042	5,198
GwernDdu01	218,976	43,779	7,131	4,876	4,427	3,885
GwernDdu04	92,792	21,657	13,400	11,687	8,586	8,329
PoleLees02	72,166	47,167	33,175	12,288	4,715	3,756
PoleLees05	94,891	51,925	24,585	10,155	7,045	6,728
SpoutFigyn	96,895	16,327	7,849	6,327	6,182	6,141
WestBlean01	107,569	19,259	9,804	7,552	7,649	7,761
WestBlean02	56,098	11,960	8,328	7,831	7,490	7,618
WestBlean03	33,230	10,074	7,910	7,651	6,592	6,689
WestBlean04	45,721	11,604	7,795	7,930	8,068	7,651

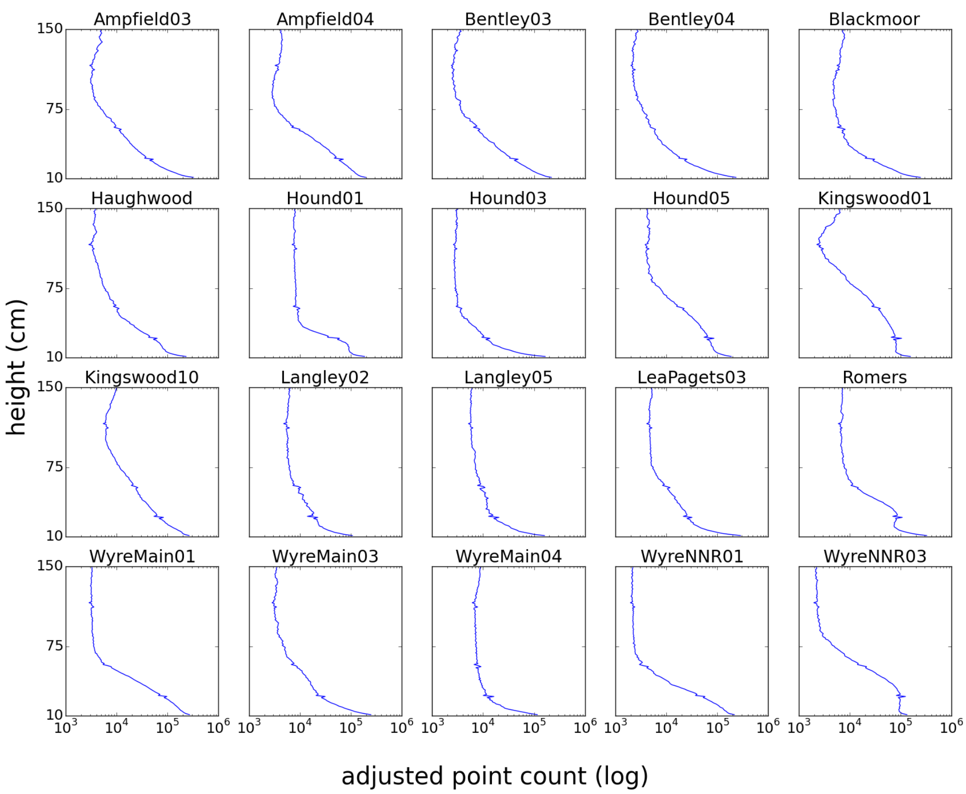

Figure 5.4: Understorey density profiles using adjusted point return count for high deer density woodland sites.

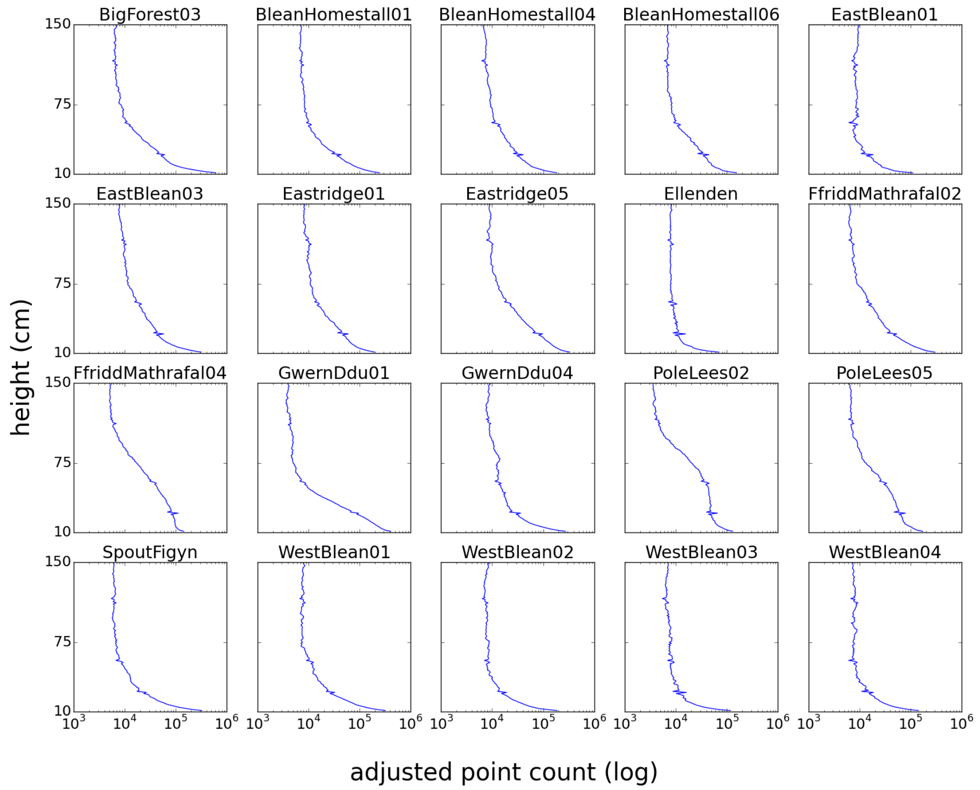

Figure 5.5: Understorey density profiles using adjusted point return count for low deer density woodland sites.

structure) within the point cloud.

(a) Gwern Ddu 01 (b) Ellenden

Figure 5.6: Ground level photos for Gwern Ddu 01 and Ellenden which were identified as having the largest difference in adjusted point returns within the 10-25 cm analysis zone. These differences can be observed in the plot photos where Ellenden has few understorey objects compared to Gwern Ddu where understorey vegetation and deadwood combine to give an object rich layer close to the ground.

5.3.2 Horizontal vegetation density within plot sites

In a similar result to the complete plot site assessment, the lower layers of understorey (10-50 cm) do not show any significant difference in the standard deviation of adjusted count across sub-sections between high and low deer density sites. The upper layers of the understorey (51-150 cm) do show a significant difference, with high deer density sites exhibiting reduced standard deviation of adjusted count across sub-sections. This suggests high deer density sites have a more uniform distribution of objects within the plot site when compared against low deer density sites. This follows expectations that deer browsing leads to a more uniform structure within the forest understorey.

The standard deviation of the mean adjusted returns across sub-sections for plots with different deer densities can be seen in Tables 5.5 and 5.6. These values represent how mean adjusted point count varies within each analysis zone (A to F) and across the five sub-plots (along the transect in each forest plot).

Using the standard deviation as an indicator of structural homogeneity (low values indicative of homogeneous structure) allows plot sites to be identified that are structurally different. Results for Eastrdige 05 show an increase in standard deviation across all five analysis zones (when compared against other sites), suggesting a horizontal heterogeneity of objects within the understorey point cloud. In comparison results for Ellenden show a decreased standard deviation, suggesting horizontal homogeneity of objects within the point cloud. This difference in object density across sub-plots within each plot site is shown in the individual understorey density profiles (Figure 5.7).

Differences in object density within vertical layers can also be observed in the plot site photographs for Eastridge 05 and Ellenden (Figure 5.8). In the photographs it can be seen that Ellenden forest shows a uniform spacing between the mutliple stems of the trees and very little understorey vegetation. Looking at the photo for Eastridge 05, relatively open patches of ground can be seen at the front of the scene and denser understorey vegetation and stems to the rear. It is this variation in density of objects that result in the increased standard deviation within sub-plots for Eastridge 05 when compared to more homogeneous sites such as Ellenden.

Table 5.5: The standard deviation of mean point return count within height bands across sub-plots for high deer density sites.

plot site	height bands (cm).					
	10-25	26-50	51-75	76-100	101-125	126-150
Ampfield03	4,115	1,267	664	203	227	346
Ampfield04	3,127	829	266	227	349	381
Bentley03	3,409	1,182	360	141	171	216
Bentley04	3,878	1,579	595	197	145	185
Blackmoor	5,619	664	263	339	375	422
Haughwood	5,713	860	580	270	213	265
Hound01	5,188	1,438	275	314	358	384
Hound03	1,898	275	218	182	175	183
Hound05	4,250	2,034	488	261	368	461
Kingswood01	3,696	1,752	1,575	485	112	366
Kingswood10	8,367	1,505	1,299	277	116	240
Langley02	593	987	495	294	199	235
Langley05	1,266	189	35	152	190	167
LeaPagets03	1,646	532	164	213	268	259
Romers	3,131	5,026	214	136	115	144
WyreMain01	5,557	2,792	306	71	75	86
WyreMain03	3,221	401	402	317	311	358
WyreMain04	1,265	210	118	108	109	123
WyreNNR01	8,624	1,789	209	147	132	131
WyreNNR03	1,668	2,187	852	87	79	96

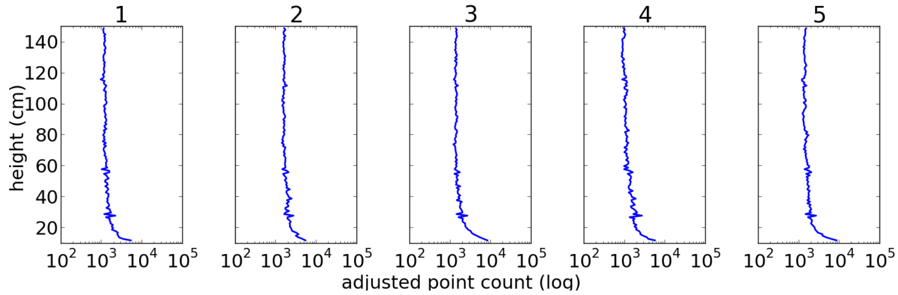

(a) Ellenden

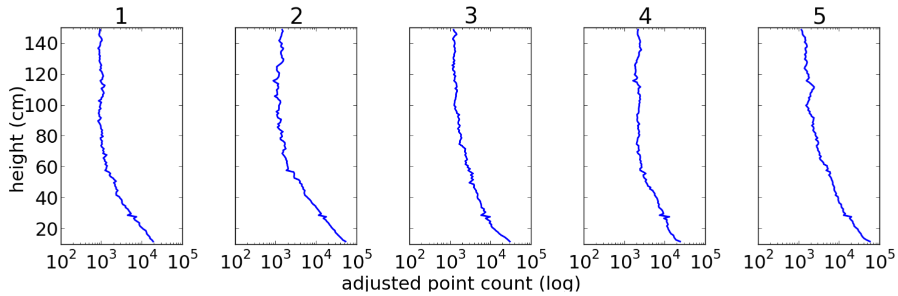

(b) Eastridge 05

Figure 5.7: Understorey density profiles for Ellenden and Eastridge 05 highlighting differences in the mean adjusted point count across sub-plots. Ellenden shows a low standard deviation indicative of similar profiles for each sub-plot 1-5. Eastridge 05 shows variation across the sub-plots 1-5, indicative of a change in density of objects across sub-plots.

(a) Ellenden (b) Eastridge 05

Figure 5.8: Plot photographs of Bentely 03 and Ffridd Mathrafal 04 showing the difference in understorey structure highlighted by a difference in standard deviation of mean point returns within analysis zones.

Table 5.6: The standard deviation of mean point return count within height bands across sub-plots for low deer density sites.

plot site	height bands (cm).					
	10-25	26-50	51-75	76-100	101-125	126-150
BigForest03	5,037	1,665	388	138	197	188
BleanHomestall01	4,904	1,130	335	132	146	143
BleanHomestall04	1,479	1,021	581	409	256	273
BleanHomestall06	4,005	1,460	400	268	302	293
EastBlean01	2,032	629	276	308	255	439
EastBlean03	4,553	1,826	607	457	344	232
Eastridge01	2,842	1,650	337	281	393	348
Eastridge05	8,466	2,426	974	503	415	424
Ellenden	497	168	171	165	180	229
FfriddMathrafal02	5,632	2,382	1,444	792	720	468
FfriddMathrafal04	3,523	1,862	1,085	378	268	188
GwernDdu01	2,820	1,502	347	288	348	328
GwernDdu04	5,787	1,993	931	566	364	318
PoleLees02	2,597	588	521	420	274	215
PoleLees05	5,970	1,381	735	504	360	402
SpoutFigyn	3,982	603	294	288	280	334
WestBlean01	4,124	476	270	335	277	313
WestBlean02	1,210	396	351	342	318	277
WestBlean03	981	359	286	229	209	200
WestBlean04	1,888	289	227	189	237	293

5.4 Discussion

5.4.1 Can TLS be used for the estimation of the vertical distribution of herbaceous layer vegetation?

Using the methods outlined here, understorey density profiles were successfully created for each of the 40 forest sites within the WoodMAD data set. These density profiles showed correspondence with deer density, supporting the use of terrestrial laser for the estimation of the vertical distribution of objects within the herbaceous layer.

Examining the links between spatial distribution of material and ecological parameters, such as diversity and productivity, has an important role in ecological studies (Scheller and Mladenoff, 2002). Whilst traditional forest survey methods can collect information on the species present within understorey communities (Song et al., 2014), the difficulty in collecting fine scale spatial information means that distribution data is commonly acquired in coarse bands (vertically) or non-contiguous quadrats (horizontally). The creation of understorey density profiles from adjusted point returns (Tables 5.3 and 5.4) gives object distribution information across vertical bands and for horizontal sub-plots, providing insights into how different forest attributes (here tested against deer density) affect density within the understorey.

The results show there was a relationship, above a height of 57 cm, between deer density and the vertical density profiles as created from TLS. The ability to detect changes in the density of objects within the understorey, at the centimetre level, shows improvements over traditional forest survey methods. An example being how, to assess regeneration rates in forest, Nagel et al. (2014) used 50 cm height classes to estimate vegetation density within sites frequented by deer. Using a finer scale measurement of vertical density, as presented here, may improve our understanding of regeneration or of animal-habitat associations within the understorey, such as the provision of shelter or the availability of light/food within different understorey layers.

In sites where deer browsing was low there was a significant increase in the number of adjusted point returns when compared to sites where deer browsing was high (Figure 5.3), this can be viewed as a general increase in the amount of understorey material where deer levels are low. Whilst this follows expectations, it also supports the use of TLS for the identification of further patterns and relationships that are perhaps not so well understood.

An example of such is how the results show no significant difference in understorey material close to the ground (10-50 cm), regardless of deer density. This suggests deer browsing may not have an effect on the herbaceous ground layer. The fact that deer density doesn't appear to have an effect on the herbaceous ground layer (unlike Suzuki et al. (2013) where deer did impact on ground level vegetation) might be explained by the transient nature of deer browsing within the plot sites surveyed (the deer were present, but perhaps did not browse as they have access to food outside the forest) and suggests that presence of deer may not be a direct indicator of ground level vegetation density.

Hegland et al. (2013) showed that herbivory within forests reduces the richness of high growing vegetation such as dwarf-shrubs and young trees, but that it increased the richness of low-growing groups such as graminoids and mosses. The Hegland et al. (2013) study supports the results seen in the understorey density profiles from TLS, where differences in the density of objects between sites of different deer density were only seen above 57 cm (i.e. deer are potentially browsing the high growing vegetation in high deer density sites).

As Newnham et al. (2015) suggest, it is through the rethinking of vegetation surveys that TLS can reach its potential. Using centimetre assessment of understorey vegetation density has shown how vertical zones of change can be identified, something that is not currently performed in surveys such as those conducted for Suzuki et al. (2013) and Hegland et al. (2013). This analysis has identified fine scale spatial relationships (vertical density) not previously examined.

It is known that structure will affect the animal-habitat associations within a forest site. Examining individual understorey profiles (Figures 5.4 and 5.5) differences in profiles can be identified within sites containing similar deer levels. Examples of this include Gwern Ddu 01, Pole Lees and West Blean 03 where obvious differences in the structural complexity of each forest site can be identified from plot site photographs (Figure 5.9). The ability to automatically detect these differences through point cloud processing across large dense data sets, shows the potential of the laser scan approach.

(a) Gwern Ddu 01

(b) Pole Lees

(c) West Blean 03

Figure 5.9: Plot photographs of Gwern Ddu 01 (a), Pole Lees (b) and West Blean 03 (c), where differences identified in the density profile can be seen within the site photograph.

In this trial the estimation of vegetation densities close to the ground used 1 cm layers, which were then assessed across 25 cm analysis zones. This shows improvements relative to the Ashcroft et al. (2014) trial, where 25 cm bins used for analysing point return data did not provide accurate results near the ground. This may be a result of an improved digital terrain model, or simpler forest floor topology, within the sites used for this trial.

Traditional forest survey methods across these sites may have identified differences in the overall cover or the species composition, but it is the fine-scale assessment using TLS that can be used to extract zones of change. An example of this is how within Pole Lees there is a zone from 60 cm to 120 cm that contains a steep density gradient indicative of increasing density of objects within the understorey. A traditional survey would provide a percentage cover estimate for the vegetation present and the species composition within quadrats. The TLS approach was used to identify a vertical zone 60 cm deep where density rapidly increases.

5.4.2 Can heterogeneity of the horizontal distribution of vegetation layers within plot sites be assessed using TLS?

In this trial five sub-plots along a central transect were used to assess horizontal heterogeneity. The standard deviation of the mean adjusted point count within height bands provided information on how changes within vertical density across subplots differed in each site. Using this it was possible to identify plots where change along the transect was low (homogenous structure, as seen in Ellenden wood - Figure 5.8a) and also where change along the transect was increased (heterogenous structure, as seen in Eastridge 05 - Figure 5.8b).

The ability to create sub-plots of different sizes from a single survey, gives the TLS approach a spatial dynamic that could not be realised using traditional methods without extensive resources. An example being how in this trial each survey was assessed as one whole plot (10 m by 50 m) and five smaller sub-plots (10 m by 10 m). Equally, the survey could be split into twenty smaller sub-plots (5 m by 5 m) or five hundred (1 m by 1 m). This flexibility from a single laser scan survey has potential to allow identification of relationships at multiple spatial scales from a single survey.

The TLS approach does not provide a complete assessment of understorey plant communities as, at the present time, different plant species cannot be identified through point cloud feature extraction. It does however, provide spatial information that can be collected relatively easily. Collecting data below the canopy also allows for assessment across all seasons, regardless of canopy state, something that aerial based solutions do not provide (Singh et al., 2015).

Using sample plots along a transect it was possible to create multiple UDP from which the horizontal heterogeneity of objects within a plot site were assessed. This method, whilst providing an assessment of how object density changes within a forest plot, does not provide a detailed analysis of the horizontal spatial relationships operating within understorey vegetation. Horizontal relationships within forest understorey structure will be examined in the following chapter through the creation of understorey cover estimates and microtopographic analysis of point return surfaces.

Chapter 6

The estimation of understorey cover and microtopography through terrestrial laser scanning

6.1 Introduction

The forest floor and lower understorey are important zones when considering the maintenance of forest ecosystems. These areas are the principle zone of decomposition and as such are critical to nutrient cycling through linking above-ground and below-ground processes (Qiao et al., 2014). As well as providing a zone for decomposition, the forest floor and lower understorey commonly support vegetation growth and habitats for ground dwelling fauna including arthropods, insects, mammals and ground nesting birds (Díaz-Aguilar et al., 2013). Understorey diversity and the abundance of understorey species are important indicators of forest health (Kerns and Ohmann, 2004) and are therefore used by ecologists when assessing forests.

The composition of the forest floor and the structure of forests are linked, with Hedwall et al. (2013) showing how increases in forest density within Swedish forests (typically as forests aged) resulted in a decrease in abundance across forest floor vegetation. Understorey cover and canopy structure have also been linked with Song et al. (2014) showing that the total abundance of herbs within plot sites were positively correlated with canopy openness and negatively correlated with the cover of lower canopies. The relationship between forest understorey and other forest features such as structure and canopy highlights the importance of surveying and analysing the understorey when considering forest systems as a whole.

Various characteristics of the forest understorey are examined by ecologists when studying forests including stem counts, light transmission and species diversity (Scheller and Mladenoff, 2002). It is understorey cover, however, that is the most common structural measure estimated by ecologists, with cover being used as a measure of vegetation abundance (Wing et al., 2012). Reich et al. (2012) describes the estimation of understorey cover as a visual assessment for species under 1 m using a system of classification groups (1%, 1–5%, 6–25%, 26–50%, 51–75% and 76–100%). This is a vegetation cover estimation that does not include material associated with any larger growth species.

The two main components of vegetation cover are the vertical and horizontal distributions of vegetation (Nudds, 1977). Horizontal understorey vegetation cover is used to help describe forest habitats and can be important when trying to understand forest competition dynamics (Chen et al., 2008). As well as a measure of abundance within forests, cover estimates can also be used to assess other factors such as fuel loading (Cram et al., 2015) and deer browsing (Boulanger et al., 2015).

The estimation of understorey cover by traditional methods can be difficult and time-consuming. This has resulted in an array of different estimation methods being used (Eskelson et al., 2011). Traditional estimation methods include cover boards, line-intercept sampling and fixed plot sampling. These methods provide percentage values for estimated cover, but results can be affected by observer bias (Macfarlane and Ogden, 2012).

Many previous studies have shown that remote sensing (both passive and active) can be used to extract forest characteristics from above the canopy, these include estimations of understorey vegetation cover. Wing et al. (2012) presented an aerial laser scanning (ALS) method for the prediction of understorey vegetation cover, giving accuracies of $\pm$ 22% and biases of $\sim$0% for a range of canopy covers. The same trial highlighted how in forest with dense canopy or where overstorey and understorey layers intermix, the ALS method may not be feasible. Singh et al. (2015) examined the use of aerial imagery and ALS for the detection of understorey invasive plants in an urban forest. This trial provided adequate assessment of invasive species over a regional scale, but concluded that surveys needed to be taken in the leaf-off season. Lone et al. (2014) showed how using

ALS data for the estimation of understorey vegetation cover greatly improved the ability to correctly predict browse biomass for Norwegian moose. This study showed the potential for ALS surveys to help in estimating the distribution of large herbivores and how ALS has the potential to be a valuable tool for ecologists and wildlife managers.

In comparison with ALS studies, those investigating the use of terrestrial laser scanning (TLS) for estimation of understorey cover are limited. Seidel et al. (2012a) examined the use of diameter at breast height (DBH) measurements from TLS to estimate understorey biomass in coppice forest, but did not provide estimates of vegetation cover. Ashcroft et al. (2014) tested the use of TLS for creating vegetation density profiles but concluded that the method could not be used accurately near the ground or in areas where the ground surface was uneven, as it was not possible to reliably distinguish the ground surface in these areas.

Although the importance of understorey vegetation cover when assessing forest abundance is known, the potential for using TLS has not currently been fully explored. As terrestrial lidar systems operate beneath the canopy and are therefore not affected by canopy state (leaf on/off), it is proposed that TLS may offer a novel approach to understorey cover estimations that can be utilised across all seasons regardless of canopy state. The use of TLS to collect high resolution point clouds may also allow for finer scale assessment of understorey cover than is currently possible using the classification groups as outlined by Reich et al. (2012).

Additional surface properties obtained through TLS have the potential to be used to identify individual understorey vegetation types (Figure 6.1). Similar surface processing methods are currently used to identify individual landforms in geomorphology (Brubaker et al., 2013). In a similar process, it has also been shown that the microtopography of forest canopies can show correlation with canopy structure (Maurer et al., 2013; Maurer et al., 2015).

The aim of this study was to address the questions: (1) can TLS be used for the estimation of the horizontal distribution of understorey vegetation cover within forest plots? and (2) are any novel understorey measurements available?

The trial used data collected as part of the WoodMAD data set. Initial expectations were that those plots classified as low deer density would show a predominance toward increased understorey cover and those classified as high deer density toward decreased cover. This was because deer browsing was expected

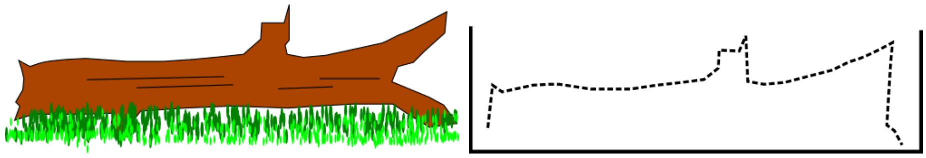

(a) Dead wood object in forest point cloud

(b) Microtopographic profile showing low levels of surface roughness.

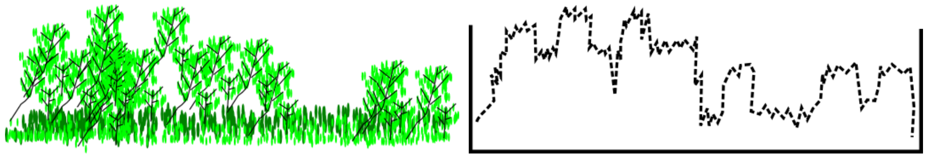

(c) Example vegetation understorey in forest point cloud.

(d) Microtopographic profile showing high levels of surface roughness.

Figure 6.1: Showing how different objects within a forest site would be expected to create different microtopographic profiles. Laser scan acquired microtopography has the potential to be used to distinguish different understorey structure types.

to cause a reduction in understorey vegetation (Suzuki et al., 2013).

In addition to understorey cover estimates, novel understorey vegetation surface parameters were examined. Using techniques developed for the study of surfaces, such as in floodplain analysis (Scown et al., 2015) and landscape evolution (Roering et al., 2013), assessments of the spatial organisation, surface character and variability of the understorey point return surface were tested. This analysis provided estimations for the understorey microtopography at each trial site.

6.2 Methods

A surface extraction method was tested following similar surface modelling techniques used in geomorphology, geology and hydrology (Lemon and Jones, 2003; Brasington et al., 2012; Raiber et al., 2012). Combining this technique with point cloud data from forest surveys decimetre analysis of understorey layers could be achieved, from which percentage cover estimates were extracted.

As understorey cover estimates were not collected by the BTO as part of the WoodMAD survey, a qualitative assessment of the 40 forest survey sites was made using photographs taken during the TLS survey. Two classifications were made for each plot. Firstly, the height of understorey vegetation was assessed and plots split into three vegetation height categories: (0) low - where the ground was visible throughout; (1) medium - patches of vegetation that blocked the ground, but where it was not a continuous covering; and (2) high - minimal ground showing through the vegetation.

Secondly, to assess the microtopography of each woodland test site against vegetation type, a qualitative assessment of the vegetation type at each survey site was made. This assessment categorised understorey vegetation type as belonging to one of six groups: (0) very little understorey; (1) low level grasses; (2) low level bramble; (3) dominated by ferns; (4) low vegetation; and (5) tall, mixed vegetation. These groups were defined using visual assessment of the photographs taken at each test site. Descriptions of the vegetation types and corresponding photographic examples can be seen in Figure 6.2.

These classifications of plot sites were qualitative classifications carried out post-survey to assess the ability of the TLS method to extract plot characteristics. As deer browsing is transient in nature (deer may be present, but not browse), is was felt that an additional classification would allow a more thorough assessment of the usefulness of the TLS approach.

In converting the vertical datum to height above ground (Chapter 3) some smoothing of the microtopographic surface was likely to have occurred. Adjustment to height above ground was achieved using a 0.5 m digital terrain model meaning that any small scale (covering less than 0.5 m^2 in the horizontal) ground surface features may have been lost. The removal of these features from the ground surface will also have removed them from the microtopographic surface.

6.2.1 Site description and data collection

All data were collected as part of the WoodMAD survey. All TLS data were acquired using a FARO Focus 3D TLS instrument.

Full details of the FARO instrument and sites visited can be found in Chapter 3 and Appendix A.

6.2.2 Data preparation

All laser scan data were registered, filtered and decimated using voxel based extraction to a level of 1 cm^3, see Chapter 3 for full details.

(a) Group 0: very little understorey

(b) Group 1: low level grasses.

(c) Group 2: low level bramble.

(d) Group 3: dominated by ferns.

(e) Group 4: low vegetation.

(f) Group 5: tall, mixed vegetation.

Figure 6.2: Showing examples of each understorey vegetation group as classified using qualitative assessment of plot photographs.

6.2.3 Estimation of understorey cover

The first step in the estimation of understorey cover was to slice the original point cloud into a data set describing only the point returns to be used during understorey cover analysis. For this trial all point returns above ground level (the ground was classified as returns in the first 10 cm) and 1.0 m height were selected. This follows a common maximum height for cover estimates, used when assessing understorey material (Reich et al., 2012; Gilliam, 2014).

The next stage was the generation of a raster surface describing understorey height from which point returns describing non-vegetation material (such as stems) could be removed. The removal of likely non-vegetation material was attempted through the creation of three individual raster surfaces describing point return count, point return height and surface slope. These were then combined to identify (likely) non-vegetation raster cells. Non-vegetation cells were those with combinations of increased return count, point height close to 1 m and surface slope near vertical. All raster data sets were generated at a resolution of 5 cm^2.

Although point cloud data was voxelised to 1 cm^3 completing the full surface processing at this resolution was considered too time-consuming to be practical. An example being how, using a standard desktop workstation (quad core with processing speed of 3.10 GHz), a single 50 m by 10 m trial site processed at 1 cm resolution was completed in about 48 hours. In comparison, using a resolution of 5 cm all surface processing was completed in 1 hour.

Vegetation surfaces with 1 cm resolution were created for Ampfield Wood 03 and Ellenden Wood to assess the sensitivity of raster resolution to the results. From this it was found that increasing the resolution resulted in a decrease in estimated cover between 11% and 15% and an increase in estimated 3D surface volume between 12% and 18% (results given in Appendix C.3 Table C.6), while greatly reducing processing time. With 40 sites to analyse the trade off between processing time and resolution, given that traditional cover estimates use coarse estimations (Reich et al., 2012), was considered acceptable for this trial.

The first surface created was of raster holding cell values equal to the point return count (referred to as the count raster). This identified vertical component within the point cloud, similar to the method outlined in Chapter 4. As vegetation components would not be expected to contain as many point returns as solid stem material and not contain the same vertical component, this step was expected to identify likely stem (vertical) material. The use of vertical component assessment close to the ground does increase the likelihood of classification errors due to increased material and point occlusion (see Chapter 4). As this was only one of three tools for the assessment of likely non-vegetation material, the effects were not expected to be significant.

Secondly, a raster containing cell values of the maximum height was generated (referred to as the height raster). As all stem material was expected to reach above the 1 m cut-off point (by definition tree stem material will grow beyond the understorey), raster cells containing values for 1 m were classified as possible stem material.

Thirdly, a raster was generated describing the slope of the understorey surface (referred to as the slope raster). This raster was created using each of the cell values from the height raster to describe the maximum gradient from one cell to its neighbours. In this way the slope of the height raster could be assessed with slope raster cells containing values in degrees between 0 and 90 (0 degrees being a flat surface parallel to the ground). The slope raster was generated as it was expected that solid forest objects such as stems, branches and dead wood would provide near vertical surfaces and so be identified through the slope analysis. In comparison, understorey vegetation was expected to show a variable surface slope due to the fact that some point returns would penetrate the vegetation.

With these three raster surfaces created (describing individual properties of the understorey point cloud), the Fuzzy Logic processing library of ESRI ArcGIS was used to combine the data sets into a single raster (Reuter and Nelson, 2009). Each of the three raster data sets were first graded from 0 to 1 (a step in the Fuzzy Logic processing library), with 0 being most likely to be vegetation material (reduced count, low height values, minimum slope) and 1 being most likely to be non-vegetation (increased count, height at 1 m, near vertical slope). In combining the three raster data sets a single understorey raster was created which was used to identify raster cells that were likely sources of non-vegetation material. Count, height, slope and combined raster examples can be see in Figure 6.3, with areas coloured red indicating cells of likely non-vegetation material.

Through visual assessments on test data sets a cut-off point of 0.78 (from a range of 0 to 1) was identified as a reliable marker for objects not likely to be understorey from the combined raster surface. Using the merged raster any cells with a value greater than 0.78 were considered null (contained no data values) and a final adjusted raster created with likely stem material removed (Figure 6.4).

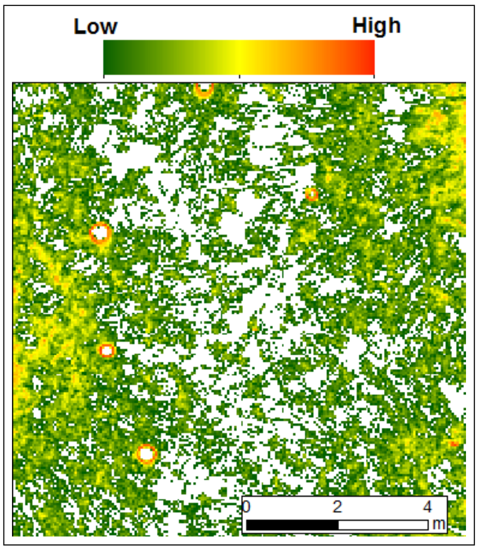

(a) Count raster

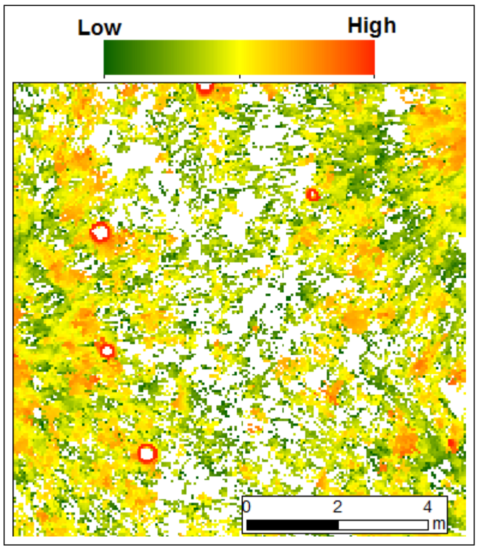

(b) Height raster

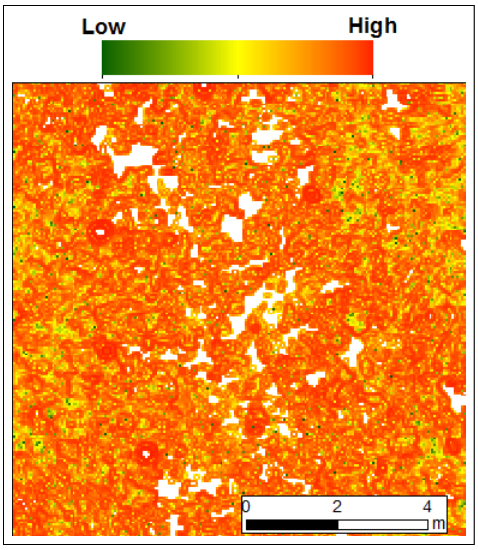

(c) Slope raster

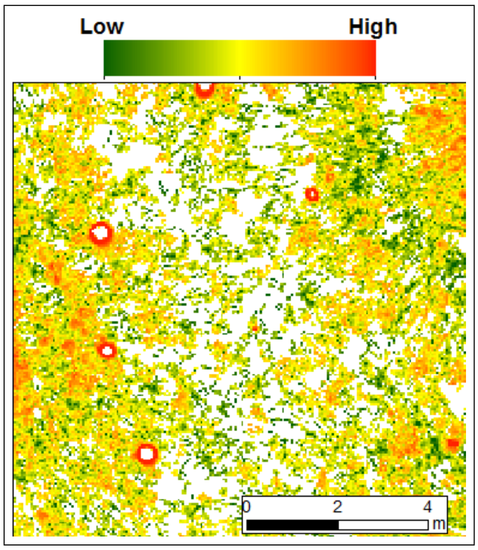

(d) Combined raster

Figure 6.3: Three normalised surface rasters, coloured by likelihood of being vegetation material, describing return count (a), height (b) and slope (c) were produced. These were then combined using fuzzy logic to form a raster (d) from which likely stem and branch material could be identified and removed. White areas are those with no data.

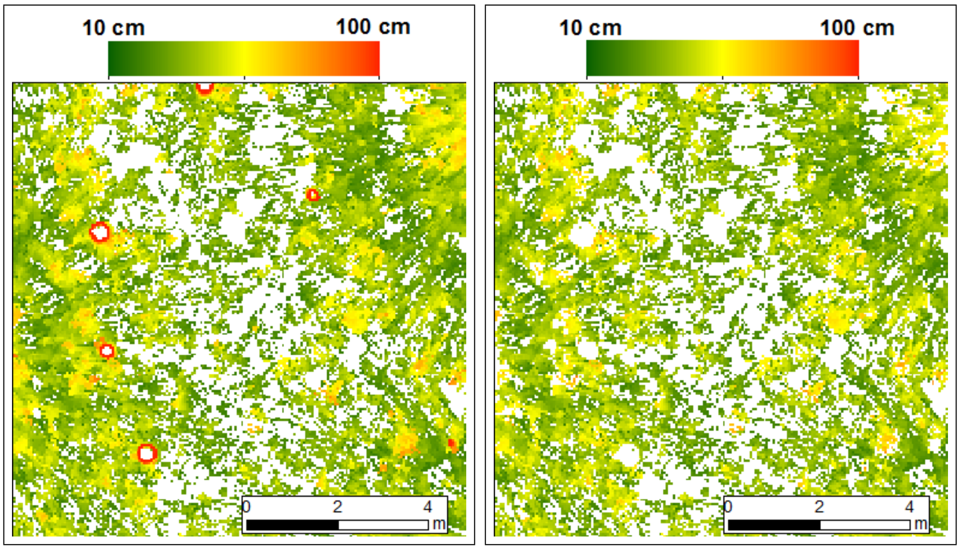

(a) original raster. (b) final raster.

Figure 6.4: Two surface height rasters showing the same area before (a) and after (b) likely stem and branch material has been removed. White grids are null values not used during processing.

The final stage in the estimation of cover was the estimation of surface areas and volumes using the processed raster surface from which likely stem material had been removed.

From the raster surface a triangulated irregular network (TIN) surface was created using the 3D analyst libraries within ESRI ArcGIS (Reuter and Nelson, 2009). TINs are vector based representations of surfaces (based on a network of non-overlapping triangles, in this case created using Delaunay triangulation) providing a variable distribution of points accurately describing terrain. Using a TIN allowed for detailed volume estimations to be made and follows existing surface modelling techniques used in landscape modelling (Jenness, 2004), hydrology (Bannister and Kennelly, 2016) and engineering geology (Dong et al., 2015). Using a second TIN describing a plane at 0 m, the volume between the understorey surface and ground level was then determined.

The ground level and understorey surface TINs were then used to estimate three values: (1) 2D area of understorey surface - a vertical projection of cover similar to that used by ecologists during visual assessment with units given in m^2; (2) 3D area of understorey surface - a non-projected surface providing an area for the complete TIN, with units given in m^2; and (3) 3D volume between uppermost understorey and ground surface - the volume between the TIN surface and the ground, with units given in m^3. A plot photo and related TIN surface can be seen in Figure 6.5.

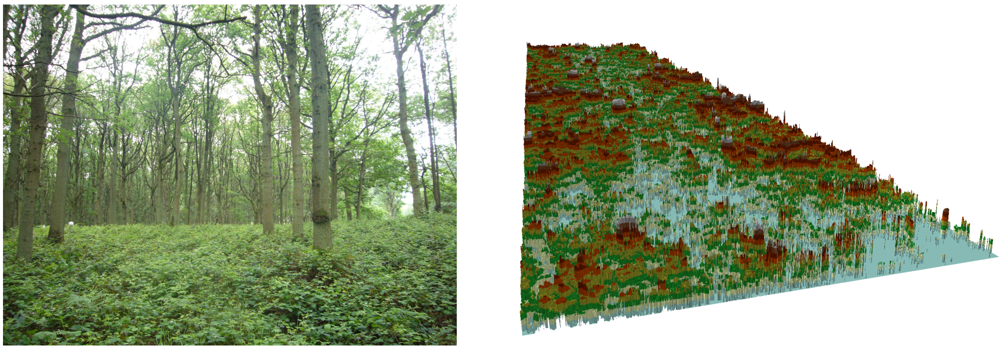

(a) Plot photo for Wyre NNR 03 (b) TIN surface calculated for Wyre NNR 03

Figure 6.5: Plot photograph and the subsequent 3D surface used for area and volume estimates for Wyre NNR plot 3. The TIN shown (b) represents the full plot measuring 10 by 50 m, coloured by height.

A graphical analysis work flow is outlined in Figure 6.6.

6.2.4 Characterising understorey microtopography and surface roughness

With the height raster created for the estimation of understorey cover, further analysis was performed to obtain surface slope and curvature properties for the understorey layer. The surface properties were extracted using a 5 cm^2 resolution height raster. Different resolution rasters will produce different results, with larger raster cells producing a 'smoothed' surface (Figure 6.7).

Slope and curvature surfaces provide an indication of the microtopography and surface roughness of each data set. From this it was possible to compare results across different plot sites, using mean values of each surface to rate plots as either "rough" or "smooth".

To extract the slope of the understorey surface the same method was used as described in section 6.2.3. To extract the curvature of the understorey the surface height raster was used to produce a curvature raster. The curvature raster described the second derivative value of the input surface on a cell-by-cell basis using the method outlined by Zevenbergen and Thorne (1987). Positive values of curvature indicate the surface is upwardly concave, negative values indicate the surface is upwardly convex and values of zero indicate a linear surface (Figure 6.8)

Standard deviation of slope was used as a descriptor of surface roughness with

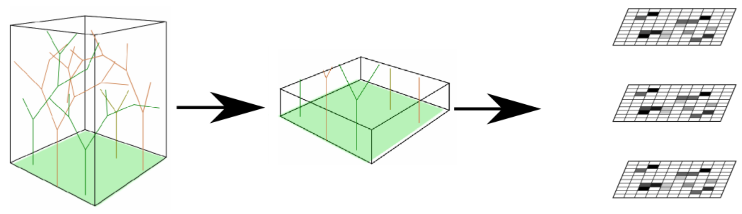

(a) initial data (b) slicing (c) height, count and slope rasters

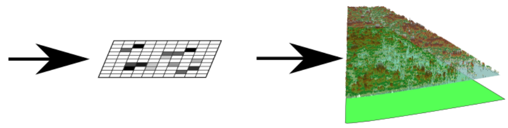

(d) final raster (e) 3D surface

Figure 6.6: Graphical work flow outlining generation of height raster with likely non-vegetation material removed covering: (a) complete point cloud adjusted to ground height; (b) understorey material selected (10-100 cm); (c) count, slope and height raster data sets created; (d) combined raster surface describing understorey point returns with likely non-vegetation material removed; and (e) understorey 3D surface used for volume and area estimates.

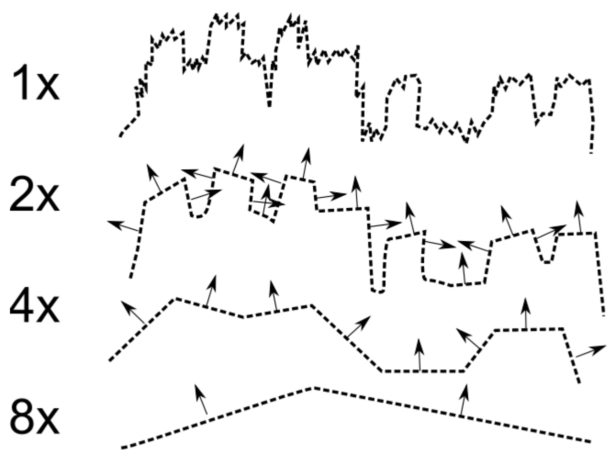

Figure 6.7: Representation of how microtopography will vary according to the resolution of the height raster (in this trial 5 cm^2). Vector normals to cell plane (the direction perpendicular to the surface) are shown as arrows. Increasing the size of the input raster (represented by 1x, 2x, 4x and 8x) has the effect of smoothing the microtopography (modified from Grohmann et al. (2011))

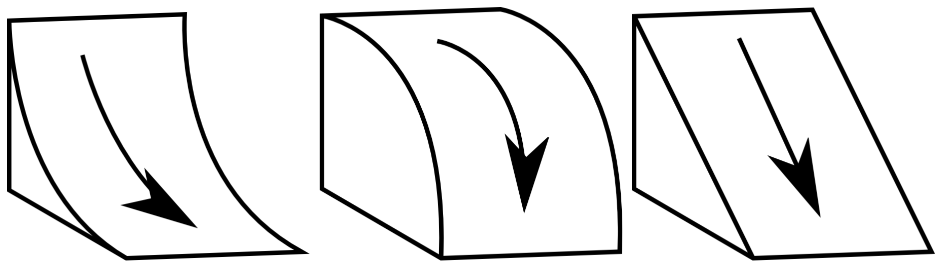

(a) positive curvature (b) negative curvature (c) zero curvature

Figure 6.8: Profile curvature is parallel to the direction of maximum slope. Positive values indicate a surface that is upwardly concave (a). Negative values indicate a surface that is upwardly convex (b). Zero values indicate a linear surface (c).

an increase in standard deviation of slope being representative of an increase in surface roughness. This follows similar analysis work flows (used here at a finer scale) outlined by Brubaker et al. (2013) for the estimation of surface roughness when using ALS to characterise terrain data.

The classification of plots on their slope and curvature values may not be sufficient for the estimation of understorey vegetation structure, which was expected to vary within a plot site. Instead, an assessment of how much and where variations occur in understorey surfaces was expected to be a more useful measure for assessing the different surface properties within the understorey of each plot site.

To provide an assessment of surface properties within plot sites, each cell from the slope and curvature raster was assessed against its neighbours with the mean calculated. This processing is referred to as moving window analysis (Figure 6.9). The expected relationship between surface properties and the resolution of the original data set and the moving window analysis is shown in Figure 6.10.

Different sizes of moving windows are used in geomorphometry to account for the different scales present within topography. For the same reason, different size grids were tested here to see which was the applicable analysis size for the microtopography of understorey vegetation. For this trial estimates using five different moving window sizes (0.5 m, 1.0 m, 1.5 m, 2.0 m and 2.5 m) were processed. The expected outcomes from the use of different moving window sizes are outlined in Figure 6.11.

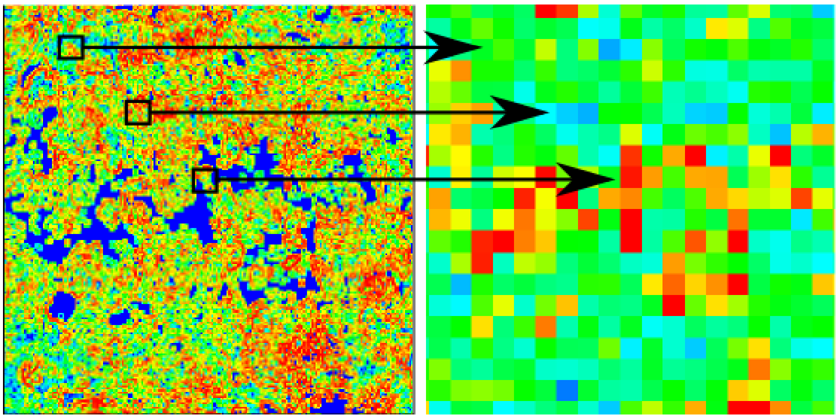

(a) Moving window 0.5 m.

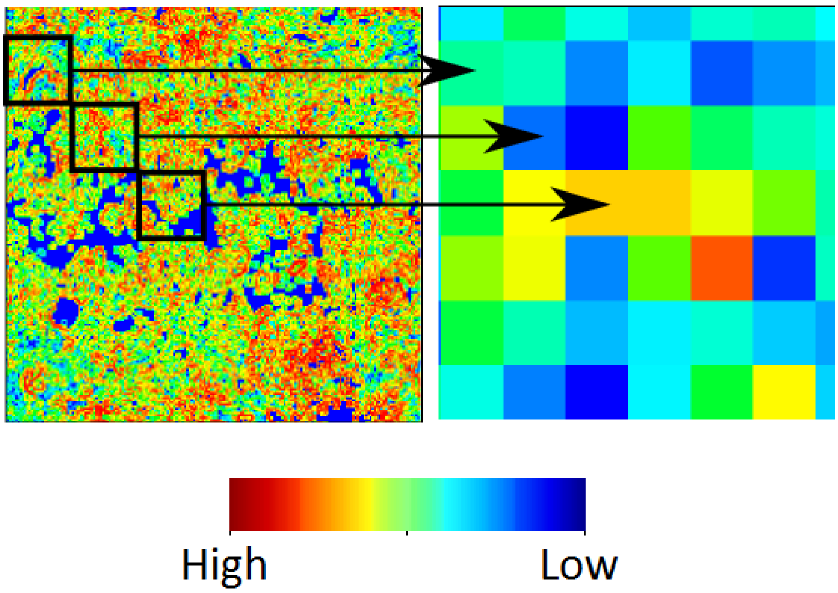

(b) Moving window 1.5 m.

Figure 6.9: A single slope raster (left hand raster) can be processed using different sized moving windows. The surface roughness raster cells (right hand raster) contain the standard deviation of the original slope raster for the extent of the moving window.

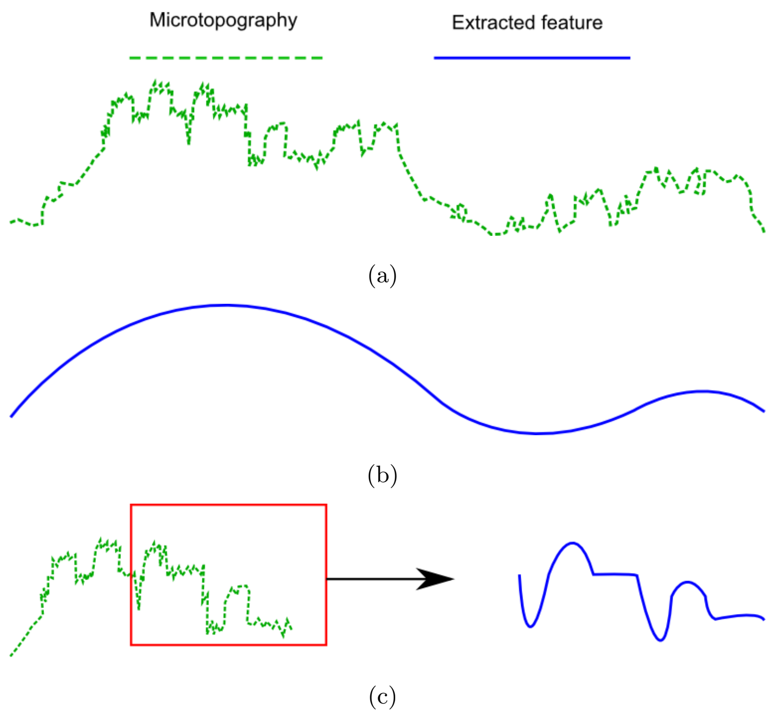

Figure 6.10: Expected effects of moving window size on the ability to detect features using surface microtopography (a). Coarse underlying features can be extracted using a large moving window (b). Finer microtopographic details can be detected using smaller moving windows (c)

6.2.5 Analysis

To assess the effect of deer density on understorey cover estimates as extracted through TLS, the mean and standard deviation of 2D area, 3D area and volume were extracted and grouped into different deer densities, estimated understorey cover and vegetation type.

In addition to cover estimates for each plot, additional microtopographic parameters of the understorey were extracted. The mean and standard deviation of slope and curvature were assessed in moving windows of different sizes. The means for the moving window analysis were then calculated for each plot site. Values for slope and curvature gave an indication of microtopography and surface roughness across the site.

A one-way analysis of variance (ANOVA) (Gelman et al., 2005) was calculated on the extracted estimates for cover and microtopography. These were grouped by the qualitative assessments for understorey and vegetation type.

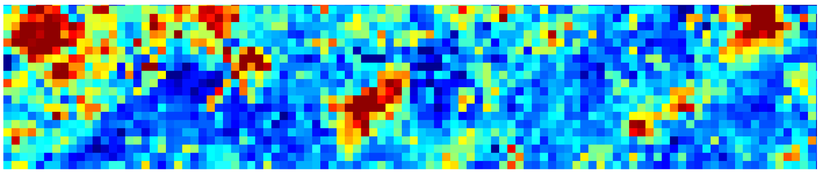

(a) 50 cm window

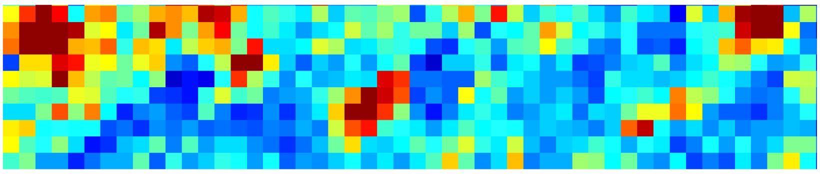

(b) 100 cm window

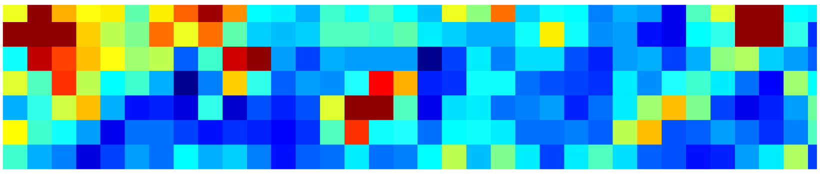

(c) 150 cm window

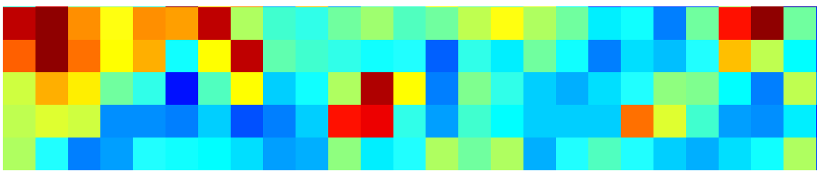

(d) 200 cm window

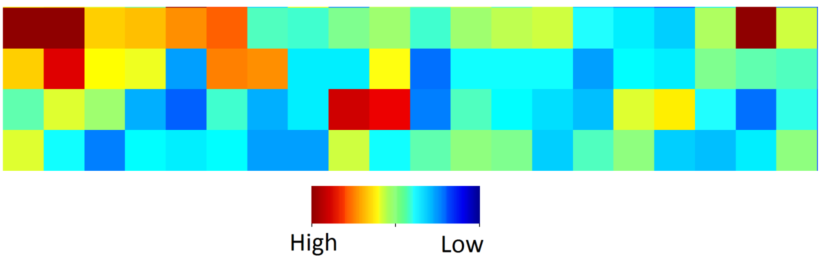

(e) 250 cm window

Figure 6.11: Different moving window sizes of 50 cm (a), 100 cm (b), 150 cm (c), 200 cm (d) and 250 cm (e) for Ampfield 03 (10 by 50 m) show that increasing the moving window size ‘smooths’ the surface roughness.

6.3 Results

6.3.1 Understorey cover estimation

Correspondence was seen between qualitative cover estimates and estimates extracted through TLS processing and analysis, with low, medium and high understorey sites showing average cover estimates of 31.9%, 57.3% and 65.6% respectively. Results for area and volume estimates can be seen in table 6.1 with box plots of the results shown in Figure 6.12. The difference in mean cover estimates for the three groups (where n=11, 14 and 15 for understorey groups 0, 1 and 2 respectively) was statistically significant for 2D area ($F_{2,39} = 28.13$, $p<0.05$), 3D area ($F_{2,39} = 27.14$, $p<0.05$) and volume ($F_{2,39} = 28.82$, $p<0.05$).

For high deer and low deer sites the mean cover estimates were 54.4% and 51.4% respectively. The mean 3D volume estimates for high deer and low deer sites were 1,165 and 1,384 m^3 respectively. The results for 2D area, 3D area and volume showed no significant difference between high and low deer density sites.

The results follow expectations that increased understorey vegetation material (as assessed qualitatively) will result in increased understorey cover estimates.

Table 6.1: Area and volume comparisons for different forest plot types extracted through TLS analysis.

Plot type	area 2d (m^2)	area 3d (m^2)	volume (m^3)	cover (%)
high deer	272.1	1164.7	50.8	54.4
low deer	257.2	1383.4	51.6	51.4
low understorey	159.4	714.4	25.4	31.9
medium understorey	286.4	1224.5	51.6	57.3
high understorey	328.1	1708.8	71.7	65.6
all plots	267.1	1265.8	51.9	53.4

Looking at individual cover estimates (individual plot results are given in Appendix C.3 Table C.7) the minimum cover estimated was 11.3% for the test site at Ellenden Wood. This was a test site that was visually assessed as having very little vegetation understorey. The maximum cover was estimated at 81.4% for Wyre NNR plot 3, this site had been visually assessed as having high levels of understorey vegetation. A visualisation of this difference is shown in Figure 6.13 where the area coverage and volume contrasts between the two sites can easily be seen.

The minimum cover estimate of 11.3% from Ellenden Wood compares to a likely assessment of cover using traditional methods of close to 0%. This difference can be explained by the presence of woody material contributing to cover estimates

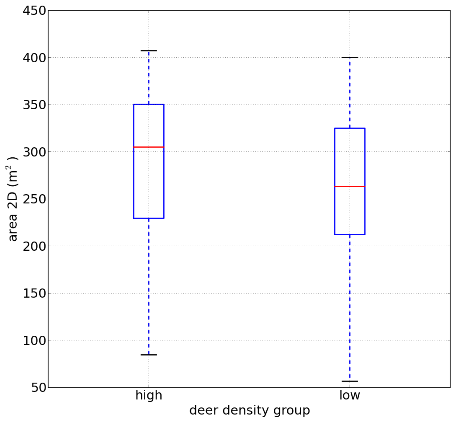

(a) 2D area grouped by deer density

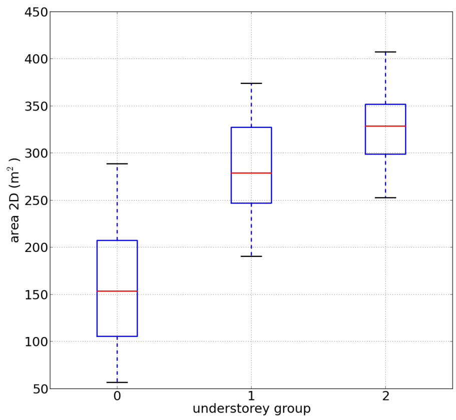

(b) 2D area grouped by understorey

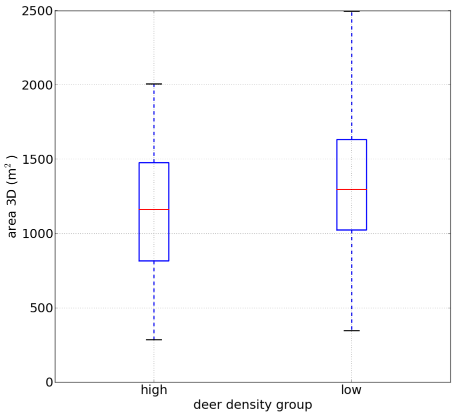

(c) 3D area grouped by deer density

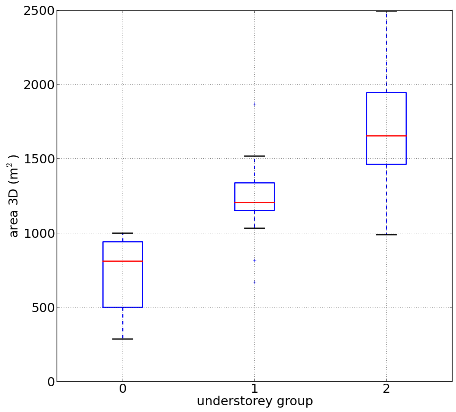

(d) 3D area grouped by understorey

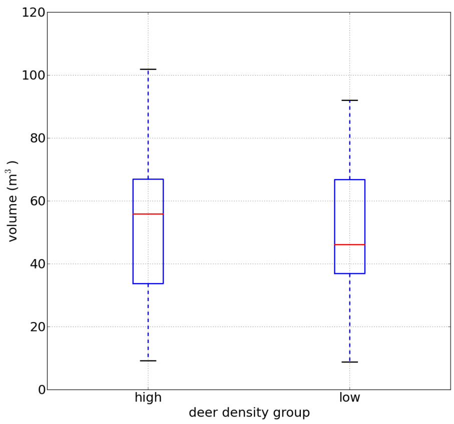

(e) volume grouped by deer density

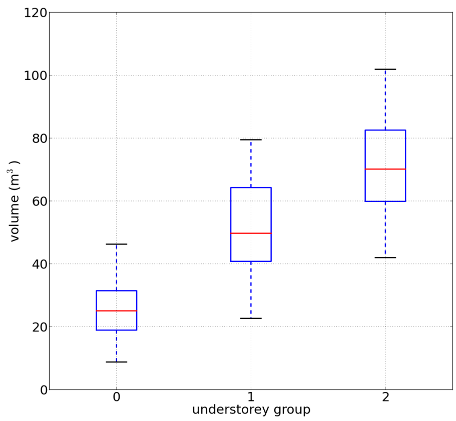

(f) volume grouped by understorey

Figure 6.12: Deer density does not show any significant difference in the results for 2D area (a), 3D area (c) or volume (e). Results sorted by qualitative assessment of understorey cover (grouped into 0 - low, 1 - medium and 2 - high) show significant differences for 2D area (b), 3D area (d) and volume (f)

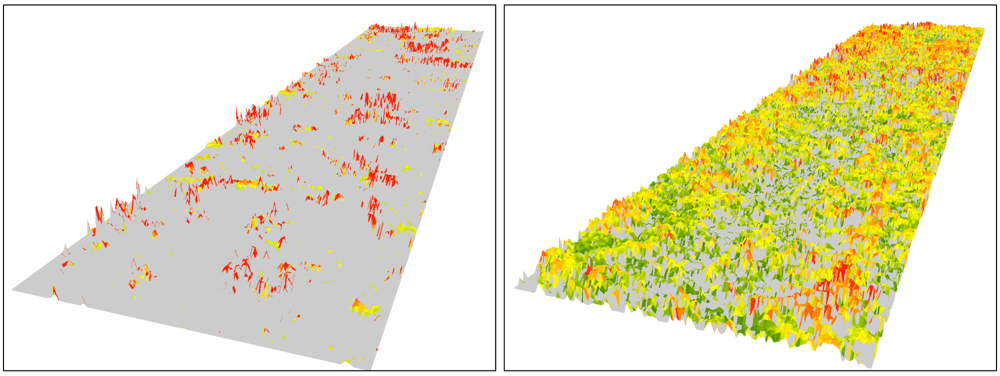

(a) Ellenden (b) Wyre NNR 03

Figure 6.13: 3D surface results for plot sites with different levels of understorey cover as extracted through TLS. Cover estimates for Ellenden (a) and Wyre NNR 03 (b) were 11.3% and 81.4% respectively. Surfaces are coloured by height.

using the TLS approach (Figure 6.14).

6.3.2 Microtopography and surface roughness

Correspondence was seen between qualitative understorey cover and vegetation type assessments and mean slope and curvature estimates extracted through TLS processing and analysis. Similar to results for cover estimation, no correspondence was seen between extracted microtopography and deer density. Box plots showing the mean curvature and slope values (extracted from a 0.5 m moving window), grouped by deer density, understorey cover and vegetation type can be seen in Figure 6.15.

Looking at the p values from ANOVA results for different moving windows sizes (0.5, 1.0, 1.5, 2.0 and 2.5 m) for extraction of mean slope and curvature, it was seen that decreased p values were observed using a 0.5 m moving window. This suggests that a finer scale approach to understorey analysis may be more appropriate when examining microtopography. Full statistical analysis results can be found in Appendix C.3 Table C.9.

The difference in extracted microtpography (using a 0.5 m moving window to calculate mean values) for the three understorey cover groups was statistically significant for curvature ($F_{2,39} = 21.590$, $p<0.05$) and slope ($F_{2,39} = 36.368$, $p<0.05$). The difference in extracted microtopgraphy for the six vegetation type groups (where n=8, 3, 11, 3, 7 and 8 for understorey groups 0, 1, 2, 3, 4, 5 and 6 respectively) also showed a significant difference for curvature ($F_{5,36} = 4.831$, $p<0.05$) and slope ($F_{5,36} = 8.101, p<0.05$).

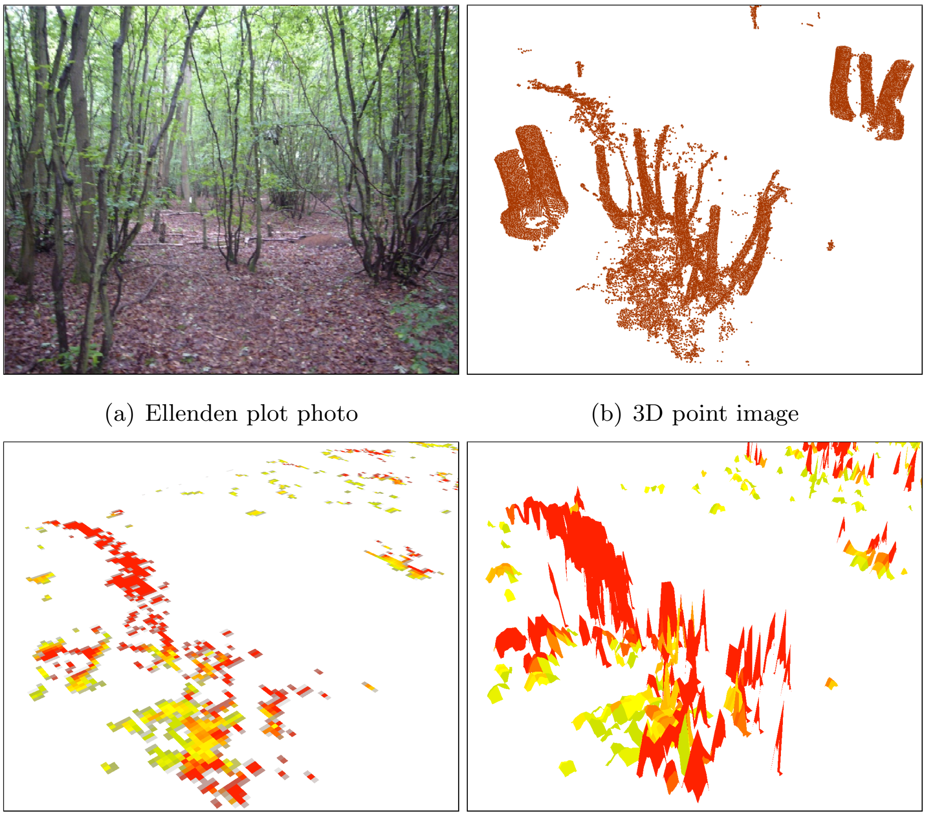

(a) Ellenden plot photo

(b) 3D point image

(c) 2D height surface

(d) 3D height surface

Figure 6.14: Understorey estimates using TLS at Ellenden Wood gave a result of 11.3% cover, showing probable over estimates due to non-vegetation material being included in the results. The plot photograph (a) shows Ellenden Wood where there is very little understorey vegetation combined with large amounts of stem material. The stem material is present in the point cloud (b), after processing (c) and in the final 3D TIN surface (d).

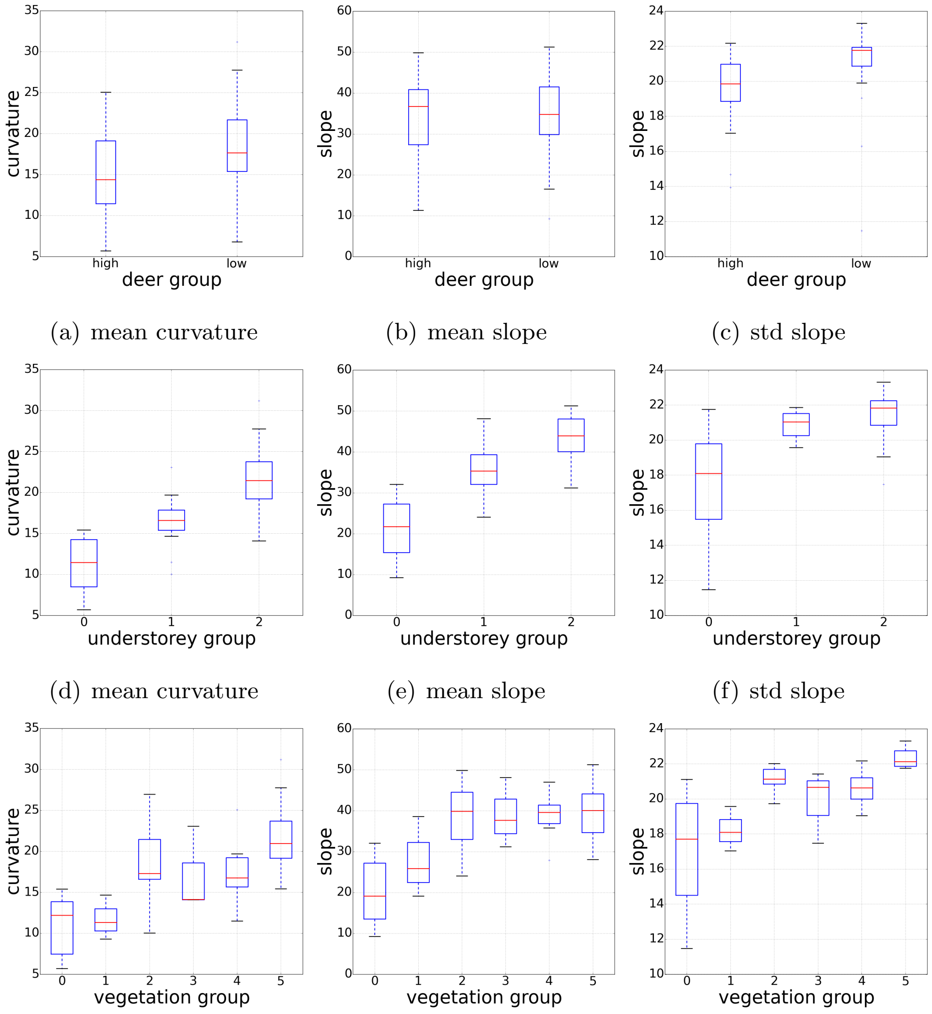

(a) mean curvature (b) mean slope (c) std slope

(d) mean curvature (e) mean slope (f) std slope

(g) mean curvature (h) mean slope (i) std slope

Figure 6.15: Deer density does not show any significant difference in the results for mean curvature (a), mean slope(b) or standard deviation of slope (c). Results for understorey cover show significant differences for mean curvature (d), mean slope (e) and mean standard deviation of slope (f). Results grouped by vegetation type also show significant differences between groups for mean curvature (g), mean slope (h) and standard deviation of slope (i).

Examining the full microtopography values across the plot sites (Appendix C.3 Table C.8) the results followed expectation with a relationship seen between increased vegetation levels and increased mean slope and curvature values. The plot site showing the smallest values for mean slope, mean curvature and mean standard deviation of slope was Ellenden with values of 9.2, 6.8 and 11.5 respectively. Ellenden shows very little understorey vegetation. In comparison Pole Lees 02 has mean slope, mean curvature and mean standard deviation of slope of 51.2, 31.2 and 23.3, respectively. Pole Lees 02 is classified as having high amounts of cover with tall, mixed vegetation. The differences in microtopgraphy surfaces for Ellenden and Pole Lees 02 can be seen in Figure 6.16.

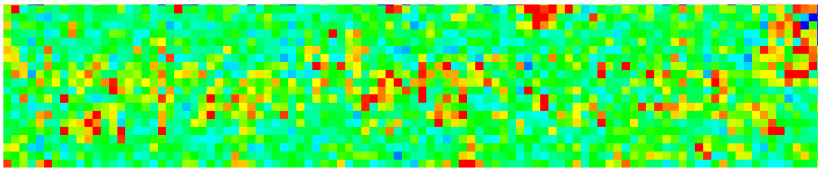

(a) slope

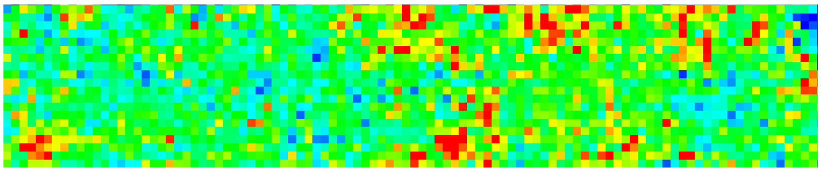

(b) curvature

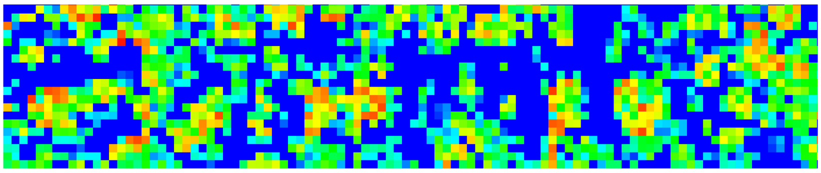

(c) slope

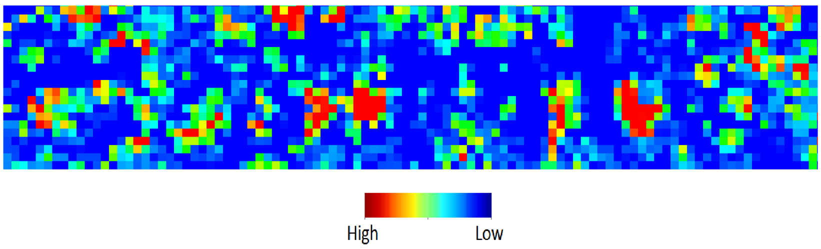

(d) curvature

Figure 6.16: The mean of slope and curvature (using a 50 cm moving window) show reduced values where very little understorey vegetation is present. Pole Lees 02 is classified as having tall, mixed vegetation and Ellenden Wood classified as having very little understorey vegetation. The difference in understorey characteristics between the two sites are visible in the moving window rasters for Pole Lees 02 (a - slope, b - curvature) and Ellenden (c - slope, d - curvature), where Ellenden shows reduced values compared to Pole Lees 02.

6.4 Discussion

6.4.1 Can TLS be used for the estimation of the horizontal distribution of understorey vegetation cover within forest plots?

The extraction of understorey cover estimates through TLS corresponds to qualitative assessments of understorey characteristics made from plot site photographs (Table 6.1). Through the use of 5 cm x 5 cm surface processing it may be possible to provide a much finer grade of cover estimates compared with the use of classification groups as outlined by Reich et al. (2012). TLS can also provide further understorey metrics such as total 3D surface and understorey volume, measurements that are not commonly collected using traditional methods.

It was seen that deer density did not have a significant effect on the estimation of understorey cover (2D and 3D) or volume as extracted from surface modelling. It was only through the use of understorey cover groups that a significant difference was seen within the results. This suggests that although deer may reduce understorey vegetation, they may not remove it completely. This follows results presented by Hegland et al. (2013) where herbivory caused an increase in low-level growth due to the removal of high growing vegetation

6.4.2 Are any novel understorey measurements available?

The novel use of 3D modelling across understorey vegetation layers, using methods similar to those developed for hydrology and geomorphology, was used to extract surface slope and curvature properties that identified relationships between understorey surfaces and vegetation type. Using microtopography estimates from understorey point clouds it was shown how those areas of low understorey complexity (with regards to understorey vegetation) showed decrease means of slope and curvature compared to plot sites with increased understorey complexity (Figure 6.16). This suggests that correlation between understorey structure (and therefore habitat type) and the microtopography of vegetation surfaces may be used for detailed assessment of understorey structural characteristics through TLS.

The results for microtopography showed a positive correspondence between both the slope and curvature values of understorey surfaces and the understorey cover and vegetation type (Figure 6.15). This suggests that as understorey cover increases and vegetation type moves from very little vegetation to mixed, tall vegetation, the slope and curvature of understorey surfaces change. This is to be expected as a flat surface (very little vegetation) would be expected to have slope and curvature values different to those for a surface with multiple objects (mixed vegetation).

The use of this novel extraction technique has the potential to increase the understanding of how the texture of forest surfaces (both at the ground level and further into the understorey) may affect forest communities. Ground level vegetation (and additional features such as woody debris) provides habitat and forage for multiple animal species (Sabatini et al., 2014) with understorey structure affecting animal-habitat associations. The spatial patterns within ground level vegetation can also provide information on processes operating within understorey communities (Scheller and Mladenoff, 2002). It is reasonable to think therefore that structural surfaces, being a product of the spatial patterns created by a combination of vegetation and forest objects, would also show correspondence with animal-habitat associations and understorey processes. Only through fine-scale 3D modelling of these surfaces will relationships be found, it is here that TLS has an important role.

Through the creation of understorey mircotopography surfaces (Figure 6.16) distinct areas of microtopography can be identified. An example being how in Figure 6.16d the majority of the site shows low slope values with small groupings of high slope values. These distinct zones of difference within the understorey microtopgraphic surface may provide information on how understorey processes operate within different forest sites. This is similar to how surface roughness estimates of forest canopies are used to model the interactions across the biosphere-atmosphere interface (Maurer et al., 2013).

This form of analysis using fine-scale assessment of different surfaces within the understorey is only possible through the use of high resolution 3D modelling and could not be performed using traditional forest ecology methods.

The use of TLS for understorey cover estimates also provides an opportunity to collect cover surveys throughout the year regardless of forest state. This is not the case using ALS as increased foliage levels during leaf-on seasons can reduce the accuracy of aerial cover estimates (Wing et al., 2012).

A source of error in TLS estimations of understorey cover is the presence of non-vegetation material within the surface used for area calculations. In this trial non-vegetation material was removed through the combination of different surfaces highlighting likely sources of solid material. Whilst removing stems that provide point returns up to a height of 1 m, the method was not as successful in removing non-vegetation materials at lower levels such as low lying branches or dead wood. The presence of this material was then included within the cover estimates resulting in a bias toward increased cover.

Figure 6.14 is representative of the error source of overestimation of cover for Ellenden wood. Non-vegetation material such as small stems and branches remain within the extracted cover surface after initial removal of likely non-vegetation material (Figure 6.14 (c)). This will bias the results towards over-estimation of cover. As this would be expected to occur in all plot sites, at this time the method may be best described as a relative cover estimation, or be taken with an appropriate awareness of error.

The vertical and horizontal geospatial components of forest structure are common measures recorded by forest ecologists when considering the 3D arrangement of forest. With the introduction of time, the 4D measurement of forest structure is possible. The following chapter will examine the use of TLS for the assessment of temporal change within forests.

Chapter 7

The use of terrestrial laser scanning for assessment of temporal change within forest understorey

7.1 Introduction

Forests are composed of multiple structural and functional components that combine to create unique habitats fuelling forest biodiversity and productivity (Paquette and Messier, 2011). These components are highly complex and are in a constant state of change. Structural and compositional changes occur within forests in different ways as forests mature. These include the progressive alteration of forest structure known as succession (from the initial stages, where fast growing saplings struggle for resources, to the dominance of stable, large trees) and cyclical change where plant communities return in the same place at intervals (Grime, 2006). Temporal changes within forests are hugely important to multiple forest characteristics such as biomass, productivity and diversity (Shugart, 1984). For this reason the study of change in forests is of fundamental importance to forest ecology (Pickett et al., 1987; Connell and Slatyer, 1977).

Temporal changes are influenced by any number of factors such as light availability, soil composition and water availability. In addition, structural and compositional changes within forest can also be brought about by disturbances within a forest including logging, storm damage, browsing or fire.

Change within forest can be considered at multiple temporal scales along the successional sequence, including: (1) the relatively brief life-cycles of grasses and wildflowers soon after a disturbance; (2) fast growth of sun-seeking pioneer species (first trees to grow after a disturbance); and (3) slow growth of long-lived late successional species. As a forest moves along the successional sequence, disturbances may occur that have the effect of reversing succession, such as when a storm fells large, late-successional species creating canopy space and increasing light penetration. In contrast, management practices or pest infestations may accelerate succession, such as through the removal of pioneer species which encourages late-successional species growth.

In addition to temporal change defined by movement along the successional sequence, cyclical changes brought about by seasonal variations are an important factor when considering temporal dynamics of forest ecosystems. Examples include the seasonal variation of species richness and diversity seen within the herbaceous understorey (Murphy and McCarthy, 2014) and the variability of understorey light availability due to seasonal patterns (Ross et al., 1986; Messier et al., 1998). Seasonal variations within the structural components of forests include the decrease in leaf area index (LAI) observed in deciduous forests caused by leaf abscission and the reduction of material within the herbaceous layer during the winter months.

Temporal variations in forests have been assessed in numerous ways using traditional survey methods including estimates from forest inventory surveys (Vanderwel et al., 2013), direct field measurements at sample plots (Fang et al., 2001; Hember et al., 2012) and tree ring cores (Río et al., 2014). These methods have primarily focused on the growth rate of trees from which further measures were extracted such as production and carbon storage. These surveys can be considered to be at a single tree to plot level spatial scale, and as focusing on the slow growth of long-lived late successional species. Furthermore, field data are commonly collected no more than once a year (low temporal resolution).

Multiple larger scale temporal assessment surveys (regional to global) have recently been performed using aerial and satellite remote sensing. These include assessing phenology within temperate forests (White et al., 2014; Guyon et al., 2014; Liu et al., 2015), biomass estimations (Goetz and Dubayah, 2011; Réjou-Méchain et al., 2015) and forest stability and disturbance assessments (Keersmaecker et al., 2014). Remotely sensed data collected by orbiting satellites can have the advantage of relatively short breaks between acquisition leading to high temporal resolution. For example, studies using Landsat imagery (**e.g. fu2014estimating**) can employ data sets collected every 14 days to build fine-scale temporal models.

Terrestrial laser scanning (TLS) has the advantage of collecting data below the canopy and at high resolution (millimetre accuracy and point spacing achievable). Liang et al. (2012) presented a method for fully automated change detection in forests using TLS data where 90% of stems that had been harvested were automatically detected between temporal scans. This study concluded that TLS offered an effective method for assessing forest growth and mortality rates. Kaasalainen et al. (2014) demonstrated how TLS could be used for detecting quantitative change in tree biomass, volume and structure, showing that changes in tree branching structure can be reproduced with about ±10% accuracy. Griebel et al. (2015) tested the use of a low cost TLS for estimating plant area index (PAI) (defined as the single sided plant area per unit ground area), with daily scans being taken over a period of two years. Results from this trial showed strong agreement when compared with monthly hemispherical images (± 0.1 PAI) and concluded that collecting three-dimensional laser scan data had strong advantages over traditional two-dimensional PAI estimations.

The work undertaken so far using TLS for temporal change detection in forests has primarily focused on forestry applications assessing timber and tree variations. It is difficult to find research relating to temporal change assessment using TLS of forest specifically targeted at forest ecology surveys within the understorey, such as characterising foliage levels or changes within the vegetation layer. Gupta et al. (2015) investigated the use of TLS for measuring the effects of fire damage on understorey vegetation through the estimation of above ground height. The study concluded that the method provided a novel approach to understorey mapping when assessing change within forest plots, but it did not present measures of forest structure relevant to forest ecologists.

The aim of this study was to address the questions: Can TLS be used to measure temporal change within the understorey for applications in forest ecology? (2) if so, what are the requirements for understorey temporal surveying (work flows)? and (3) are any novel temporal assessments available?

It was expected that the seasonal changes seen within forest structure (reduction of understorey and foliage material in winter) would be present within the TLS extracted data sets.

7.2 Methods

Through construction of a permanent trial site the application of TLS for temporal assessment of forest could be tested. Using the structural assessment methods outlined previously in Chapters 4, 5 and 6, the vertical component, understorey density profiles and understorey cover estimates were calculated for three surveys carried out over the length of a year. The temporal surveys took place in summer (leaf-on), winter (leaf-off) and the following summer (leaf-on).

Using surface deformation monitoring techniques commonly applied in fields including geomorphology (Wilkinson et al., 2015) and engineering geology (Hu et al., 2015), novel temporal change assessment within the understorey vegetation layer were conducted. Through the use of temporal microtopographic surfaces, deformation maps (which in this application may be described as understorey vegetation change maps) were generated to help describe the structural changes seen in understorey vegetation.

7.2.1 Site description

Permanent TLS survey subplots were installed within a previously constructed ecological survey area in Kirton Wood (SSSI), Nottinghamshire. Full details of the site can be found in Chapter 3.

7.2.2 Permanent survey plots

For this trial three permanent TLS survey subplots were established within the previously constructed ecological survey area at Kirton Wood. The three trial subplots were chosen to be non-contiguous allowing for work to be completed with minimal trampling. To reduce disturbance within the ecological survey area the subplots were selected as the corner grids of the existing ecological survey site (Figure 7.1).

Permanent survey control points were installed at each subplot to allow the accurate transformation of laser scan point clouds into the same coordinate reference system (CRS) at each survey location. With each subplot having its own CRS, direct comparison between temporal surveys was possible.

For the permanent control points two earth anchor markers were buried at each subplot to a depth of 0.5 m (Figure 7.2). One marker was positioned in the centre of each subplot and one outside at a distance of approximately 1.5 m from the edge. The use of tripod mounted FARO traverse spheres positioned over the

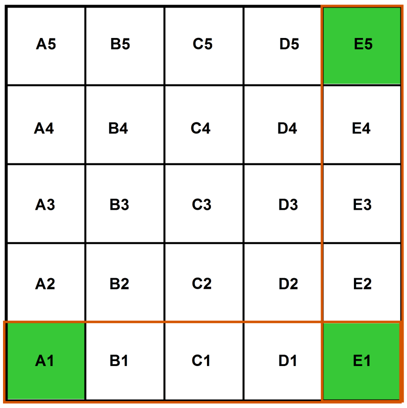

Figure 7.1: Ecological survey area within Kirton Wood.
Existing grid squares with laser scan test sites coloured green. The survey area measures 50 by 50 m (general location details given in Chapter 3, Figure 3.1).

control points allowed for the accurate location of the permanent markers within the temporal laser scan point clouds.

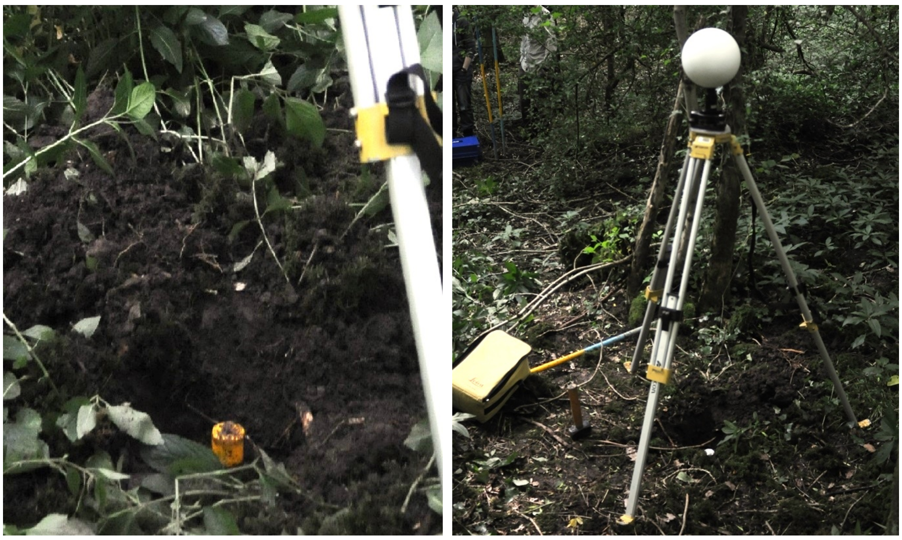

(a) ground anchor (b) tripod mounted survey sphere

Figure 7.2: Temporal surveying was made possible through the installation of permanent survey ground markers (a) and the use of tripod mounted target spheres (b), allowing independent laser scans to be transformed into the same coordinate reference system.

7.2.3 Data collection

The laser scan data used for this trial were collected over a twelve month period from June 2013 to June 2014. Data were collected during three survey visits encompassing seasonal change: (1) summer (27 June 2013); (2) winter (21

February 2014); and (3) summer (25 June 2014).

Survey data were collected using a FARO Focus 3D (120) TLS instrument. Full specifications can be found in Chapter 3. For referencing of scans two FARO traverse spheres were used. The traverse spheres are large (ø 100 mm), painted with a matt reflective paint (giving a very strong return value) and can be tribrach (a survey grade bracket) mounted on tripods allowing for accurate positioning and levelling over known points.

7.2.4 Data transformation

In ecological surveys the fundamental vertical datum is the ground surface, with estimates of tree height and understorey depth given as the height above ground. When assessing temporal surveys for ecological studies in this trial a single digital terrain model (DTM) for each subplot provided the most effective way of assessing temporal change with respect to the ground surface.

Generation of accurate DTM surfaces from TLS surveys is dependent on the density of the vegetation at the survey site, with thick vegetation obscuring the ground and increasing the likelihood of errors in the terrain surface (Fan et al., 2014; Jalonen et al., 2015). With vegetation levels decreased in winter, the winter survey was considered the most appropriate temporal scan to use for the creation of a DTM in this study.

To allow the accurate transformation of all surveys into the CRS of the winter survey, the centroid coordinates of the FARO traverse target spheres were used as fixed points between scans, with the targets being accurately positioned over the ground control for every survey. FARO Scene software (Pueschel, 2013) was used to model the traverse spheres in the winter survey and extract the XY planar coordinates of the centroid. These coordinates were then used as known points for the centroid of the corresponding sphere in both the summer surveys.

To determine the height of the target spheres a height hook measuring tape was used to obtain the height of the tribrach above the ground anchor. This was then added to a fixed distance from tribrach to sphere to provide a value for the height of the sphere centroid above the ground anchor (Figure 7.3). In this way the coordinates of the centroid of the target spheres from all temporal surveys were determined in the same CRS. Registration was then performed using FARO Scene (Figure 7.4).

All surveys were registered with only minor errors. Baseline distances between registration spheres positioned over the fixed ground anchors were measured and

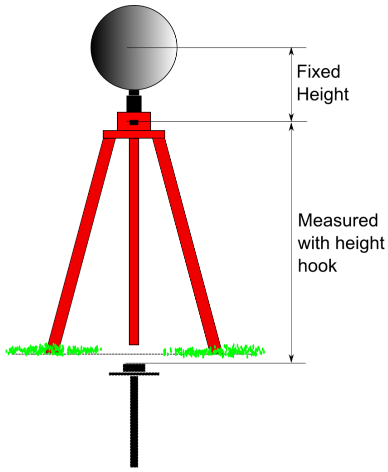

Figure 7.3: Measuring the height of the target centroid above the ground anchor.

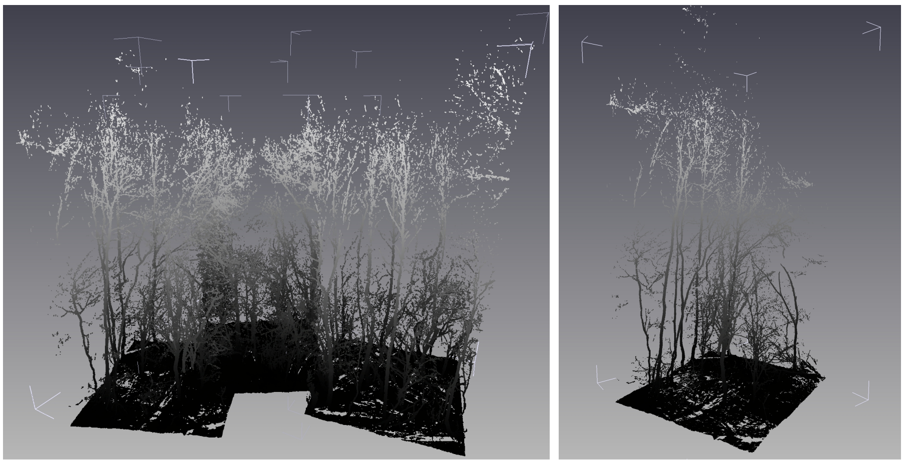

(a) individual seasonal surveys

(b) a single CRS containing all three seasonal surveys

Figure 7.4: Processing point clouds into the a single CRS allows for a common vertical datum to be used. Three surveys (winter, summer, winter) cannot be compared directly in their own, unique CRS (a). Combining the three surveys into a single CRS (b) allows for direct comparison between surveys.

compared for each survey (Table 7.1). The maximum error seen between target baselines distances was 7 mm with the maximum standard deviation of the baseline distance being 4 mm. The registration errors seen within all temporal surveys fall within acceptable levels, with 7 mm planimetric errors not considered significant in ecological studies when positioning stems (Freeman and Ford, 2002).

Table 7.1: Errors within baseline distances between control points for different surveys. The maximum error was 7 mm seen between summer 2013 and summer 2014 survey in plot A1.

sub plot	control point baseline distance (m)			std (m)
	summer 2013	winter 2014	summer 2014	
A1	6.125	6.129	6.132	0.004
E1	10.092	10.090	10.090	0.001
E5	7.268	7.267	7.262	0.003

With all subplot point clouds transformed to the same CRS, voxelisation and correction to the DTM were carried out using the methods outlined in Chapter 3.

7.2.5 Data processing

The data processing steps used here for assessing vertical component, understorey density and understorey cover follow the methods outlined previously in Chapters 4, 5 and 6, respectively. Data were processed for each survey with temporal assessments carried out using these results.

For the assessment of novel understorey vegetation change maps, a series of surface difference calculations were performed between temporal surveys at individual subplots. The source data for the change maps were the triangulated irregular network (TIN) data sets created as part of the understorey cover estimates. Using the 3D Analyst library within ESRI ArcMap (Reuter and Nelson, 2009), surface difference maps were created describing areas where the TIN surface had: (1) decreased; (2) increased; and (3) remained the same between temporal surveys.

7.2.6 Analysis

The data analysis steps used here for assessing the vertical component, understorey density and understorey cover follow the analysis methods outlined previously in Chapters 4, 5 and 6, respectively.

7.3 Results

7.3.1 Vertical to non-vertical index

All data were processed across height bands 50-200 cm. The temporal surveys are labelled as summer 2013 (I), winter 2014 (II) and summer 2014 (III).

The surveys taken during winter 2014 at plots A1, E1 and E5 show decreased VNVI values when compared to those from the summer 2013 survey (Table 7.2), representative of an decrease in the relative amount of non-vertical (foliage) material during the winter survey.

The VNVI values increase from winter 2014 to summer 2014 for subplots E1 and E5, this represents an increase in the relative amount of non-vertical (foliage) material. When looking at the winter 2014 and summer 2014 survey for plot A1, the increase in VNVI is not observed. For this survey the mean VNVI values for summer and winter were -0.439 and -0.417 respectively, showing the summer survey tending towards vertical dominance.

For all subplots the highest values of VNVI were seen within the summer 2013 survey (Figure 7.5), representative of an increase in foliage amount during the summer 2013 survey.

Table 7.2: VNVI values across temporal surveys for trial plots A1, E1 and E5. Extracted values (min, max, mean, std) are for 10 cm height bands within the 50-200 cm analysis zone.

survey	subplot	min VNVI	max VNVI	mean VNVI	std VNVI
Summer 2013	A1	-0.509	0.027	-0.276	0.181
	E1	0.078	0.697	0.260	0.136
	E5	0.010	0.628	0.277	0.163
Winter 2014	A1	-0.582	-0.274	-0.417	0.094
	E1	-0.447	-0.090	-0.270	0.101
	E5	-0.531	-0.164	-0.359	0.120
Summer 2014	A1	-0.677	-0.193	-0.439	0.151
	E1	-0.130	0.263	0.015	0.113
	E5	-0.026	0.379	0.155	0.108

7.3.2 Understorey density profile

The understorey density profiles across all three subplots show the winter 2014 survey as producing a decrease in material observed compared against the summer 2013 and 2014 surveys (Figure 7.6). Both subplots A1 and E1 show maximum density of material within the summer 2014 survey. Subplot E5 shows

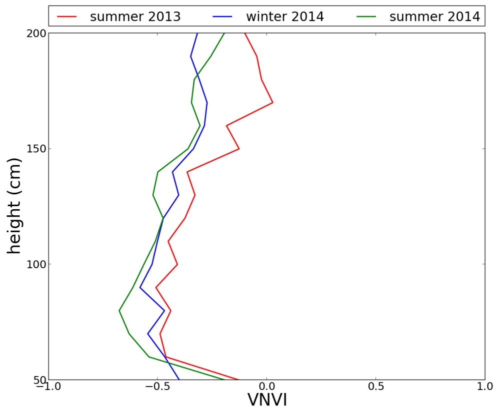

(a) subplot A1

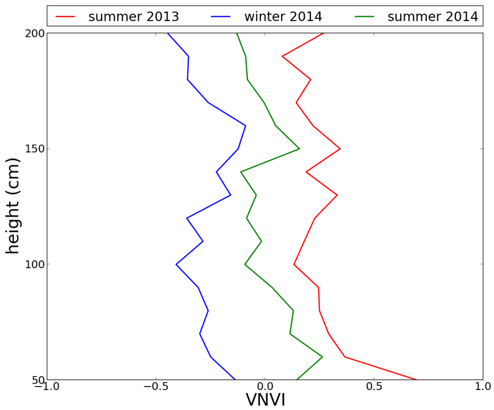

(b) subplot E1

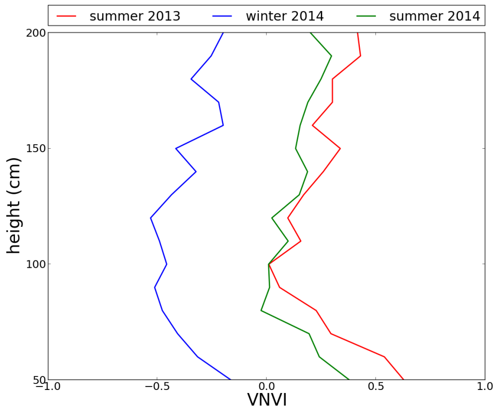

(c) subplot E5

Figure 7.5: Temporal assessment of the vertical to non-vertical ratio for individual subplots shows that the winter 2014 survey shows a tendency towards dominance of vertical components in subplots E1 and E5 when compared to summer 2013 and summer 2014 surveys. Subplot A1 shows decreased variation between seasonal surveys when compared against subplots E1 and E5.

summer 2013 having the maximum density values.

All three subplots show similar adjusted returns across temporal surveys from 150 cm down to where understorey vegetation starts. This is at approximately 40 cm, 60 cm and 60 cm for subplots A1, E1 and E5 respectively. Below this height there is a clear increase in understorey density of objects in the summer surveys compared against winter.

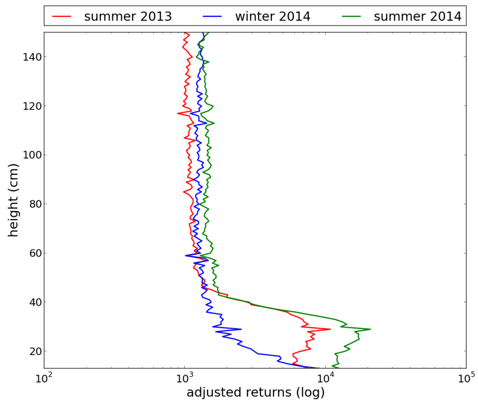

(a) subplot A1

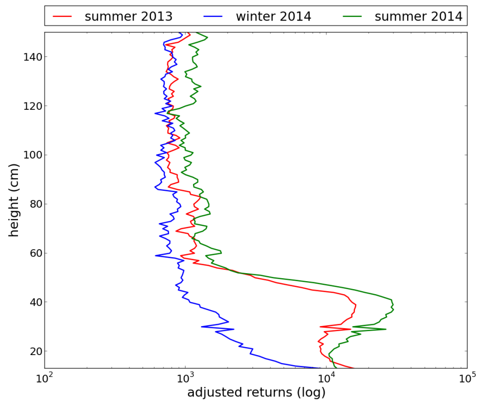

(b) subplot E1

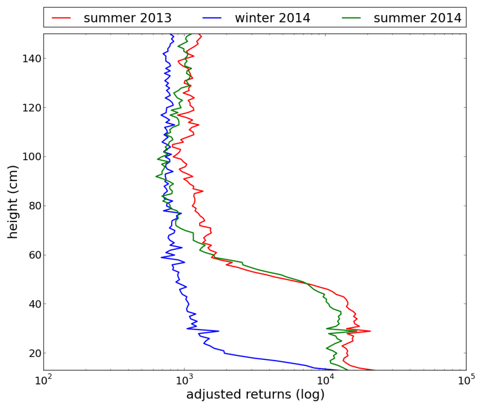

(c) subplot E5

Figure 7.6: Understorey density profiles for individual subplots over temporal surveys show that the winter and summer surveys have similar point return numbers from 60-150 cm. Below 60 cm the summer surveys show a sharp increase in point returns (density), indicative of increased vegetation close to the ground level during the summer.

7.3.3 Understorey cover

Results for the understorey 2D area, 3D area and volume estimates can be seen in Table 7.3 and Figure 7.7. For all subplots the 2D area, 3D area and volume estimates are greatly reduced in the winter 2014 survey compared against both summer surveys. Subplots E1 and E5 show similar 2D area, 3D area and volume estimates estimates for summer 2013 and summer 2014, with subplot A1 showing an increase in 2D area, 3D area and volume estimates between summer 2013 and 2014.

Table 7.3: Understorey cover estimates for temporal surveys across trial plots A1, E1 and E5.

survey	subplot	area 2D (m^2)	area 3D (m^2)	volume (m^3)
Summer 2013	A1	47.8	196.7	8.4
	E1	72.2	339.8	18.0
	E5	74.6	349.1	18.2
Winter 2014	A1	12.7	48.0	1.5
	E1	18.6	71.9	2.0
	E5	17.5	56.4	1.7
Summer 2014	A1	62.4	228.7	11.6
	E1	77.7	335.0	20.0
	E5	75.4	343.8	17.3

7.3.4 Understorey microtopography

Results for the microtopography analysis can be seen in Figures 7.8 and 7.9. There is a reduction in the mean of slope values in winter 2014 compared against both summer surveys. Whereas, the standard deviation of slope values remains similar across all surveys for all three subplots, suggesting surface roughness does not change between surveys.

Temporal volume changes as calculated from the microtoplogy surfaces can be seen in Table 7.4. Here it is seen that 3D volumes as described by the surface all decrease from summer 2013 to winter 2014 and then increase from winter 2014 to summer 2014. Surface change maps showing net gain and net loss over time for all subplots are shown in Figure 7.10. from these it was seen that from summer to winter there was an overall net loss of material and from winter to summer there was a net gain. From summer to summer there were equal areas of net gain and loss.

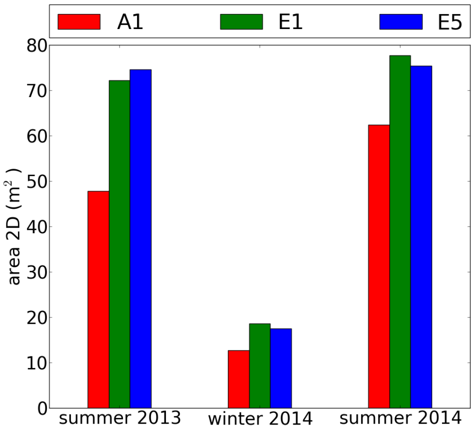

(a) Area 2D

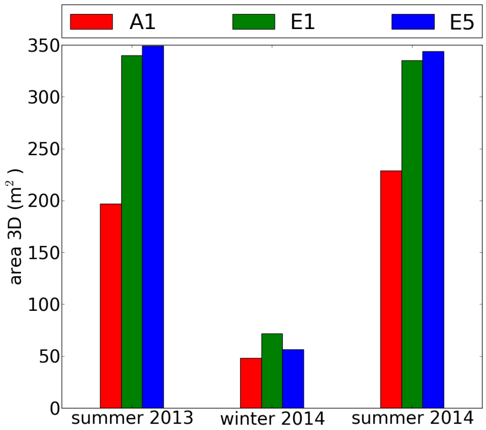

(b) Area 3D

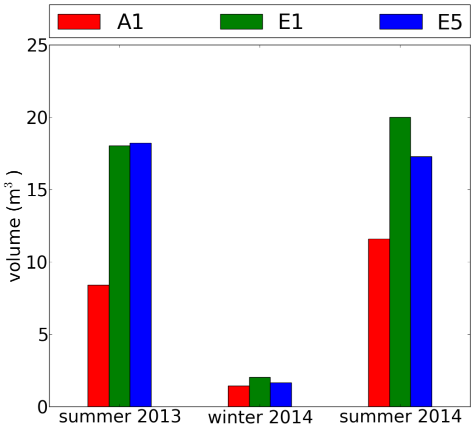

(c) Volume

Figure 7.7: 2D area, 3D area and volume results for all subplots show reduced values for the winter survey when compared against the summer surveys, indicative of a decrease in vegetation material within the understorey during the winter.

Table 7.4: Volume changes for temporal surveys across trial plots A1, E1 and E5.

survey comparison	subplot	volume change (m^3)
summer 2013 to winter 2014	A1	-6.885
	E1	-15.907
	E5	-16.509
winter 2014 to summer 2014	A1	+10.109
	E1	+17.939
	E5	+15.532
summer 2013 to summer 2014	A1	+3.182
	E1	+2.006
	E5	-0.992

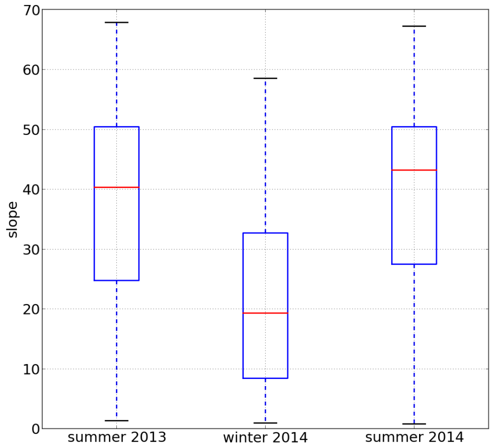

(a) subplot A1

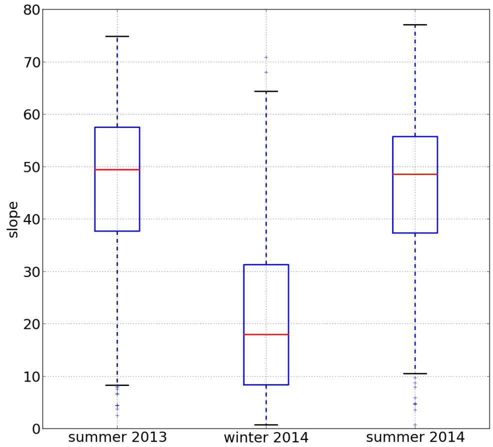

(b) subplot E1

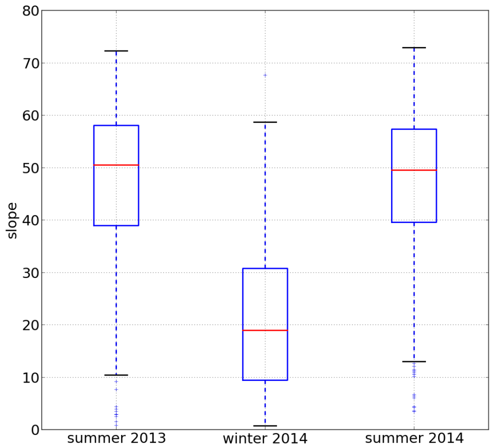

(c) subplot E5

Figure 7.8: Mean of slope values across different subplots (A1, E1, E5) grouped by survey all show a significant difference in the mean slope values between the summer and winter surveys. This is indicative of different microtopographic properties between summer and winter.

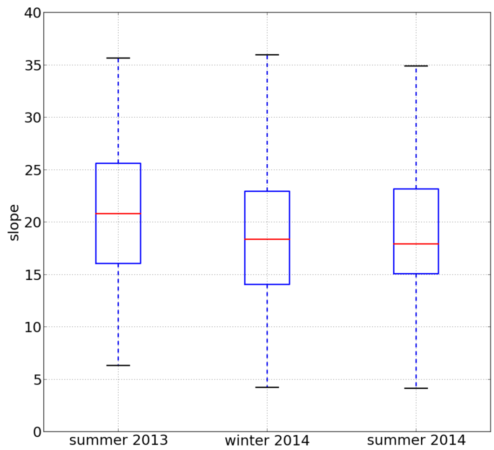

(a) subplot A1

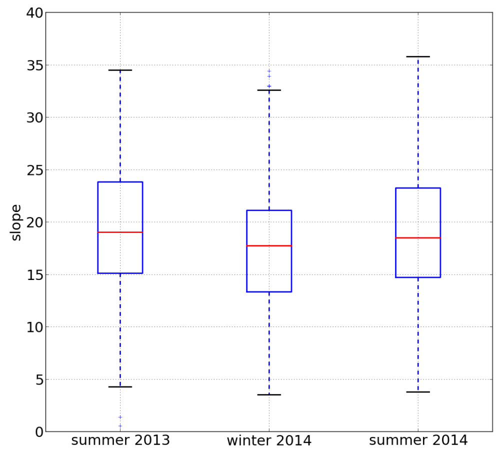

(b) subplot E1

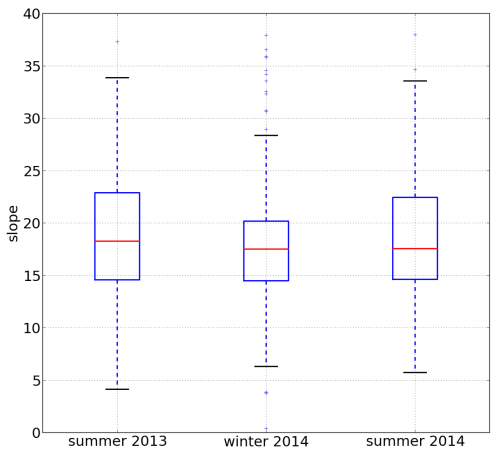

(c) subplot E5

Figure 7.9: Standard deviation of slope values across different subplots (A1, E1, E5) grouped by survey do not show a significant difference in the standard deviation of slope values between the summer and winter surveys. This is indicative of similar surface roughness properties across seasonal surveys.

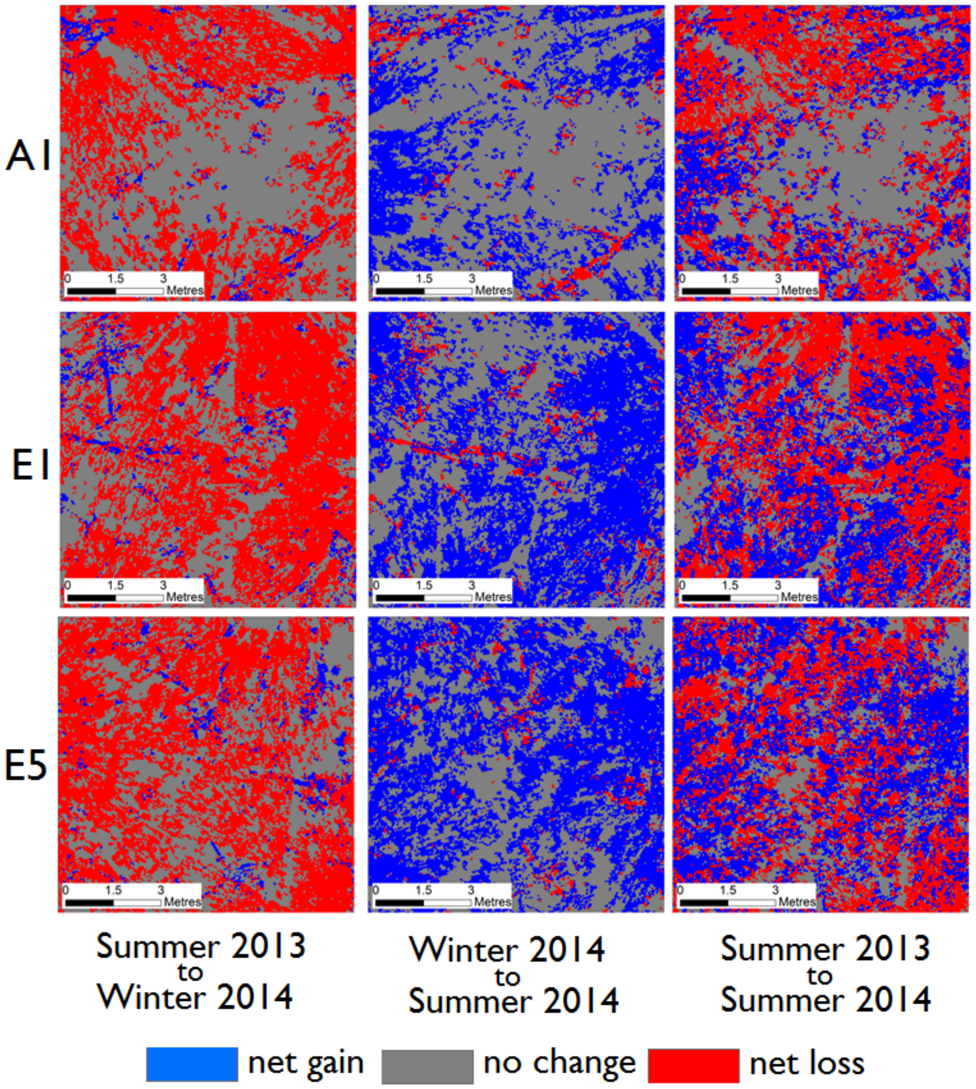

Figure 7.10: Understorey change maps for subplots with comparisons between summer 2013 and winter 2014, winter 2014 and summer 2014, and summer 2013 and summer 2014. Between summer and winter surveys an overall net loss is seen. Between winter and summer surveys an overall net gain is seen. Summer to summer surveys show equal gain and loss of material.

7.4 Discussion

7.4.1 Can TLS be used to measure temporal change within the understorey for applications in forest ecology?

TLS data collected in a dedicated survey plot using permanent ground control have been used to measure temporal change within the vertical component, understorey density and vegetation cover of forest plots. As Griebel et al. (2015) noted, TLS offers clear advantages over traditional methods of temporal forest survey through its ability to collect 3D data. This approach offers a relatively quick, efficient, non-destructive assessment. The use of a standardised methodology, utilising a common digital terrain model (DTM) and fixed ground control across all temporal surveys, as described here, provides a framework from which further data can be acquired.

All of the results showed correspondence between season of survey and structural features extracted through TLS. The estimations of understorey vertical components, vegetation density and cover all followed expectations of a reduction in foliage and ground level growth during the winter due to leaf abscission and vegetation die back. This can be seen in the reduction in mean vertical to non-vertical index, mean understorey point returns and cover estimates within the winter survey when compared against both summer surveys. This highlights the potential of TLS to provide new analysis techniques for the assessment of structural change with time, relevant to forest ecology studies.

Once permanent control has been installed the TLS method can provide a much finer temporal scale for forest surveys, where traditional temporal surveys using tree cores or diameter measurements are not taken more than once a year (Fang et al., 2001; Hember et al., 2012; Río et al., 2014).

Looking at the results for VNVI extraction there is a clear reduction in the non-vertical component during the winter survey when compared to the summer surveys for subplots E1 and E5. Subplot A1 shows similar VNVI values across all three temporal surveys. This raises the question, what is causing the vertical component to remain the same within subplot A1 across the temporal surveys. Potential reasons include: (1) increased vertical proportion caused by increased non-vertical material within vertical voxels; or (2) increased vertical proportion caused by low quantities of non-vertical material. The first possibility implies the result is a methodological artifact and cannot be excluded. The second possibility is that the result is a consequence of differences in non-vertical component within subplot A1 compared to subplots E1 and E5.

Examining the understorey density profiles from adjusted point counts (Figure 7.6), the difference between subplots A1, E1 and E5 identified in VNVI assessment is not present. With adjusted point count remaining similar across all subplots and temporal surveys, this shows there wasn't an increase in the volume of objects within subplot A1 during the summer survey when compared against subplots E1 and E5. With similar object densities (adjusted return counts) within all point clouds, it is sensible to assume that VNVI similarities seen in plot A1 are due to differences in non-vertical component. If the decrease in VNVI within summer surveys was due to an increase in non-vertical material within vertical voxels, a corresponding increase in return count would also be expected.

7.4.2 What are the requirements for understorey temporal surveying?

The trial outlined here used permanent control markers to provide common points between temporal surveys. It is the use of accurate ground control that provides confidence in the temporal assessment.

An alternative method of referencing scan data to the same CRS was considered (the iterative closest point (ICP) algorithm). This process uses common surface geometry within scan data sets to provide fixed points used for registration and is commonly used for mobile laser scanning systems (Ryding et al., 2015). This was not chosen for this trial however, as using surface geometry to reference data was not thought to be a practical solution when it was the movement of surface geometry (due to temporal change) that was being assessed.

Errors in digital terrain models can be caused by dense vegetation. These errors would then propagate into any analysis based on heights derived from the DTM. Through using a single DTM generated in winter and transforming all summer data into this system, the errors caused by dense vegetation would be reduced. This method does introduce possible transformation errors when bringing all data into the a common coordinate reference system (CRS). Based on existing studies on DTM errors due to vegetation (Fan et al., 2014; Jalonen et al., 2015) and those examining transformation errors in point clouds (Becerik-Gerber et al., 2011), it was felt that the minimum error would be introduced through transformation errors, if care was taken to position the targets accurately at each survey.

7.4.3 Are any novel temporal assessments available?

Using a TLS approach allows for the fine scale measurement of structure in forest vegetation with respect to cyclical changes brought about by the seasons. This includes the novel creation of temporal change maps (Figure 7.10) to the decimetre level. These change maps show an increased resolution of cover estimates compared to traditional methods of cover assessment, such as the classification groups outlined by Reich et al. (2012), but also offer possible insights into how understorey vegetation changes within a trial site. This can be seen in the change maps and understorey volume differences produced between the summer surveys (Figure 7.10 and Table 7.4), where the change maps can be used to identify areas of net loss and gain of material between temporal surveys.

This form of temporal assessment within forests would be far too time-consuming and costly to consider using traditional ecology survey methods. In this trial temporal change maps were created that describe the areas of relative vegetation growth and reduction across temporal surveys.

The development of a work flow for temporal surveys using TLS allows for a standardised method of assessing change within forest plots. The extent of these temporal surveys is still limited to small-scale plot sites. Introducing new methods of TLS data collection may allow for increased areas of forest to be surveyed. The following chapter examines the novel use of handheld mobile laser scanning (HMLS) for the rapid collection of forest point cloud data, greatly increasing survey speed and resulting in an increase in the point cloud coverage.

Chapter 8

Using handheld mobile laser scanning for forest surveys

8.1 Introduction[1]

Recent improvements in the speed, accuracy and affordability of terrestrial laser scanning (TLS) systems have opened the possibility of major enhancements to existing studies by providing detailed information on three-dimensional forest structures (Leeuwen and Nieuwenhuis, 2010). This can be achieved by combining the results of multiple scans to recreate complex habitats (Lovell et al., 2011; Dassot et al., 2011). Such new tools allow replicable controlled measures of many forest features relevant to ecologists, environmental scientists and foresters, including the dimensions and heterogeneity of canopies, size and distribution of canopy gaps, leaf area index (LAI – leaf area per unit ground area) and total surface area of stems and leaves.

At the present time TLS, while demonstrating the potential of the technology, has been typically used for the measurement of small-scale sample plots within larger woodland sites. An obstacle to the uptake of TLS for larger-scale forest monitoring projects is the time and costs associated with building point clouds of sufficient size to adequately describe the forest environment. With line-of-sight often limited to several metres, multiple scan locations are required to produce data sets that can be used for accurate feature extraction (Watt and Donoghue, 2005). This limitation means that a TLS generated point cloud describing an entire woodland plot of a substantial size is currently too time-consuming and

[1]This chapter has been modified from Ryding et al. (2015)

costly to be considered.

Mobile laser scanning (MLS) systems offer a potential solution to the problem of creating ground-based point clouds with the necessary geospatial extent whilst maintaining accuracy (Pueschel et al., 2013) and minimising time and cost. MLS is a technology that uses a navigation module to determine the position of a laser whilst the laser takes measurements of the environment. A typical MLS system combines a laser scanning instrument, a moving platform and a positioning and navigation device such as a Global Navigation Satellite System (GNSS) receiver and inertial measurement unit (IMU). This configuration limits their use to relatively open environments such as highways and infrastructure corridors. MLS also often contain large, heavy equipment normally making them only suitable for vehicle mounted operation and as such they are currently predominantly mounted on road vehicles for urban mapping (Holopainen et al., 2013), although all-terrain vehicles have also been tested for the mapping of forests (Yang et al., 2013a). Liang et al. (2014b,a) have also demonstrated a MLS instrument mounted on an all-terrain vehicle and as a backpack-carried personal laser scanning system (PLS) for use within forest plots.

In this study the potential for handheld mobile laser scanning (HMLS) to provide point clouds of similar precision and accuracy to those currently being produced through TLS applications was explored. An assessment of laser scan survey times when compared against the field survey method was also carried out. The survey was completed in a complex, semi-natural woodland stand rather than managed woodland with roads and paths running through it.

The aim of this proof of concept study was to address four main questions: (1) Can TLS measurements of forests be replicated using HMLS? (2) does the use of HMLS provide any advantages in practical ease over TLS or field survey methods? (3) are any novel measurements available? and (4) what are the remaining challenges for the application of HMLS in forest monitoring.

8.2 Methods

8.2.1 Instrumentation

The FARO Focus 3D TLS instrument and ZEB1 HMLS instrument were used during this trial. See Section 3 for full instrumentation details.

8.2.2 Site description

All data were collected at the permanent survey plot within Kirton Wood (SSSI), Nottinghamshire. See Chapter 3 for full site details.

For this trial three permanent laser scan survey subplots were established within the previously constructed ecological survey area at Kirton Wood. The three trial subplots were chosen to be non-contiguous allowing for work to be completed with minimal trampling. To reduce disturbance within the ecological survey area the subplots were selected as the corner grids of the existing ecological survey site (Figure 8.1).

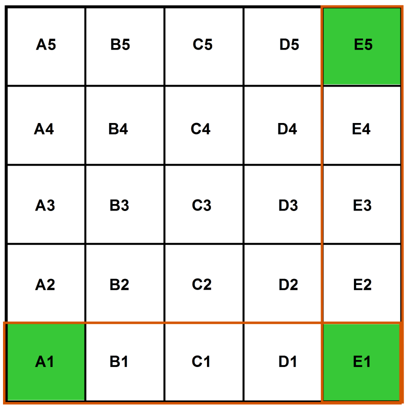

Figure 8.1: Ecological survey area within Kirton Wood.
Existing grid squares with laser scan test sites coloured green. The survey area measures 50 by 50 m (general location details given in Chapter 3, Figure 3.1).

8.2.3 Data collection

Scans were taken using the methods outlined in Section 3.

Using these set up specifications an individual subplot area could be surveyed using the FARO Focus 3D in half an hour (not including set-up time). Whereas, using the ZEB1 a subplot could be surveyed in less than five minutes.

In addition to the three subplots surveyed using both instruments, the ZEB1 was also used to collect data between subplots A1 and E1 and between subplots E1 and E5, zones of approximately 500 m^2. These data sets were collected to appraise the ability of the handheld system to quickly produce large point clouds, with the same area estimated to need over four hours using the FARO Focus 3D. The trajectory path for this data collection between subplots E1 and E5 can be seen in Figure (8.2b).

The survey path taken during handheld surveying is critical when considering

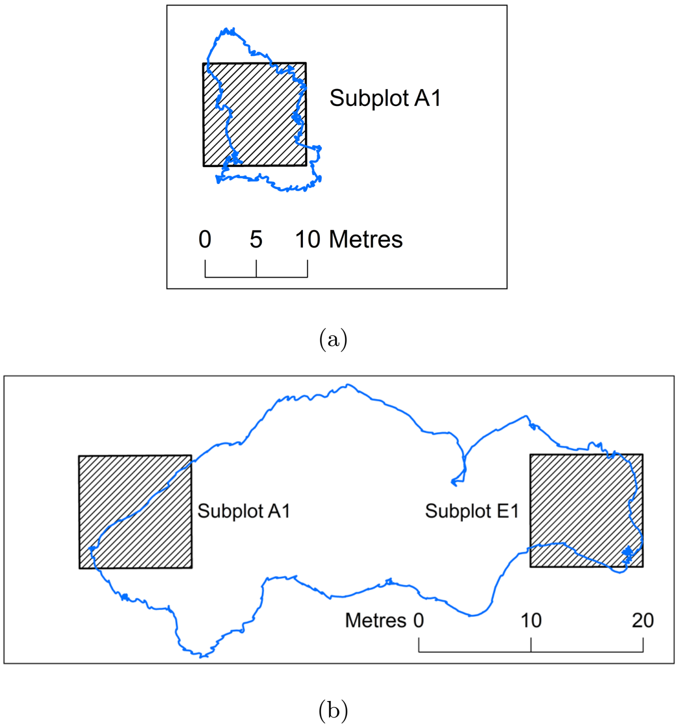

Figure 8.2: Trajectory for HMLS survey of (a) subplot A1 and (b) zone between subplots.

the usefulness of the method for producing point clouds of the required point accuracy and density. The manufacturers of the ZEB1 state a swath distance of no more than 30 m. In this trial a swath of 5.0 m was attempted within the subplot areas. Between subplots A1 and E1 the swath distance widened to 15 m, this was caused by dense understory and ground cover making it difficult to keep to a fixed survey line.

8.2.3.1 Traditional ecological survey methods

Data were collected one subplot at a time with a team of four ecologists working over two days in October 2008. Diameter at breast height (DBH) was recorded in mm using a standard measuring tape for every stem $\leq$ 1 cm. In addition to stem DBH, species and status (dead or alive) were also recorded. Stem positions were calculated using the method of intersection from measurements taken to two corner markers within each subplot.

8.2.4 Data processing

The data processing times are similar for both the FARO and ZEB1 once the point clouds have been produced. The FARO registration processing times will vary considerably dependent on influences such as density of woodland, location of targets *etc*. The ZEB1 registration processing is approximately equal to the data capture time.

8.2.4.1 FARO Focus 3D

For each sample plot the individual FARO scans were registered using the Scene laser scanner software (Pueschel, 2013). This is designed for registration and processing. Filters were used on the point cloud to remove any likely sources of noise or stray points. Any return with a reflectance value of less than 300 was removed from the data set, this value being the default filter used to remove point noise within the Scene software. Reflectance values for the FARO Focus 3D are given within the range 0 to 2047, which is manufacturer-dependent. Additionally, for each scan return a distance from a point to its nearest neighbours within the surrounding area was determined. If over 50% of a point's neighbouring returns were at a range of more than 2 cm the return was classified as an outlier and removed. This is a standard filter used within Scene software for the removal of stray points.

8.2.4.2 ZEB1

Once the data had been captured using the ZEB1, they were uploaded to the 3D Laser Mapping (3DLaserMapping, 2016) secure servers for processing. The data were processed on the servers at a timing ratio of 1:1, with five minutes of data collection taking five minutes to process. The data processing is charged on a pay-as-you-go basis, based on the distance travelled during data collection. Subplot A1 was processed online at a cost of £6.08, with the total online processing for this trial costing £47.78 (cost in 2014). Once processed the data were downloaded in the .las delivery format, which is compatible with a variety of point cloud software. The returned data were in a local coordinate reference system (CRS) based on the start position of the survey.

A condition value along the ZEB1 survey path is also provided through the online processing. This is a value calculated during ZEB1 processing representing the correspondences created during the matching process and relates to the quality of the matching in the output point cloud. It takes into consideration the orientation and compatibility of the correspondences used and can be taken as an indication of how reliable the matching process has been throughout data collection. A poor condition is considered to be a value under 0.2. For this trial condition values ranged from 0.5 to 0.8 therefore the quality of the matched points was considered high.

8.2.4.3 Transformation to local coordinate reference system

For this study the local coordinate system of the ZEB1 point cloud became the reference for comparison with the FARO point cloud, allowing for direct comparison of the two lidar data sets within the same model space. To enable co-registration all points on the survey spheres from the ZEB1 point cloud were isolated and modelled enabling a centroid coordinate to be determined. This was completed using the Leica Cyclone software (Eitel et al., 2013). The centroid coordinates were then used as control points for registering the scans.

Results for the co-registration can be seen in Table 8.1. Subplots A1 and E1 show mean distance errors of 4 and 3 mm respectively, subplot E5 shows mean distance errors of 16 mm. Registration errors for the three subplots all fall within acceptable levels with 16 mm planimetric error not considered significant when positioning stems in ecological studies (Freeman and Ford, 2002). The variation in co-registration errors does however highlight the importance of redundancy when registering scans using targets (Becerik-Gerber et al., 2011; Alba and Scaioni, 2007). Only three common survey spheres could be modelled between scan locations for subplot E5, giving little redundancy, whereas for both subplots A1 and E1 five common survey spheres were successfully modelled.

Table 8.1: Co-registration errors using sphere centroid coordinates.

Subplot	No. control points	mean distance error (mm)	min distance error (mm)	max distance error (mm)
A1	5	4	2	6
E1	5	3	1	15
E5	3	16	9	40

8.2.5 Feature extraction

The process of surface creation and adjustment was automated through the use of a Python script utilising the spatial analyst library of ESRI Arcmap. This allowed the registered point cloud from both the FARO and ZEB1 data sets to be processed identically (Figure 8.3). A digital terrain model was created first and all heights adjusted to height above ground. Slices were taken through each subplot data set at heights from 1.2 m and 1.4 m. Stem mapping and DBH estimations were then performed on these 20 cm slices.

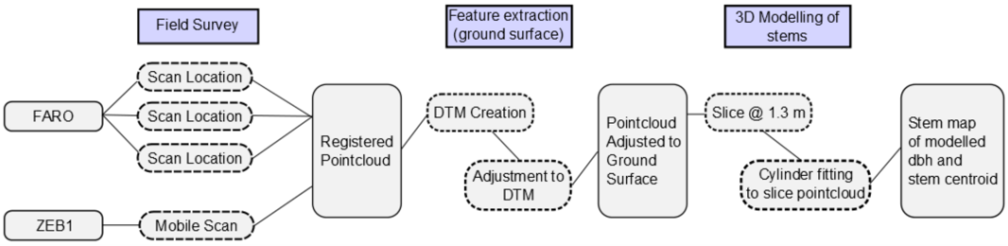

Figure 8.3: Workflow for data collection and processing during HMLS trial

Leica Cyclone software was used to model the stems from which centroid estimations and DBH values could be extracted. Using the sliced data sets, cylinders were fit to all stem objects for both FARO and ZEB1 data sets. This was a manual process. Each cylinder was then isolated and its DBH and centroid at 1.3 m above ground determined.

8.2.6 Comparison with historic field data

For comparison of laser scan derived values against the stem centroid and DBH estimations from 2D historic field data, a translation and rotation to align with the data sets was necessary. This was a manual process with identical translation and rotation values applied to both the ZEB1 and FARO data sets.

8.2.7 Analysis

For the analysis of results the ZEB1 dataset was evaluated against the FARO, which was considered to be the control model. This provides a direct comparison of the HMLS and TLS approaches to forest surveying. The time taken and resultant survey coverage for both laser scan methods and the field survey were also assessed.

The results of the stem modelling were assessed on objects that could be identified in the FARO data set. Omission differences are where stems are present in the control data set, but not in the model. Commission differences are those where stems are not present in the control, but are in the model (Desclée et al., 2006).

Accuracies of the stem mapping and DBH estimations were gauged using root mean squared error (RMSE), relative RMSE, bias and relative bias:

$$\text{RMSE} = \sqrt{\frac{\sum_{i=1}^{n}(X_{obs,i} - X_{control,i})^2}{n}} \tag{8.1}$$

$$\text{relative RMSE} = \frac{RMSE}{\bar{x}} \tag{8.2}$$

$$\text{Bias} = \frac{1}{n}\sum_{i=1}^{n}(X_{obs,i} - X_{control,i}) \tag{8.3}$$

$$\text{relative bias} = \frac{bias}{\bar{x}} \tag{8.4}$$

Where *obs,i* is the i$^{\text{th}}$ observation, *control,i* is the i$^{\text{th}}$ control, $\bar{x}$ is the mean of control values, and n is the number of estimations.

8.3 Results

8.3.1 Direct HMLS to TLS comparison

Using the FARO data set 54 stems were modelled across all three subplots with the minimum/maximum DBH estimates being 3 cm and 45 cm respectively. Using the ZEB1 data set 49 stems were modelled across all three subplots with minimum/maximum DBH estimates being 5 cm and 45 cm respectively (Table 8.2). This represents an omission difference of 9% for the ZEB1 compared to the FARO. The results of the DBH estimations and stem mapping can be seen in Tables 8.3 and 8.4 with point cloud comparisons in Figure 8.4 and the distribution of DBH estimation differences in Figure 8.5.

Table 8.2: Number of stems detected by ZEB1 and FARO

Subplot	FARO	ZEB1	omission difference (%)
A1	23	21	9
E1	13	12	8
E5	18	16	11

(a) (b) (c)

Figure 8.4: Point cloud comparisons for (a) FARO (b) ZEB1 and (c) combined data sets. Images show cross section of survey (10 m wide).

Table 8.3: RMSE results for diameter at breast height (dbh) and stem positioning (plan) using no filter, only examining stems with DBH >10 cm and stems with DBH <10 cm.

type	filter	RMSE (cm)				relative RMSE (%)			
		subplot				subplot			
		All	A1	E1	E5	All	A1	E1	E5
plan	none	3.1	2.6	3.1	3.5	-	-	-	-
plan	Ø > 10 cm	2.1	1.9	2.4	1.7	-	-	-	-
plan	Ø < 10 cm	3.9	3.2	4.5	4.3	-	-	-	-
dbh	none	2.9	3.5	2.9	1.9	23	29	20	17
dbh	Ø > 10 cm	1.5	1.5	1.8	0.9	9	9	11	5
dbh	Ø < 10 cm	3.9	4.8	4.8	2.3	46	69	75	33

Table 8.4: Bias results for diameter at breast height (dbh) and stem positioning (plan) using no filter, only examining stems with DBH >10 cm and stems with DBH <10 cm.

type	filter	bias (cm)				relative bias (%)			
		subplot				subplot			
		All	A1	E1	E5	All	A1	E1	E5
plan	none	2.3	2.0	2.5	2.3	-	-	-	-
plan	Ø >10 cm	1.7	1.5	2.1	1.5	-	-	-	-
plan	Ø <10 cm	2.8	2.6	3.7	2.8	-	-	-	-
dbh	none	0.3	0.5	0.3	0.0	2.4	4.6	2.2	-0.3
dbh	Ø >10 cm	0.9	-1.2	-0.7	-0.6	-5.6	-7.4	-4.4	-3.2
dbh	Ø <10 cm	1.6	2.5	3.4	0.3	19.5	35.6	53.6	4.3

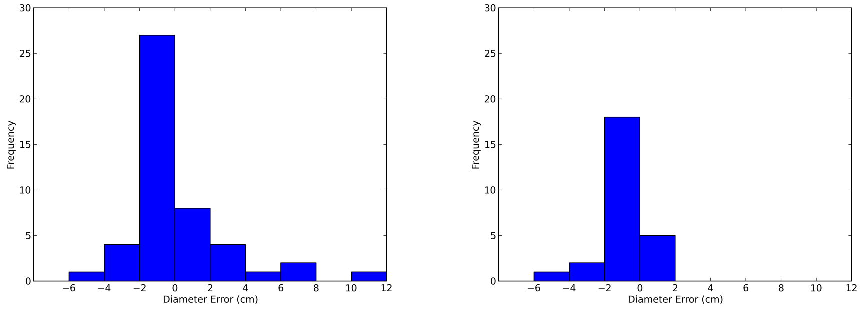

(a) (b)

Figure 8.5: Distribution of DBH estimation differences between ZEB1 and FARO values with (a) no filter and (b) DBH > 10 cm.

8.3.2 Comparison of laser scanning results against field survey method

Survey times were recorded and can be seen in Table 8.5. For the static lidar survey a 10 m x 10 m subplot was completed by two operators in thirty minutes using the FARO system, although if taking into account walking between plot sites and setting up this time is extended to one hour. For the handheld approach, each 10 m x 10 m subplot was surveyed by one person in five minutes. In addition, using the ZEB1 it was possible to traverse the area between subplot sites (Section 8.2.3) and collect the survey data in little over ten minutes. For the field survey data collection the Kirton Wood test area (50 m x 50 m) was surveyed by a team of four ecologists over two days.

Table 8.5: Times and coverages for different methods of Kirton wood survey.

Instrument	Personnel	Area (m^2)	Time taken (min)	Survey coverage per surveyor m^2/min
FARO	2	100	60	0.85
ZEB1 (A1)	1	100	5	20
ZEB1 (A1-E5)	1	500	10	50
Field survey	4	2500	1440	0.43

8.4 Discussion

8.4.1 Can TLS measurements of forests be replicated using HMLS?

The data set and resultant point cloud captured using the handheld system was used to extract DBH and stem map information to a comparable accuracy to those obtained from data sets collected using TLS survey techniques (Tables 8.3 and 8.4.

The handheld approach allows the user to easily direct the scanner toward points of interest and can capture data from the whole survey area, rather than at three set-up points as is usual with a static survey. In this test the user walked steadily through the plot collecting data, but a more directed survey aiming the scanner at all stems may increase modelling accuracy and reduce omission errors. A slower operational gait may also allow for a higher resolution point cloud creation, something that needs to be examined in further trials of the hardware. This was a proof of concept study, allowing for a more vigorous methodology to be developed in future trials.

The cases of stem omission in the ZEB1 data set were caused by insufficient points returned from the handheld system to accurately describe the surface of a stem. These instances caused a modelling error in the Cyclone software and can be classed as complete modelling failure. Omission errors can be caused by point occlusion within the point cloud. Shadowing is the main factor in point occlusion which can increase in areas of high stem density and increased understorey.

Both plan positioning and DBH estimations show greater errors when stems of DBH < 10 cm are examined (Tables 8.3 and 8.4). For stems with DBH < 10 cm the smaller surface area of the target results in fewer point returns and therefore fewer data from which the stem surface can be modelled. With the most important element of above ground biomass being trees of DBH > 10 cm (Alba and Scaioni, 2007) the use of a filter to eliminate smaller stems and saplings is a practice used in forest modelling (Desclée et al., 2006). Removing stems with DBH < 10 cm results in increased accuracy for the plan position and DBH estimations. If the intended application is to assess total basal area then the aggregate effect of these DBH errors will be to add a little more uncertainty to the total value while saving a large amount of survey time.

The manufacturer's stated accuracies differ greatly for the two instruments with stated accuracies being ± 2 mm for the FARO and ± 30 mm for the ZEB1. The reduction in point accuracy when using the ZEB1 comes with an increase in data collection efficiency, so this is a trade-off that would need to be assessed for individual survey needs.

DBH estimations show predominance toward underestimation using the handheld system when compared against the FARO (Figure 8.5). The lower DBH estimations from the ZEB1 instrument are possibly due to the modelling methodology not accounting for the increased point noise seen within the ZEB1 data set (Bailey and Durrant-Whyte, 2006). When extracting surfaces the Cyclone software fits cylinders to the inner diameter of the point cloud. With increased surface noise that can be seen in the ZEB1 approach (Figure 8.6) this may result in decreased diameter estimations. Surface noise is caused by multiple sources such as object surface texture and registration errors. With a decreased range accuracy compared to static instruments such as the FARO, the ZEB1 does contain significantly more uncertainty when modelling surfaces. Using a different modelling methodology, such as using a different software that accounts for increased surface noise, may increase modelling accuracies and minimise bias.

The trial highlights the potential for a handheld system to replace static lidar for surveying complex, difficult to access forest plots and for recording DBH and plan position. When examining stems with a DBH >10 cm the utilisation of a handheld survey approach provides an acceptable accuracy (for most forestry applications) in DBH and position estimates whilst increasing the possible survey extent. The method may not however, currently provide the required surface accuracy for the reconstruction of trees for precise volume or biomass estimations, or the required DBH and position accuracies when examining stems with a DBH of <10 cm.

8.4.2 Does the use of HMLS provide any advantages in practical ease over TLS or field survey methods?

Of the methodologies tested the handheld laser scanner showed a much greater area of coverage per hour of survey than the TLS approach or the field survey (Table 8.5), significantly reducing the time spent at the forest plot. From the subplot surveys it is estimated that the ZEB1 approach is approximately 12 times faster than if using a TLS. This is comparable with James and Quinton (2014) who demonstrated the ZEB1 as being approximately 40 times faster than a TLS when surveying complex topography. In the same study it was also concluded that even with limitations in data density and accuracy shown in the ZEB1 system, its usefulness in difficult environments would make it a highly practical

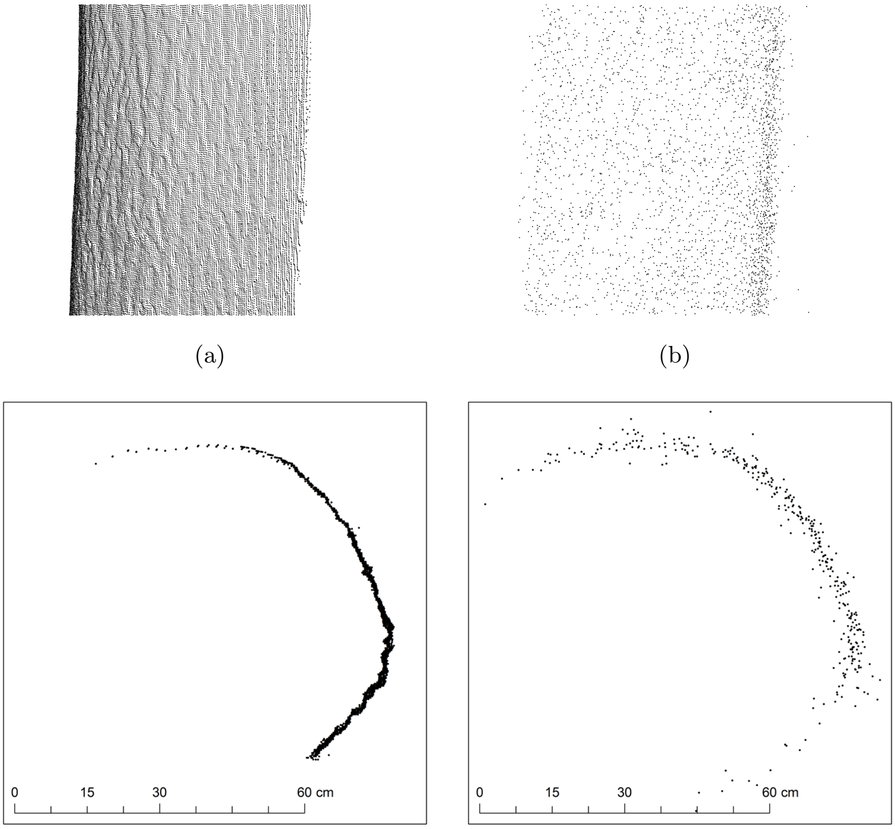

(a) (b)

(c) (d)

Figure 8.6: Point cloud stem comparisons for side view of FARO (a) and ZEB1 (b) and planar view from FARO (c) and ZEB1 (d). The data shown is a 10 cm vertical slice through the same stem point cloud. It can be seen that the ZEB1 contains much noisier data when compared against the FARO. This results in less accurate surface modelling when using the ZEB1.

survey solution.

The forest plot surveyed for this trial was considered complex with dense understory. The terrestrial survey time of one hour per subplot may have been longer than in open woodland or plantations. In addition, for both laser scan methods additional processing work is required away from the plot site to extract DBH and positional estimates from the point cloud.

The lack of survey targets in the handheld approach reduces set-up time for the survey when compared against the static laser scan. Data collection using the handheld scanner is carried out simply by walking through a plot. With this ease of survey comes the possibility of survey data being integrated with other tasks resulting in a combined approach to survey work.

There is potential for more cost-effective surveys using the handheld approach. With reduced survey time comes the associated reduction in operational costs. There is also the reduced hardware costs, with a ZEB1 instrument currently (in 2015) costing £14,000. This is less than a TLS instrument, which can range typically at this time from £25,000 to £80,000 depending on manufacturer. Processing costs are more difficult to compare between the two systems with initial processing of the ZEB1 data being priced on a per metre basis, currently approximately £200 per kilometre of survey path. TLS systems do not have this external processing cost, although registration has to be completed in-house.

Further work also needs to be carried out examining the effect of survey path on point cloud accuracy and survey time. A longer survey path including multiple swaths crossing the site in all directions may increase the usefulness of the handheld approach when considered for feature extraction, but this will also increase survey time.

Liang et al. (2014a) have also demonstrated the usefulness of personal scanning systems within the forest environment. In their study they used a backpack mounted MLS (10 kg) to survey a 2000 m^2 forest plot in two minutes, giving a survey coverage of 1000 m^2 per minute, highlighting the effectiveness of personal scanning systems for fast surveying. It is difficult to directly compare the two studies because stand characteristics in each trial were very different. The equipment used by Liang et al. (2014a) is likely to be less portable, especially within dense vegetation. Nevertheless, both tools indicate the potential for further development of the methodology.

8.4.3 Are any novel measurements available?

When using a handheld system it should be possible to obtain a more complete model of the plot site than the three scan location approach common in TLS forest surveys. Every step taken using a handheld instrument is a new scan location and so the environment captured with the survey can be modelled in more detail.

Examining the resultant point cloud obtained from the handheld instrument it can be seen that more detail is collected on understorey and low level features than with the equivalent TLS point cloud (Figure 8.4). Using a handheld instrument allows data from complex zones of interest (such as the understorey) to be collected with decreased occlusion. This is because each rock of the scanner head is similar to a new scan location in a static survey, meaning obstacles can be walked around to obtain large amounts of points returns. This highlights the potential of the ZEB1 system for detailed analysis of forest structural parameters incorporating ground level features.

8.4.4 What are the remaining challenges for the application of HMLS in forest monitoring?

In this test a relatively small plot area was surveyed with the ZEB1 scan data collected in short bursts of less than ten minutes. Further tests need to be carried out in the woodland environment to assess the usefulness of the handheld approach for larger scale surveys.

With longer survey paths required for extended surveys comes the problem of maintaining a sufficient point density for the extraction of features to be successful. This presents itself in the stem omission differences within this trial (Table 8.2), which would be expected to increase for longer surveys such as that shown in Figure 8.2b.

An important factor in the development of point cloud data sets for use within forest modelling will be the automation of data processing. Without automation these very large, complex data sets are too time-consuming to process manually and would not be considered a practical survey solution. Existing software for point cloud processing to extract information such as volumes could be used with a point cloud from the ZEB1. The increased point noise seen within the ZEB1 cloud may limit automation of the processing; this needs to be examined in detail in further studies.

In this trial it was not possible to extract the species of tree or its status (alive or dead) from the laser scan data. Achieving this may involve a hybrid survey approach whereby additional setup requirements, such as reflective strips to identify dead trees are used in conjunction with the handheld laser instrument.

The introduction of handheld mobile laser scanning into the field of forest ecology, viewed alongside extraction techniques presented in Chapters 4, 5, 6 and 7, supports the use of ground based lidar technology to increase our understanding of the structural properties of forests and how structure affects further ecological attributes such as diversity and productivity.

Chapter 9

Conclusions

The main aim of this study was to assess the application of commercially available terrestrial laser scanning (TLS) for the estimation of forest understorey structural attributes, beyond those currently extracted from aerial laser scanning (ALS) and TLS systems. The study was specifically designed for UK lowland, broad-leaved forests, although the methods described have potential relevance to multiple forest types.

Whilst traditional methods for forest survey offer reliable, low cost estimations of forest parameters they are not suitable for assessing the 3D properties of forest sites at high resolution. The potential of TLS for the assessment of 3D spatial relationships within forest is great given the high accuracy and resolution of commercially available laser scanning equipment, combined with the use of automated data processing.

Previous studies that have tested the use of TLS for ecological surveys have commented on its potential but these studies have tended to replicate existing metrics rather than explore new ones (McMahon et al., 2015; Eitel et al., 2013; Davies and Asner, 2014). Whereas, it is the new metrics and indices, such as those presented in this study, that may allow TLS to reach its full potential.

The success of ALS for forestry surveys should provide an example for TLS. The ability to collect very large (regional) data sets quickly and efficiently has seen its introduction into multiple governmental forestry inventory programmes with large cost savings involved. If ALS surveys offers clear advantages of survey size and cost savings, it needs to be recognised that there should be other clear advantages to forest surveyors when using TLS, be this in area coverage, novel metrics or a combination of both.

The results from this study show that commercially available TLS instruments can be used to provide novel estimations of forest structural parameters. They also show how forest survey data can be collected much quicker and over larger areas (when using a handheld approach) than when compared against traditional forest ecology surveys.

The novel measurements of vertical to non-vertical index (VNVI), understorey density and cover, also provide additional information on the structure of forests beyond the dendrometric parameters commonly collected using TLS in forests. The ability to acquire data regardless of canopy state also gives a ground based approach advantages over an aerial approach where dense canopy can create a barrier to effective data collection.

Through the development of new measures that can only be extracted through detailed 3D modelling of forest structure, this study has identified new ways in which TLS can be used to increase the understanding of the complex structural relationships operating within forests at multiple spatial scales.

With the development of work flows for the extraction of different structural attributes from forest point clouds, this study has identified possible replicable measures that can be used to assess forest understorey vegetation. Although designed specifically for UK lowland, broad-leaved forest, these work flows have the potential to be applied across a range of forest types. Points to consider when planning further studies in different forest types are the density of stems and understorey and their relevance to line-of-sight and the effect different forest densities will have on processing parameters.

The density of stems and understorey will affect how the survey is designed and how far apart the instrument setups need to be. The general guidelines covering line-of-sight and range to objects (as covered in Chapter 3) will apply to different forest types, but the specific grid spacing needed to make sure all objects are 'seen' by the instrument may change.

In a similar way the processing parameters, such as VNVI cutoff point, may need evaluating for different forest types. The values presented in this study were derived from data collected in the UK, across similar woodlands, of a similar age. The value for VNVI cutoff (the point from which vertical point density is considered to approximate stem material) is not expected to be the same across different forest types due to the specific structural properties inherent within distinct forest types (i.e. the expected difference in vertical material between a rain and boreal forest). Structural changes due to movement along the successional sequence may also require processing parameters to be reevaluated.

Using the generation of a vertical to non-vertical index (VNVI) presented in Chapter 4, it was possible to identify patterns within the vertical structure of forests relating to deer browsing. This method offers an improvement over existing studies examining deer browsing by allowing the effects of deer browsing to be assessed to 10 cm. Traditional methods for estimating vegetation with relevance to deer browsing are proven and understandable, as surveying stems in 10 cm height bands using traditional methods would be very time-consuming, but it does highlight the additional analysis benefits that using TLS combined with extraction of VNVI can bring to a forest survey.

The VNVI approach to point cloud analysis provides a relatively fast method for the extraction of structural attributes without the need for extensive modelling or manual data processing. After initial filtering and trimming of data sets, the extraction of a VNVI can be fully automated allowing for large, multiple data sets to be processed efficiently. This has the potential to be used for even larger studies where data processing would need to be fully automated for efficient analysis work flows.

The classification of forest plot components into vertical and non-vertical based on the two stage analysis using vertical alignment of gridded point returns and clustering of points does have limitations. Dense foliage may cause an overestimation of vertical component through providing returns in multiple adjacent vertical voxels. It may also be the case that dense foliage would cause vertical component to be misclassified as non-vertical through point occlusion.

Building on the classification of forest plot components into vertical and non-vertical the development of an understorey density profile (UDP) for the 40 WoodMAD data sets highlighted the use of TLS for examining vertical density within forest plots (Chapter 5). Using the MacArthur-Horn transformation data sets were corrected for point occlusion and a profile created describing density of understorey material.

In sites where deer browsing was low there was a significant increase in the number of adjusted point returns when compared to sites where deer browsing was high, this can be viewed as a general increase in the amount of understorey material where deer levels are low. Whilst this follows expectations, it also supports the use of TLS for the identification of further patterns and relationships that are perhaps not so well understood.

In examining the understorey density profiles, variations of forest density with height were isolated and patterns identified at the centimetre scale. This level of spatial analysis was highlighted by the BTO as having potential benefits when examining bird nesting patterns, above and beyond traditional methods of forest survey. This analysis work flow was also used to identify woodland sites with unique density profiles indicative of structural features (such as the presence of ground level growth or bare ground), it is these applications of TLS analysis that have the potential to provide much more detailed assessment of forest structure with respect to animal-habitat associations than is currently common.

In addition to plot scale density profiles, the sub-division of plots into sub-plots allowed for the heterogeneity of vertical density to be assessed. This technique allowed changes in object density along transects to be identified, changes that may have been smoothed over using a single plot site approach.

The TLS approach for creating understorey density profiles does not provide a complete assessment of understorey plant communities as, at the present time, different plant species cannot be identified through point cloud feature extraction. It does however, provide spatial information that can be collected in three dimensions, something that is not provided through traditional survey methods.

For the examination of horizontal component within forest plots, the trial outlined in Chapter 6 showed how TLS analysis can be used to replicate the existing forest measure of understorey cover. Results showed correspondence with a qualitative assessment of each plot site and cover estimates extracted from forest point clouds. TLS was also used to provide further understorey metrics such as total 3D surface and understorey volume, measurements that are not commonly collected using traditional methods.

The use of fine resolution laser scanning also allowed for estimation of cover at the decimetre level, this is an improvement on the classification of cover into cover groups as described by Reich et al. (2012) using traditional estimation methods. There is also the potential for removing user bias through automation of processing and extraction of metrics directly from point cloud data sets. This further enhances the ability of TLS to offer a realistic alternative to traditional direct measurements of understorey cover.

The novel use of 3D modelling across understorey vegetation layers, using methods similar to those developed for hydrology and geomorphology, was used to extract surface slope and curvature properties that identified relationships between understorey surfaces and vegetation type. The use of this novel extraction technique has the potential to increase our understanding of how the texture of forest surfaces (both at the ground level and further into the understorey) may affect forest communities. Ground level vegetation (and additional features such as woody debris) provides habitat and forage for multiple animal species (Sabatini et al., 2014) with understorey structure affecting animal-habitat associations. The spatial patterns within ground level vegetation can also provide information on processes operating within understorey communities (Scheller and Mladenoff, 2002). The correspondence seen between slope and curvature values of understorey vegetation surfaces and vegetation type shows the potential of TLS for the creation of new metrics describing the spatial relationships operating within the understorey.

In addition to the development of new analysis work flows and measures outlined in this trial, Chapter 7 examined the use of TLS for temporal surveys. With forests being such a dynamic environment this is an important aspect of forest surveying. The results provide correspondence between the expected structural changes witnessed within forest (leaf abscission in winter, leaf growth in spring) and the structural changes as extracted from TLS acquired point clouds.

Using a TLS approach allowed for fine scale measurement of structure in forest vegetation with respect to cyclical changes brought about by seasonal change. This included the novel creation of temporal change maps showing an increased resolution of cover estimates compared to traditional methods of cover assessment and offering possible insights into how understorey vegetation structure changes within a trial site over time.

The new methods for the assessment of understorey vegetation structure, outlined in chapters 6 and 7, were tested using qualitative assessments of plot site photographs that divided the survey areas into different cover and vegetation types. If the methods are accepted, an assessment of plot sites based on VNVI and UDP (outlined in chapters 4 and 5) should allow understorey vegetation cover and temporal change to be quantified with reference to these new metrics, avoiding the use of qualitative assessments.

Handheld mobile laser scanning (HMLS) has shown the potential to complement TLS by providing increased survey coverage and allowing point cloud data processing to be considered for areas which are otherwise difficult to access (Chapter 8). The integration of laser scanning and inertial movement technologies, used in conjunction with the concept of simultaneous localisation and mapping (SLAM) within the ZEB1 instrument offer an exciting new development in the production of point clouds from HMLS. In using SLAM technology the reliance on satellite positioning is removed and the user can operate in environments where satellite signals are poor or non-existent. The need for a pre-installed network of survey targets is also eliminated as a moving time window of trajectory data from each scan is used to compute the 3D point cloud.

The ZEB1 HMLS approach offers potential when considered for forest surveys. With dense canopy, difficult terrain, complicated structure and limited line-of-sight the forest environment limits the effectiveness of TLS systems to gather point cloud data beyond the small-scale permanent sample plots currently in use. Using the ZEB1 an HMLS survey can be conducted as easily as walking through a plot and the creation of point clouds with increased geospatial extent becomes feasible.

Limitations in the HMLS approach are currently associated with the maximum survey time allowed by the hardware. Resolution of the point cloud to allow acceptable feature extraction may also be an issue when using the ZEB1 HMLS approach. These deficiencies and also further applications need to be examined in future studies.

In combination, the trials outlined here suggest that TLS for forest surveys offers an enhanced range of metrics than those currently collected through traditional methods of survey, or from previous TLS. Fine-scale analysis, combined with replicable work flows, provide advantages over traditional methods that may help TLS to reach its full potential. Using novel metrics and maintaining standardised survey methodology, TLS and HMLS offer a new approach to forest surveys that has been shown to be a reliable tool for the extraction of structural attributes, the estimation of vegetation cover, the development of microtopology analysis of understorey surfaces and for temporal change assessment.

Chapter 10

Recommendations for future research and work

This study has provided work flows for data extraction that can be used for the assessment of forest structural properties. These work flows can be considered as starting with a point cloud which can be acquired in any number of ways. Point clouds used in this study were collected using static terrestrial laser scanning (TLS) instruments and handheld mobile laser scanning (HMLS) instruments, although the methodologies described could be applied to point clouds collected by any means. It is the extraction of features from point clouds and the collection of point cloud data itself that present the largest challenges when considering further work.

One important aspect of using point clouds for the measurement of forest structural attributes that would allow the method to be more widely used is the development and improvement of algorithms that extract the desired parameters from large, complex data sets.

Currently, research is predominantly focused on TLS hardware as this provides the required accuracy and creates detailed point clouds from which highly accurate models can be made. With technological advances such as the introduction of HMLS that allow for more rapid surveying, but with reduced accuracy, the focus of feature extraction may need to move away from the notion of precise surface modelling and move to a more generalised modelling approach such as through voxel based extraction rather than surface modelling.

Further studies are also recommended to assess the application of the data collection methods and analysis techniques developed here for sites along the successional sequence and sites across multiple forest types. How the methodologies will change with forest type, including the effect of forest type on processing parameters needs to be understood in more detail.

A detailed analysis of the developed methods compared against traditional methods should also be considered. This would include direct tests of traditional methods against TLS derived values at various sites. Different applications within forest ecology and forestry (such as when assessing bird habitats or timber production) use different traditional methods, so each application would need an individual assessment. What is learnt about TLS data collection for timber reserves may not hold when considering habitat mapping.

If the methods outlined in the study are accepted and used, an assessment of plot sites based on VNVI and UDP (outlined in chapters 4 and 5) should allow understorey vegetation cover and temporal change to be quantified with reference to these new metrics, avoiding the use of qualitative assessments.

In addition to accurate, high resolution point clouds acquired through TLS surveying, there is the possibility that 3D data collection can be 'out-sourced' to low cost devices such as smart phones (Escribano-Rocafort et al., 2014; Tichy, 2016).

It is suggested that further research be conducted on the use of low-cost survey alternatives from which point clouds can be produced. How, and to what extent, does the resolution and accuracy of the surveying instrument influence the extracted results and do the results meet the required levels of accuracy and repeatability. If low cost hardware that can be utilised through mass data gathering, such as crowd sourcing events, produces data sets and resultant point clouds that contain the required accuracy for simple analysis, this may offer a companion to the high resolution, high cost TLS technique.

As well as considering different methods for the collection of point cloud data within forests, the relationships between the spatial properties of point cloud data and animal-habitat associations also need to be examined in more detail.

An example of this is how this study utilised a very large data set acquired as part of the WoodMAD trials aimed at the assessment of the effects of deer browsing on woodland song bird habitats. As such, the data was specifically targeted at those sites with different deer densities. Whilst this allowed for the assessment of structural properties extracted from point clouds with particular reference to those features expected to be altered by deer browsing, it is recommended that other animal-habitat associations be examined.

Appendices

Appendix A

Instrumentation

FARO® Laser Scanner Focus^{3D} X 130

The New Powerful X Series Laser Scanner

Mid range scanning - up to 130m

Its range up to 130m allows the Focus^{3D} X 130 for laser scanning in all kinds of applications in the architecture, BIM, heritage, forensics, shipbuilding, construction, process industry, CGI, and many others.

Xtra positioning - integrated GPS receiver

Effortlessly determine the position of the scanner. This helps to facilitate the registration process and provides the exact time and location of the users' scans.

Xtra portable

The Focus^{3D} X 130 has the size of only 24 x 20 x 10 cm and a weight of just 5.2kg. Waterproof Pelicase and a ergonomic backpack incl. tripod holder make the device truly portable.

Wireless LAN

WLAN remote control permits you to start, stop, and view scans at a distance.

Best value for money

The new Focus^{3D} X 130 delivers extraordinary performance at affordable rates, unique to the market.

X-series laser scanner for mid-range applications

The new X-series laser scanner FARO Focus^{3D} X 130 is a powerful high-speed 3D scanner for all kinds of applications.

The ultra-portable Focus^{3D} X 130 enables fast, straightforward, and yet accurate measurements of façades, complex structures, production and supply facilities, accident sites, and large-volume components. Combining the highest-precision scanning technology with authentic mobility and ease-of-use, the new device offers reliability, flexibility, and real-time views of recorded data. The 3D scan data can easily be imported into all commonly used software solutions for accident reconstruction, architecture, civil engineering, construction, forensics or industrial manufacturing.

With a battery runtime of 4.5 hours, the laser scanner has also a high level of flexibility and endurance. The Focus' light weight, small size and SD-card makes the scanner truly mobile.

Benefits

The new FARO Focus^{3D} X 130 is the powerful and affordable tool for mid-range 3D documentation applications.

One million points/second scanning rate, ease-of-use, portability, scanning range up to 130m, integrated GPS, very low noise as well as WLAN remote control make it a universal tool for all kinds of working enviroments.

FARO® Laser Scanner Focus^{3D} X 130

www.faro.com

Performance Specifications Focus^{3D} X 130

Ranging unit

Unambiguity interval:	>130m
Range Focus^{3D} X 130:	0.6m - 130m indoor or outdoor with upright incidence to a 90% reflective surface
Measurement speed (pts/sec):	122,000 / 244,000 / 488,000 / 976,000
Ranging error[1]:	±2mm

Ranging noise[2]	@10m	@10m - noise compressed[3]	@25m	@25m - noise compressed[3]
@ 90% refl.	0.3mm	0.15mm	0.3mm	0.15mm
@ 10% refl.	0.4mm	0.2mm	0.5mm	0.25mm

Colour unit

Resolution:	Up to 70 megapixel colour
Dynamic colour feature:	Automatic adaption of brightness
Parallax:	Co-axial design

Deflection unit

Field of view (vertical/horizontal):	300° / 360°
Step size (vertical/horizontal):	0.009° (40,960 3D-Pixel on 360°) / 0.009° (40.960 3D-Pixel on 360°)
Max. vertical scan speed:	5.820rpm or 97Hz

Laser (optical transmitter)

Laser class:	Laser class 1
Wavelength:	1550nm
Beam divergence:	Typical 0.19mrad (0,011°) (1/e, halfangle)
Beam diameter at exit:	Typical 2.25mm (1/e)

Data handling and control

Data storage:	SD, SDHC™, SDXC™; 32GB card included
Scanner control:	Via touchscreen display and WLAN
New WLAN access:	Remote control, scan visualisation are possible on mobile devices with Flash®

Multi-Sensor

Dual axis compensator:	Levels each scan: Accuracy 0.015°; Range ± 5°
Height sensor:	Via an electronic barometer the height relative to a fixed point can be detected and added to a scan.
Compass[4]:	The electronic compass gives the scan an orientation. A calibration feature is included.
GPS:	Integrated GPS receiver

CLASS 1
LASER PRODUCT

[1] Ranging error is defined as a systematic measurement error at around 10m and 25m, one sigma [2] Ranging noise is defined as a standard deviation of values about the best-fit plane for measurement speed of 122,000 points/sec.[3] A noise-compression algorithm may be activated thereby compressing raw data noise by a factor of 2 or 4. Subject to change without prior notice .[4] Ferromagnetic objects can disturb the earth magnetic field and lead to inaccurate measurements

General

Power supply voltage:	19V (external supply) 14.4V (internal battery)
Power consumption:	40W and 80W (while battery charges)
Battery life:	4.5 hours
Ambient temperature:	5° - 40°C
Humidity:	Non-condensing
Cable connector:	Located in scanner mount
Weight:	5.2kg
Size:	240 x 200 x 100mm
Maintenance / calibration:	Annual

ISO 9001 BUREAU VERITAS Certification

ANAB ACCREDITED

GSA Contract Holder

Global Offices: Australia ▪ Brazil ▪ China ▪ France ▪ Germany
India ▪ Italy ▪ Japan ▪ Malaysia ▪ Mexico ▪ Netherlands
Philippines ▪ Poland ▪ Portugal ▪ Singapore ▪ Spain ▪ Switzerland
Thailand ▪ Turkey ▪ United Kingdom ▪ USA ▪ Vietnam

www.faro.com
Freecall 00 800 3276 7253
info@faroeurope.com


Geo SLAM™
Survey
in motion
GeoSLAM develops game-changing survey solutions
for the measurement and mapping of multi-level
three-dimensional environments.
Fast
Accurate
Proven
Efficient
ZEB1
Geo SLAM
geoslam.com

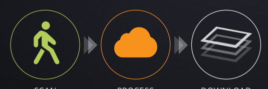

How it works

Walk and Scan

Grab the ZEB1, our lightweight hand-held laser-scanner and walk through your target survey environment to record more than 40,000 measurement points/second.

Process Online

Upload your raw scan data to the GeoSLAM Cloud where Simultaneous Localisation and Mapping (SLAM) software will transform your survey measurements into a fully registered point cloud.

Download 3D

Replace large upfront software costs and annual maintenance charges with our pay-as-you-go data processing and 3D download service.

Advantages

- lightweight
- easy to operate
- rapid data capture
- +/- 0.1% accuracy
- online processing
- automatic registration
- pay-as-you-go
- 5-Year warranty available

Applications

ZEB1 is used to complete measured surveys of building interiors, to document road traffic accidents and crime scenes, to map underground mine and cave networks, to measure property for real estate valuations, and to facilitate contingency planning.

Unlike trolley based SLAM systems, the hand-held ZEB1 is easy-to-use in multi-level environments such as stairways and mines; making it ideal for surveying challenging indoor and underground spaces.

Building Survey Example

Scan time = **15 minutes** | Floor area = **370m²**

Scan size = **25 million points** | Processing cost = **$15**

Buildings | Forestry | Manufacturing | Mining | Retail

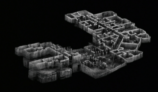

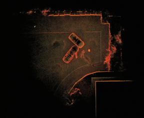

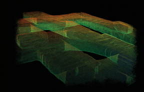

Specifications

Data Acquisition Speed	43,200 measurement points/second
3D Measurement Accuracy	+/- 0.1% (typically)
Maximum Range	Up to 30m (15m outdoors)
Laser Safety Class	Class 1 Eye Safe
Angular Field of View	270 x ~100 degrees
Weight of Scanner Head	665g
Dimensions of Scanner Head	60 x 60 x 360mm

WHAT OUR CUSTOMERS SAY

"GeoSLAM's solutions are changing the way we survey buildings. We can now measure building plans 10 times faster than we used to with total station or traditional survey equipment."

Morten Thoft, COWI, Denmark

"We are streamlining our business on the back of this game-changing technology from GeoSLAM which is revolutionising our process for surveying underground mines."

William Hedges, ICL Fertilisers, UK

Geoslam Limited Unit 11 Moorbridge Court Bingham Nottingham NG13 8GG United Kingdom
+44 (0)1949 831 814 | info@geoslam.com

geoslam.com

Appendix B

Plot information

Table B.1: Plant species, abbreviations and scientific names

Plant species	Abbreviation	Scientific name
Ash	AH	*Fraxinus excelsior*
Birch	BI	*Betula spp.*
Hawthorn	HAW	*Crataegus monogyna*
Hazel	HAZ	*Corylus avellana*
Holly	HOL	*Ilex aquifolium*
Oak	OK	*Quercus spp.*
Sycamore	SYC	*Acer pseudoplatanus*

Table B.2: Plot descriptions provided by British Trust for Ornithology. Easting, northing and bearing values are the coordinates in OS British National Grid and bearing value (°) for the start location of each survey transect.

Site name	easting	northing	bearing	Stand details
Ampfield 03	439678	124506	20	OK 50yrs
Ampfield 04	440147	125186	57	OK 50yrs
Bentley 03	424927	128915	196	OK overstood + dense
Bentley 04	425335	128982	246	mature OK+AH
Big Forest 03	315361	309924	181	mature OK 60yrs,HAZ,HAW
Blackmoor	423361	129378	38	mature OK,overstood coppice
Blean Homestall 01	610184	159619	52	mature OK + MBL
Blean Homestall 04	610822	159965	149	mature OK + HAZ
Blean Homestall 06	611210	159844	321	mature OK + HAZ
East Blean 01	617713	164456	232	mature OK+AH,HAZ understorey
East Blean 03	618170	164679	98	OK high forest + cut HAZ
Eastridge 01	340044	301736	100	semi-mature MBL (AH,BI,WI),very dense understorey
Eastridge 05	339015	300797	234	mature BI,OK,AH
Ellenden	610335	161895	267	OK all ages,some is overstood coppice
Ffridd Mathrafal 02	311638	310858	308	OK p20,HAZ,OK,HAW,HOL understorey
Ffridd Mathrafal 04	312046	311234	270	OK p52,OK,HAZ,MBL understorey,CON nat regen <20%
Gwern Ddu 01	313587	310155	69	OK p62 + WI,BI older nat regen
Gwern Ddu 04	313986	310491	48	OK p52,HAZ,HAW understorey

Haughwood	358630	237944	266	mature OK,sparse understorey
Hound 01	422263	130790	20	OK standards,overstood HAZ
Hound 03	422680	130130	218	mature OK+AH
Hound 05	423320	130454	27	mature OK,HAZ
Kingswood 01	346719	212581	214	mature OK,HAZ
Kingswood 10	347678	211986	201	AH/OK,HAZ,bluebells,bramble
Langley 02	423283	120762	108	mature OK,overstood HAZ
Langley 05	423805	120709	316	mature BI+MBL
Lea Pagets 03	359933	234208	240	mature OK with HAZ,HAW,WCH,diverse ancient woodland groundflora
Pole Lees 02	339179	304649	172	OK,more densely stocked,smaller stems,bramble
Pole Lees 05	339370	304472	261	mature OK with AH,BI,diverse ancient woodland groundflora
Romers	360455	263158	220	mature OK/AH high forest,multi-storey,multi-aged,HAZ,HAW,dense bluebell carpet
Spout Figyn	315517	311071	340	mature OK,some AH,BI,SYC with HAZ,bramble
West Blean 01	614275	164133	260	mature OK
West Blean 02	614645	163925	175	mature OK
West Blean 03	615296	163461	130	OK high forest + cut HAZ
West Blean 04	616595	164597	228	OK high forest + cut HAZ
Wyre main 01	374526	277479	135	OK,some BI,Yew,some OK + HOL understorey
Wyre main 03	373735	276215	65	very old OK
Wyre main 04	374000	276190	355	OK/BI nat regen,some bramble
Wyre NNR 01	375765	276433	275	mature OK (former OK coppice with OK standards,singled out in 1920s,not thinned since),bramble,bracken bluebells
Wyre NNR 03	375567	275740	161	mature OK (former OK coppice with OK standards,singled out in 1920s,not thinned since),bramble,bracken bluebells

Bearing: 20

Ampfield 03

E: 439678
N: 124506

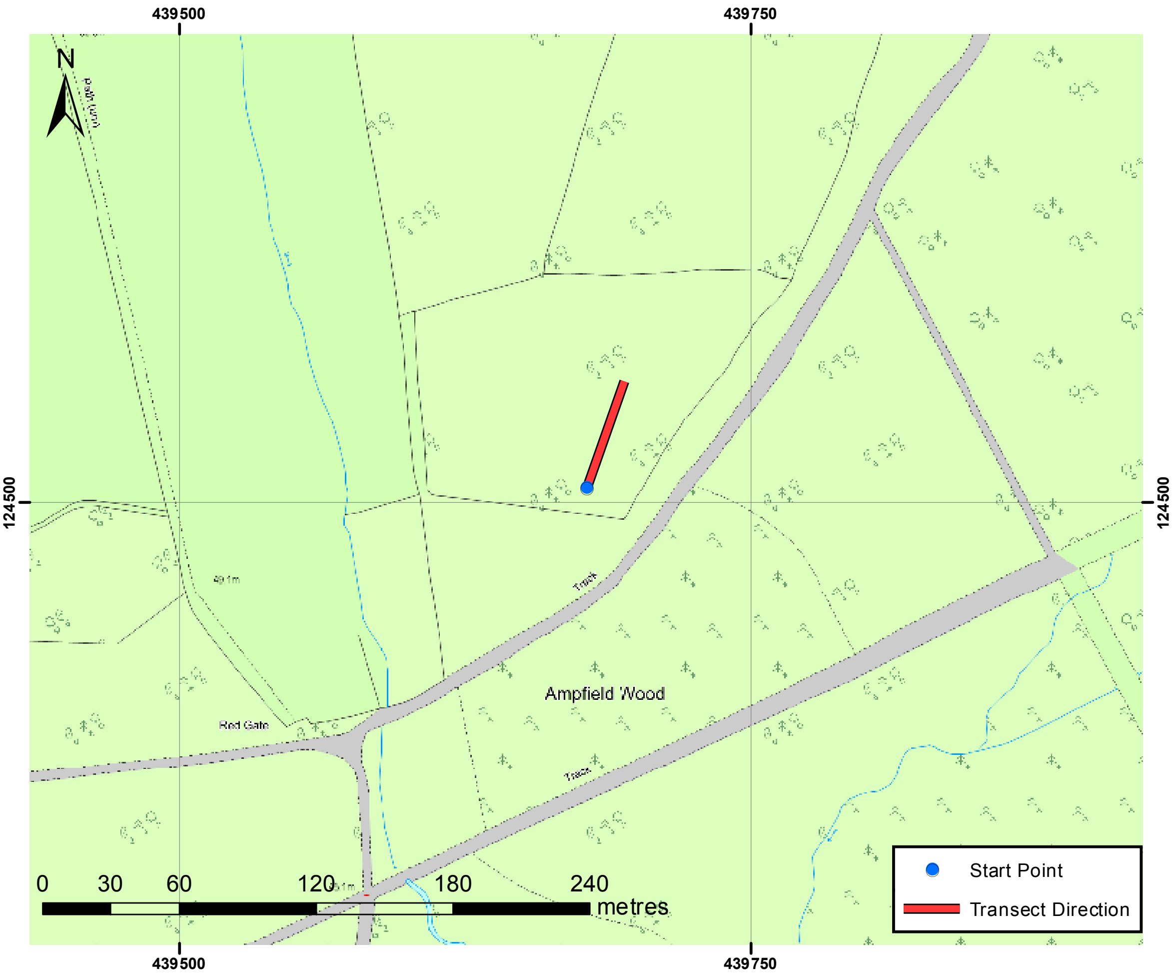

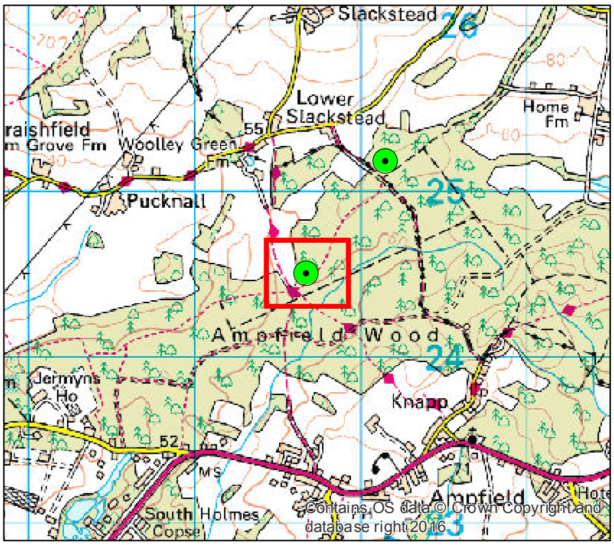

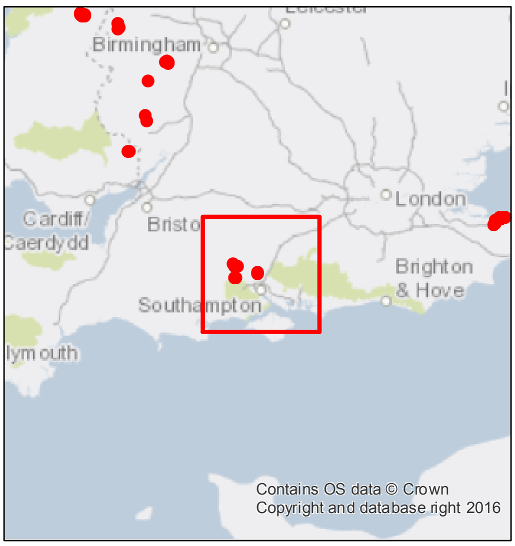

Bearing: **56**

Ampfield 04

E: **440147**
N: **125186**

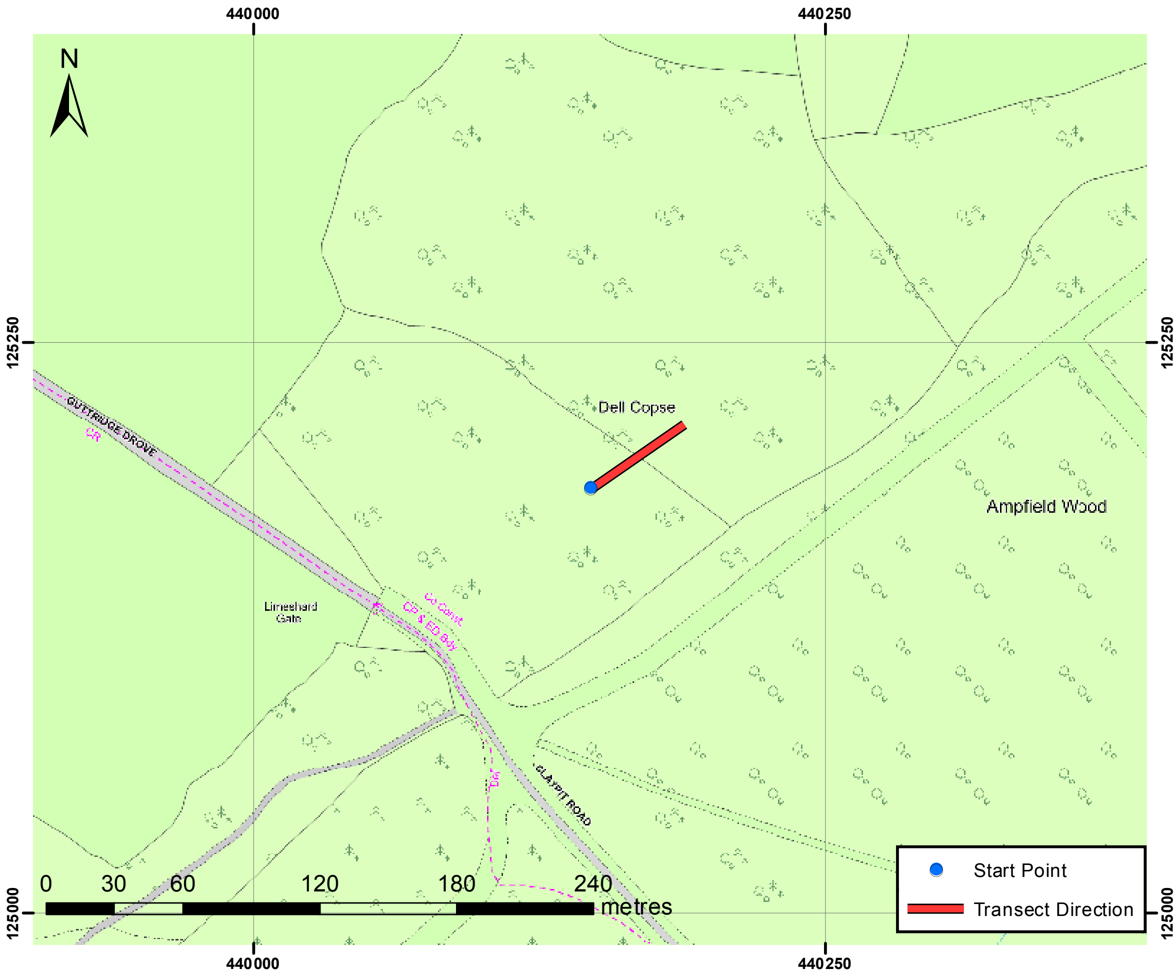

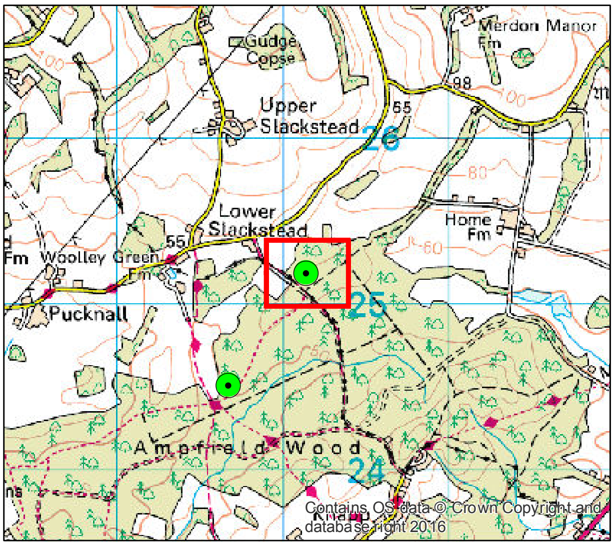

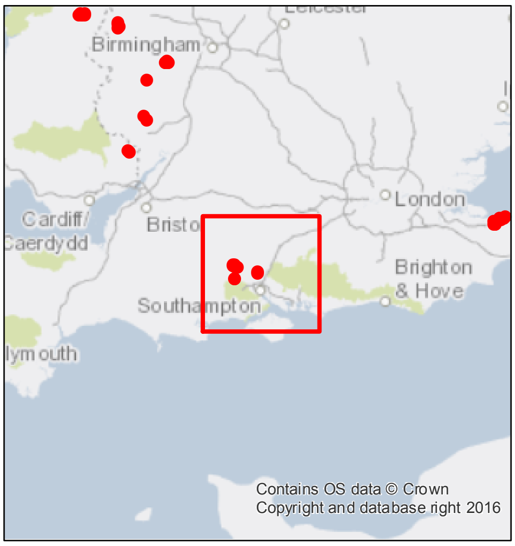

Bearing: 196

Bentley 03

E: 424927
N: 128915

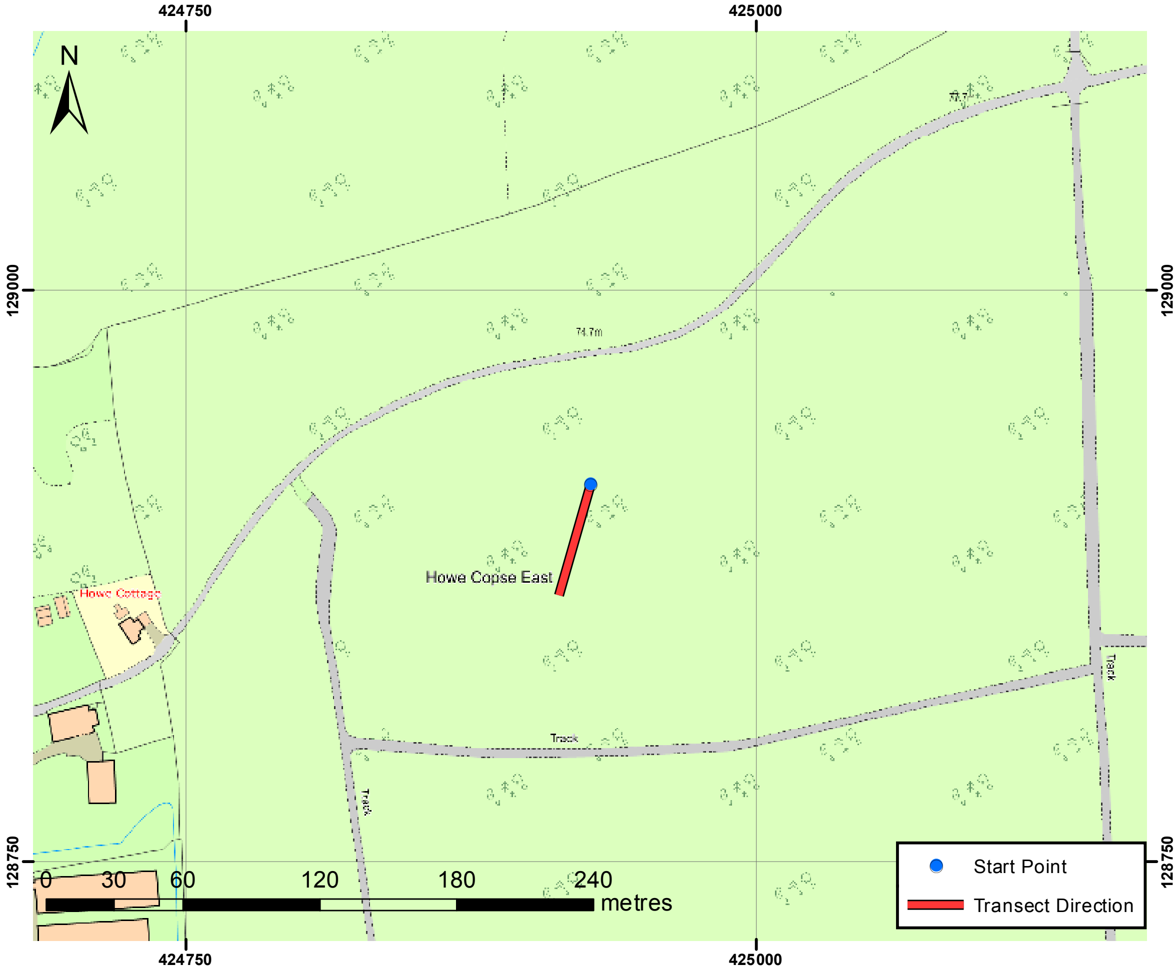

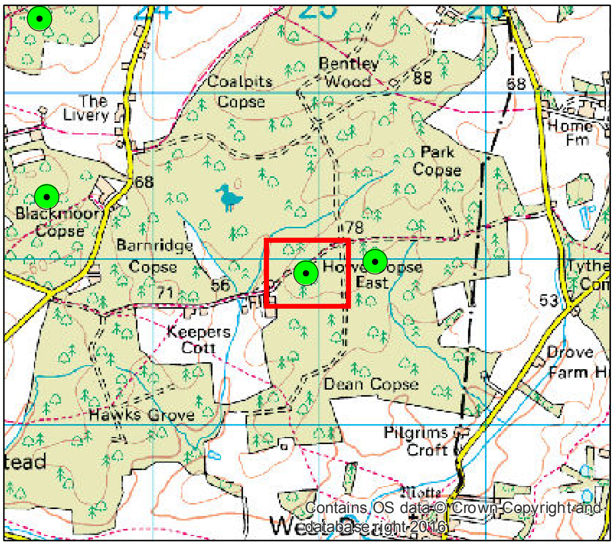

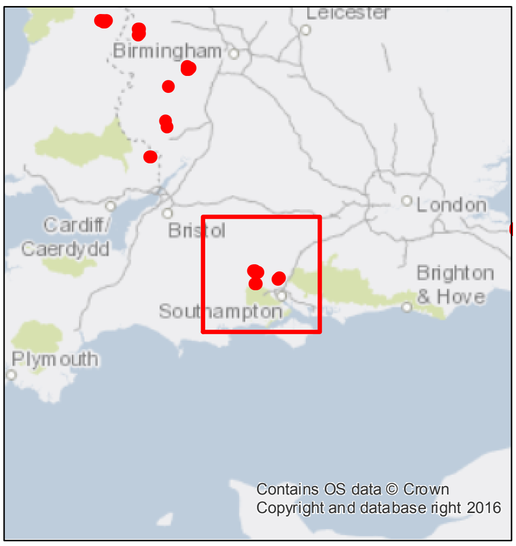

Bearing: 246

Bentley 04

E: 425335
N: 128982

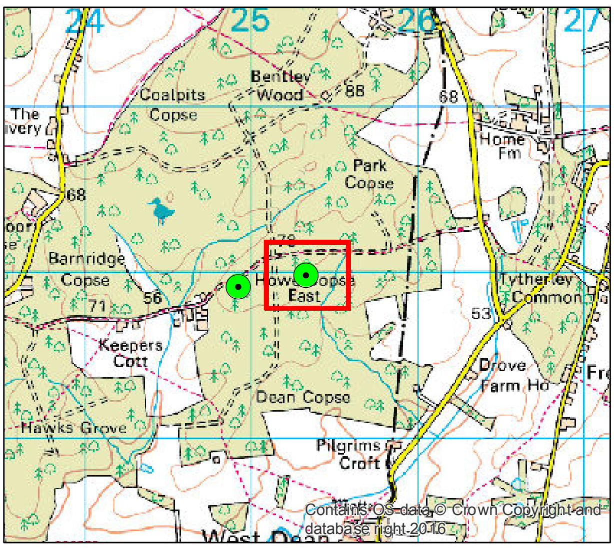

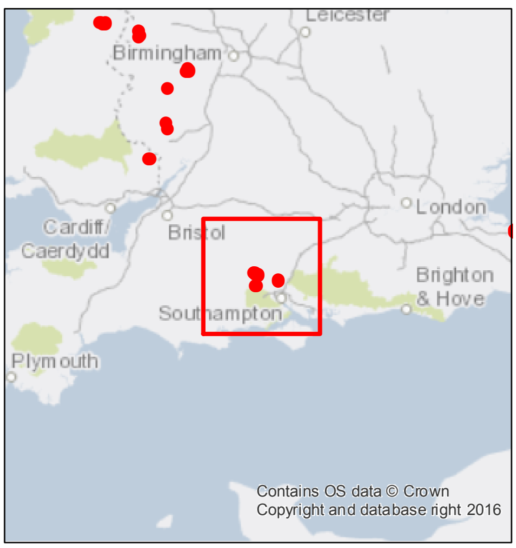

Bearing: 181

Big Forest 03

E: 315361
N: 309924

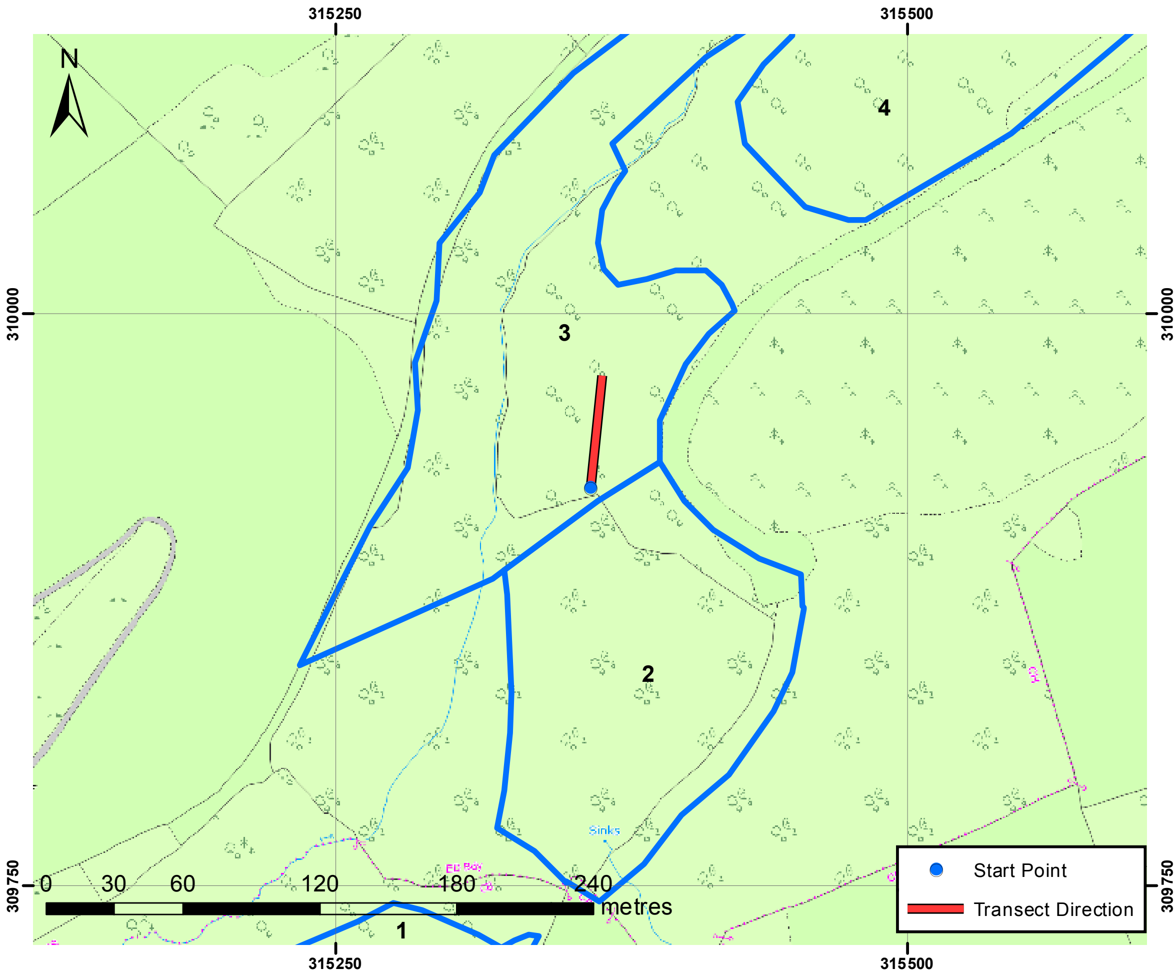

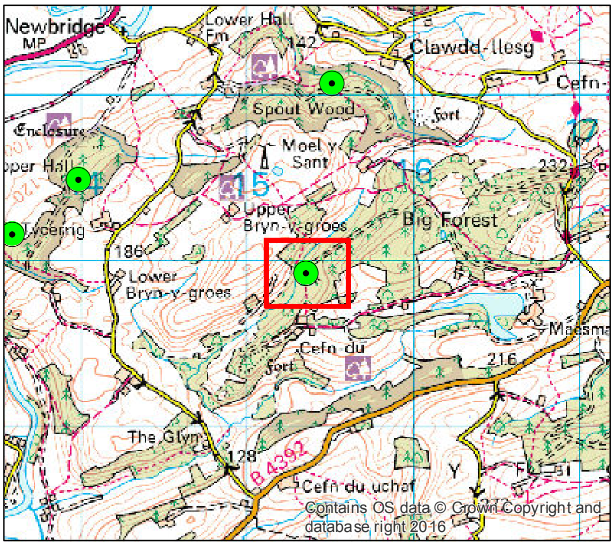

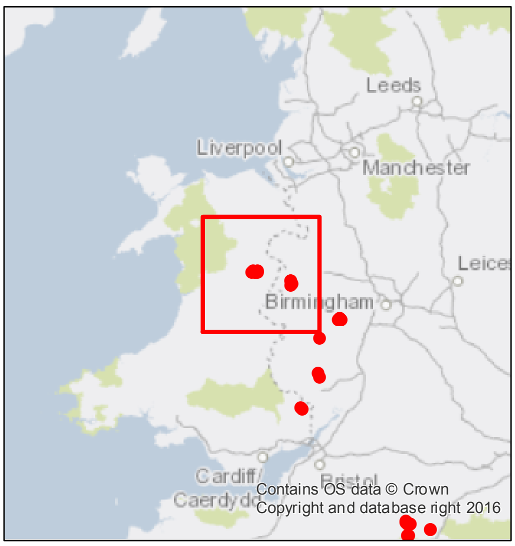

Bearing: 38

Blackmoor Wood

E: 423361
N: 129378

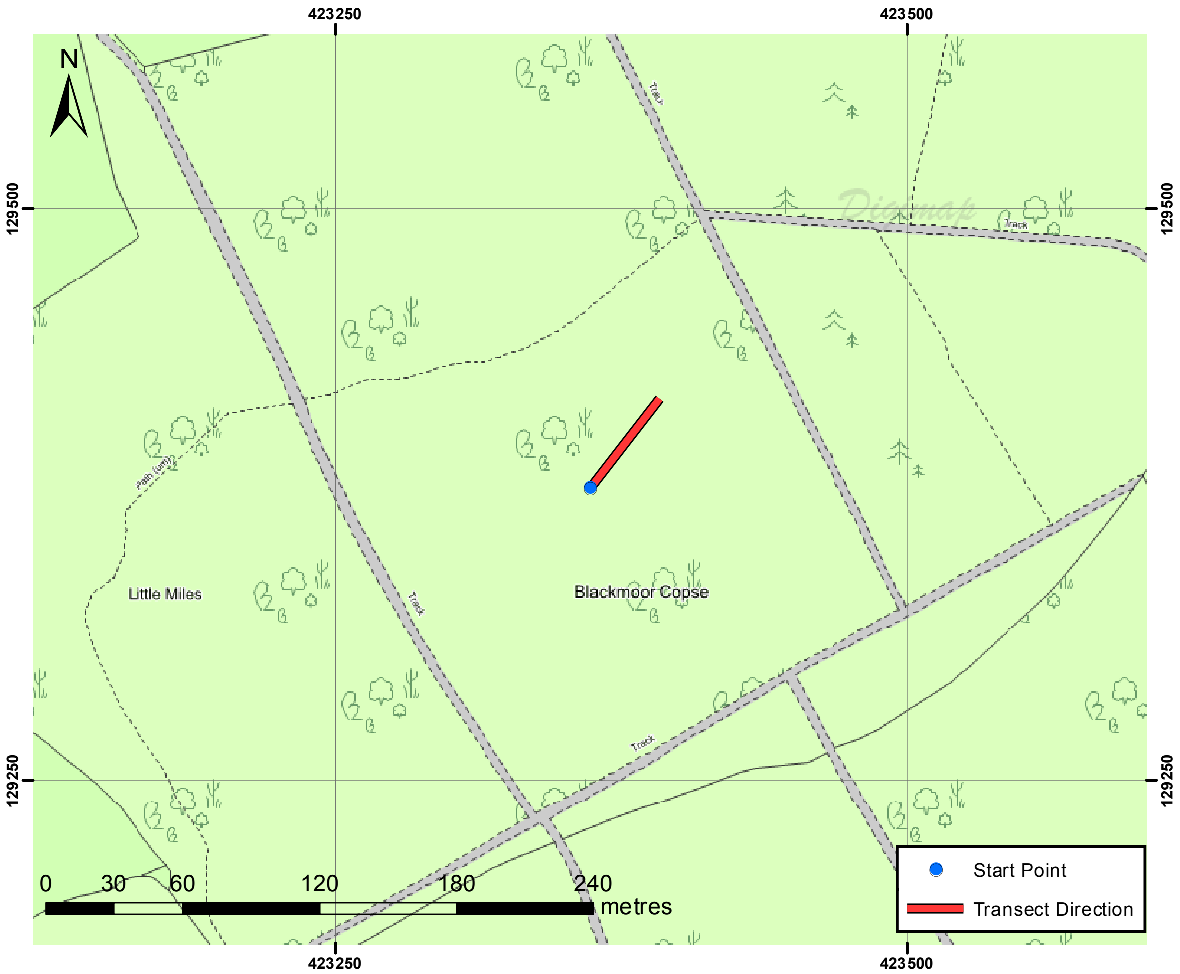

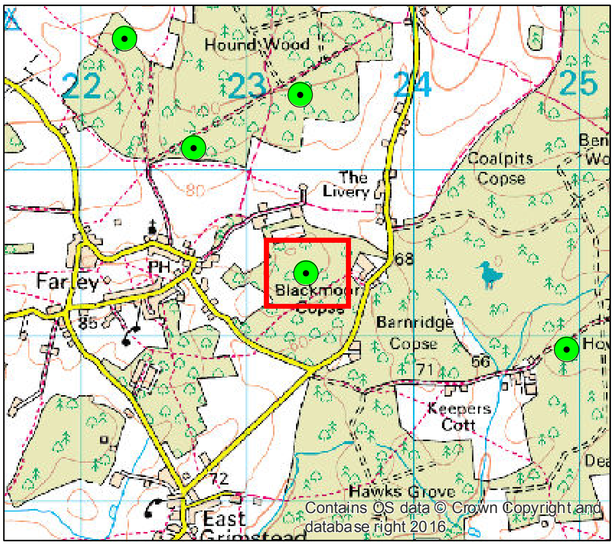

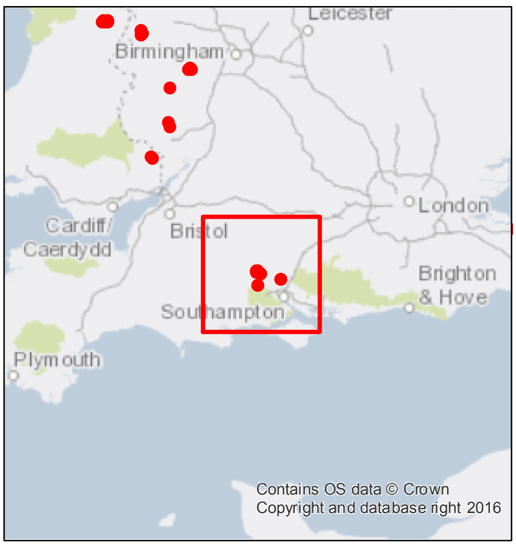

Bearing: 52

Blean Homestall 01

E: 610184
N: 159619

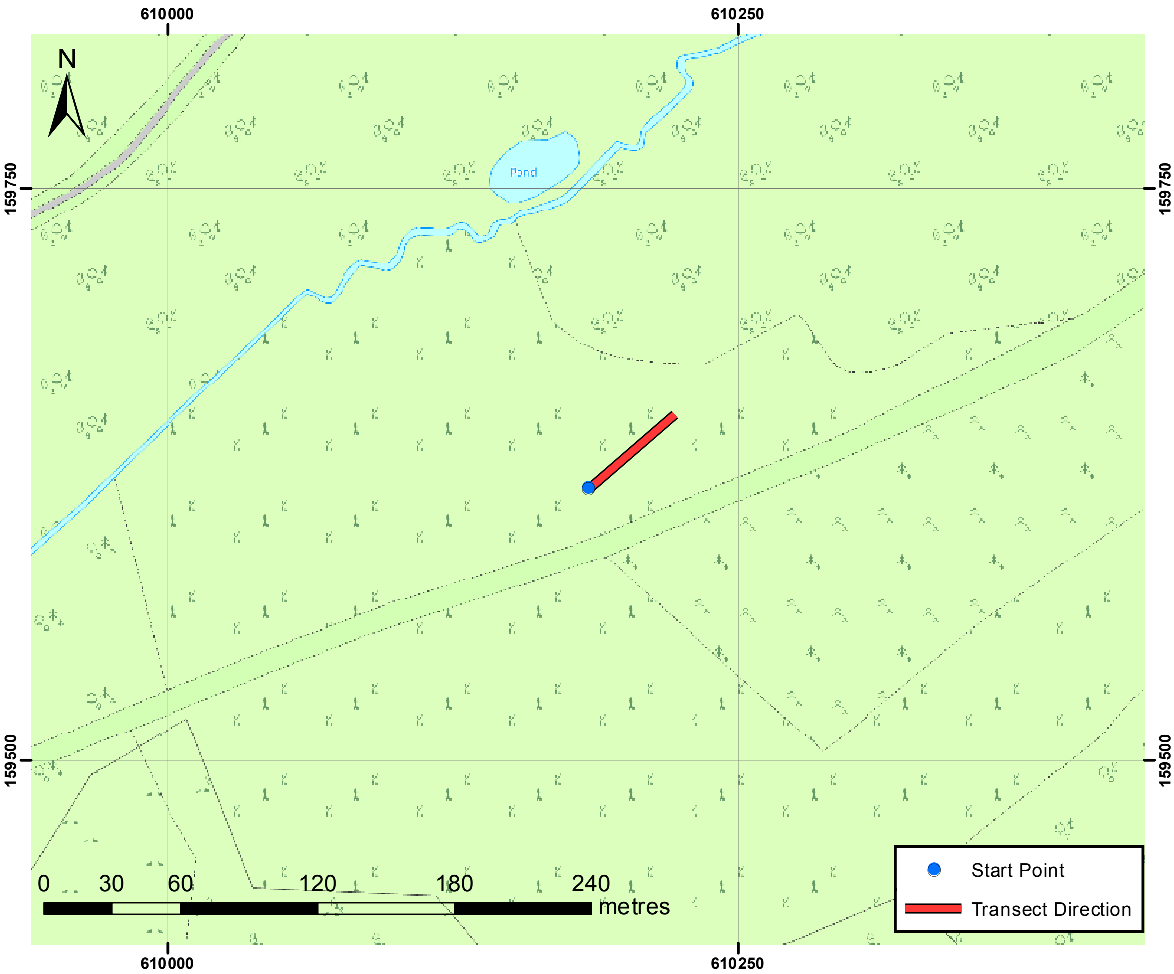

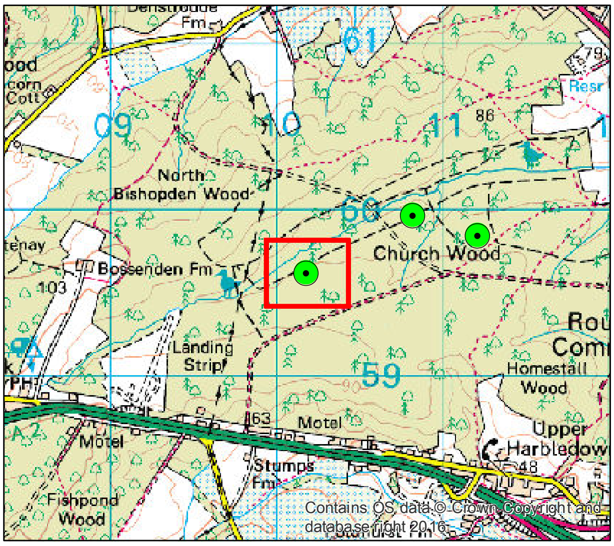

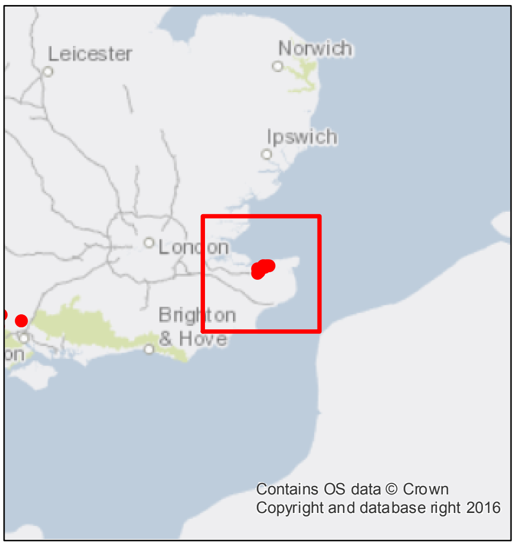

Bearing: 149

Blean Homestall 04

E: 610822
N: 159965

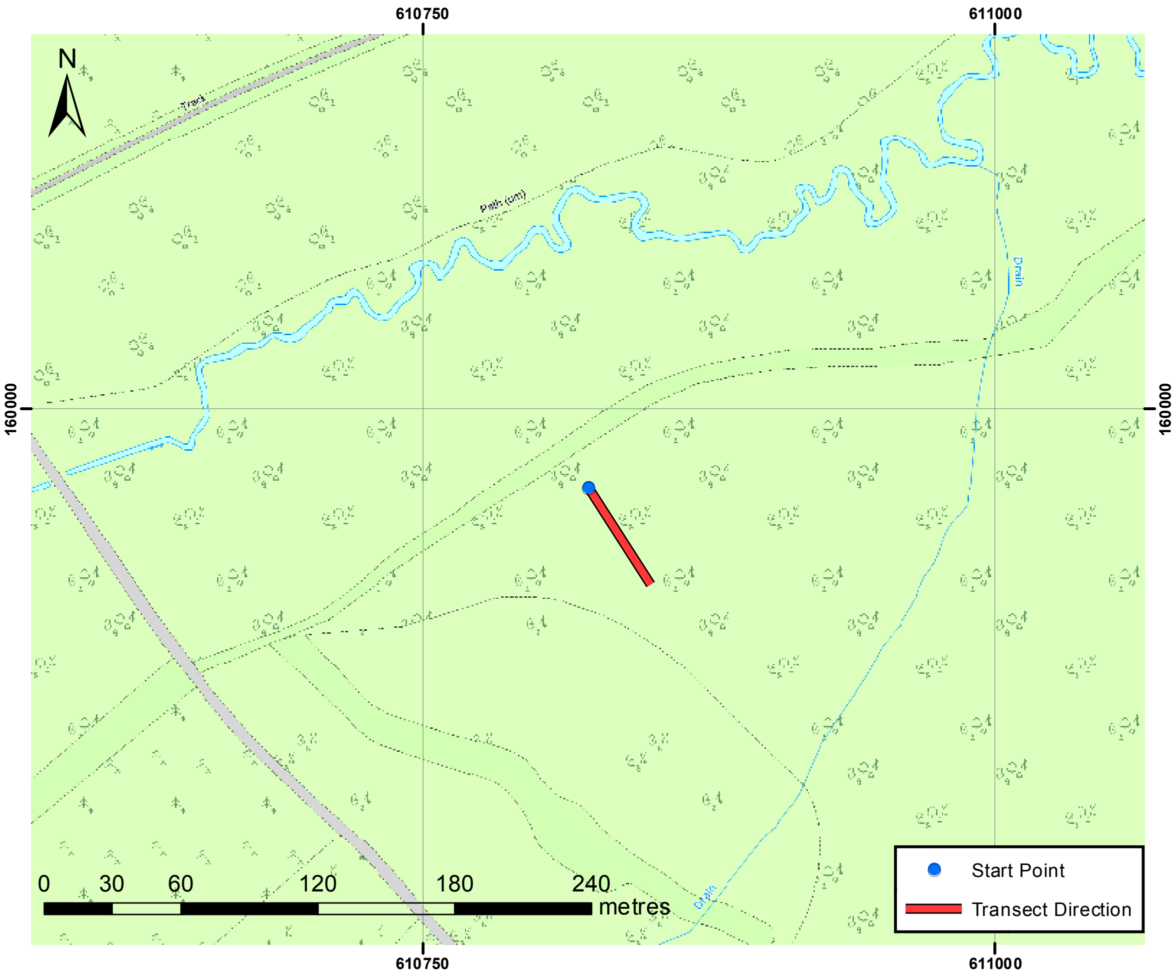

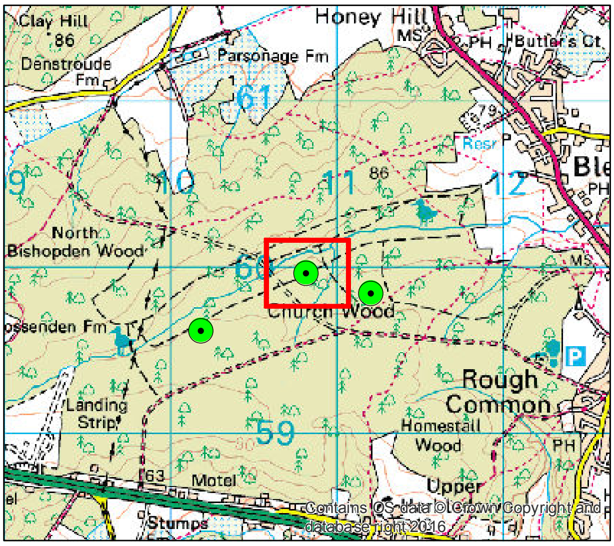

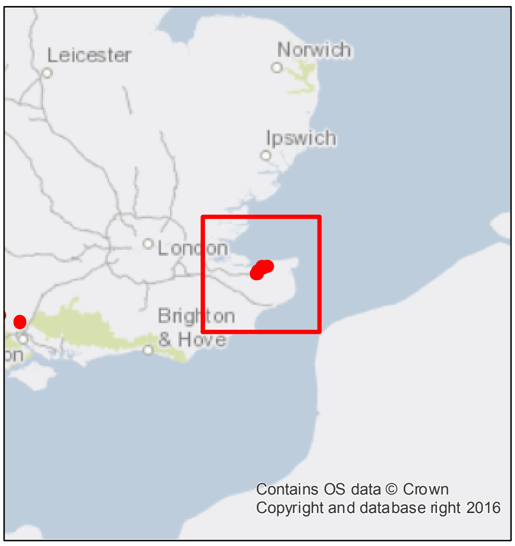

Bearing: 321

Blean Homestall 06

E: 611210
N: 159844

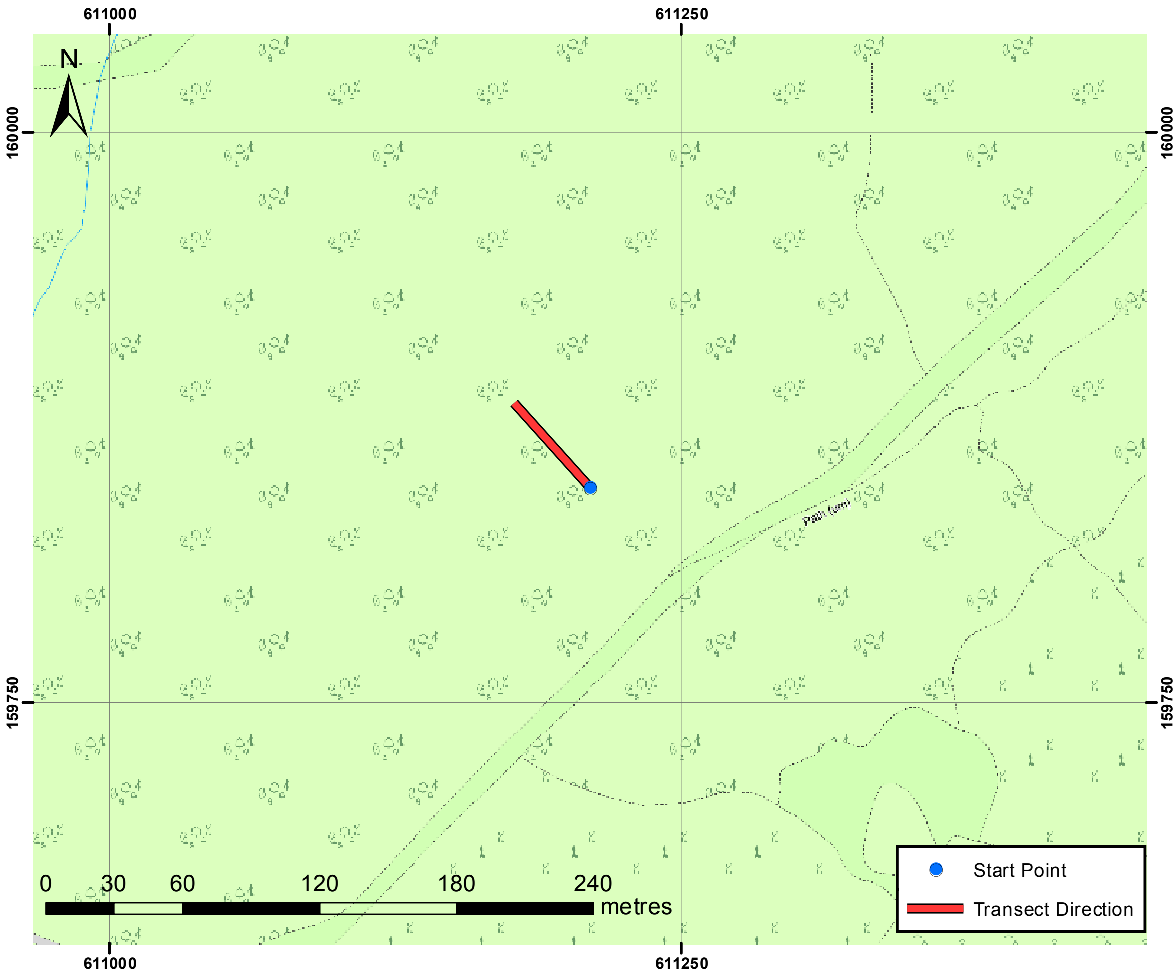

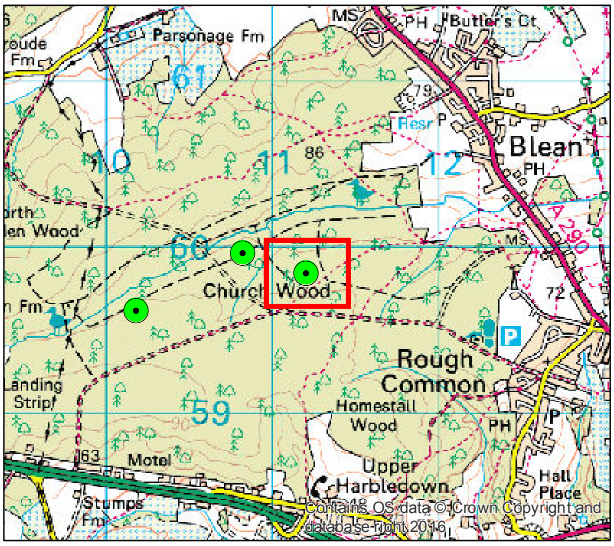

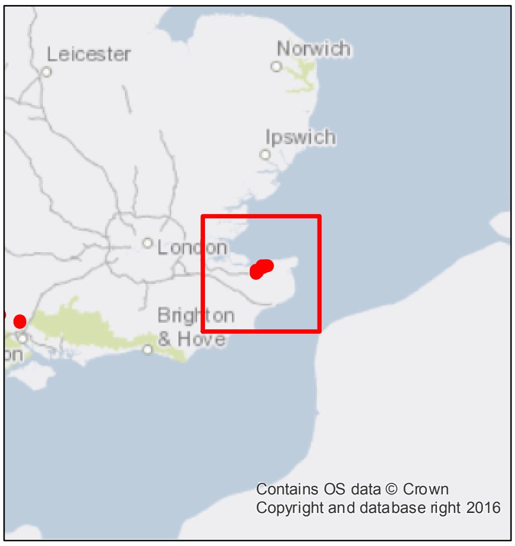

Bearing: 232

East Blean 01

E: 617713
N: 164456

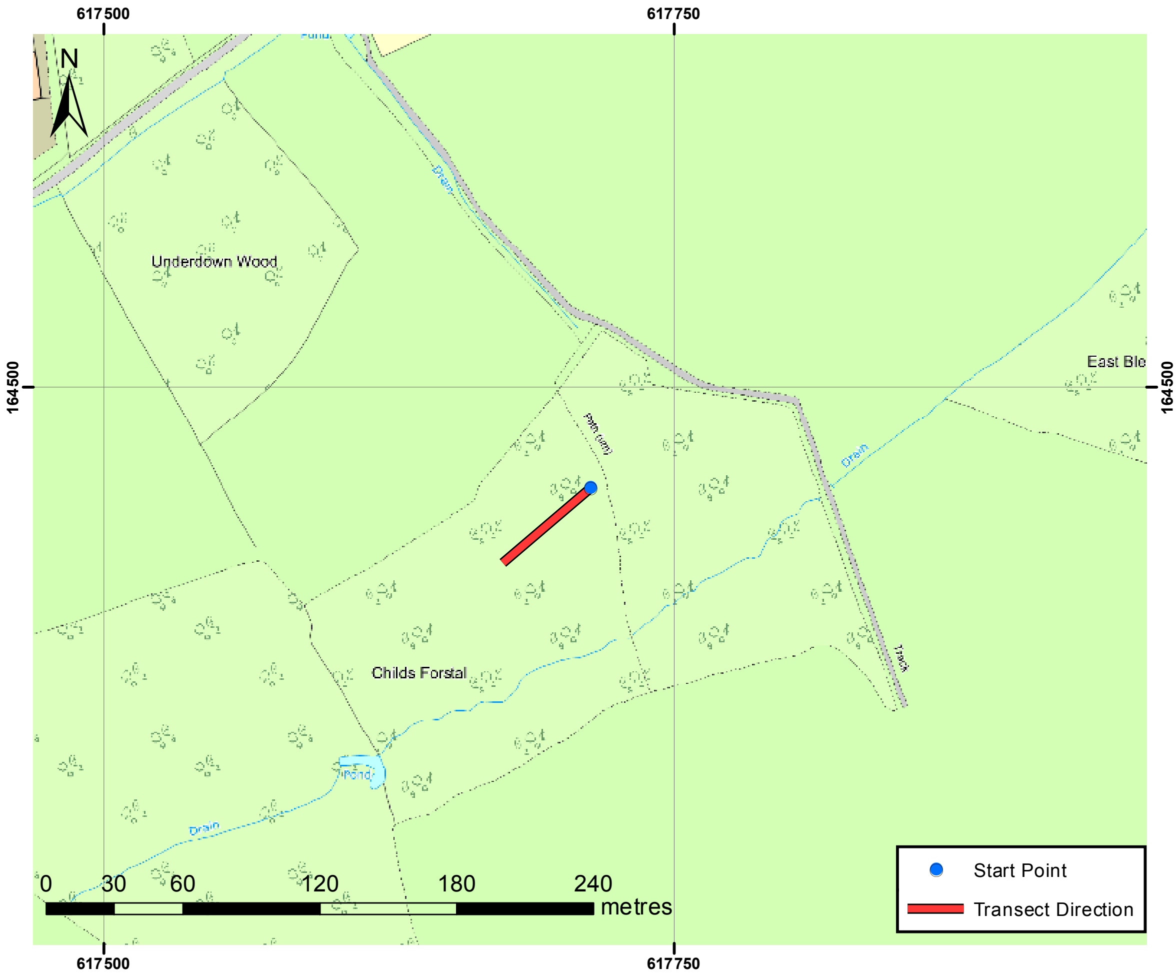

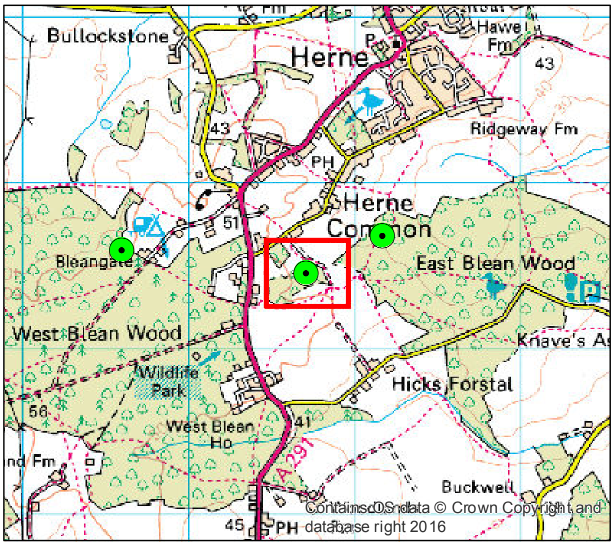

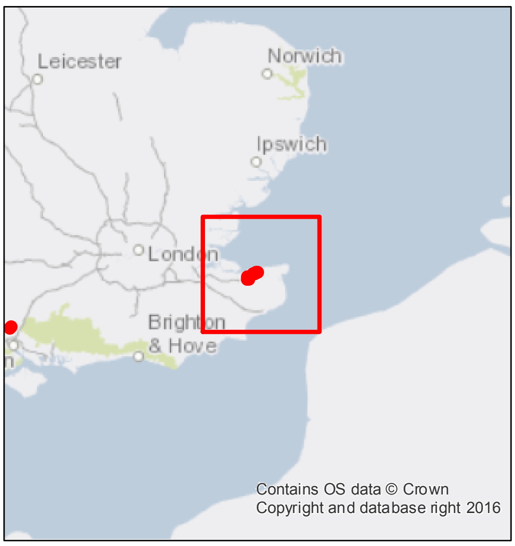

Bearing: 98

East Blean 03

E: 618170
N: 164679

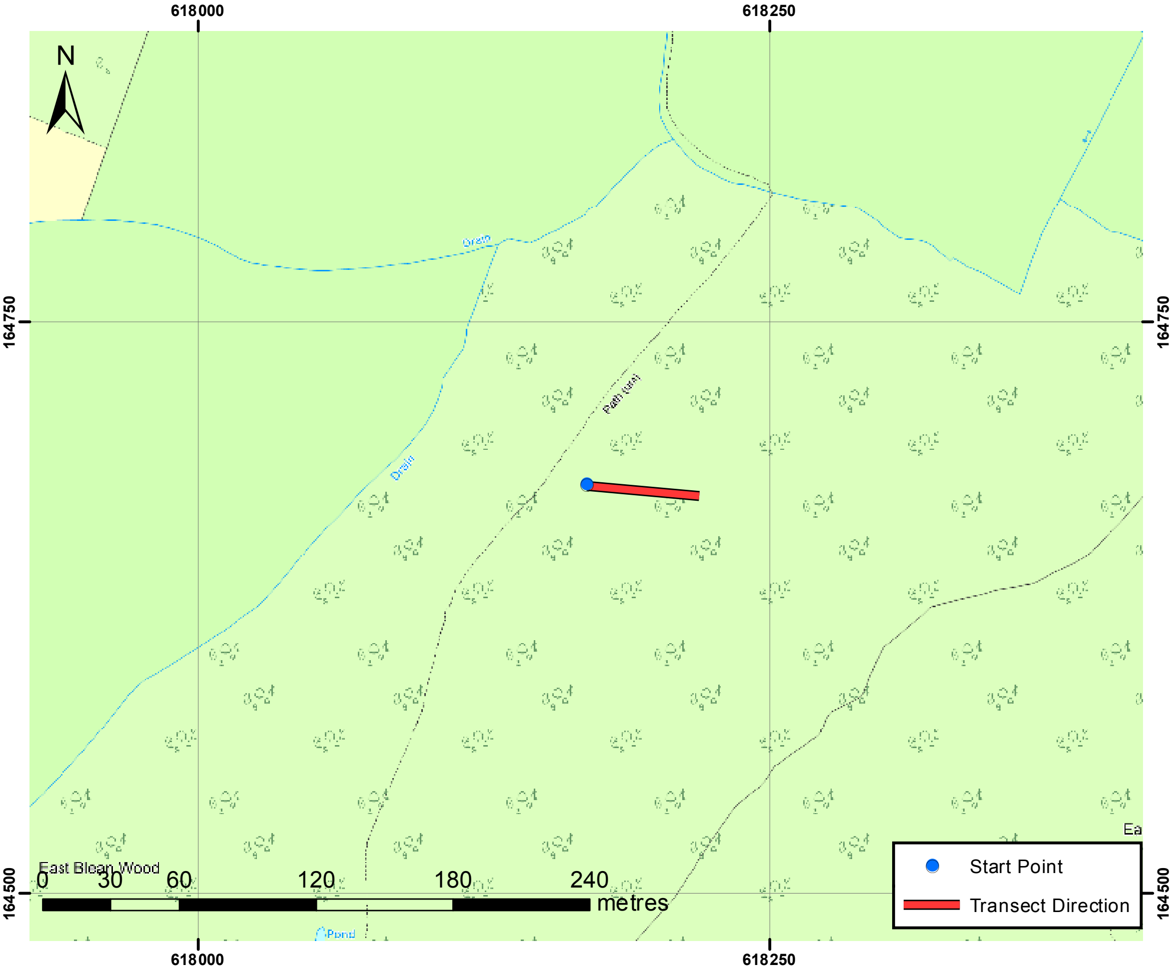

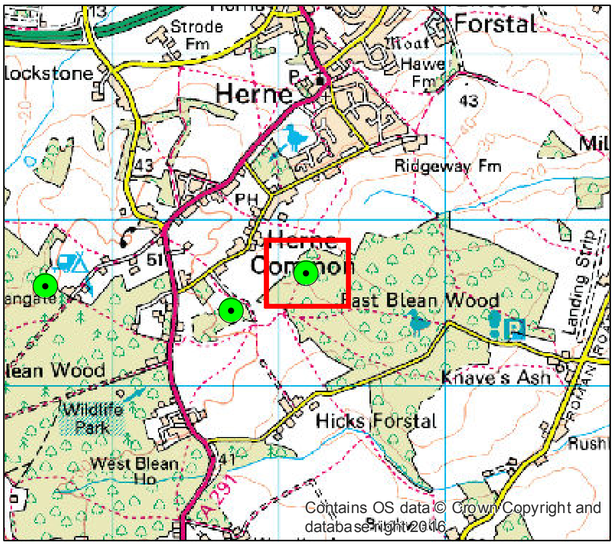

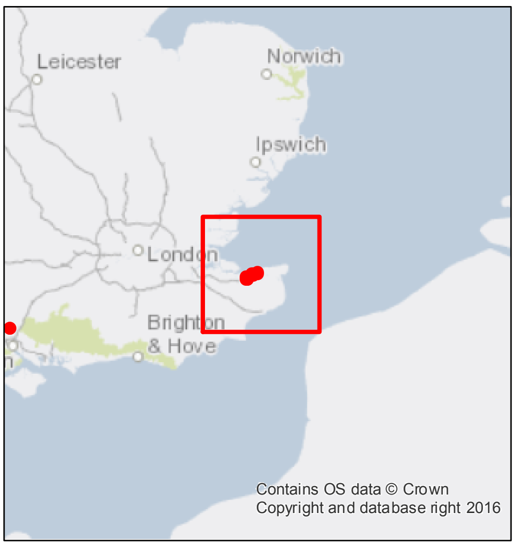

Bearing: 100

Eastridge 01

E: 340044
N: 301736

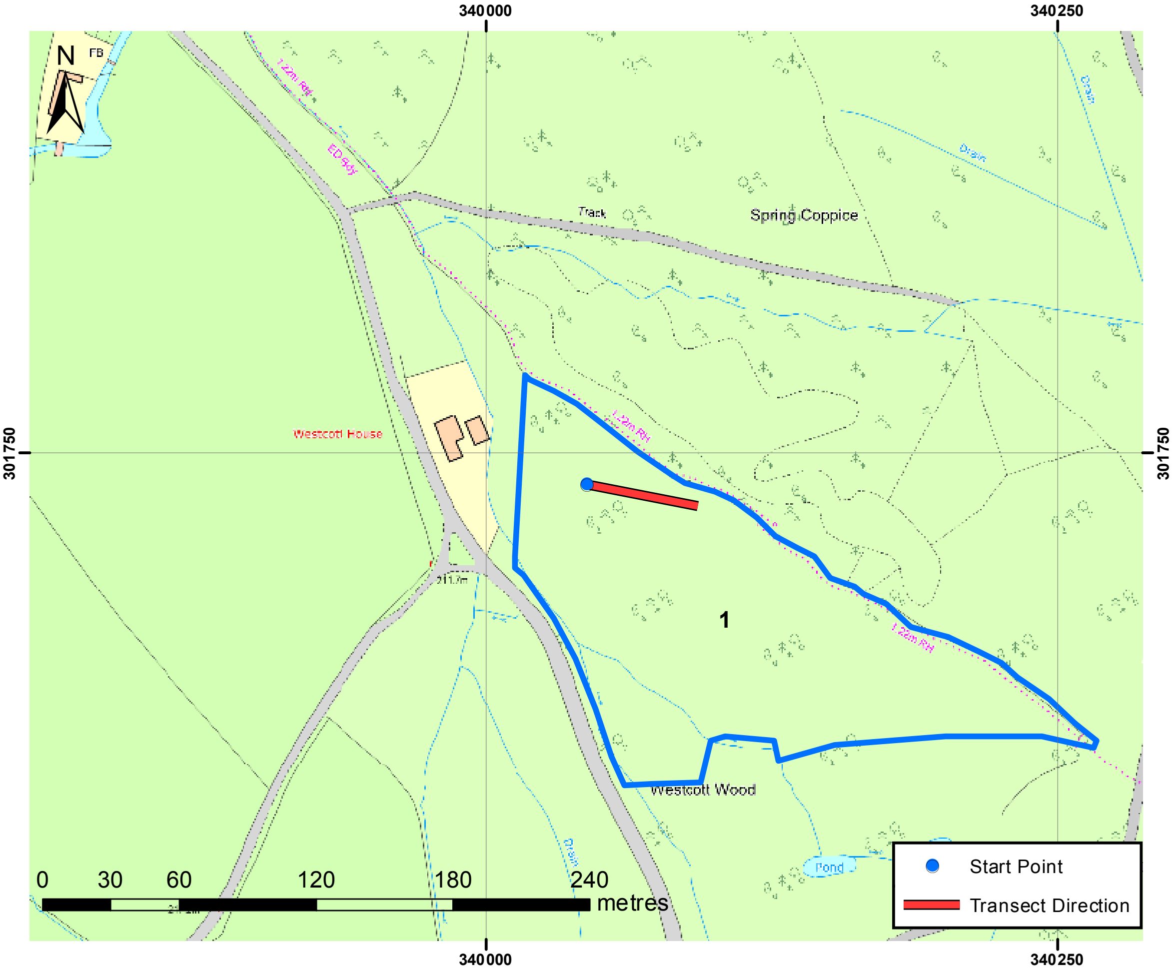

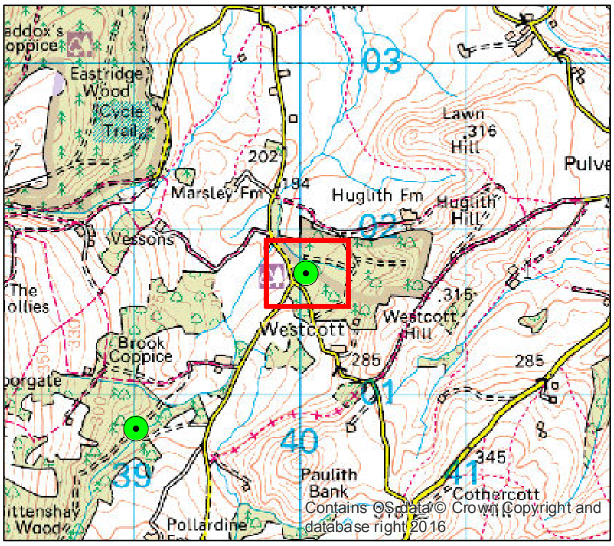

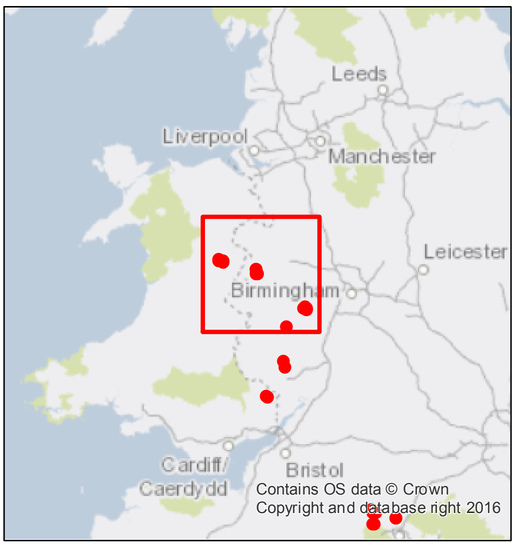

Bearing: **234**

Eastridge 05

E: **339015**
N: **300797**

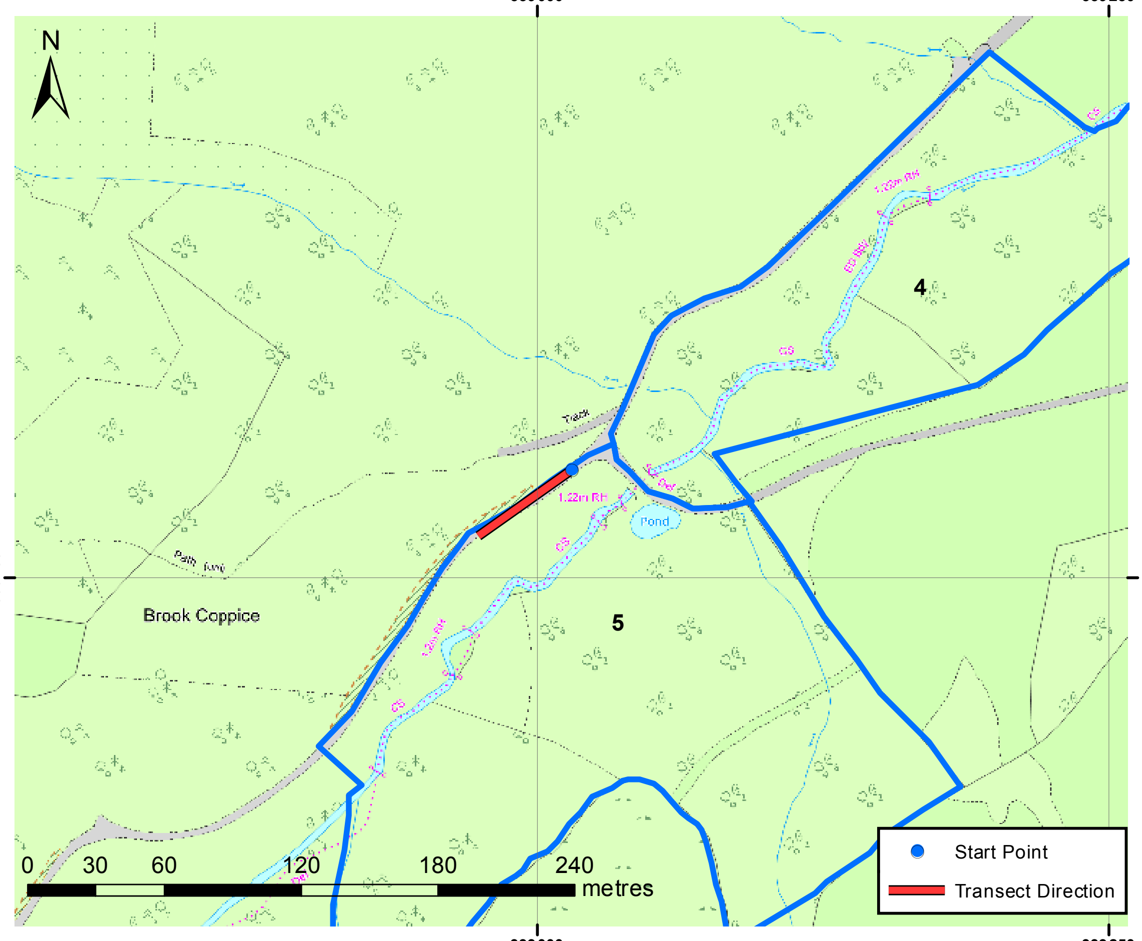

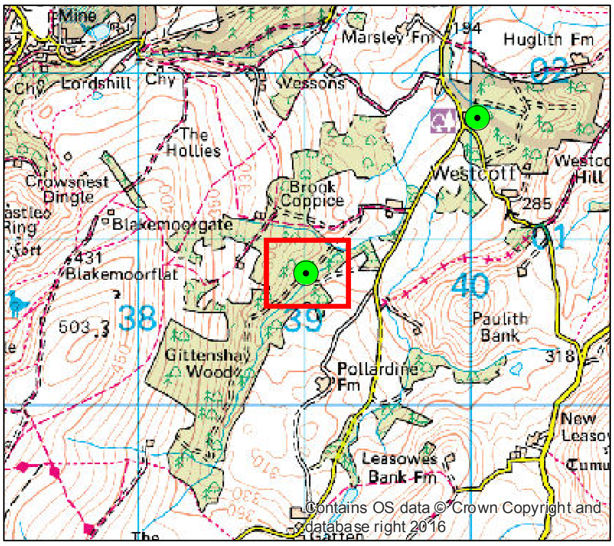

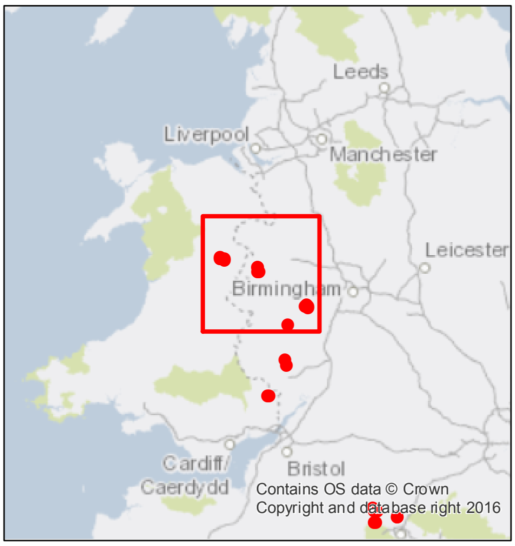

Bearing: 267

Ellenden Wood

E: 610335
N: 161895

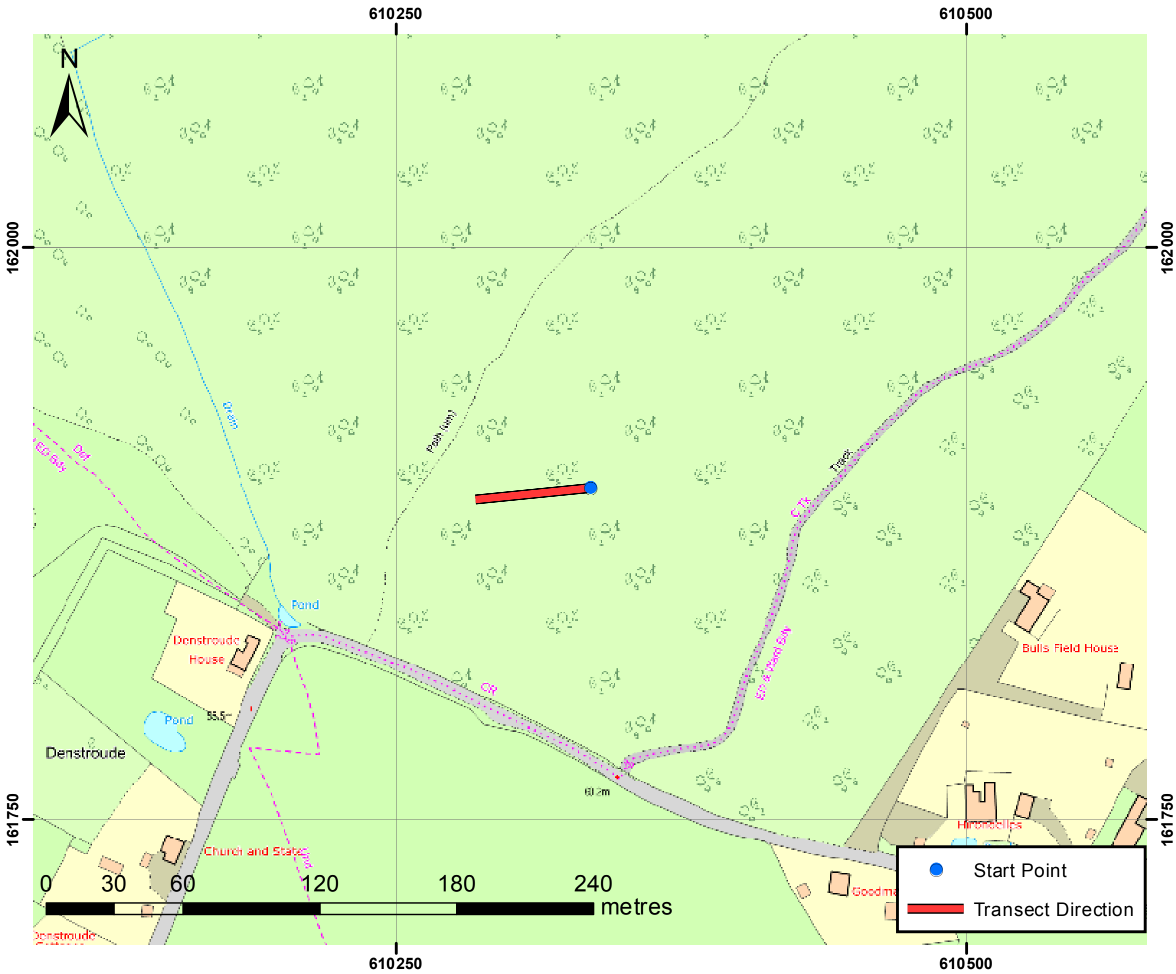

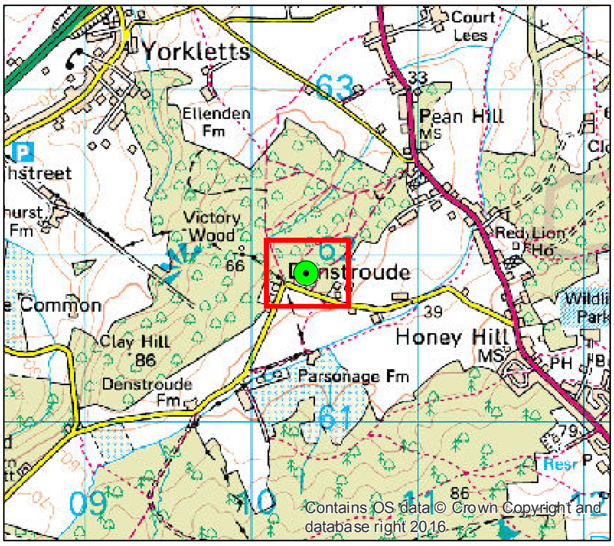

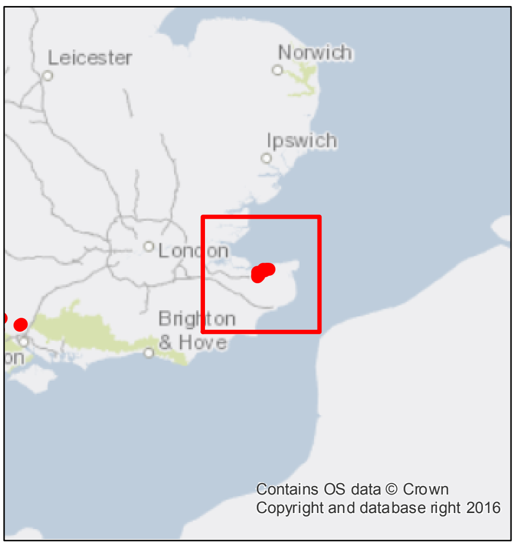

Bearing: 308

Ffridd Mathrafal 02

E: 311638
N: 310858

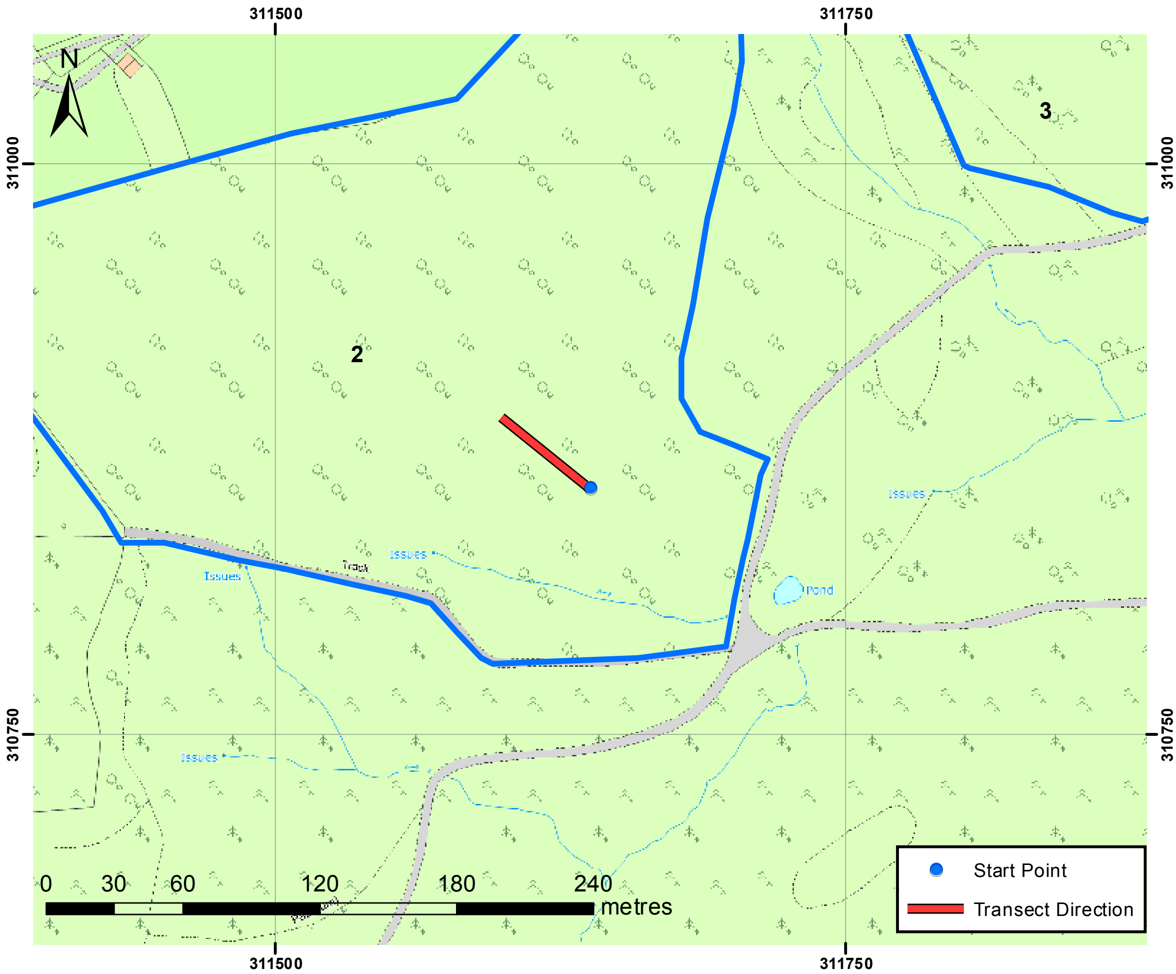

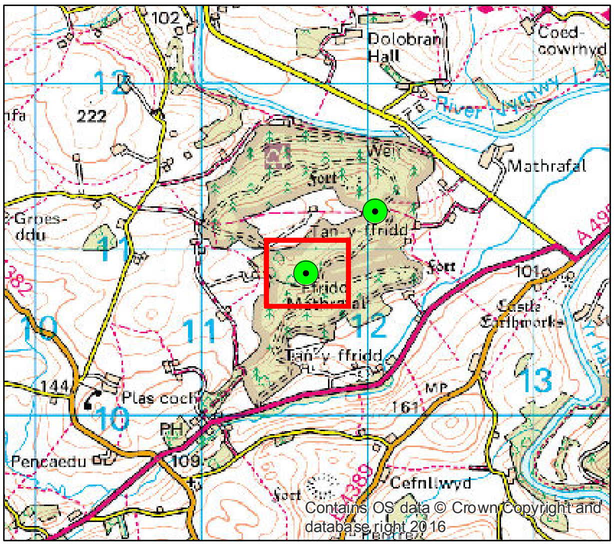

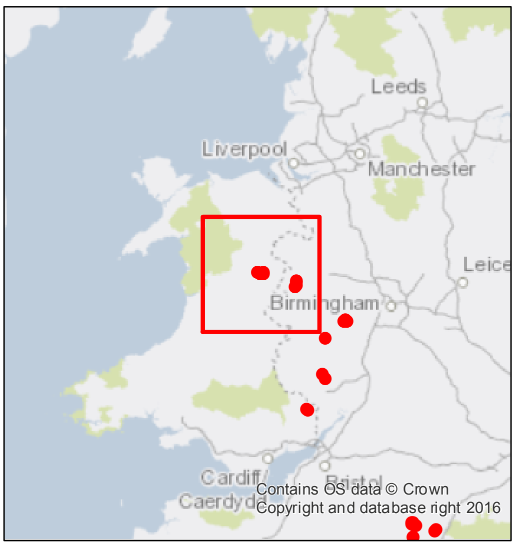

Bearing: 270

Ffridd Mathrafal 04

E: 312046
N: 311234

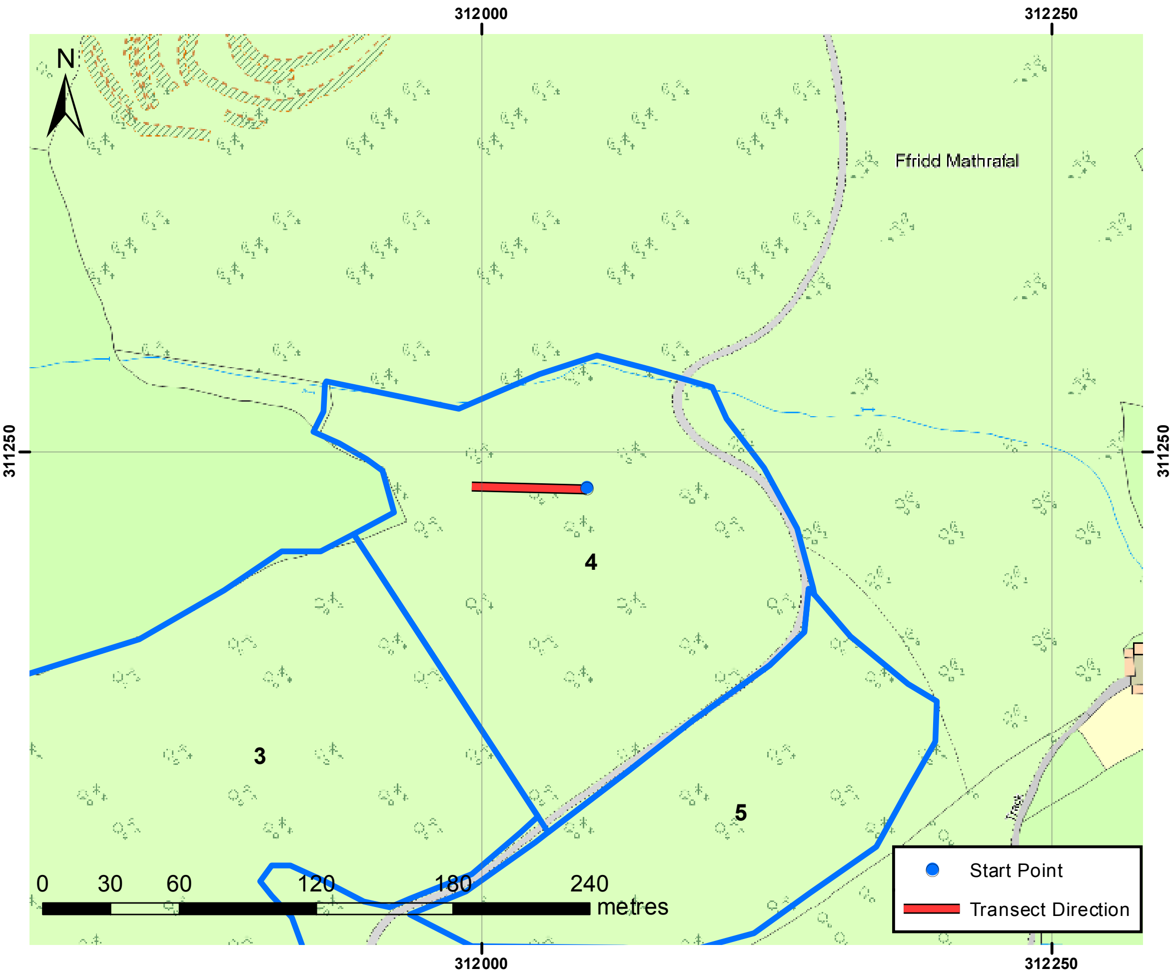

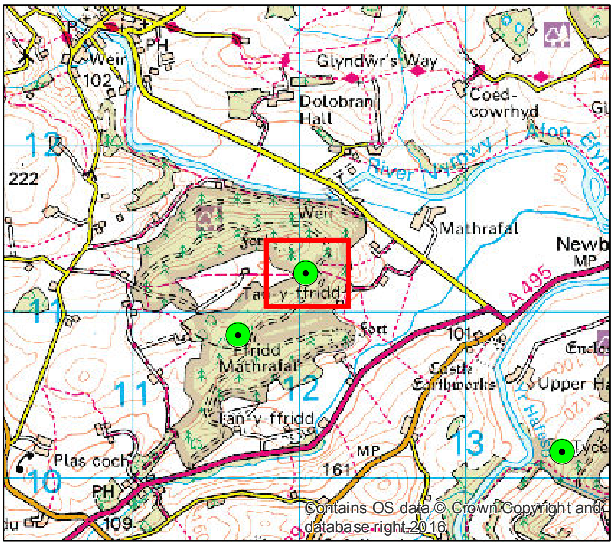

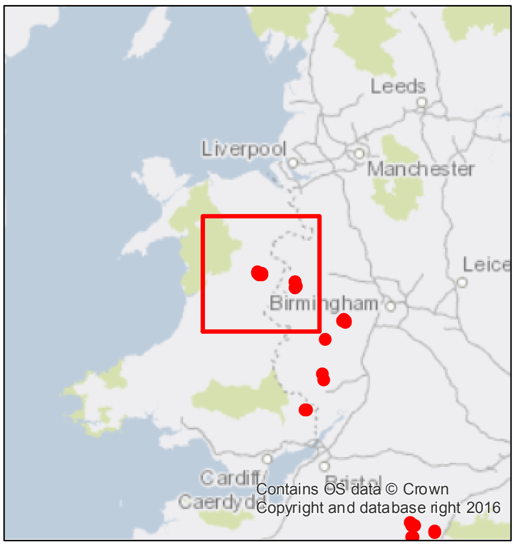

Bearing: 69

Gwern Ddu 01

E: 313587
N: 310155

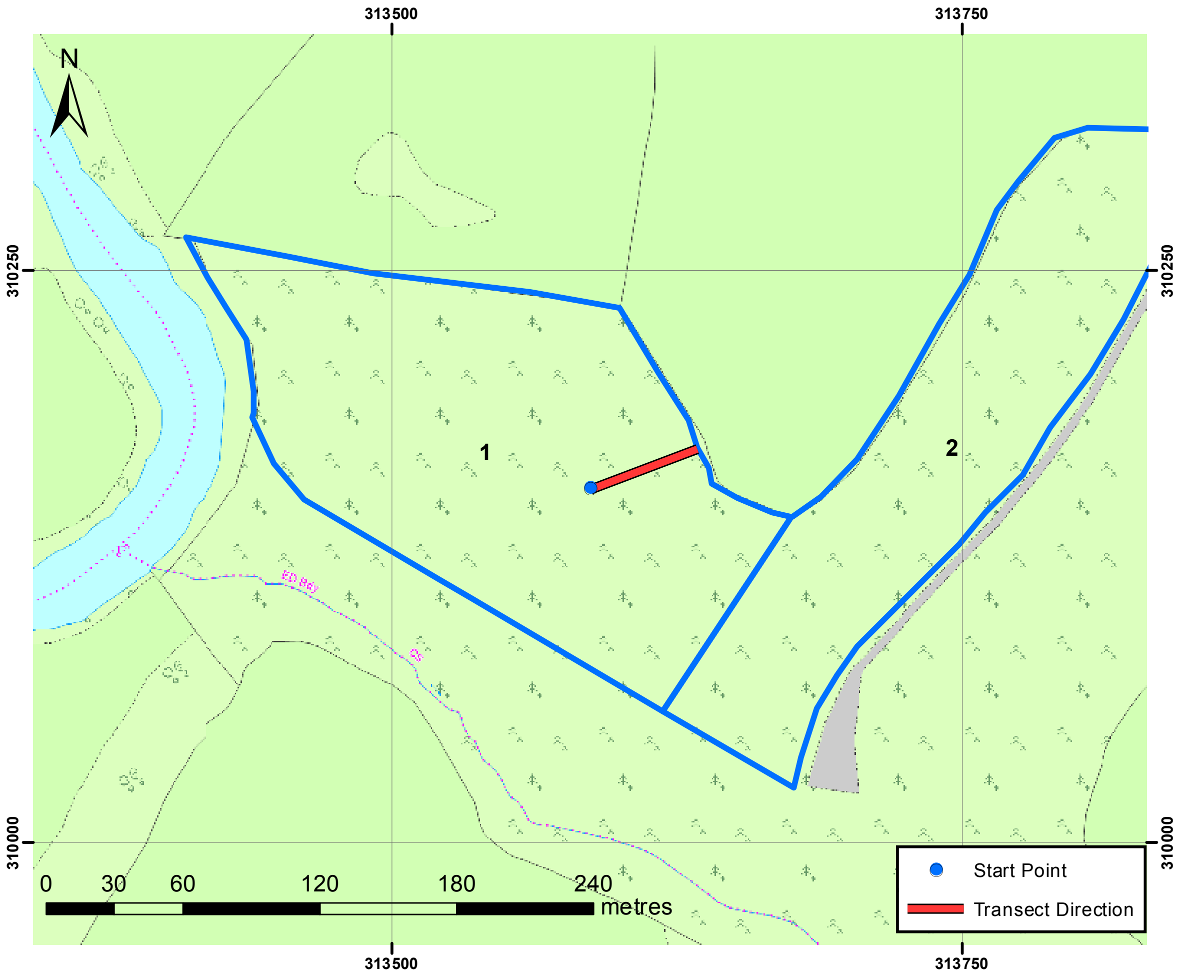

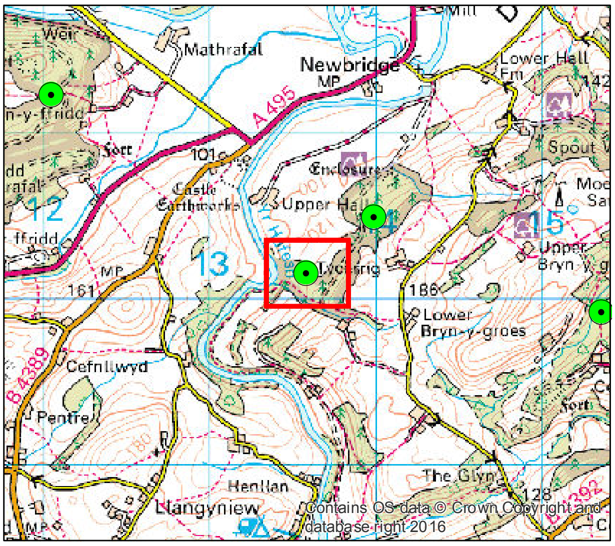

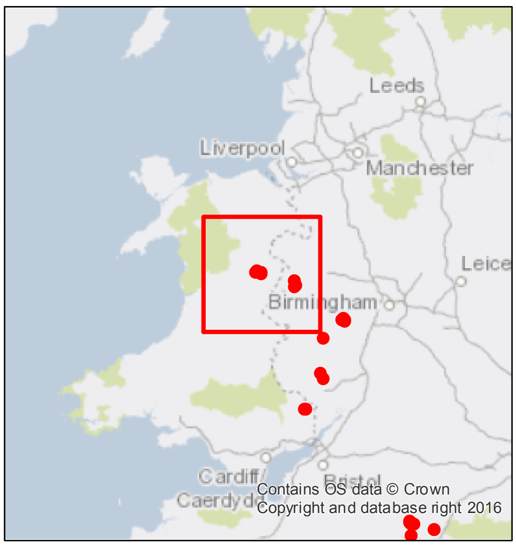

Bearing: 48

Gwern Ddu 04

E: 313986
N: 310491

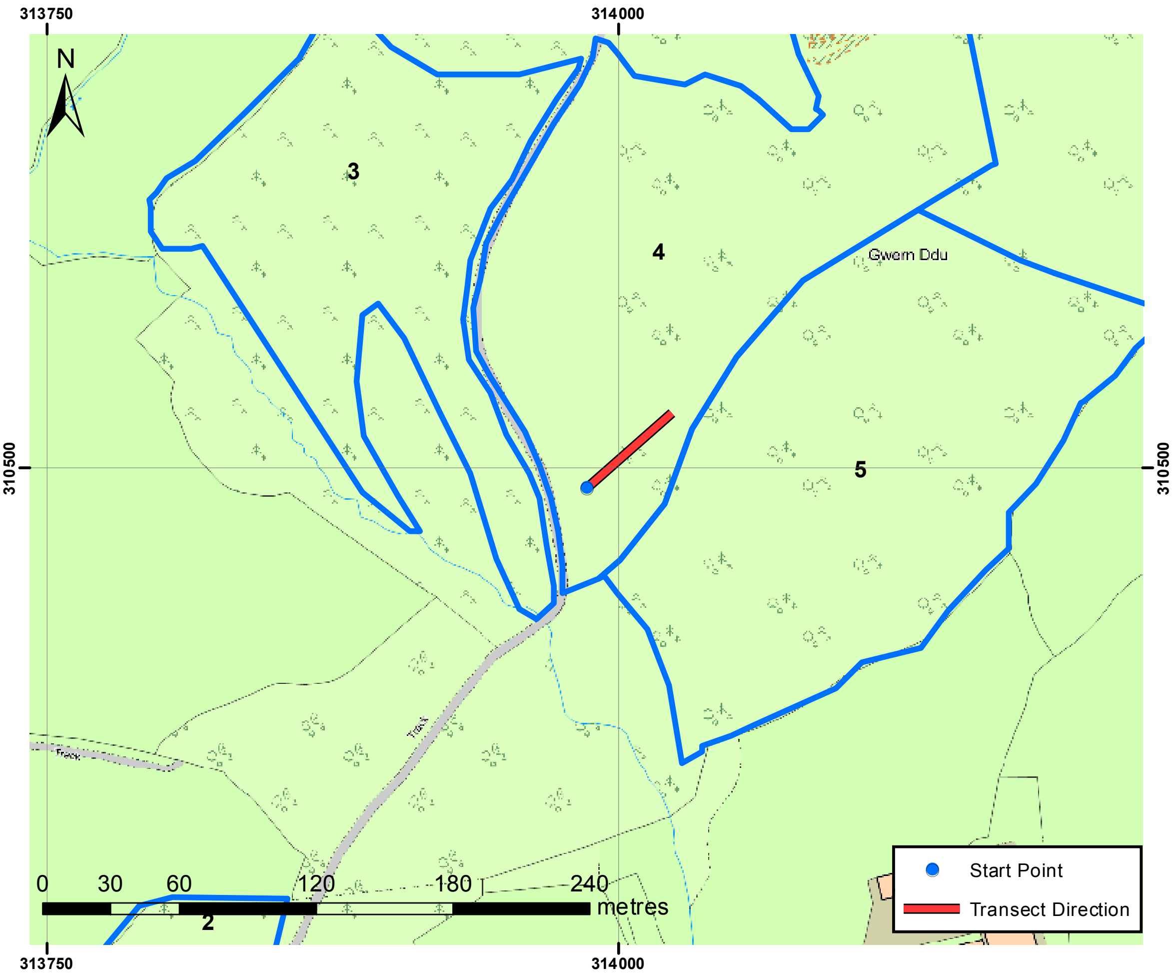

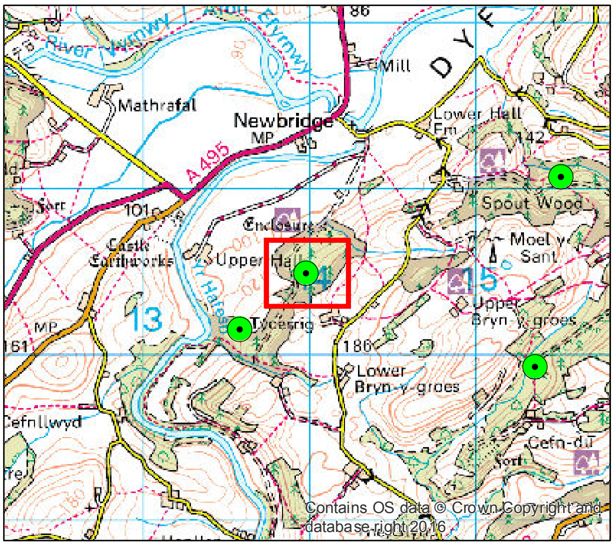

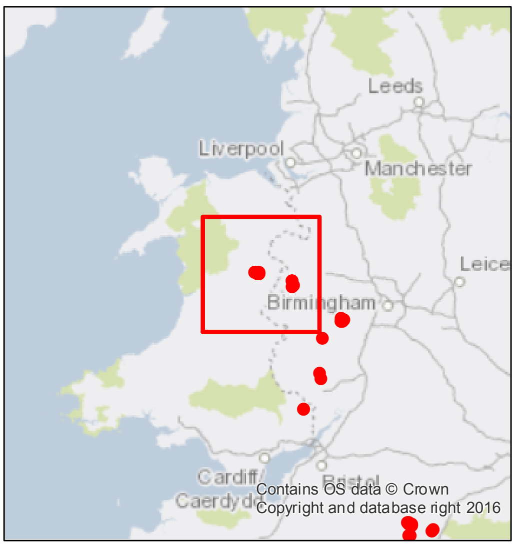

Bearing: 266

Haugh Wood

E: 358630
N: 237944

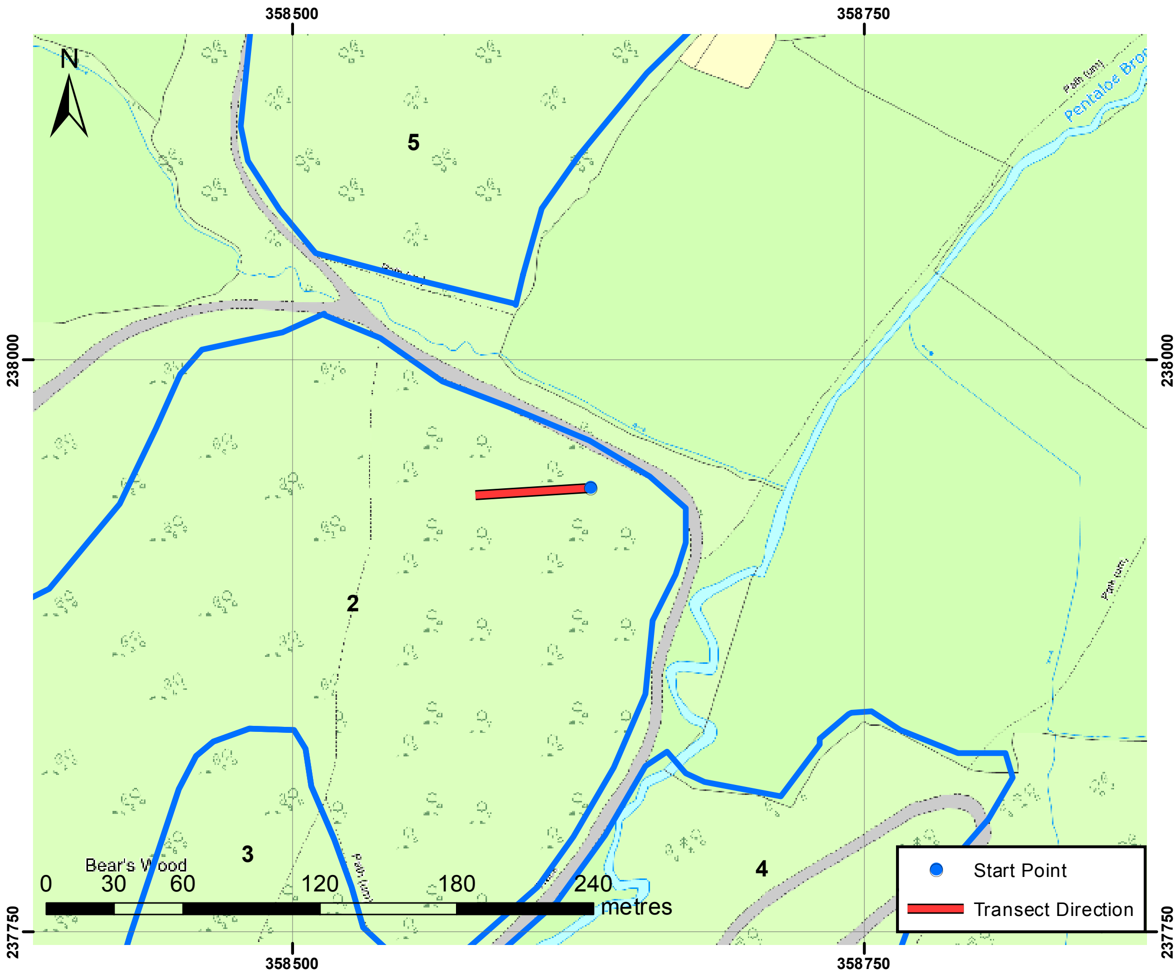

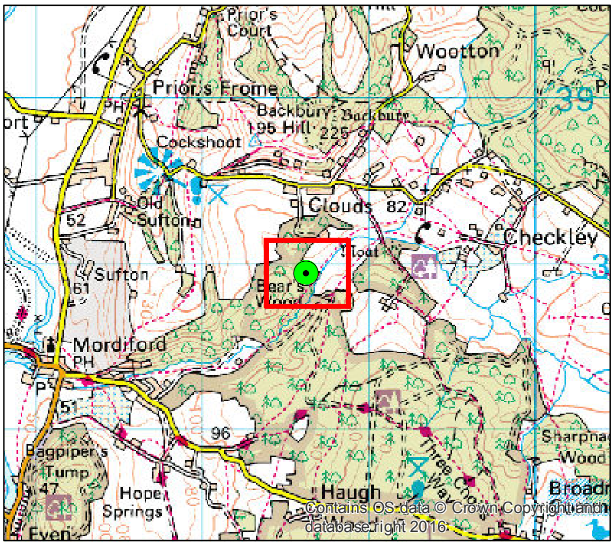

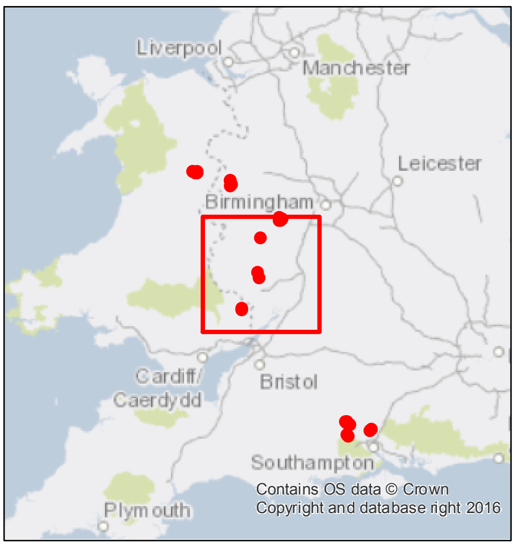

Bearing: 20

Hound Wood 01

E: 422263
N: 130790

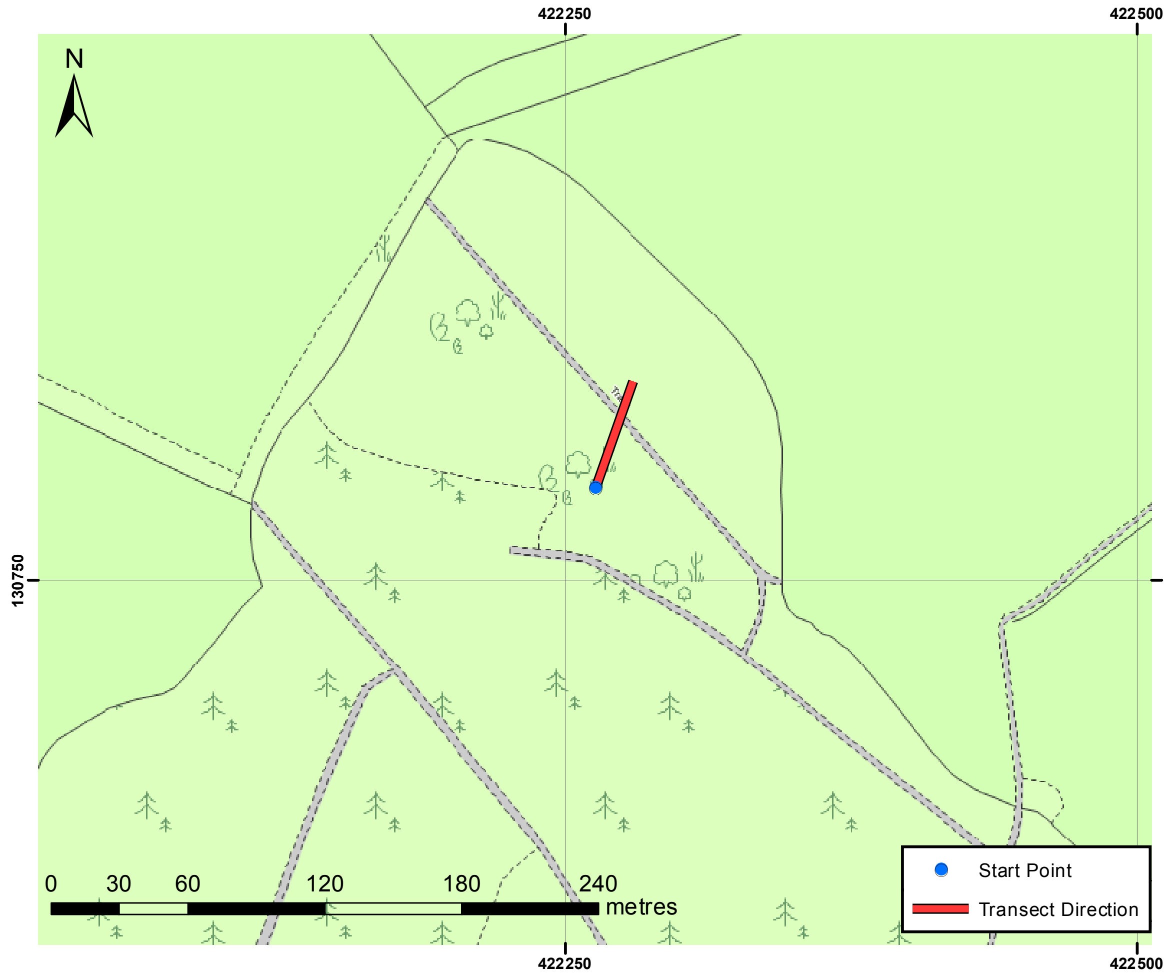

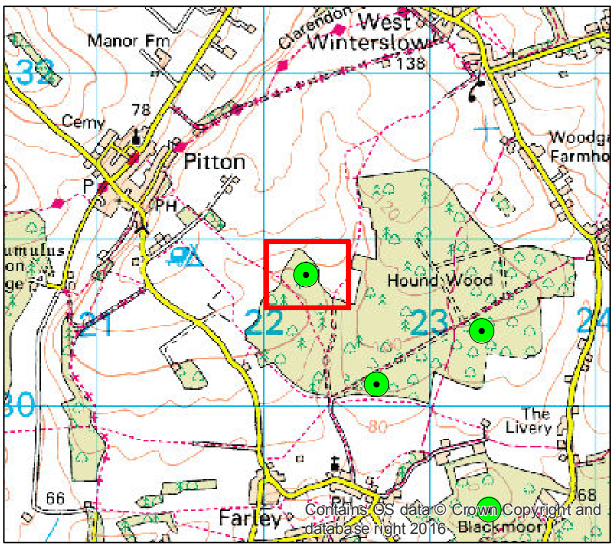

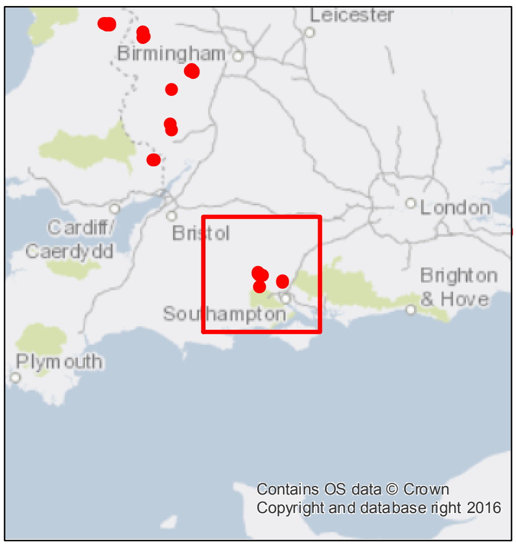

Bearing: 218

Hound Wood 03

E: 422680
N: 130130

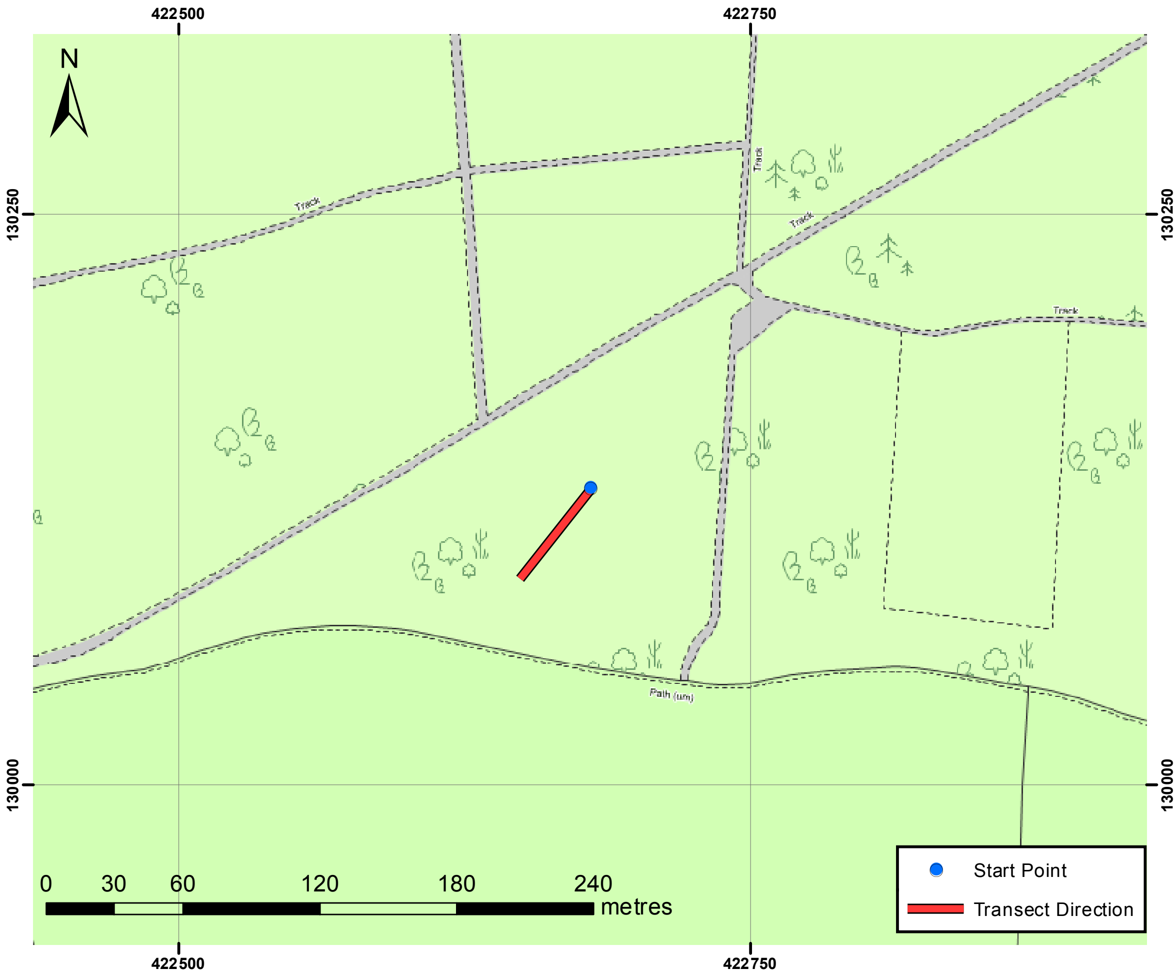

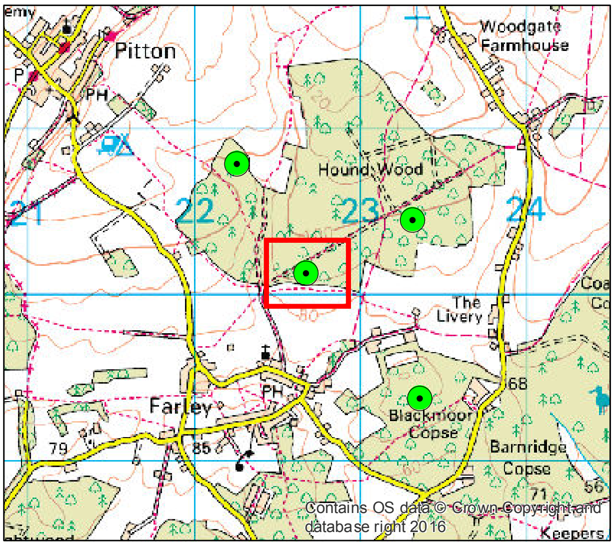

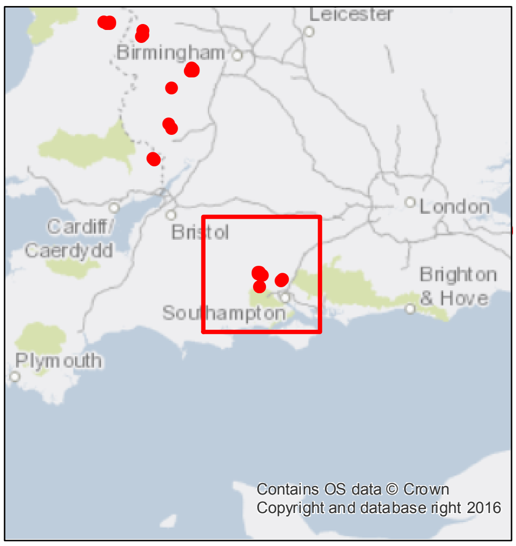

Bearing: 27

Hound Wood 05

E: 423320
N: 130454

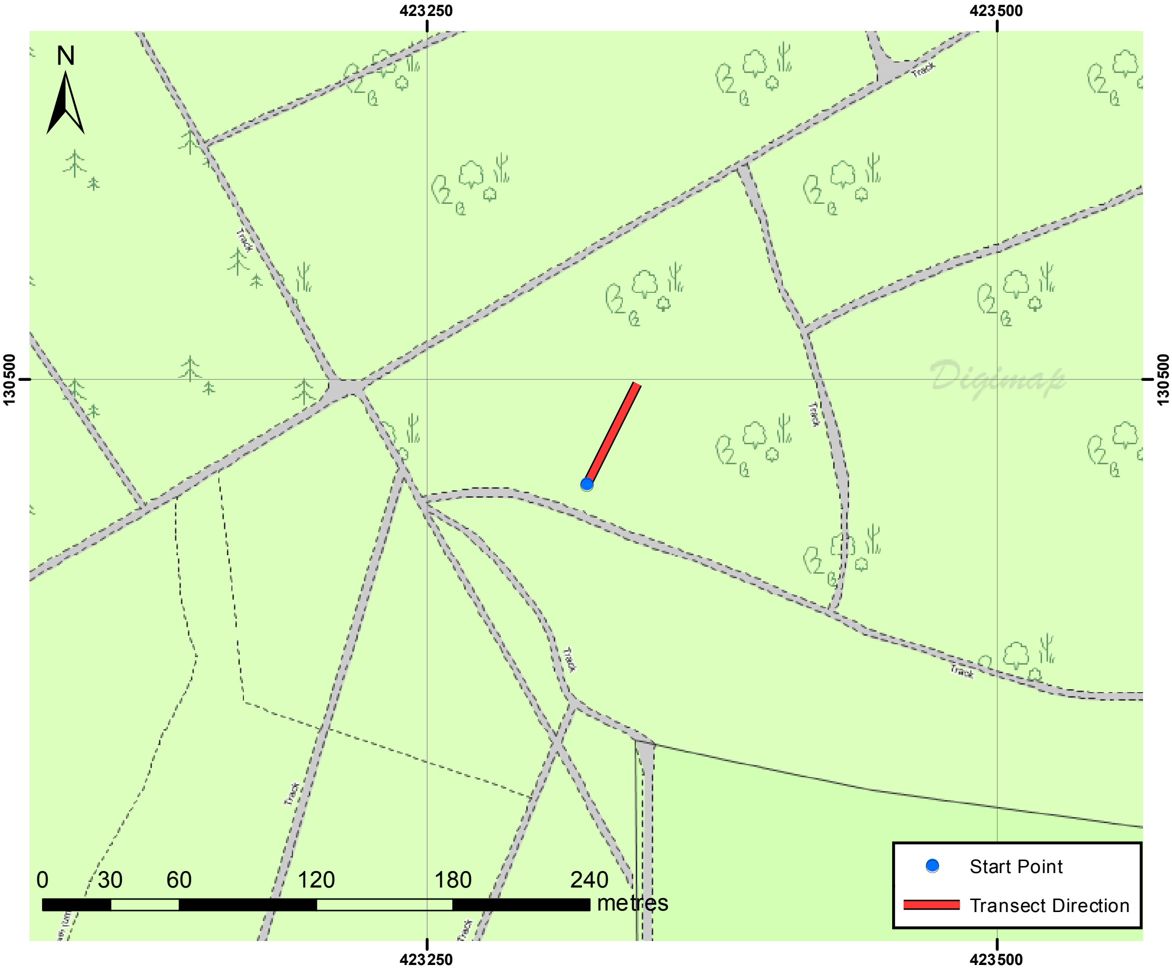

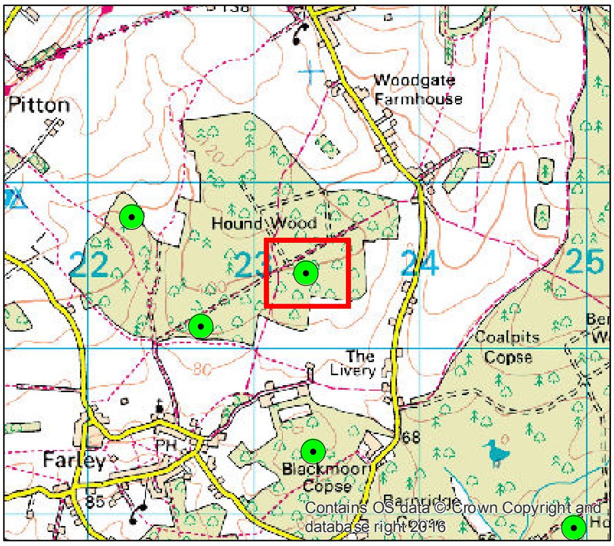

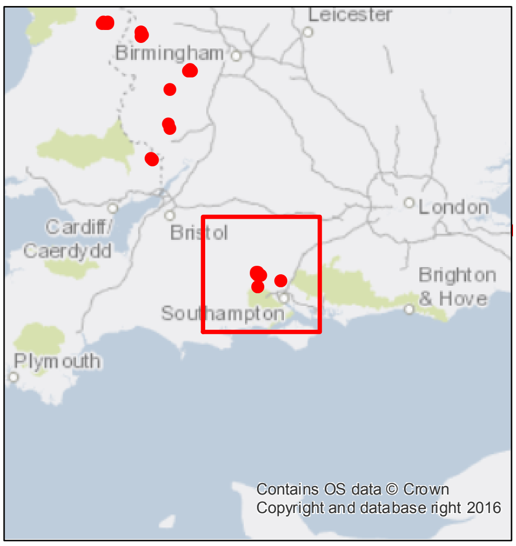

Bearing: 214

Kingswood 01

E: 346719
N: 212581

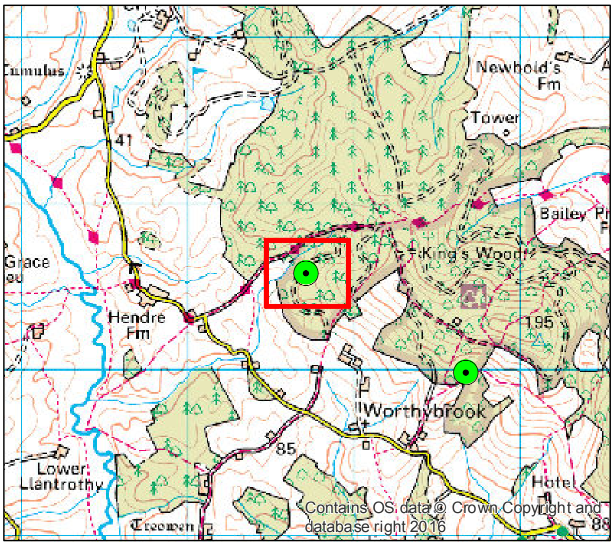

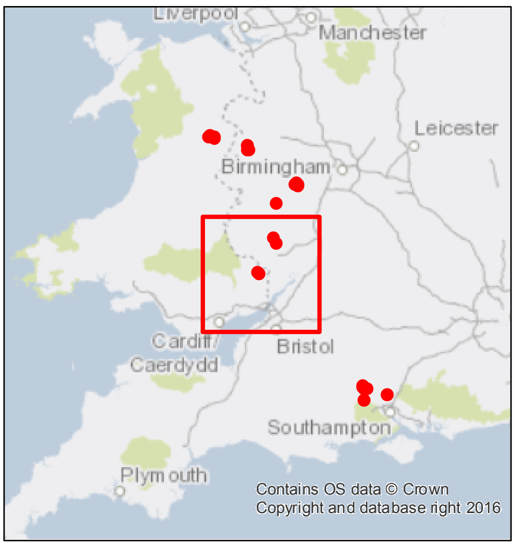

Bearing: 201

Kingswood 10

E: 347678
N: 211986

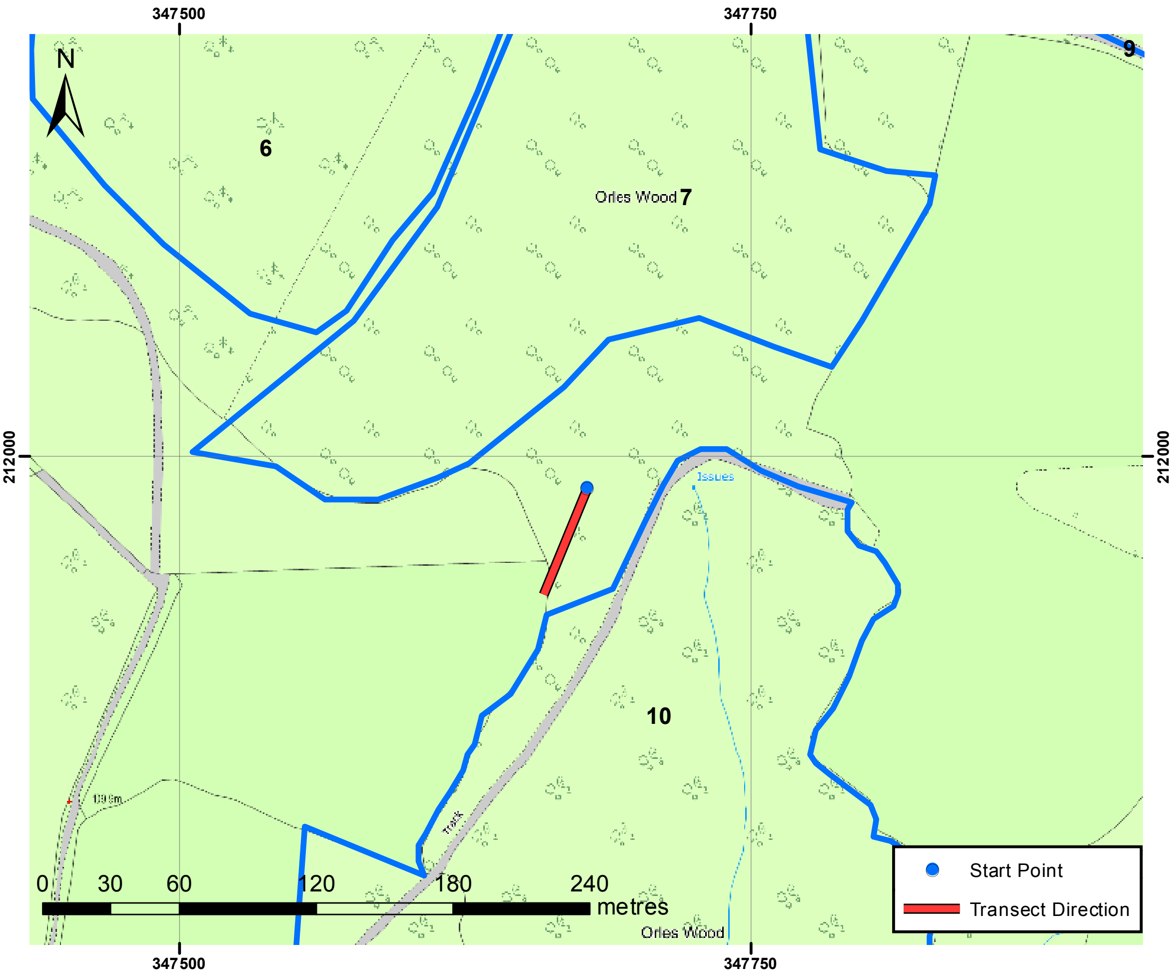

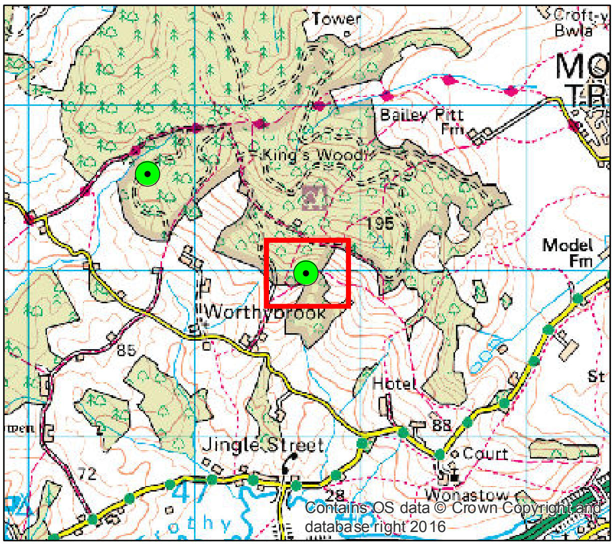

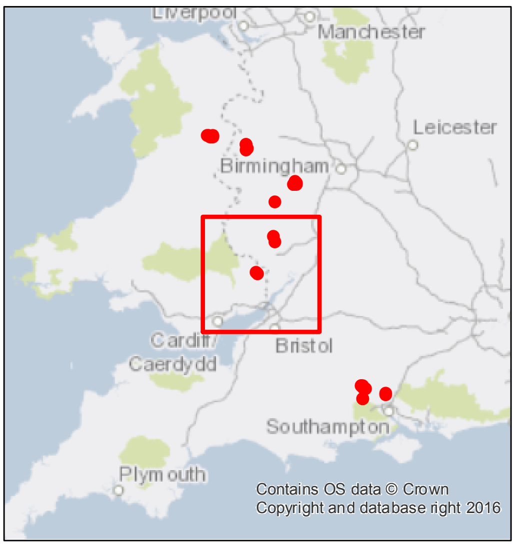

Bearing: 108

Langley 02

E: 423283
N: 120762

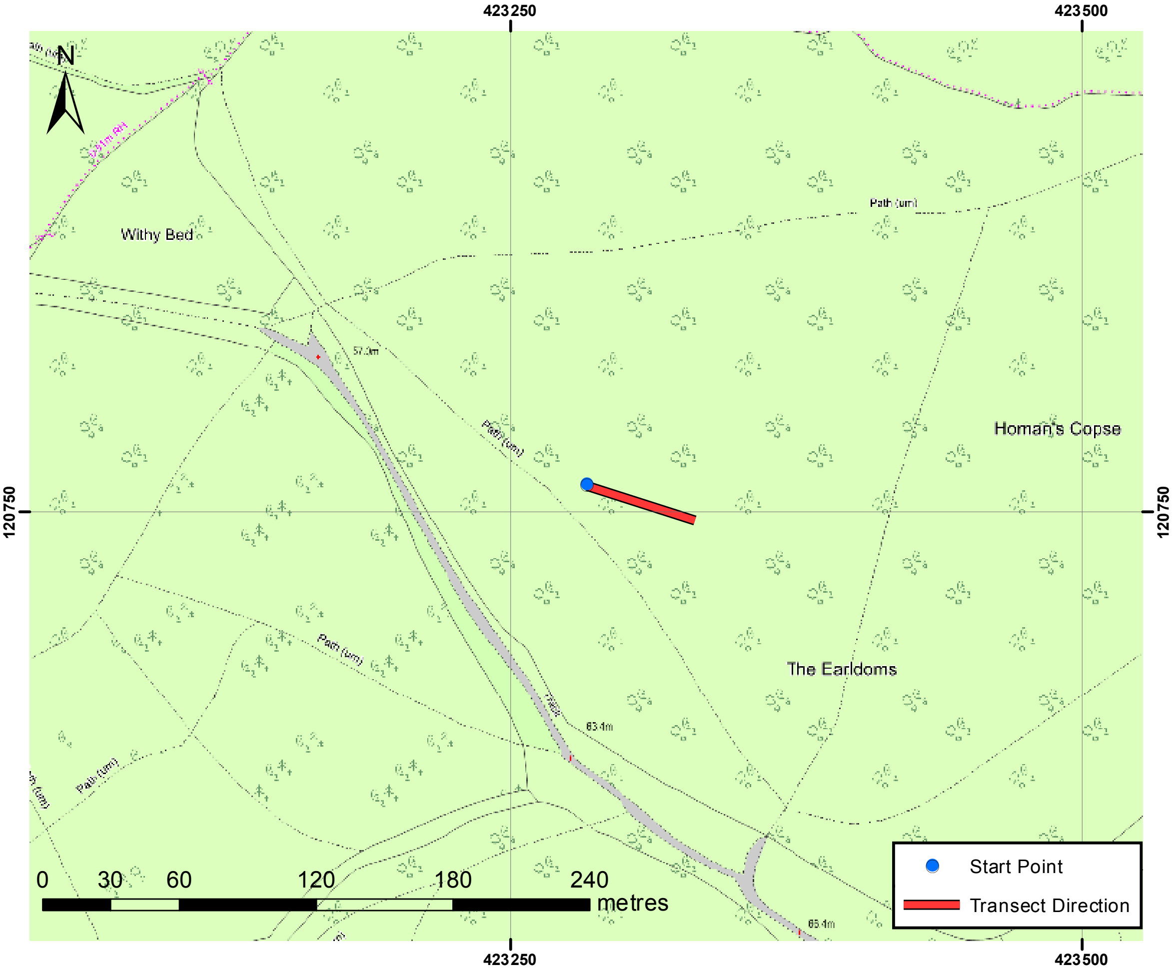

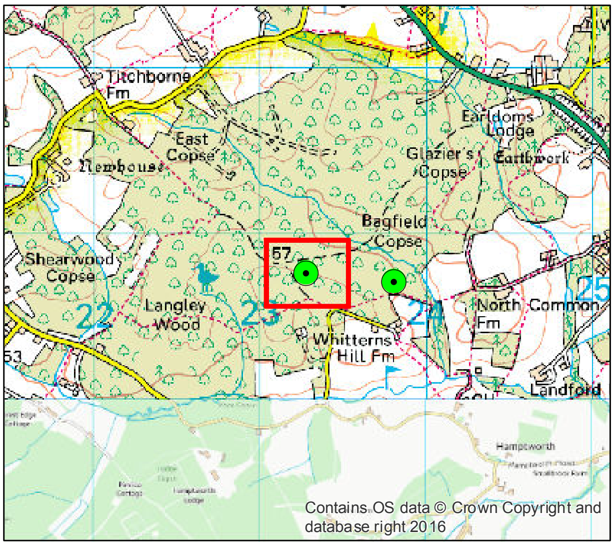

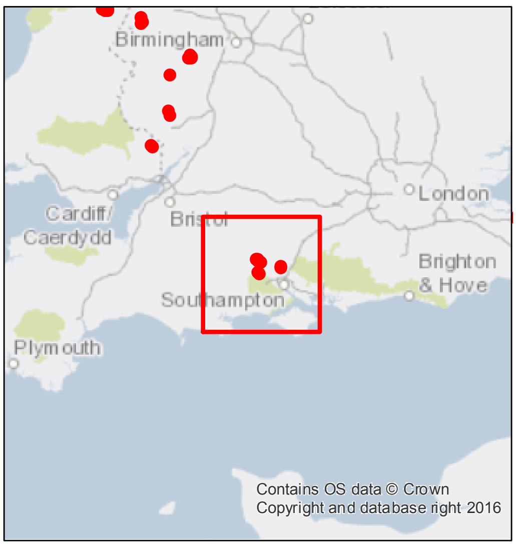

Bearing: 316

Langley 05

E: 423805
N: 120709

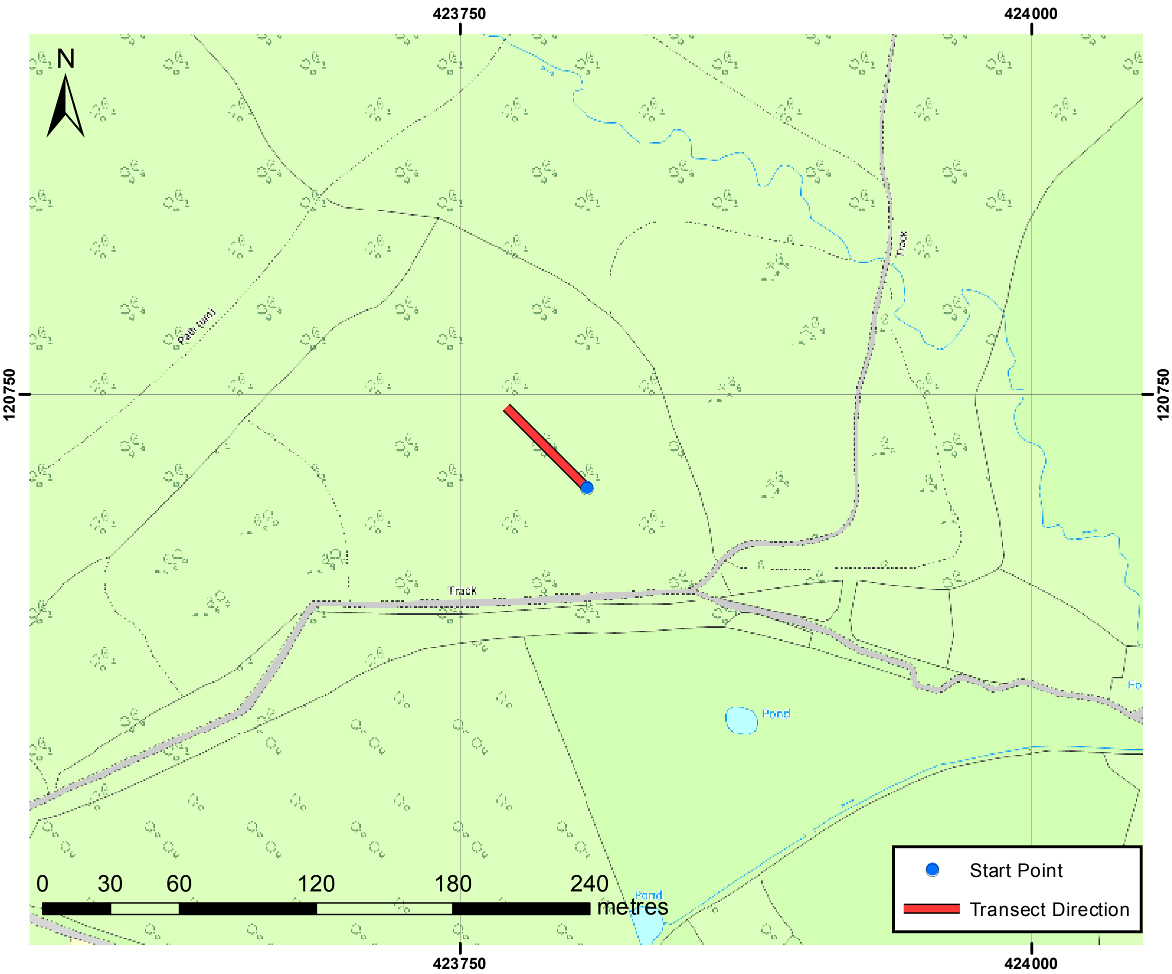

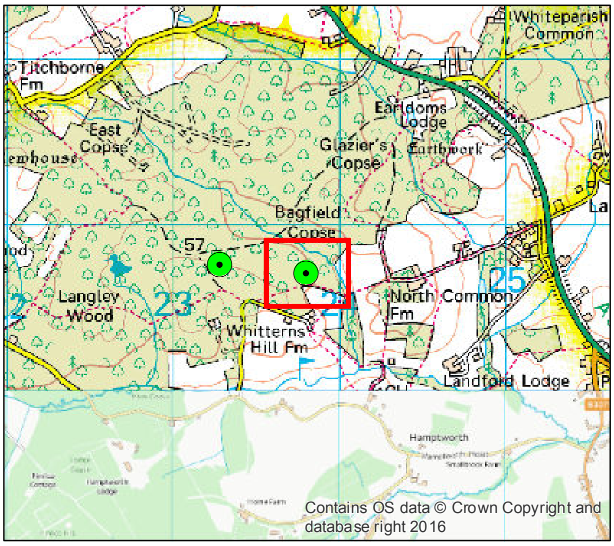

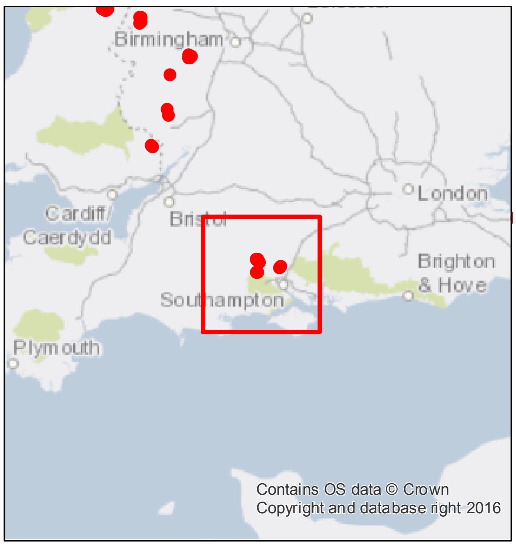

Bearing: **240**

Lea Pagets 03

E: **359933**
N: **234208**

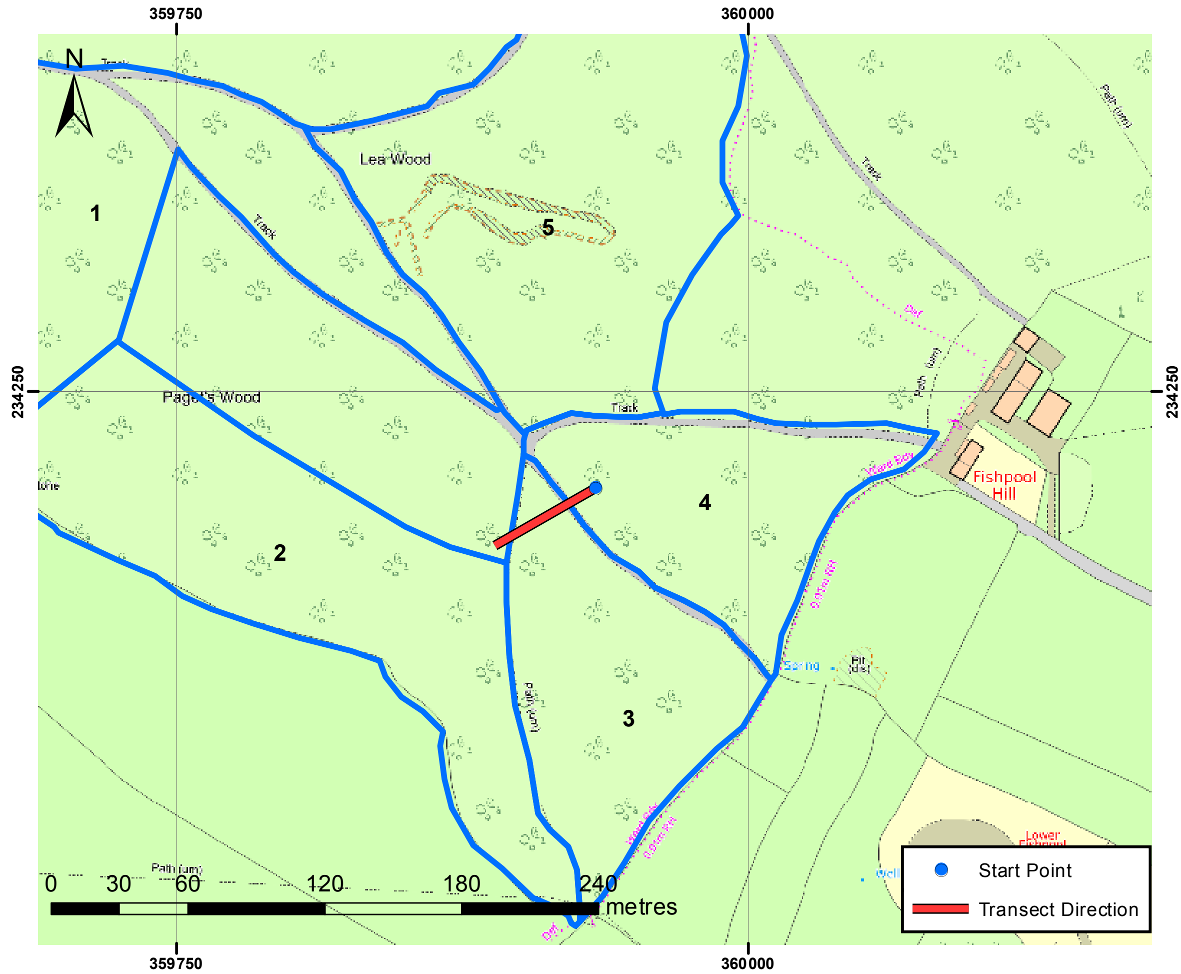

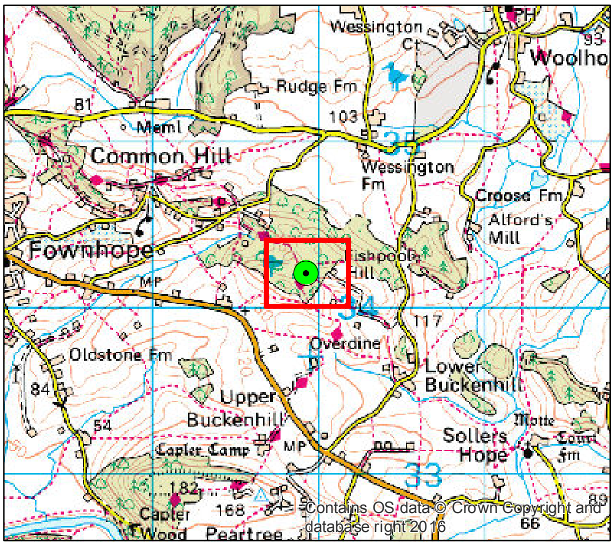

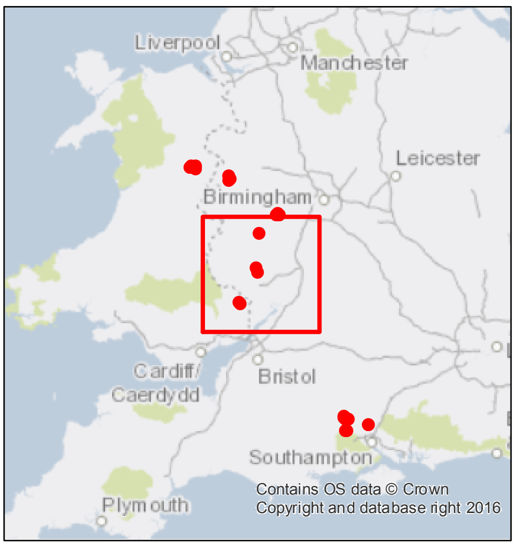

Bearing: 172

Pole Lees 02

E: 339179
N: 304649

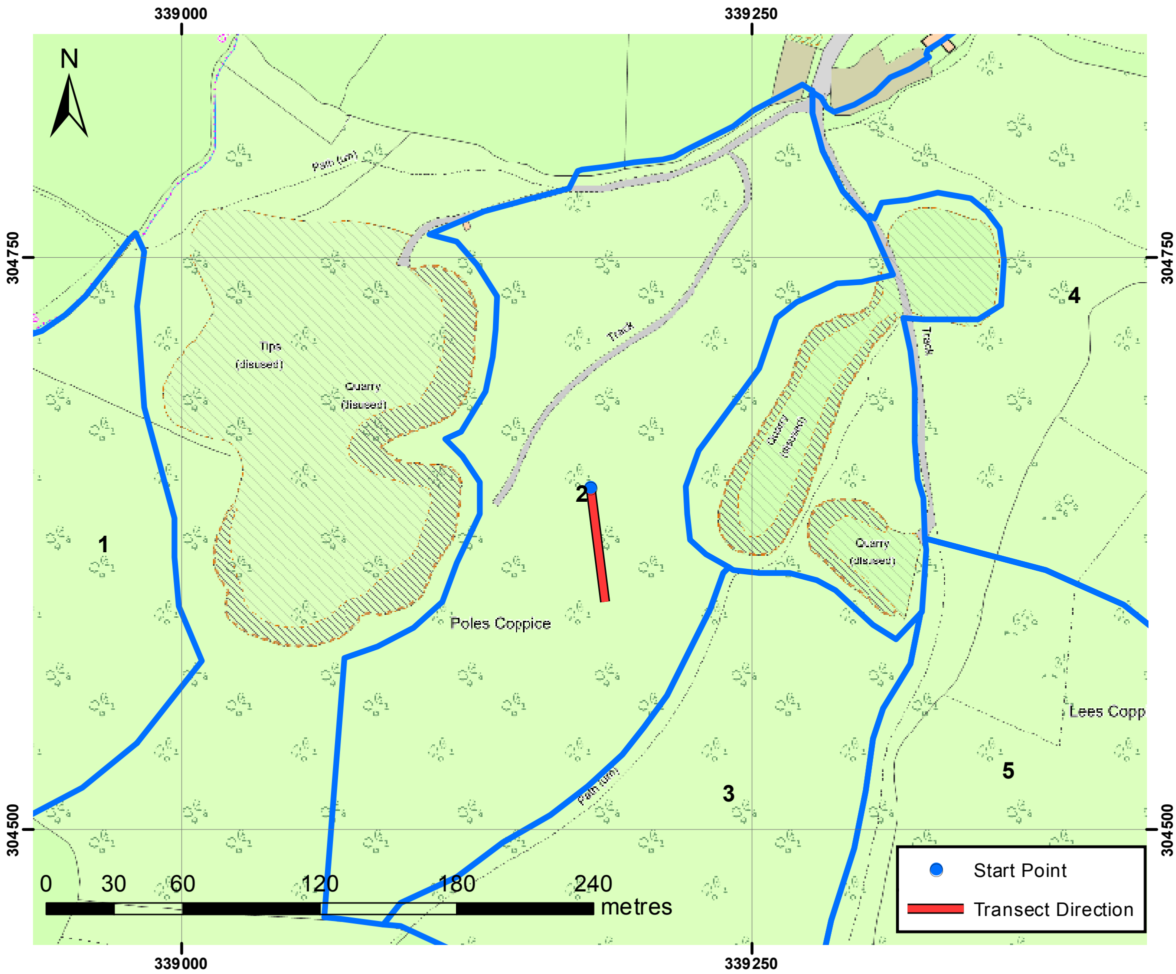

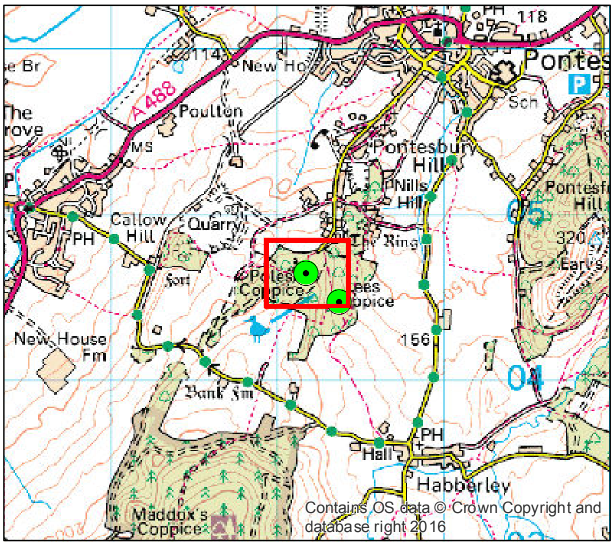

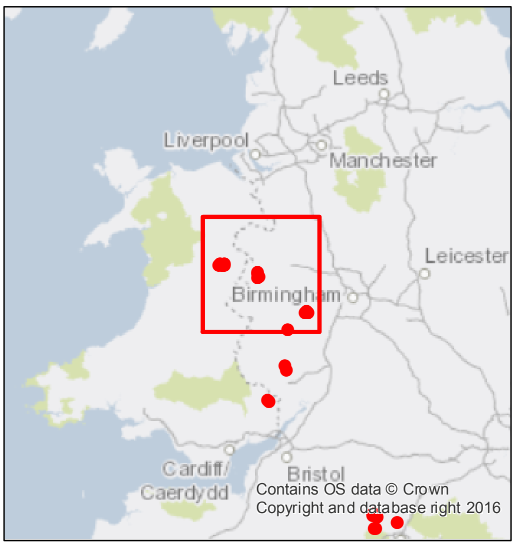

Bearing: 261

Pole Lees 05

E: 339370
N: 304472

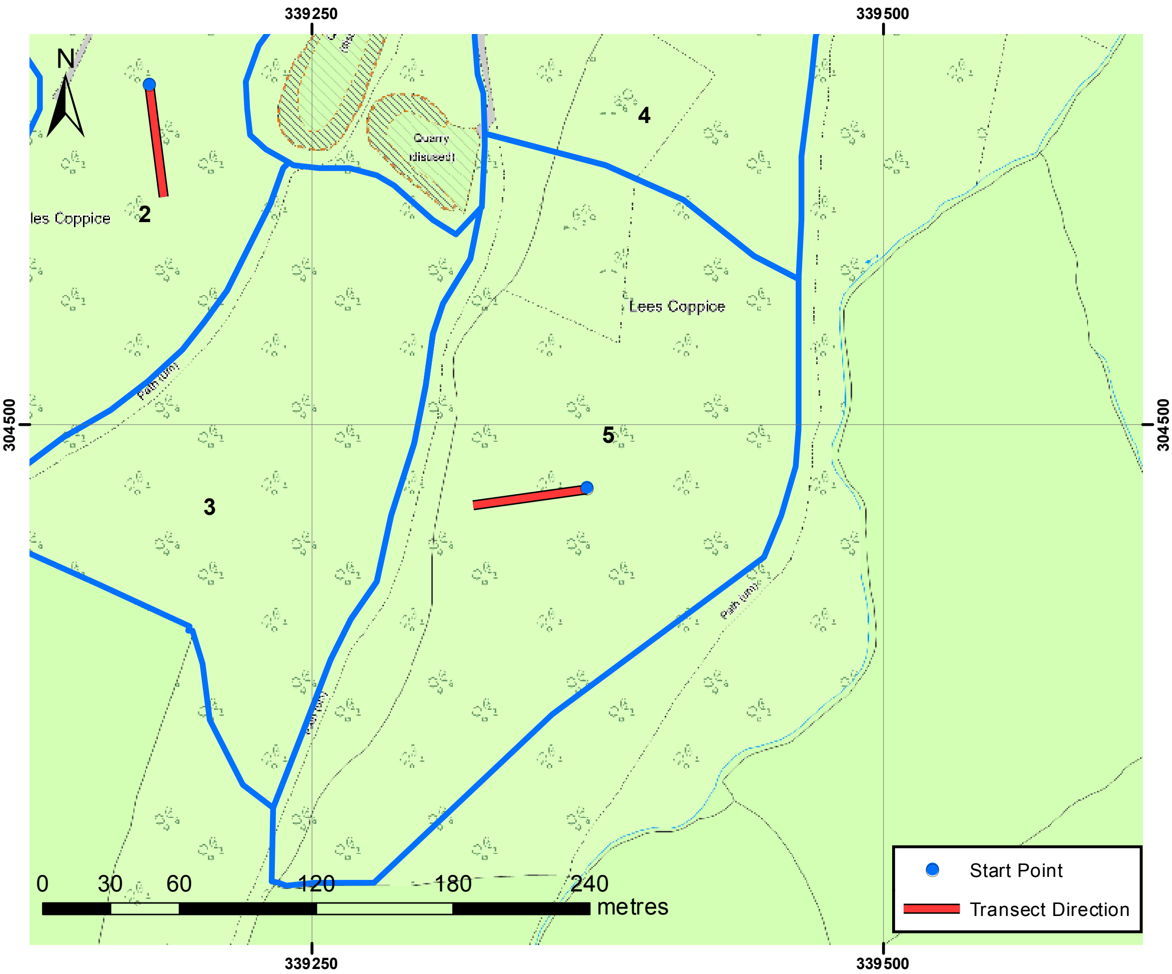

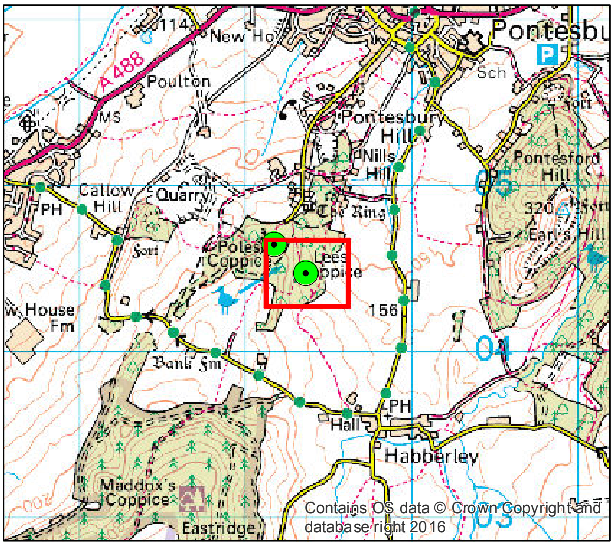

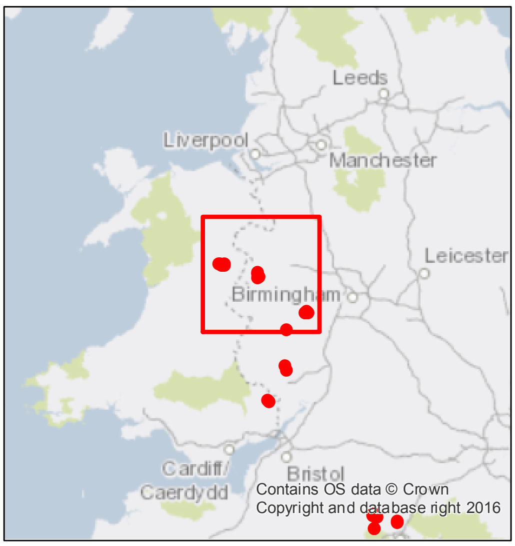

Bearing: 220

Romers Wood

E: 360455
N: 263158

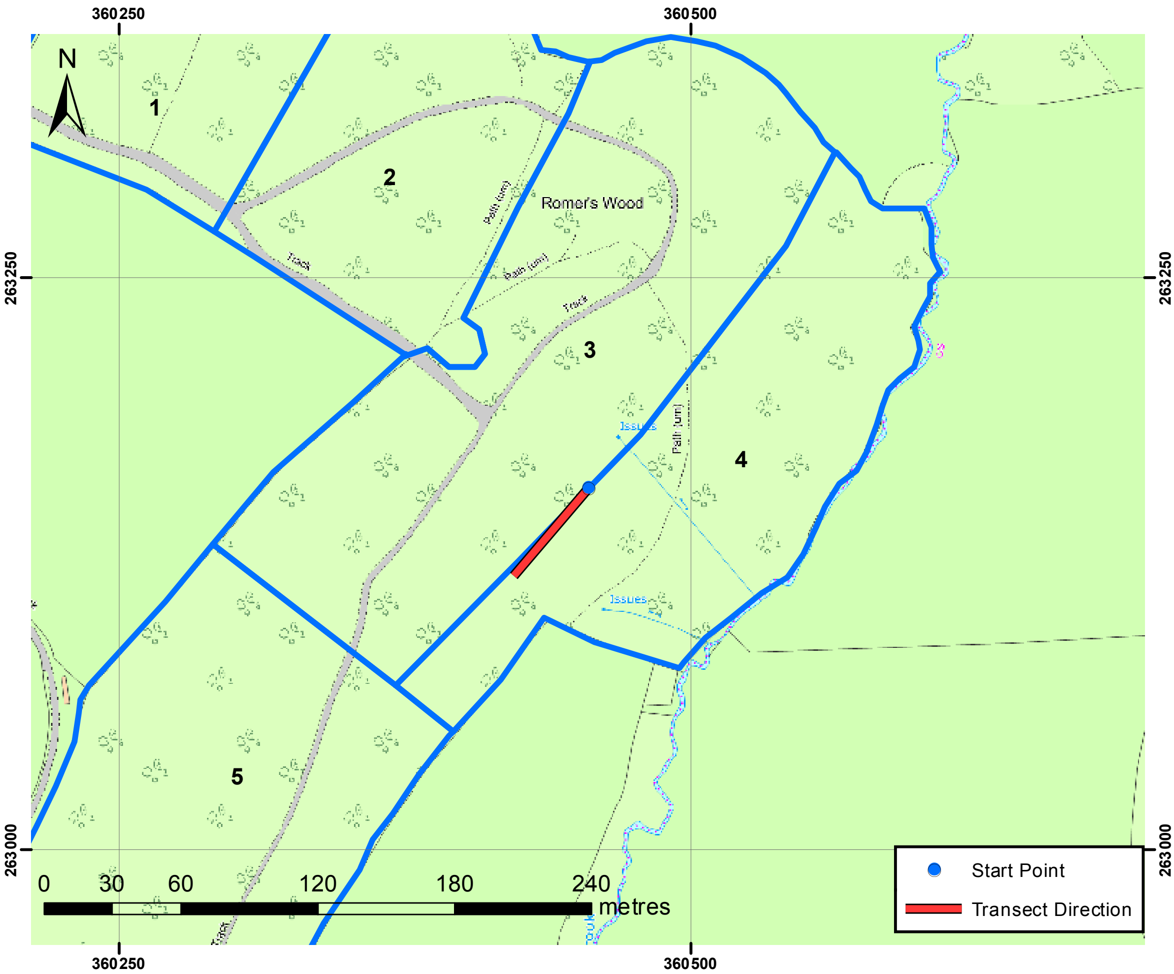

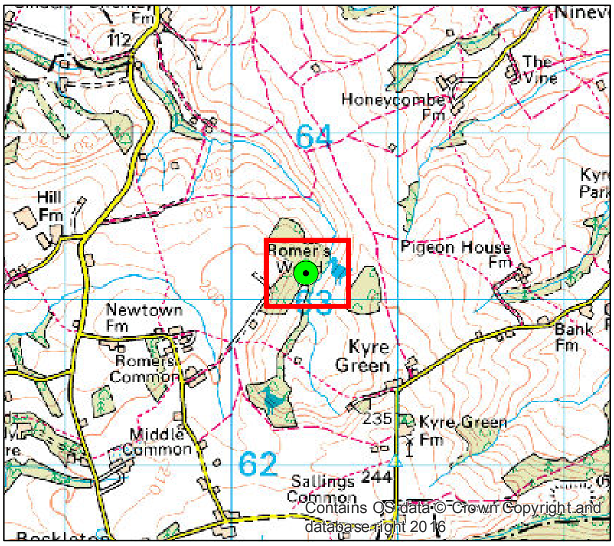

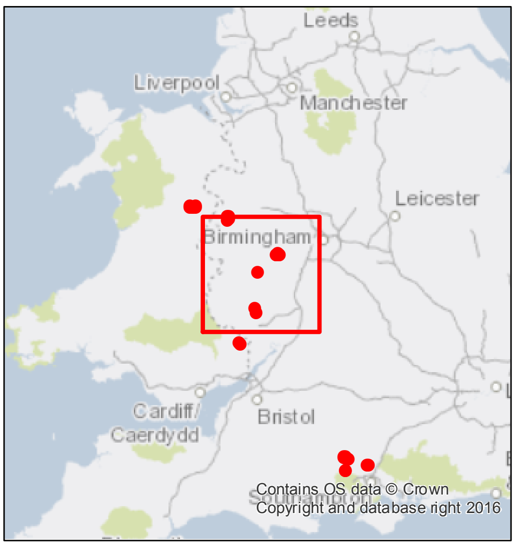

Bearing: 340

Spout Figyn

E: 315517
N: 311071

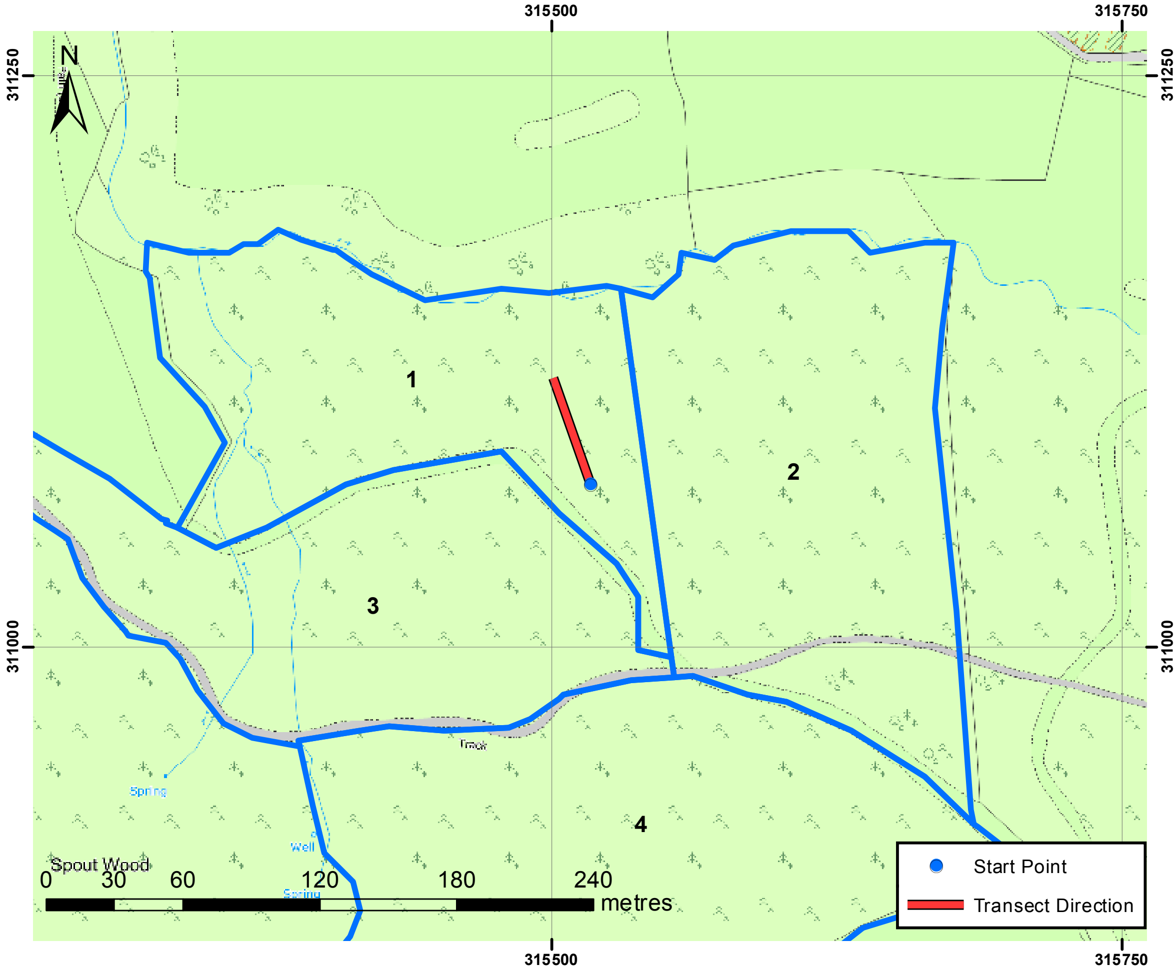

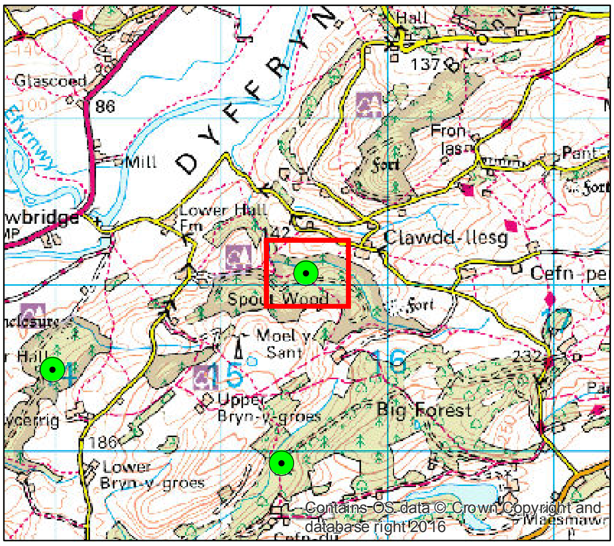

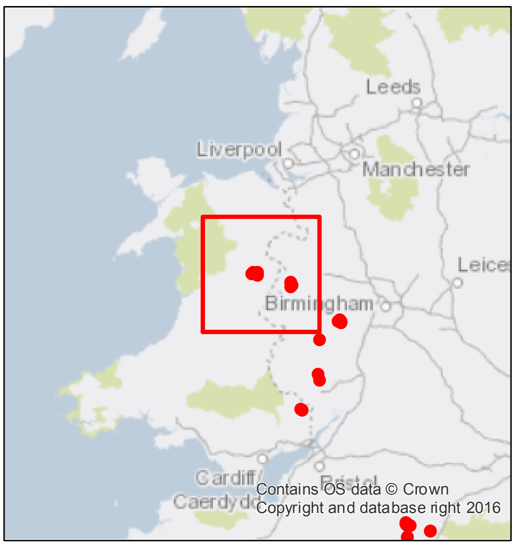

Bearing: 260

West Blean 01

E: 614275
N: 164133

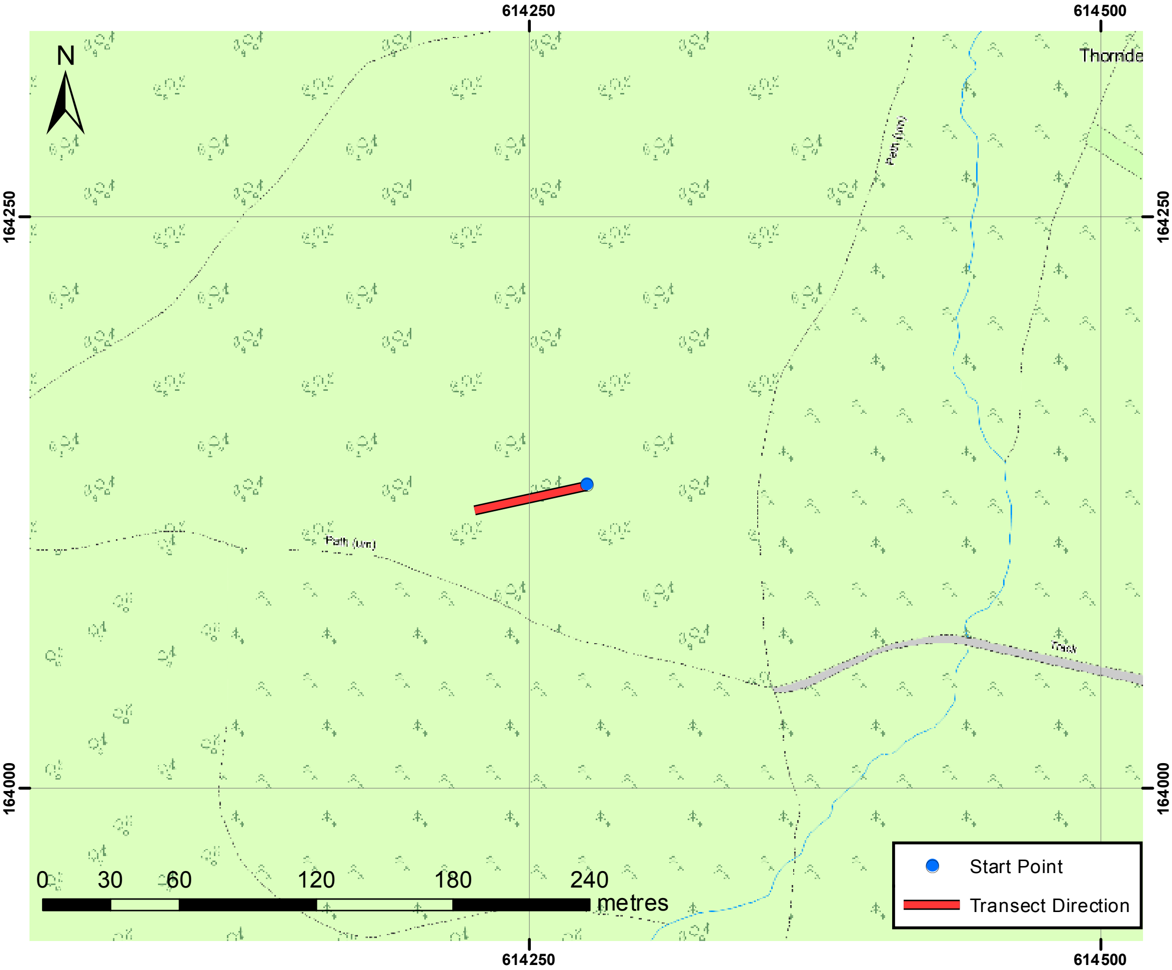

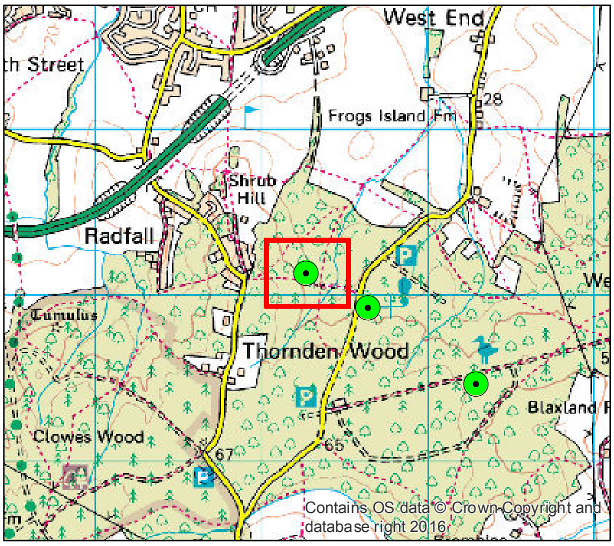

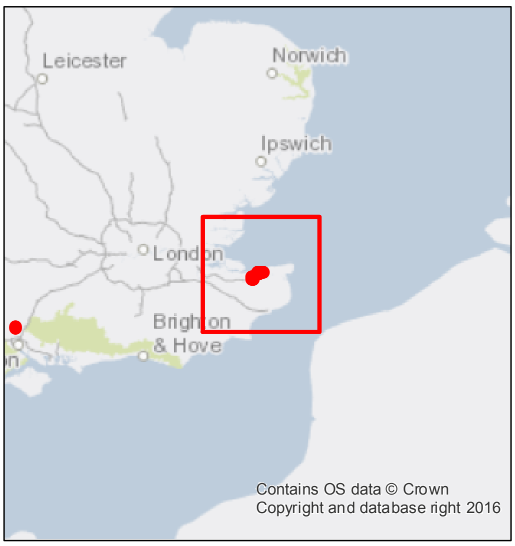

Bearing: 175

West Blean 02

E: 614645
N: 163925

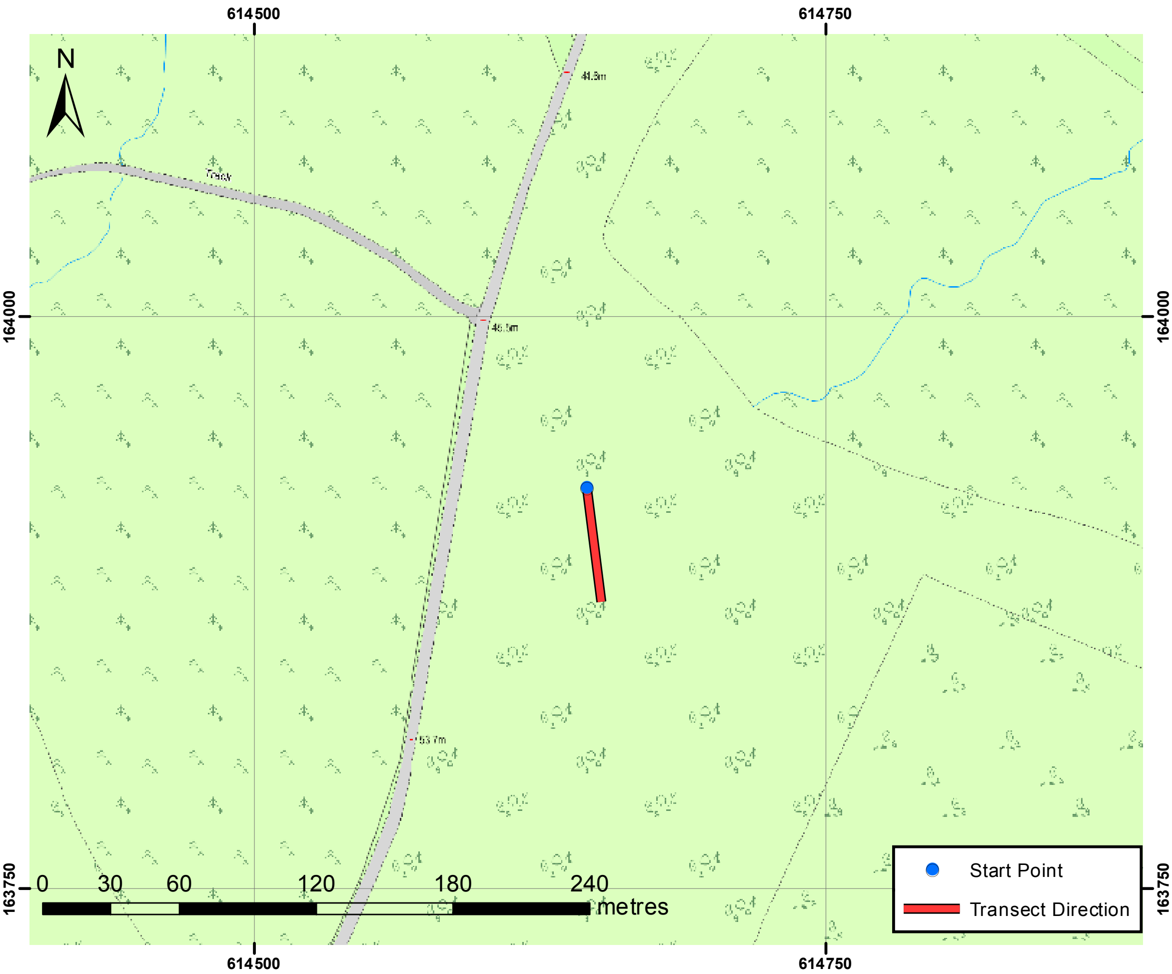

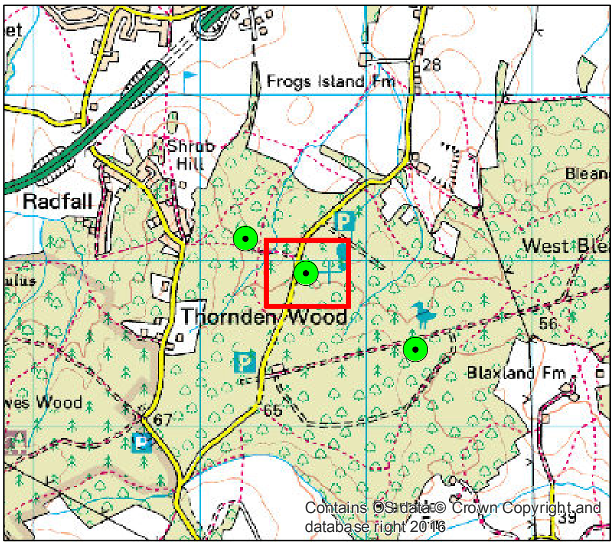

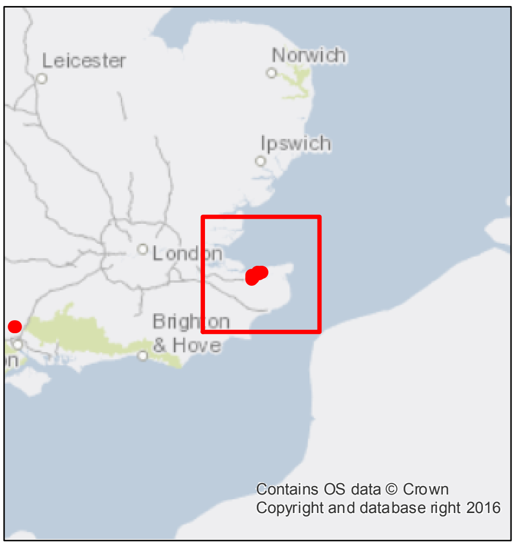

Bearing: 130

West Blean 03

E: 615296
N: 163461

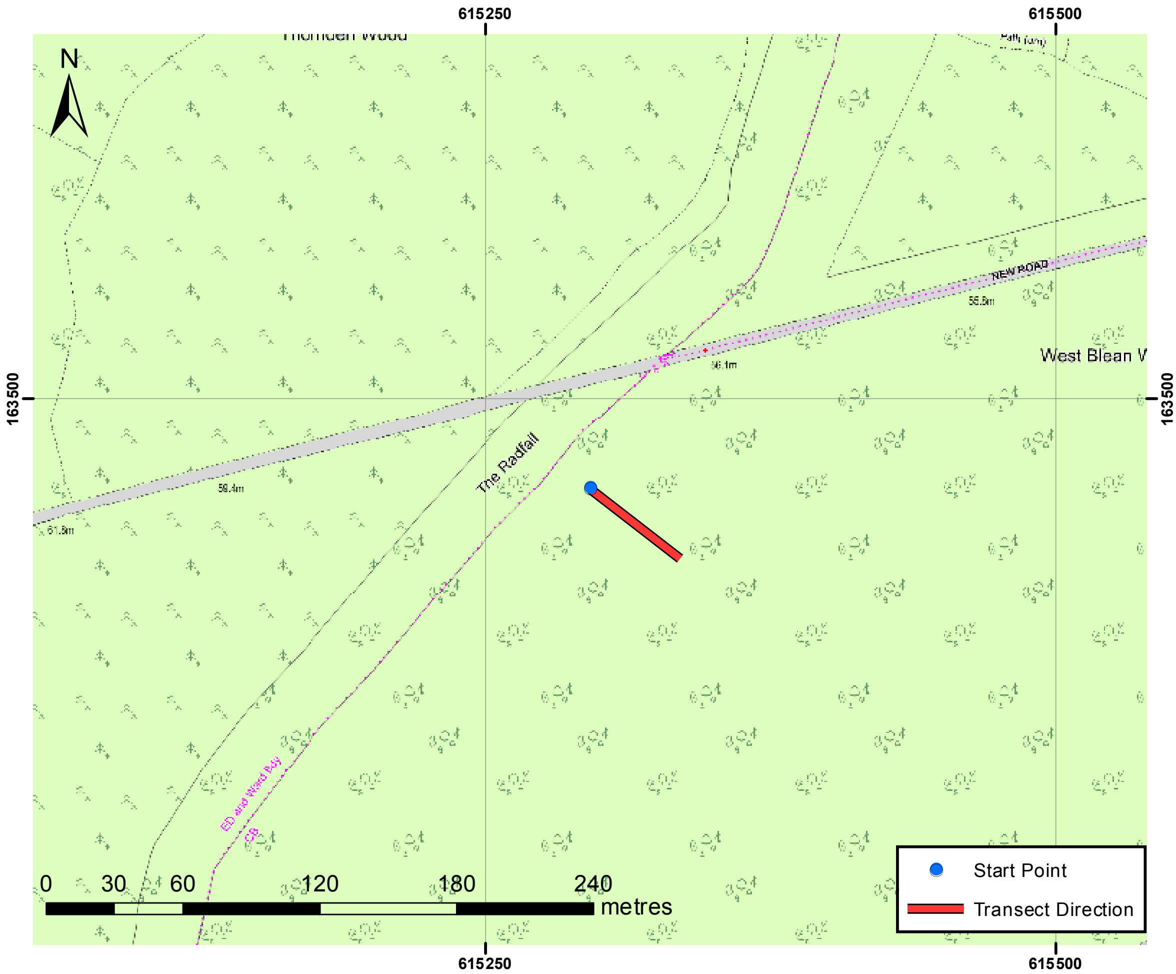

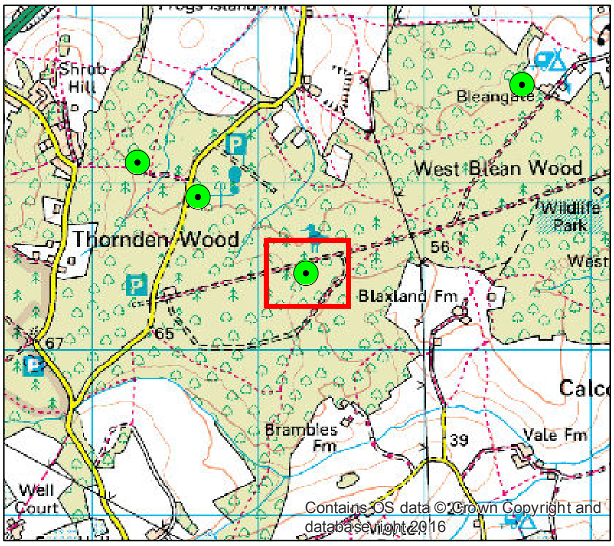

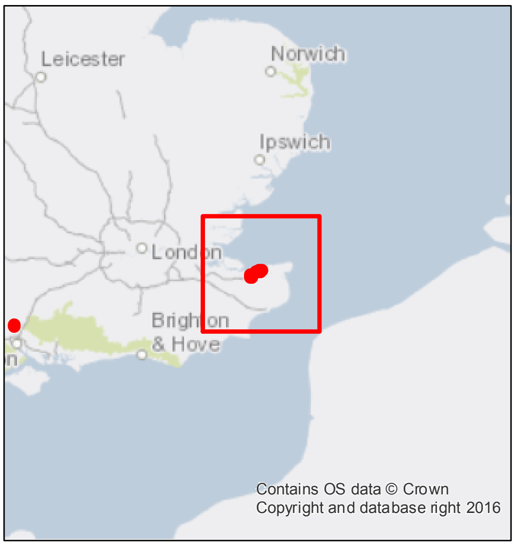

Bearing: 228

West Blean 04

E: 616595
N: 164597

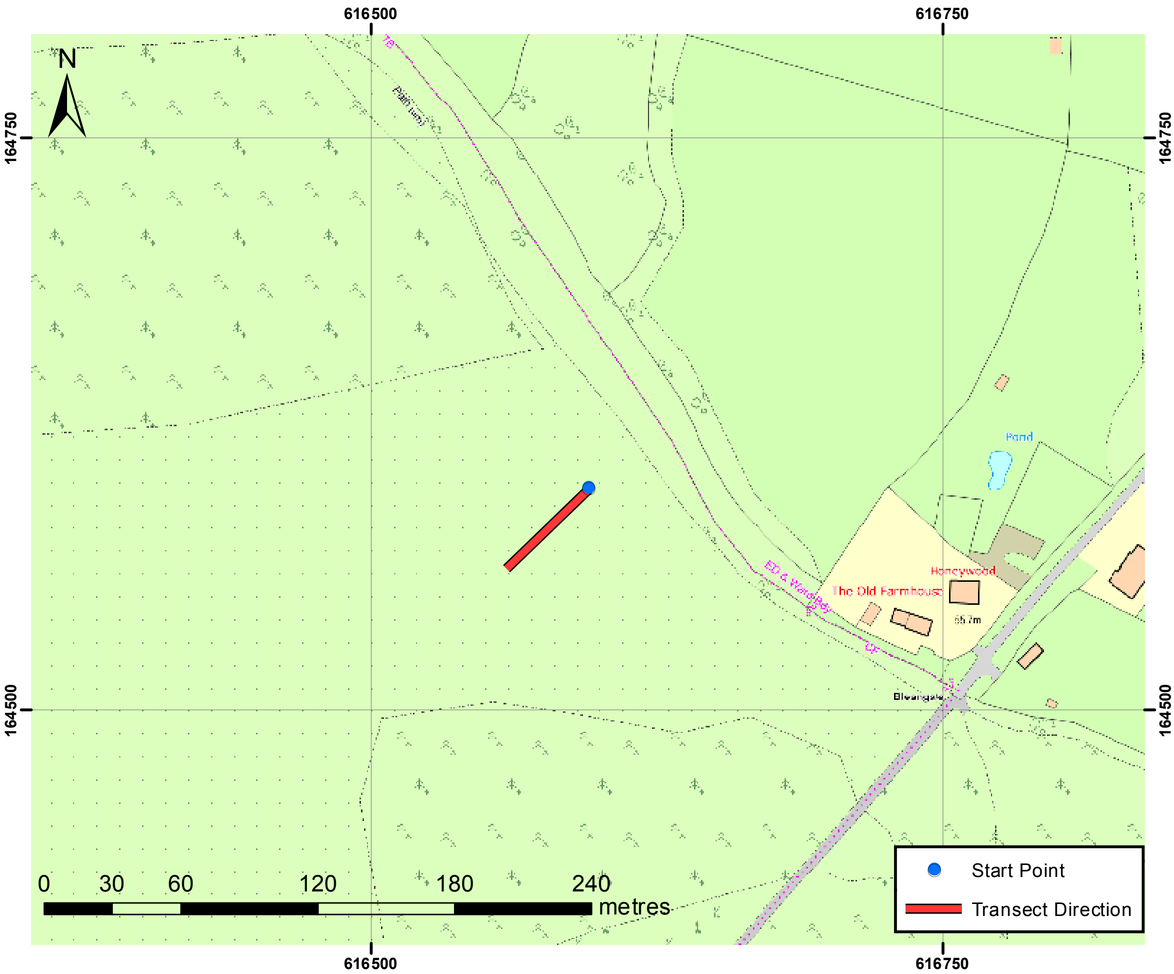

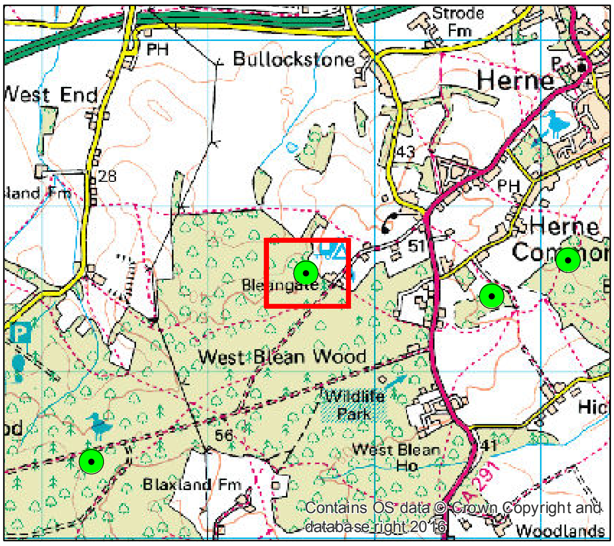

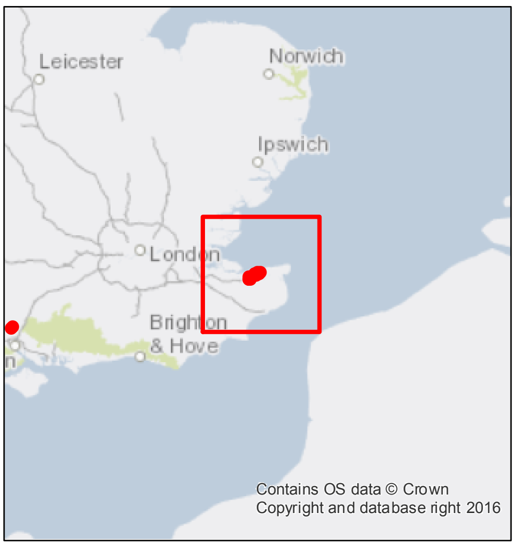

Bearing: 135

Wyre Forest Main 01

E: 374526
N: 277479

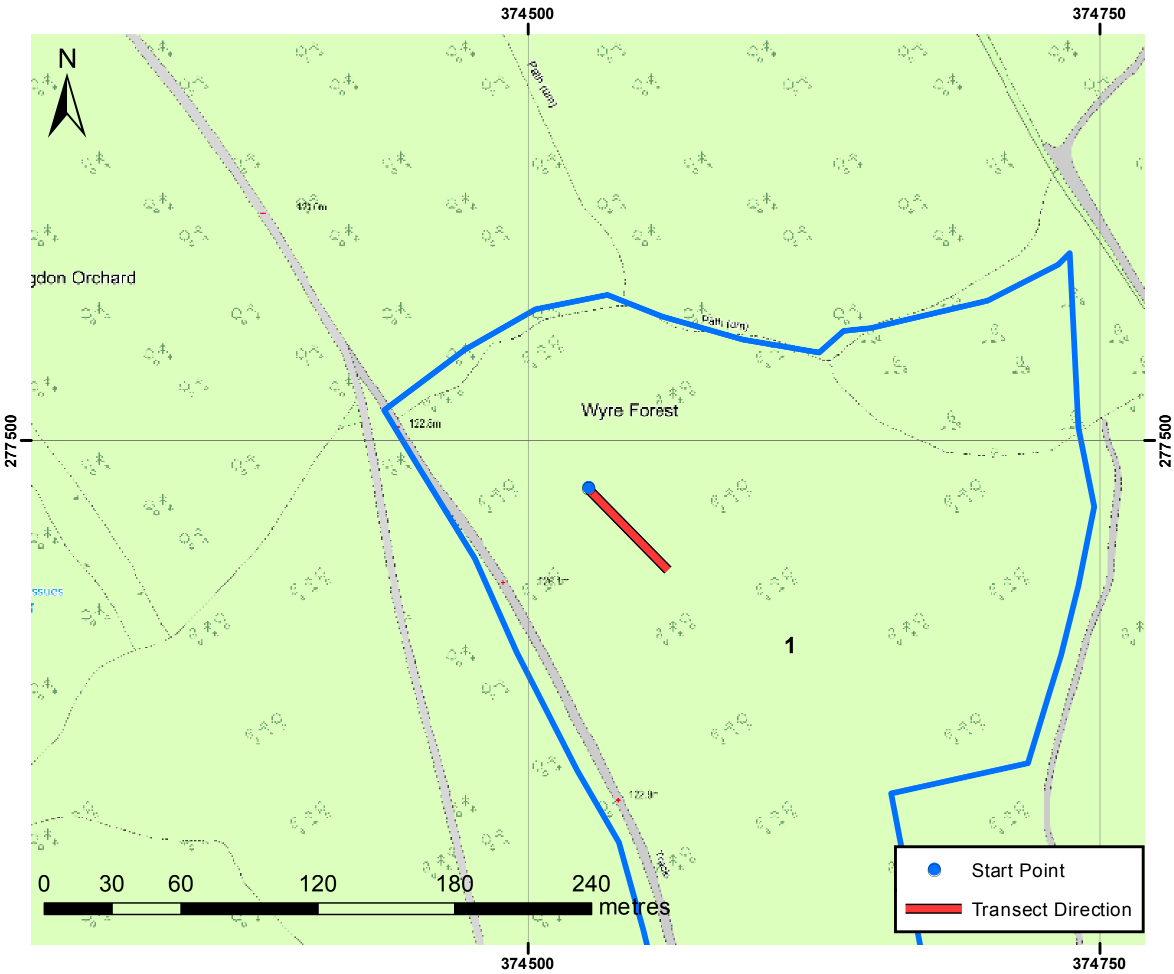

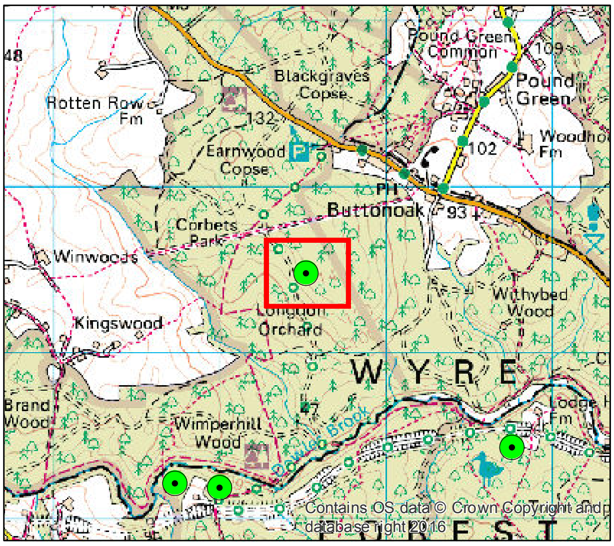

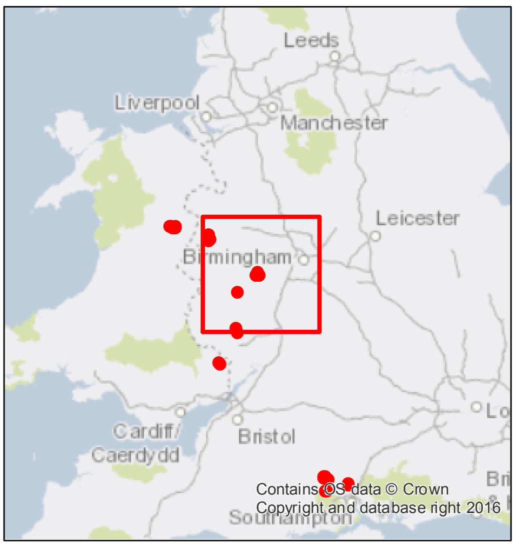

Bearing: 65

Wyre Forest Main 03

E: 373735
N: 276215

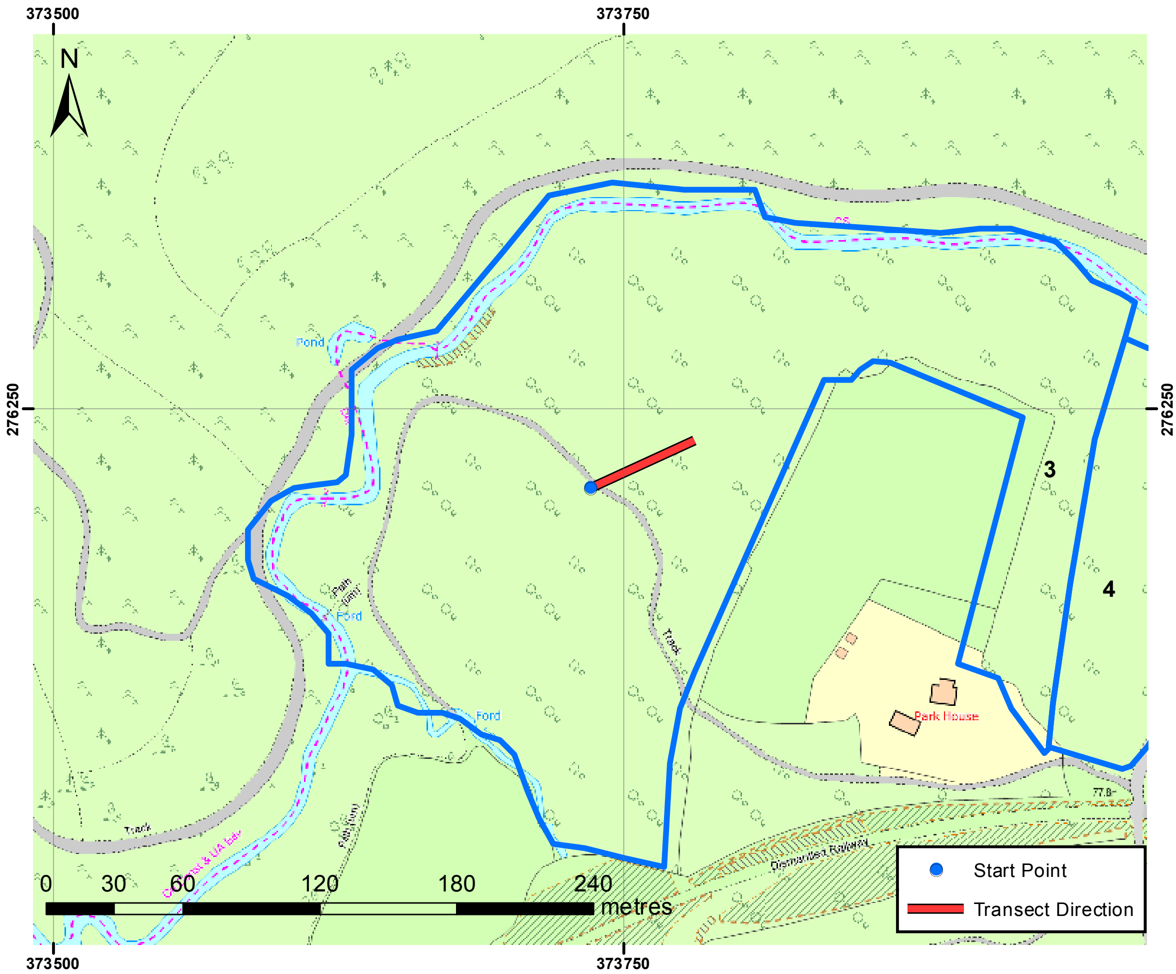

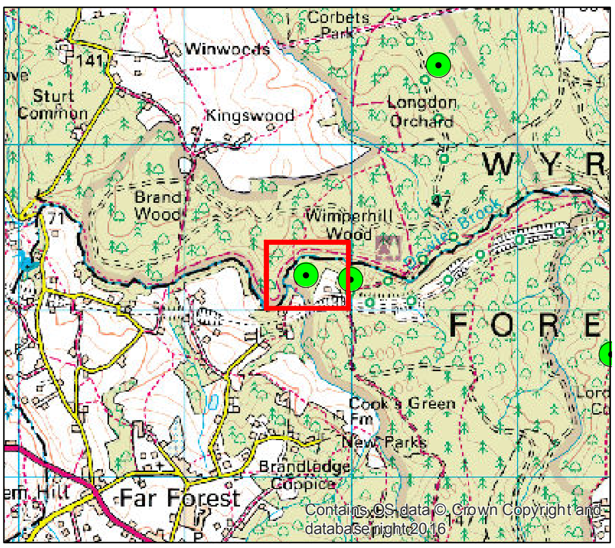

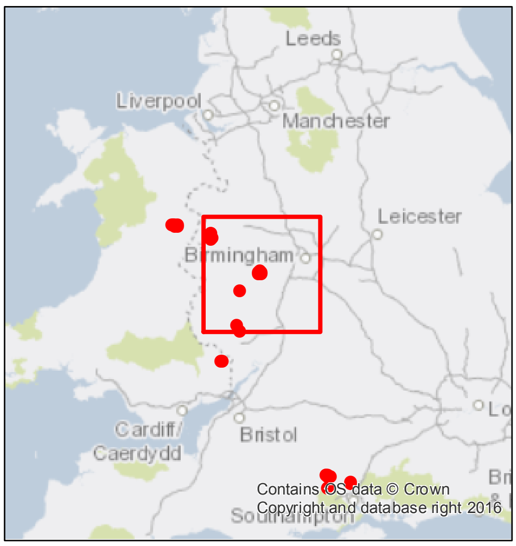

Bearing: 355

Wyre Forest Main 04

E: 374000
N: 276190

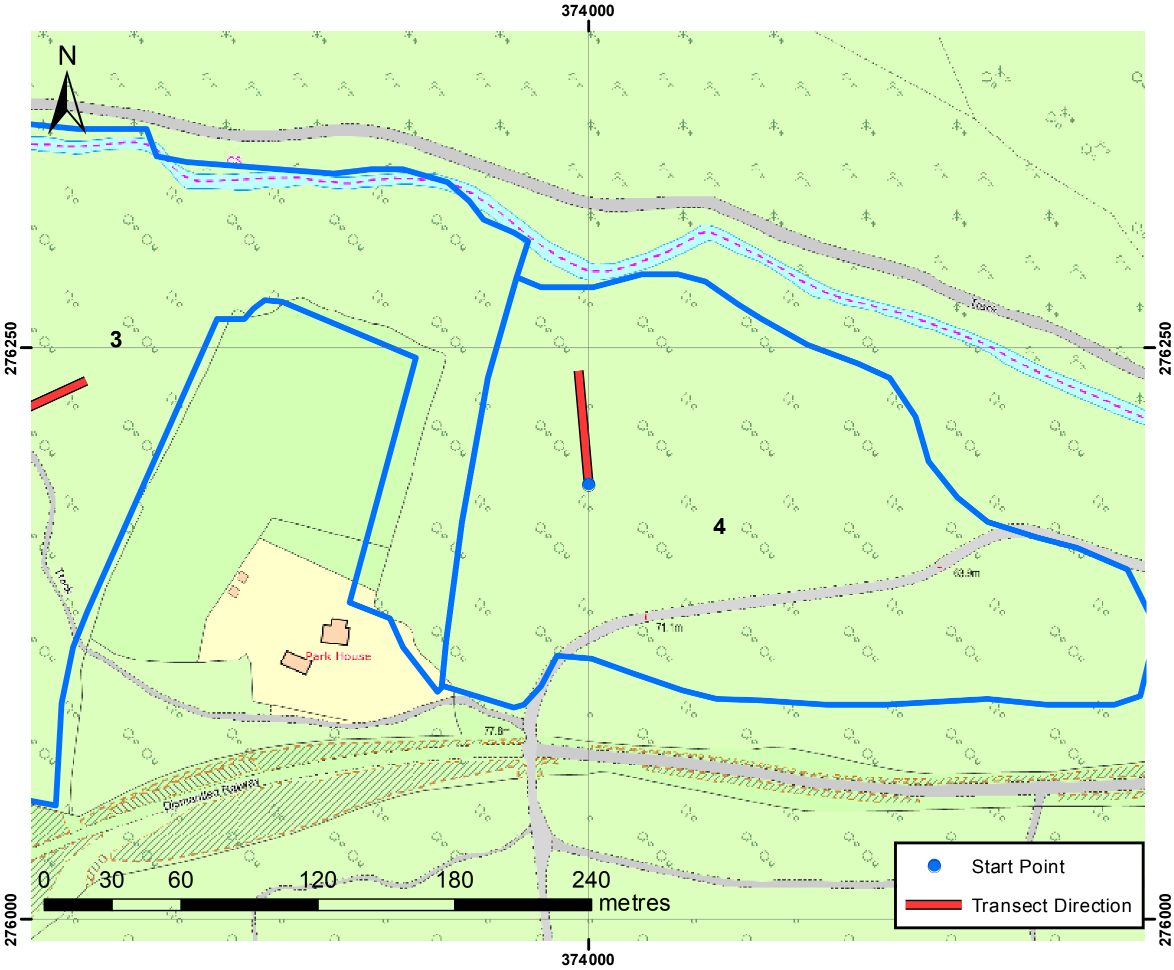

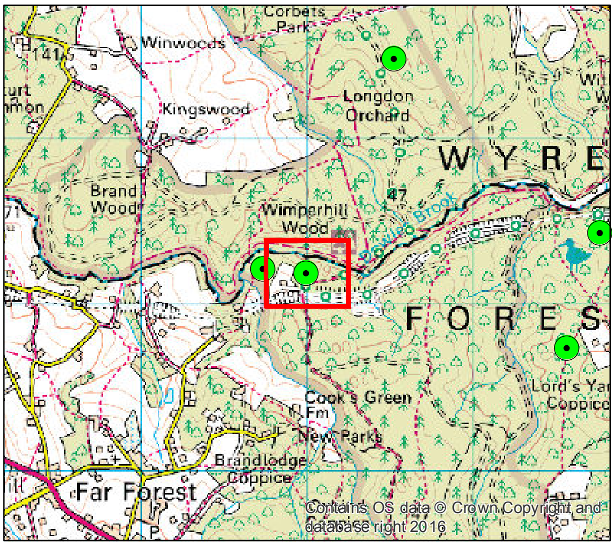

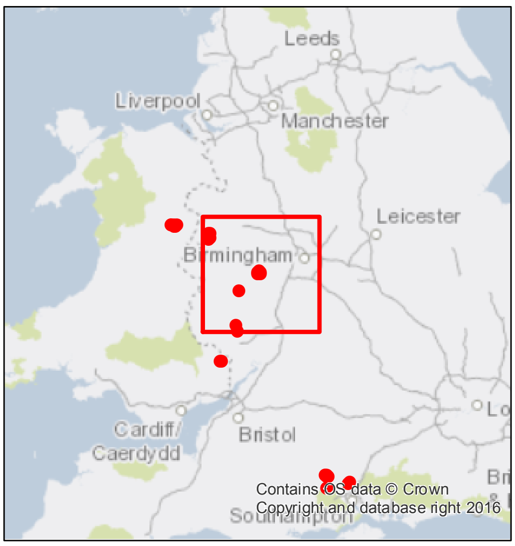

Bearing: 275

Wyre Forest NNR 01

E: 375765
N: 276433

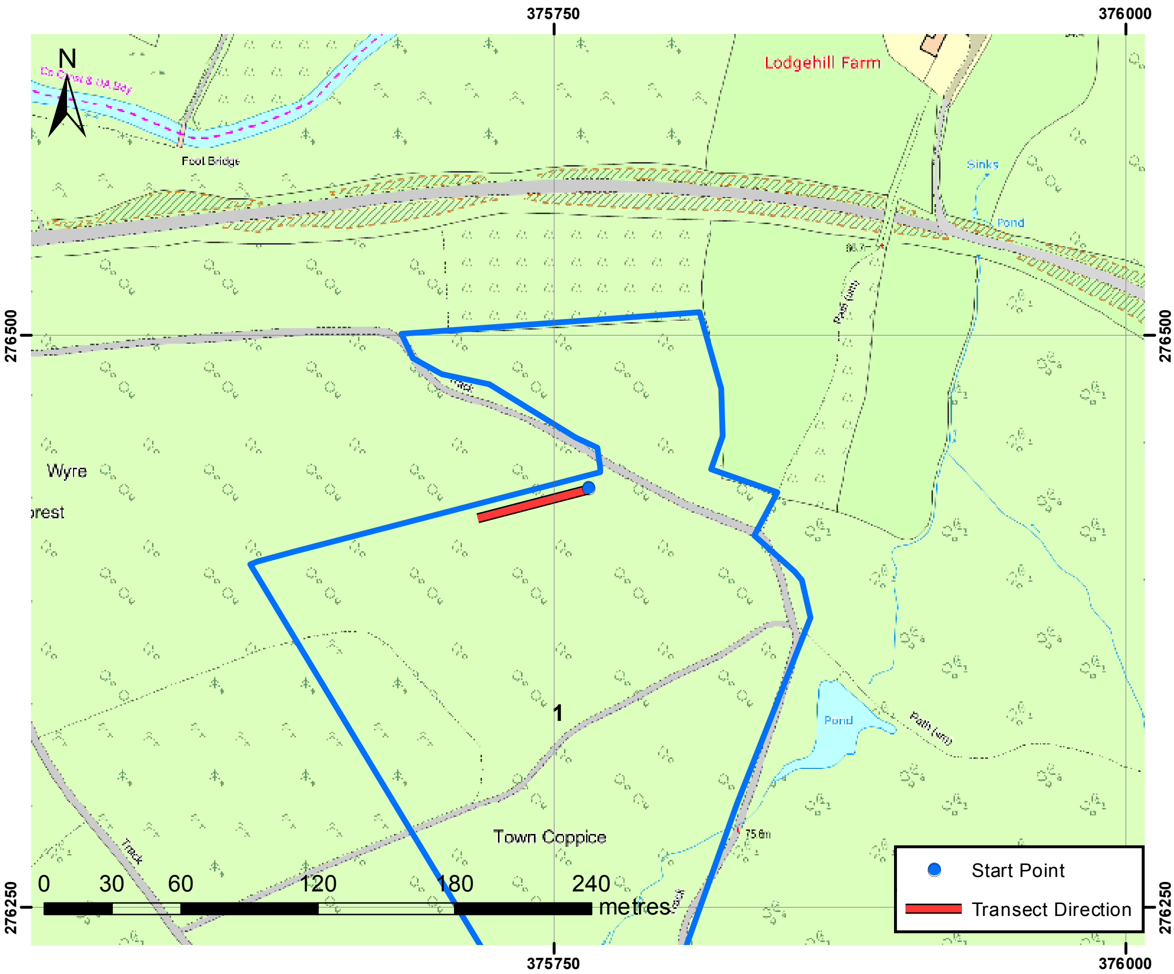

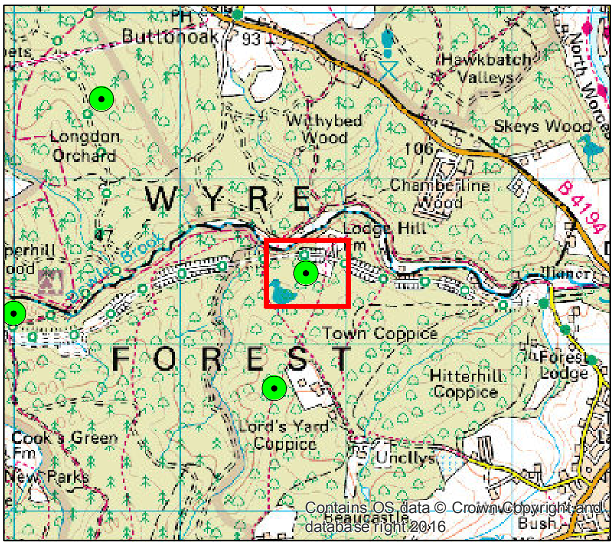

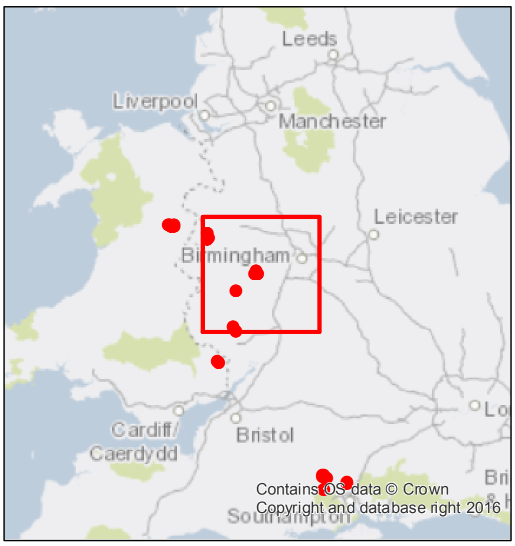

Bearing: 161

Wyre Forest NNR 03

E: 375567
N: 275740

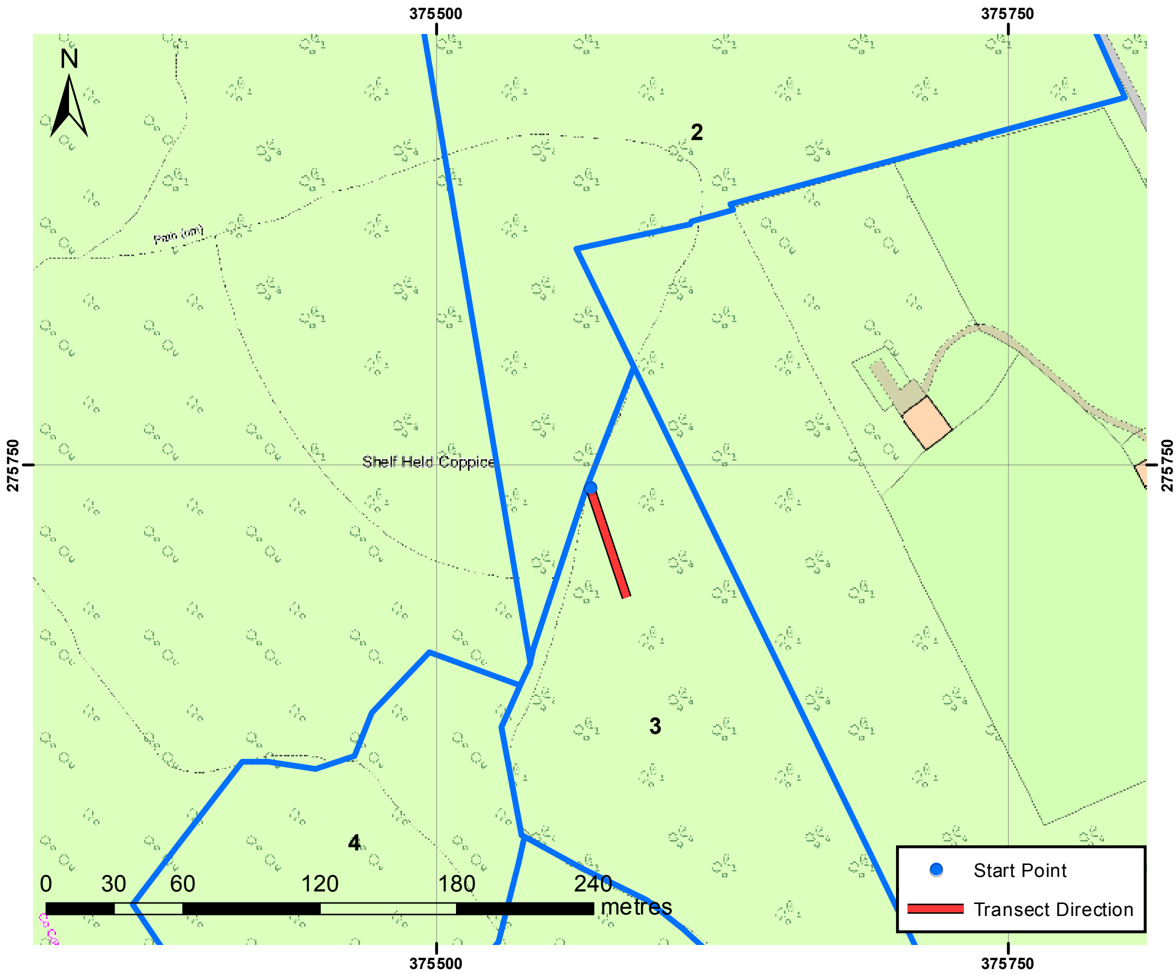

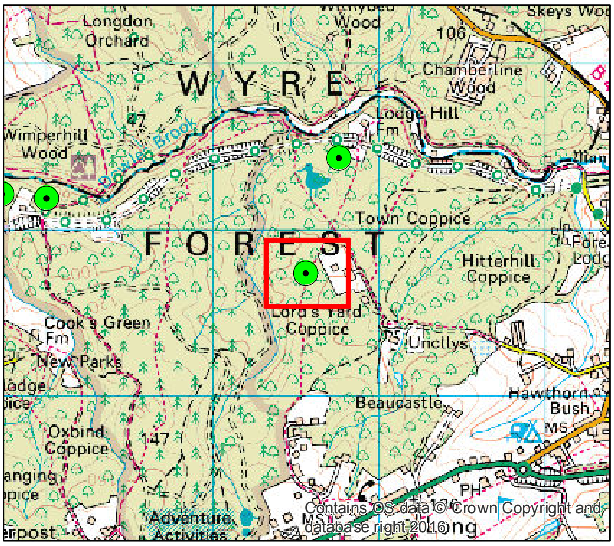

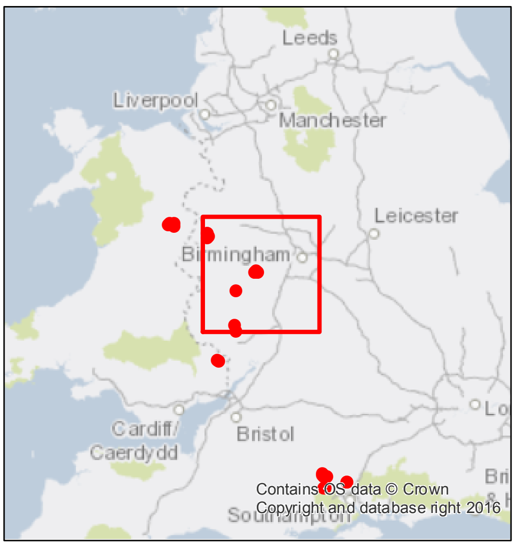

Appendix C

Expanded results

C.1 Estimating the vertical component of forest using terrestrial laser scanning

Table C.1: VNVI values for height bands 50-190cm within high deer density plots

plot	height band (cm)														
	50	60	70	80	90	100	110	120	130	140	150	160	170	180	190
Ampfield03	0.38	0.28	0.17	-0.07	-0.39	-0.59	-0.62	-0.52	-0.38	-0.31	-0.34	-0.40	-0.28	-0.22	-0.16
Ampfield04	0.52	0.41	0.12	-0.29	-0.69	-0.83	-0.77	-0.58	-0.42	-0.25	-0.25	-0.15	-0.18	-0.10	-0.04
Bentley03	0.38	0.24	-0.03	-0.21	-0.66	-0.72	-0.66	-0.57	-0.54	-0.45	-0.23	-0.10	-0.07	0.06	0.02
Bentley04	0.08	0.08	-0.10	-0.30	-0.46	-0.68	-0.79	-0.85	-0.83	-0.82	-0.72	-0.58	-0.54	-0.42	-0.34
Blackmoor	-0.01	-0.18	-0.31	-0.33	-0.45	-0.44	-0.27	-0.17	-0.05	0.05	0.11	0.14	0.14	0.22	0.19
Haughwood	0.64	0.56	0.42	0.34	0.24	0.20	0.04	-0.14	-0.18	-0.17	-0.18	-0.12	-0.00	0.04	0.11
Hound01	-0.11	-0.41	-0.45	-0.50	-0.49	-0.46	-0.44	-0.39	-0.40	-0.37	-0.35	-0.29	-0.22	-0.02	-0.06
Hound03	-0.27	-0.61	-0.78	-0.88	-0.91	-0.92	-0.89	-0.86	-0.73	-0.66	-0.58	-0.62	-0.55	-0.58	-0.55
Hound05	0.44	0.36	0.23	0.08	-0.10	-0.16	-0.25	-0.18	-0.08	-0.07	-0.09	-0.09	-0.08	-0.03	0.14
Kingswood01	0.35	0.38	0.39	0.34	0.30	0.16	0.02	-0.21	-0.14	-0.12	-0.12	0.10	0.29	0.34	0.40
Kingswood10	0.16	0.28	0.24	0.22	0.20	0.27	0.21	0.08	-0.08	-0.34	-0.45	-0.58	-0.54	-0.38	-0.23
Langley02	-0.11	-0.29	-0.55	-0.61	-0.66	-0.66	-0.63	-0.59	-0.51	-0.41	-0.31	-0.25	-0.17	-0.10	-0.16
Langley05	-0.01	-0.13	-0.26	-0.30	-0.46	-0.53	-0.61	-0.55	-0.65	-0.69	-0.63	-0.50	-0.32	-0.27	-0.20
LeaPagets03	0.20	0.05	-0.29	-0.58	-0.62	-0.65	-0.53	-0.60	-0.56	-0.40	-0.26	-0.20	-0.10	-0.04	0.00
Romers	0.50	0.44	0.42	0.49	0.18	0.13	0.01	-0.03	-0.09	-0.09	-0.08	-0.02	-0.00	0.04	0.05
WyreMain01	0.25	0.08	-0.20	-0.48	-0.79	-0.93	-0.96	-0.98	-0.98	-0.97	-0.97	-0.94	-0.90	-0.86	-0.82
WyreMain03	0.35	0.06	-0.15	-0.44	-0.67	-0.79	-0.90	-0.83	-0.63	-0.48	-0.43	-0.30	-0.31	-0.24	-0.27
WyreMain04	-0.74	-0.80	-0.86	-0.85	-0.82	-0.82	-0.79	-0.69	-0.55	-0.33	-0.18	-0.15	-0.05	-0.02	0.02
WyreNNR01	0.55	0.08	-0.53	-0.78	-0.87	-0.95	-0.96	-0.94	-0.97	-0.96	-0.97	-0.95	-0.95	-0.92	-0.78
WyreNNR03	0.57	0.53	0.52	0.18	-0.32	-0.81	-0.94	-0.98	-0.99	-0.99	-0.98	-0.97	-0.95	-0.97	-0.95

Table C.2: VNVI values for height bands 50-190cm within low deer density plots

plot	height band (cm)														
	50	60	70	80	90	100	110	120	130	140	150	160	170	180	190
BigForest03	0.43	0.13	0.23	0.21	0.09	-0.03	-0.14	-0.18	-0.14	-0.08	-0.01	0.10	0.14	0.23	0.24
BleanHomestall01	0.26	0.09	-0.11	-0.20	-0.21	-0.23	-0.24	-0.25	-0.28	-0.22	-0.24	-0.22	-0.17	-0.13	-0.10
BleanHomestall04	0.23	0.08	0.09	0.11	0.04	0.09	0.00	-0.01	-0.01	0.04	0.03	0.06	0.09	0.24	0.18
BleanHomestall06	0.36	0.24	0.14	0.00	-0.14	-0.22	-0.26	-0.17	-0.15	-0.09	-0.14	-0.12	-0.12	-0.12	-0.07
EastBlean01	0.17	0.21	0.21	0.26	0.21	0.14	0.13	0.11	0.14	0.19	0.14	0.13	0.18	0.22	0.29
EastBlean03	0.36	0.31	0.16	0.11	0.06	-0.03	-0.06	-0.02	-0.10	-0.12	-0.15	-0.13	-0.10	-0.05	-0.01
Eastridge01	0.46	0.41	0.36	0.36	0.38	0.24	0.25	0.25	0.17	0.19	0.13	0.10	0.15	0.20	0.19
Eastridge05	0.29	0.33	0.29	0.22	0.19	0.17	0.06	0.09	0.06	0.14	0.04	0.06	0.05	0.08	0.11
Ellenden	-0.44	-0.49	-0.54	-0.49	-0.45	-0.44	-0.45	-0.46	-0.44	-0.47	-0.43	-0.39	-0.41	-0.39	-0.37
FfriddMathrafal02	0.37	0.41	0.37	0.23	0.28	0.23	0.18	0.21	0.17	0.24	0.28	0.39	0.44	0.48	0.47
FfriddMathrafal04	0.32	0.44	0.54	0.56	0.55	0.48	0.38	0.32	0.22	0.20	0.17	0.15	0.14	0.09	0.11
GwernDdu01	0.41	0.40	0.41	0.24	0.11	0.04	-0.10	-0.16	-0.30	-0.20	-0.23	-0.31	-0.35	-0.37	-0.37
GwernDdu04	0.10	0.28	0.20	0.12	0.14	0.11	0.15	0.20	0.21	0.26	0.25	0.35	0.41	0.47	0.51
PoleLees02	0.42	0.48	0.52	0.51	0.49	0.46	0.31	0.27	0.11	0.02	0.11	0.06	-0.06	-0.06	0.01
PoleLees05	0.57	0.57	0.56	0.50	0.32	0.21	0.11	0.04	0.01	-0.03	0.02	0.05	0.10	0.17	0.27
SpoutFigyn	0.32	0.20	0.12	-0.01	-0.08	-0.15	-0.14	-0.14	-0.16	-0.16	-0.12	-0.10	-0.00	0.05	0.06
WestBlean01	0.39	0.31	0.24	0.17	0.16	0.07	0.16	0.12	0.13	0.10	0.12	0.11	0.11	0.23	0.22
WestBlean02	0.12	0.08	0.06	0.09	0.05	0.07	0.03	0.03	-0.00	0.07	0.14	0.25	0.27	0.31	0.28
WestBlean03	0.23	0.15	0.06	0.08	0.12	0.13	0.09	0.02	-0.05	-0.00	0.01	0.10	0.17	0.22	0.22
WestBlean04	0.21	0.15	0.15	0.12	0.13	0.11	0.16	0.16	0.11	0.15	0.28	0.20	0.22	0.22	0.21

Table C.3: VNVI values for each plot site across high deer density sites within height band 200-990 cm.

plot	VNVI values				
	min	max	mean	std	variance
Ampfield03	-0.11	0.78	0.39	0.26	0.067
Ampfield04	-0.08	0.42	0.18	0.12	0.014
Bentley03	-0.11	0.66	0.39	0.17	0.031
Bentley04	-0.33	0.58	0.11	0.23	0.051
Blackmoor	0.11	0.95	0.68	0.21	0.045
Haughwood	0.06	0.66	0.46	0.15	0.022
Hound01	-0.07	0.95	0.62	0.28	0.081
Hound03	-0.61	0.90	0.43	0.40	0.163
Hound05	0.09	0.71	0.43	0.16	0.027
Kingswood01	0.27	0.78	0.56	0.13	0.017
Kingswood10	-0.09	0.86	0.58	0.21	0.043
Langley02	-0.15	0.84	0.58	0.23	0.051
Langley05	-0.31	0.85	0.46	0.34	0.114
LeaPagets03	0.15	0.76	0.57	0.14	0.019
Romers	0.02	0.99	0.70	0.26	0.070
WyreMain01	-0.84	0.27	-0.27	0.23	0.054
WyreMain03	-0.27	0.61	0.27	0.20	0.040
WyreMain04	0.02	0.76	0.49	0.19	0.036
WyreNNR01	-0.60	0.64	0.23	0.32	0.102
WyreNNR03	-0.97	0.11	-0.45	0.32	0.104

Table C.4: VNVI values for each plot site across low deer density sites within height band 200-990 cm.

plot	VNVI values				
	min	max	mean	std	variance
BigForest03	0.33	0.99	0.73	0.17	0.027
BleanHomestall01	-0.04	0.95	0.59	0.33	0.106
BleanHomestall04	0.20	0.98	0.77	0.22	0.050
BleanHomestall06	-0.09	0.91	0.58	0.26	0.066
EastBlean01	0.27	0.91	0.67	0.18	0.034
EastBlean03	-0.01	0.85	0.51	0.22	0.049
Eastridge01	0.15	0.83	0.54	0.15	0.023
Eastridge05	0.08	0.87	0.59	0.21	0.043
Ellenden	-0.42	0.95	0.47	0.43	0.188
FfriddMathrafal02	0.33	0.83	0.66	0.10	0.009
FfriddMathrafal04	0.14	0.55	0.36	0.11	0.012
GwernDdu01	-0.46	0.36	-0.03	0.19	0.037
GwernDdu04	0.45	0.96	0.77	0.13	0.018
PoleLees02	-0.17	0.62	0.24	0.21	0.046
PoleLees05	0.18	0.64	0.42	0.13	0.016
SpoutFigyn	0.14	0.94	0.65	0.21	0.043
WestBlean01	0.00	0.70	0.26	0.16	0.026
WestBlean02	0.28	0.97	0.77	0.15	0.023
WestBlean03	0.21	0.87	0.63	0.16	0.026
WestBlean04	0.25	0.77	0.51	0.11	0.013

Figure C.1: Forest plot photos for high deer density sites

Figure C.2: Forest plot photos for low deer density sites

Figure C.3: VNVI profiles across zone A with sub-figures divided into managed (a) and unmanaged (b) plots.

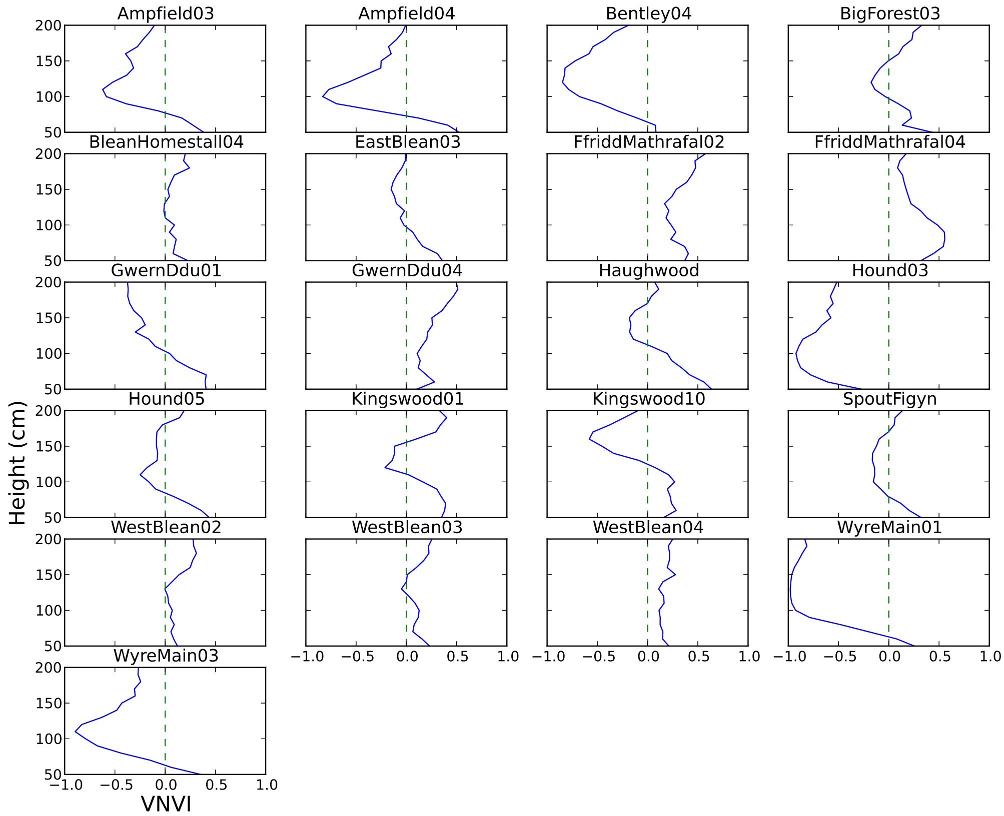

(a) managed

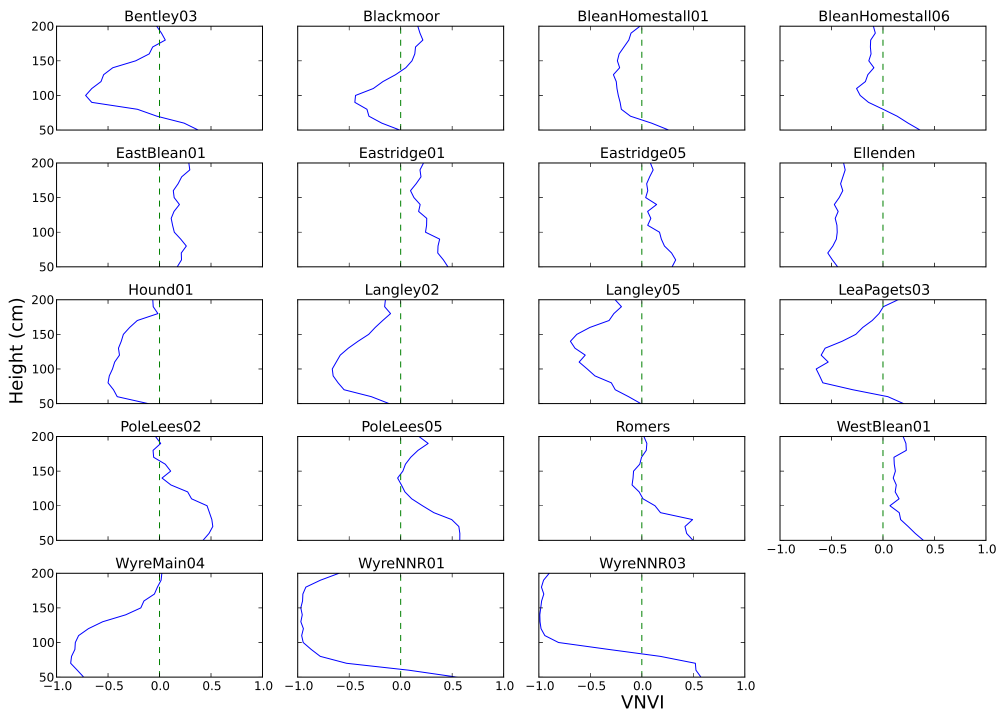

(b) unmanaged

Figure C.4: Mean and standard deviations of vertical cluster count within height bands (zone B) for high/low deer density and managed/unmanaged forest plots.

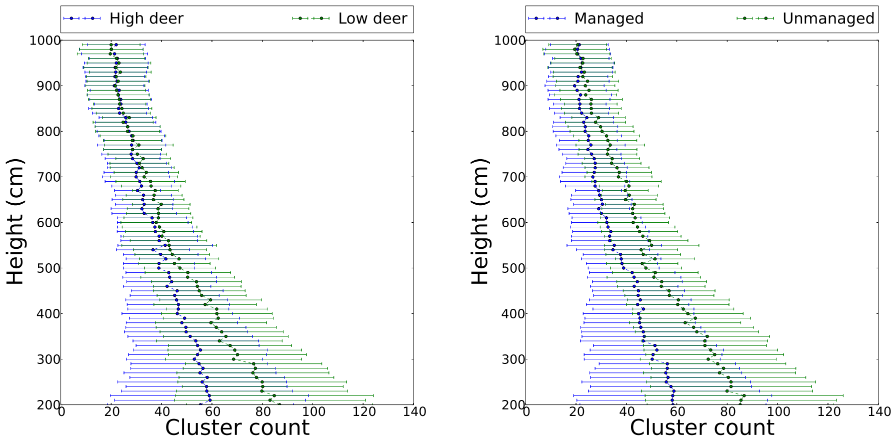

(a) deer density (b) management

Figure C.5: Mean and standard deviations of nearest neighbour within height bands (zone B) for high/low deer density and managed/unmanaged forest plots.

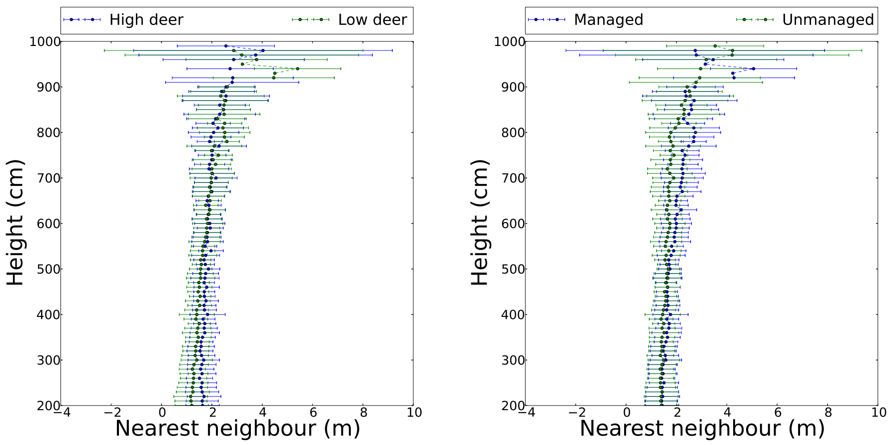

(a) deer density (b) management

C.2 Vertical density profiles

Table C.5: Showing mean values and standard deviation in understorey UDP across the sub-sections for each plot site. Values are given returns per cm.

plot site	subsections							
	0 - 50 cm		51 - 100 cm		101 - 150 cm		151 - 200	
	mean	std	mean	std	mean	std	mean	std
Ampfield03	4463	1992	173	106	61	8	28	12
Ampfield04	6549	1489	178	48	96	20	35	13
Bentley03	4302	1165	91	30	32	5	14	4
Bentley04	1611	1466	58	40	20	2	11	5
BigForest03	9657	8333	276	82	113	10	48	8
Blackmoor	2182	1824	137	12	92	9	38	11
BleanHomestall01	3550	2140	276	38	126	7	43	7
BleanHomestall04	2720	1040	377	69	146	19	48	10
BleanHomestall06	3066	2188	323	55	149	18	44	11
EastBlean01	885	858	249	18	163	7	61	13
EastBlean03	6170	3022	572	106	208	34	59	12
Eastridge01	5993	1397	604	107	243	30	80	18
Eastridge05	10398	5478	523	109	184	25	52	14
Ellenden	629	197	239	9	131	6	42	7
FfriddMathrafal02	6055	5072	417	244	150	54	50	14
FfriddMathrafal04	11326	2258	887	221	110	23	34	10
GwernDdu01	9178	2113	110	27	43	11	12	6
GwernDdu04	4495	3432	480	157	180	17	62	10
Haughwood	5727	3344	276	178	78	16	26	12
Hound01	3549	1892	269	11	147	15	56	13
Hound03	651	582	39	6	24	4	10	5
Hound05	6029	2010	236	74	66	8	28	18
Kingswood01	9553	2348	631	285	62	23	42	24
Kingswood10	12002	5649	631	364	153	9	72	18
Langley02	777	257	139	56	65	7	26	7
Langley05	1096	363	159	17	73	6	28	5
LeaPagets03	2142	1129	153	30	69	7	26	4
PoleLees02	6975	2218	946	151	79	22	20	7
PoleLees05	8956	4177	890	207	181	20	70	18
Romers	9903	1714	347	85	137	7	48	4
SpoutFigyn	3076	1104	255	21	130	21	47	11
WestBlean01	4150	2029	281	23	140	20	52	9
WestBlean02	1398	609	249	19	140	13	55	13
WestBlean03	751	577	201	15	101	7	33	7
WestBlean04	1259	734	252	14	145	13	49	8
WyreMain01	9623	2449	129	73	52	3	20	4
WyreMain03	1686	1118	113	37	48	8	17	9
WyreMain04	904	300	223	12	134	9	51	10
WyreNNR01	5544	3495	100	26	46	10	15	7
WyreNNR03	10049	695	189	100	26	3	9	4

C.3 Extraction of understorey cover and microtopography

Table C.6: Area estimates extracted at 1 cm resolution show a decrease in 2D area and an increase in 3D area when compared against estimates extracted using 5 cm resolution.

plot site	resolution	area 2D (m^2)	area 3D (m^2)	volume (m^3)	cover (%)
Ampfield03	1 cm	285.0	1438.2	42.3	57.0
	5 cm	318.3	1270.5	57.8	63.7
Ellenden	1 cm	49.1	421	7.6	9.8
	5 cm	56.4	345.5	8.7	11.3

Table C.7: Area and volume estimates extracted through terrestrial laser scan analysis for each plot site.

site name	deer density	understorey	area 2D (m^2)	area 3D (m^2)	volume (m^3)	cover (%)
Ampfield03	High	medium	318.3	1270.5	57.8	63.7
Ampfield04	High	high	353.4	1505.9	69.1	70.7
Bentley03	High	medium	293.2	1166.3	53.8	58.6
Bentley04	High	low	218.8	810.6	32.4	43.8
BigForest03	Low	medium	373.6	1518.8	65.5	74.7
Blackmoor	High	medium	233.0	815.4	34.2	46.6
BleanHomestall01	Low	medium	263.7	1181.9	44.1	52.7
BleanHomestall04	Low	medium	217.4	1147.4	39.0	43.5
BleanHomestall06	Low	medium	246.0	1244.3	45.7	49.2
EastBlean01	Low	low	104.6	665.0	20.9	20.9
EastBlean03	Low	high	277.7	1596.2	54.8	55.5
Eastridge01	Low	high	291.8	1740.5	63.2	58.4
Eastridge05	Low	high	338.4	1789.7	70.1	67.7
Ellenden	Low	low	56.4	345.5	8.7	11.3
FfriddMathrafal02	Low	high	305.8	1532.7	56.3	61.2
FfriddMathrafal04	Low	high	349.1	2272.4	92.0	69.8
GwernDdu01	Low	high	400.2	1420.8	80.1	80.0
GwernDdu04	Low	high	252.6	1349.2	46.3	50.5
Haughwood	High	medium	330.3	1359.0	64.1	66.1
Hound01	High	low	288.5	958.7	46.1	57.7
Hound03	High	medium	190.4	666.8	22.7	38.1
Hound05	High	medium	351.0	1868.3	79.4	70.2
Kingswood01	High	high	325.2	2006.8	81.3	65.0
Kingswood10	High	medium	316.2	1465.9	64.3	63.2
Langley02	High	low	106.1	419.6	16.8	21.2
Langley05	High	low	153.5	577.1	21.1	30.7
LeaPagets03	High	low	238.0	923.9	38.5	47.6
PoleLees02	Low	high	324.0	2494.9	90.6	64.8
PoleLees05	Low	high	328.3	2236.7	83.6	65.7
Romers	High	high	365.3	1655.3	80.6	73.1
SpoutFigyn	Low	medium	249.4	1031.5	39.6	49.9
WestBlean01	Low	medium	262.4	1226.1	45.6	52.5
WestBlean02	Low	low	195.6	999.5	30.4	39.1
WestBlean03	Low	low	132.7	877.5	25.0	26.5
WestBlean04	Low	low	175.2	997.3	30.1	35.0
WyreMain01	Medium	medium	365.5	1180.5	66.2	73.1
WyreMain03	Medium	high	252.2	986.3	41.9	50.4
WyreMain04	Medium	low	84.3	284.2	9.2	16.9
WyreNNR01	Medium	high	349.9	1160.6	63.5	70.0
WyreNNR03	Medium	high	406.9	1884.2	101.8	81.4

Table C.8: Understorey surface properties for individual plot sites.

site name	mean slope	mean curvature	mean std slope
Ampfield03	37.9	15.7	20.6
Ampfield04	43.9	18.9	21.0
Bentley03	35.8	15.6	21.0
Bentley04	25.9	11.3	18.1
BigForest03	41.4	18.7	20.1
Blackmoor	27.8	11.5	19.9
BleanHomestall01	34.8	16.8	21.9
BleanHomestall04	31.3	16.4	21.5
BleanHomestall06	34.6	17.3	21.8
EastBlean01	16.5	11.4	16.3
EastBlean03	40.1	21.5	22.9
Eastridge01	41.9	22.3	22.7
Eastridge05	44.8	22.5	21.6
Ellenden	9.2	6.8	11.5
FfriddMathrafal02	40.0	20.4	21.9
FfriddMathrafal04	50.5	27.8	21.8
GwernDdu01	41.4	16.7	19.1
GwernDdu04	34.7	19.5	22.3
Haughwood	39.8	17.1	20.6
Hound01	32.1	12.9	19.1
Hound03	24.0	10.0	19.7
Hound05	48.1	23.1	21.4
Kingswood01	47.0	25.1	22.2
Kingswood10	39.6	19.7	21.4
Langley02	14.3	7.7	14.7
Langley05	19.1	9.3	17.0
LeaPagets03	29.3	13.5	19.7
PoleLees02	51.2	31.2	23.3
PoleLees05	49.1	27.0	22.0
Romers	44.1	20.9	21.1
SpoutFigyn	30.5	15.3	21.1
WestBlean01	34.3	18.0	21.9
WestBlean02	28.1	15.4	21.8
WestBlean03	21.7	15.0	19.9
WestBlean04	26.4	15.4	21.1
WyreMain01	38.6	14.7	19.6
WyreMain03	31.1	14.1	20.7
WyreMain04	11.3	5.7	14.0
WyreNNR01	37.6	14.1	17.5
WyreNNR03	49.8	22.0	19.8

Table C.9: The P values provided through ANOVA from the extracted mean microtopography estimates for the five vegetative groups (where n=8, 3, 11, 3 and 7 for understorey groups 0, 1, 2, 3, 4 and 5 respectively) are reduced when using a finer scale resolution of moving window. For this reason a 50 cm moving window was used for the assessment of results.

resolution	measure	statistic	significant	F	p
50 cm	slope	std	yes	5.733	0.00178951
		mean	yes	8.101	0.00019921
	curvature	std	yes	4.486	0.00657120
		mean	yes	4.831	0.00453328
100 cm	slope	std	no	2.606	0.05800135
		mean	yes	8.080	0.00020292
	curvature	std	yes	3.942	0.01201483
		mean	yes	4.838	0.00450315
150 cm	slope	std	no	1.496	0.23124325
		mean	yes	8.109	0.00019789
	curvature	std	yes	3.658	0.01660629
		mean	yes	3.219	0.02774301
200 cm	slope	std	no	1.278	0.30322428
		mean	yes	8.080	0.00020287
	curvature	std	yes	3.410	0.02214991
		mean	yes	3.500	0.01994788
250 cm	slope	std	no	1.074	0.38883255
		mean	yes	8.080	0.00020282
	curvature	std	yes	3.265	0.02624652
		mean	yes	3.583	0.01811986

References

3DLaserMapping (2016). *D Laser Mapping is a world-leading provider of mobile mapping and monitoring solutions.* http://www.3dlasermapping.com.

Ackermann, Friedrich (1999). "Airborne laser scanning - present status and future expectations". In: *ISPRS Journal of Photogrammetry and Remote Sensing* 54.2, pp. 64–67.

Aerts, Raf and Olivier Honnay (2011). "Forest restoration, biodiversity and ecosystem functioning." In: *BMC ecology* 11.1, p. 29.

Alba, M and M Scaioni (2007). "Comparison of techniques for terrestrial laser scanning data georeferencing applied to 3-D modelling of cultural heritage". In: *The International Archives of the Photogrammetry, Remote Sensing and Spatial Information Sciences* 36.5/W47, p. 8.

Aldoma, Aitor, Zoltan-Csaba Marton, Federico Tombari, Walter Wohlkinger, Christian Potthast, Bernhard Zeisl, Radu Bogdan Rusu, Suat Gedikli, and Markus Vincze (2012). "Point Cloud Library". In: *IEEE Robotics & Automation Magazine* 1070.9932/12.

Appuhn, Karl (2000). "Inventing Nature: Forests, Forestry, and State Power in Renaissance Venice". In: *The Journal of Modern History* 72.4, pp. 861–889.

Ashcroft, Michael B, John R Gollan, and Daniel Ramp (2014). "Creating vegetation density profiles for a diverse range of ecological habitats using terrestrial laser scanning". In: *Methods in Ecology and Evolution* 5.3, pp. 263–272.

Axelsson, Peter (2000). "DEM generation from laser scanner data using adaptive TIN models". In: *International Archives of Photogrammetry and Remote Sensing* 33.B4/1; PART 4, pp. 111–118.

Bailey, Tim and Hugh Durrant-Whyte (2006). "Simultaneous localization and mapping (SLAM): Part II". In: *IEEE Robotics & Automation Magazine* 13.3, pp. 108–117.

Bannister, R and P Kennelly (2016). "Incorporating Stream Features into Groundwater Contouring Tools Within GIS." In: *Ground water* 54.2, pp. 286–290.

Baraloto, Christopher and Pierre Couteron (2010). "Fine-scale Microhabitat Heterogeneity in a French Guianan Forest". In: *Biotropica* 42.4, pp. 420–428.

Barbier, Stéphane, Frédéric Gosselin, and Philippe Balandier (2008). "Influence of tree species on understory vegetation diversity and mechanisms involved - a critical review for temperate and boreal forests". In: *Forest Ecology and Management* 254.1, pp. 1–15.

Becerik-Gerber, Burcin, Farrokh Jazizadeh, Geoffrey Kavulya, and Gulben Calis (2011). "Assessment of target types and layouts in 3D laser scanning for registration accuracy". In: *Automation in Construction* 20.5, pp. 649–658.

Béland, Martin, Dennis D Baldocchi, Jean-Luc Widlowski, Richard A Fournier, and Michel M Verstraete (2014a). "On seeing the wood from the leaves and the role of voxel size in determining leaf area distribution of forests with terrestrial LiDAR". In: *Agricultural and Forest Meteorology* 184, pp. 82–97.

Béland, Martin, Jean-Luc Widlowski, and Richard A Fournier (2014b). "A model for deriving voxel-level tree leaf area density estimates from ground-based LiDAR". In: *Environmental Modelling & Software* 51, pp. 184–189.

Bergner, Adam, Mustafa Avcı, Hasan Eryiğit, Nicklas Jansson, Mats Niklasson, Lars Westerberg, and Per Milberg (2015). "Influences of forest type and habitat structure on bird assemblages of oak (Quercus spp.) and pine (Pinus spp.) stands in southwestern Turkey". In: *Forest Ecology and Management* 336, pp. 137–147.

Besl, Paul J and Neil D McKay (1992). "A method for registration of 3-D shapes". In: *IEEE transactions on pattern analysis and machine intelligence* 14.2, pp. 239–256.

Beyer, Hawthorn L (2012). "Geospatial Modelling Environment (Version 0.7. 2.1)". In: *Spatial Ecology, LLC.*

Bickford, C Allen (1952). "The sampling design used in the forest survey of the Northeast". In: *Journal of Forestry* 50.4, pp. 290–293.

Bienert, A, R Queck, A Schmidt, Ch Bernhofer, and HG Maas (2010). "Voxel space analysis of terrestrial laser scans in forests for wind field modeling". In: *International Archives of Photogrammetry, Remote Sensing and Spatial Information Sciences* 38.Part 5, pp. 92–97.

Bienert, A, S Scheller, and E Keane (2007). "Tree detection and diameter estimations by analysis of forest terrestrial laserscanner point clouds". In: *ISPRS workshop on laser scanning*, pp. 50–55.

Bienert, A, S Scheller, E Keane, G Mullooly, and F Mohan (2006a). "Application of terrestrial laser scanners for the determination of forest inventory parameters". In: *International Archives of Photogrammetry, Remote Sensing and Spatial Information Sciences* 36.5.

Bienert, Anne, Hans-Gerd Maas, and Steffen Scheller (2006b). "Analysis of the information content of terrestrial laserscanner point clouds for the automatic determination of forest inventory parameters". In: *Workshop on 3D Remote Sensing in Forestry*. Vol. 14, p. 15.

Bitelli, Gabriele, Andrea Simone, Fabrizio Girardi, and Claudio Lantieri (2012). "Laser scanning on road pavements: A new approach for characterizing surface texture". In: *Sensors* 12.7, pp. 9110–9128.

Bonham, Charles D (2013). *Measurements for terrestrial vegetation*. John Wiley & Sons.

Bornaz, Leandro, Andrea Lingua, and Fulvio Rinaudo (2003). "Multiple scan registration in LIDAR close range applications". In: *Int. Arch. Photogram. Rem. Sens. Spatial Inform. Sci* 34, pp. 72–77.

Bosse, Michael, Robert Zlot, and Paul Flick (2012). "Zebedee: Design of a spring-mounted 3-d range sensor with application to mobile mapping". In: *Robotics, IEEE Transactions on* 28.5, pp. 1104–1119.

Boudon, Frédéric, Chakkrit Preuksakarn, Pascal Ferraro, Julien Diener, Philippe Nacry, Eero Nikinmaa, and Christophe Godin (2014). "Quantitative assessment of automatic reconstructions of branching systems obtained from laser scanning". In: *Annals of botany* 114.4, pp. 853–862.

Boulanger, Vincent, Christophe Baltzinger, Sonia Saïd, Philippe Ballon, Jean-Francois Picard, and Jean-Luc Dupouey (2015). "Decreasing deer browsing pressure influenced understory vegetation dynamics over 30 years". In: *Annals of Forest Science* 72.3, pp. 367–378.

Bouvier, Marc, Sylvie Durrieu, Richard A Fournier, and Jean-Pierre Renaud (2015). "Generalizing predictive models of forest inventory attributes using an area-based approach with airborne LiDAR data". In: *Remote Sensing of Environment* 156, pp. 322–334.

Brasington, J, D Vericat, and I Rychkov (2012). "Modeling river bed morphology, roughness, and surface sedimentology using high resolution terrestrial laser scanning". In: *Water Resources Research* 48.11.

Brolly, Gábor, Géza Király, and Kornél Czimber (2013). "Mapping Forest Regeneration from Terrestrial Laser Scans". In: *Acta Silvatica et Lignaria Hungarica* 9.1, pp. 135–146.

Brubaker, Kristen M, Wayne L Myers, Patrick J Drohan, Douglas A Miller, and Elizabeth W Boyer (2013). "The use of LiDAR terrain data in characterizing surface roughness and microtopography". In: *Applied and Environmental Soil Science* 2013.

Buckland, ST, IBJ Goudie, and DL Borchers (2000). "Wildlife population assessment: past developments and future directions". In: *Biometrics* 56.1, pp. 1–12.

Buckley, Simon J, JA Howell, HD Enge, and TH Kurz (2008). "Terrestrial laser scanning in geology: data acquisition, processing and accuracy considerations". In: *Journal of the Geological Society* 165.3, pp. 625–638.

Buongiorno, Joseph, Sally Dahir, Hsien-Chih Lu, and Ching-Rong Lin (1994). "Tree size diversity and economic returns in uneven-aged forest stands". In: *Forest Science* 40.1, pp. 83–103.

Burton, Julia I, Lisa M Ganio, and Klaus J Puettmann (2014). "Multi-scale spatial controls of understory vegetation in Douglas-fir-western hemlock forests of western Oregon, USA". In: *Ecosphere* 5.12, art151.

Burton, Julia I., David J. Mladenoff, Murray K. Clayton, and Jodi A. Forrester (2011). "The roles of environmental filtering and colonization in the fine-scale spatial patterning of ground-layer plant communities in north temperate deciduous forests". In: *Journal of Ecology* 99.3, pp. 764–776.

Butchart, Stuart H M, Matt Walpole, Ben Collen, Arco van Strien, Jörn P W Scharlemann, Rosamunde E a Almond, Jonathan E M Baillie, Bastian Bomhard, Claire Brown, John Bruno, Kent E Carpenter, Geneviève M Carr, Janice Chanson, Anna M Chenery, Jorge Csirke, Nick C Davidson, Frank Dentener, Matt Foster, Alessandro Galli, James N Galloway, Piero Genovesi, Richard D Gregory, Marc Hockings, Valerie Kapos, Jean-Francois Lamarque, Fiona Leverington, Jonathan Loh, Melodie a McGeoch, Louise McRae, Anahit Minasyan, Monica Hernández Morcillo, Thomasina E E Oldfield, Daniel Pauly, Suhel Quader, Carmen Revenga, John R Sauer, Benjamin Skolnik, Dian Spear, Damon Stanwell-Smith, Simon N Stuart, Andy Symes, Megan Tierney, Tristan D Tyrrell, Jean-Christophe Vié, and Reg Watson (2010). "Global biodiversity: indicators of recent declines." In: *Science (New York, N.Y.)* 328.5982, pp. 1164–8.

Cabaleiro, M, B Riveiro, P Arias, JC Caamaño, and JA Vilán (2014). "Automatic 3D modelling of metal frame connections from LiDAR data for structural engineering purposes". In: *ISPRS Journal of Photogrammetry and Remote Sensing* 96, pp. 47–56.

Calders, Kim, John Armston, Glenn Newnham, Martin Herold, and Nicholas Goodwin (2014). "Implications of sensor configuration and topography on vertical plant profiles derived from terrestrial LiDAR". In: *Agricultural and Forest Meteorology* 194, pp. 104–117.

Calders, Kim, Glenn Newnham, Andrew Burt, Simon Murphy, Pasi Raumonen, Martin Herold, Darius Culvenor, Valerio Avitabile, Mathias Disney, John Armston, et al. (2015). "Nondestructive estimates of above-ground biomass using terrestrial laser scanning". In: *Methods in Ecology and Evolution* 6.2, pp. 198–208.

Chen, Jun, Masae Shiyomi, Charles D Bonham, Taisuke Yasuda, Yoshimichi Hori, and Yasuo Yamamura (2008). "Plant cover estimation based on the beta distribution in grassland vegetation". In: *Ecological research* 23.5, pp. 813–819.

Cifuentes, Renato, Dimitry Van der Zande, Jamshid Farifteh, Christian Salas, and Pol Coppin (2014). "Effects of voxel size and sampling setup on the estimation of forest canopy gap fraction from terrestrial laser scanning data". In: *Agricultural and Forest Meteorology* 194, pp. 230–240.

Connell, Joseph H and Ralph O Slatyer (1977). "Mechanisms of succession in natural communities and their role in community stability and organization". In: *American naturalist*, pp. 1119–1144.

Cram, Douglas S, Terrell T Baker, Alexander G Fernald, Andres F Cibils, and Dawn M VanLeeuwen (2015). "Fuel and Vegetation Trends after Wildfire in Treated versus Untreated Forests". In: *Forest Science* 61.4, pp. 753–762.

Dale, Virginia H and Suzanne C Beyeler (2001). "Challenges in the development and use of ecological indicators". In: *Ecological indicators* 1.1, pp. 3–10.

Danson, F Mark, Rachel Gaulton, Richard P Armitage, Mathias Disney, Oliver Gunawan, Philip Lewis, Guy Pearson, and Alberto F Ramirez (2014). "Developing a dual-wavelength full-waveform terrestrial laser scanner to characterize forest canopy structure". In: *Agricultural and Forest Meteorology* 198, pp. 7–14.

Danson, F Mark, David Hetherington, Felix Morsdorf, Benjamin Koetz, and Britta Allgower (2007). "Forest canopy gap fraction from terrestrial laser scanning". In: *Geoscience and Remote Sensing Letters, IEEE* 4.1, pp. 157–160.

Dassot, Mathieu, Thiéry Constant, and Meriem Fournier (2011). "The use of terrestrial LiDAR technology in forest science: application fields, benefits and challenges". English. In: *Annals of forest science* 68.5, pp. 959–974.

Davies, Andrew B and Gregory P Asner (2014). "Advances in animal ecology from 3D-LiDAR ecosystem mapping". In: *Trends in ecology & evolution* 29.12, pp. 681–691.

Desclée, Baudouin, Patrick Bogaert, and Pierre Defourny (2006). "Forest change detection by statistical object-based method". In: *Remote Sensing of Environment* 102.1, pp. 1–11.

Díaz-Aguilar, Irma, Sylvie A Quideau, Heather C Proctor, Barbara E Kishchuk, and John R Spence (2013). "Influence of stand composition on predatory mite (Mesostigmata) assemblages from the forest floor in western Canadian boreal mixedwood forests". In: *Forest Ecology and Management* 309, pp. 105–114.

Dong, Mei, Christoph Neukum, Hui Hu, and Rafig Azzam (2015). "Real 3D geotechnical modeling in engineering geology: a case study from the inner city of Aachen, Germany". In: *Bulletin of Engineering Geology and the Environment* 74.2, pp. 281–300.

Douglas, Ewan S., Alan Strahler, Jason Martel, Timothy Cook, Christopher Mendillo, Robert Marshall, Supriya Chakrabarti, Crystal Schaaf, Curtis Woodcock, Zhan Li, Xiaoyuan Yang, Darius Culvenor, David Jupp, Glenn Newnham, and Jenny Lovell (2012). "DWEL: A Dual-Wavelength Echidna Lidar for ground-based forest scanning". In: *2012 IEEE International Geoscience and Remote Sensing Symposium*, pp. 4998–5001.

Dufrêne, Marc and Pierre Legendre (1997). "Species assemblages and indicator species: the need for a flexible asymmetrical approach". In: *Ecological monographs* 67.3, pp. 345–366.

Durrant-Whyte, Hugh and Tim Bailey (2006). "Simultaneous localization and mapping: part I". In: *Robotics & Automation Magazine, IEEE* 13.2, pp. 99–110.

Durupt, Alexandre, Sebastien Remy, Guillaume Ducellier, and Benoit Eynard (2008). "From a 3D point cloud to an engineering CAD model: a knowledge-product-based approach for reverse engineering". In: *Virtual and Physical Prototyping* 3.2, pp. 51–59.

Eichhorn, MP (2010). "Spatial organisation of a bimodal forest stand". In: *Journal of forest research* 15.6, pp. 391–397.

Eitel, Jan UH, Lee A Vierling, and Troy S Magney (2013). "A lightweight, low cost autonomously operating terrestrial laser scanner for quantifying and monitoring ecosystem structural dynamics". In: *Agricultural and Forest Meteorology* 180, pp. 86–96.

Escribano-Rocafort, Adrián G, Agustina B Ventre-Lespiaucq, Carlos Granado-Yela, Antonio López-Pintor, Juan A Delgado, Vicente Muñoz, Gabriel A Dorado, and Luis Balaguer (2014). "Simplifying data acquisition in plant canopies-Measurements of leaf angles with a cell phone". In: *Methods in Ecology and Evolution* 5.2, pp. 132–140.

Eskelson, Bianca NI, Lisa Madsen, Joan C Hagar, and Hailemariam Temesgen (2011). "Estimating riparian understory vegetation cover with beta regression and copula models". In: *Forest Science* 57.3, pp. 212–221.

Fan, Lei, William Powrie, Joel Smethurst, Peter M Atkinson, and Herbert Einstein (2014). "The effect of short ground vegetation on terrestrial laser scans at a local scale". In: *ISPRS Journal of Photogrammetry and Remote Sensing* 95, pp. 42–52.

Fang, Jingyun, Anping Chen, Changhui Peng, Shuqing Zhao, and Longjun Ci (2001). "Changes in forest biomass carbon storage in China between 1949 and 1998". In: *Science* 292.5525, pp. 2320–2322.

Fernández-Sarría, A, L Martínez, B Velázquez-Martí, M Sajdak, J Estornell, and JA Recio (2013a). "Different methodologies for calculating crown volumes of *Platanus hispanica* trees using terrestrial laser scanner and a comparison with classical dendrometric measurements". In: *Computers and Electronics in Agriculture* 90, pp. 176–185.

Fernández-Sarría, A, B Velázquez-Martí, M Sajdak, L Martínez, and J Estornell (2013b). "Residual biomass calculation from individual tree architecture using terrestrial laser scanner and ground-level measurements". In: *Computers and Electronics in Agriculture* 93, pp. 90–97.

Forest, Li (2014). *LiForest*. http://www.liforest.com/.

Franklin, Jerry F and Robert Van Pelt (2004). "Spatial aspects of structural complexity in old-growth forests". In: *Journal of Forestry* 102.3, pp. 22–28.

Franklin, Jerry F, Thomas A Spies, Robert Van Pelt, Andrew B Carey, Dale A Thornburgh, Dean Rae Berg, David B Lindenmayer, Mark E Harmon, William S Keeton, David C Shaw, et al. (2002). "Disturbances and structural development of natural forest ecosystems with silvicultural implications, using Douglas-fir forests as an example". In: *Forest Ecology and Management* 155.1, pp. 399–423.

Frayer, WE and George M Furnival (1999). "Forest survey sampling designs: a history". In: *Journal of Forestry* 97.12, pp. 4–10.

Freeman, Elizabeth A and E David Ford (2002). "Effects of data quality on analysis of ecological pattern using the K (d) statistical function". In: *Ecology* 83.1, pp. 35–46.

Frerker, Katie, Autumn Sabo, and Donald Waller (2014). "Long-Term Regional Shifts in Plant Community Composition Are Largely Explained by Local Deer Impact Experiments". In: *PloS one* 9.12, e115843.

Fröhlich, Christofer and Markus Mettenleiter (2004). "Terrestrial laser scanning–new perspectives in 3D surveying". In: *International archives of photogrammetry, remote sensing and spatial information sciences* 36.Part 8, W2.

Fuller, RJ, PE Bellamy, A Broome, J Calladine, MP Eichhorn, RM Gill, and GM Siriwardena (2014). *Effects of woodland structure on woodland bird populations - an assessment of the effects of changes in woodland structure on bird populations as a result of woodland management practices and deer browsing.* http://randd.defra.gov.uk.

Gajardo, John, Mariano García, and David Riaño (2014). "Applications of Airborne Laser Scanning in Forest Fuel Assessment and Fire Prevention". In: *Forestry Applications of Airborne Laser Scanning.* Springer, pp. 439–462.

García, Mariano, F Mark Danson, David Riano, Emilio Chuvieco, F Alberto Ramirez, and Vishal Bandugula (2011). "Terrestrial laser scanning to estimate plot-level forest canopy fuel properties". In: *International Journal of Applied Earth Observation and Geoinformation* 13.4, pp. 636–645.

Gaulton, R, FM Danson, G Pearson, PE Lewis, and M Disney (2010). "The Salford Advanced Laser Canopy Analyser (SALCA): A multispectral full waveform LiDAR for improved vegetation characterisation". In: *Proceedings of the Remote Sensing and Photogrammetry Society Conference, Remote Sensing and the Carbon Cycle, London, UK.* Vol. 5.

Gelman, Andrew et al. (2005). "Analysis of variancewhy it is more important than ever". In: *The Annals of Statistics* 33.1, pp. 1–53.

Gill, Robert M A, M L Thomas, and D Stocker (1997). "The use of portable thermal imaging for estimating deer population density in forest habitats". In: *Journal of Applied Ecology*, pp. 1273–1286.

Gill, Robin and Robert J Fuller (2007). "The effects of deer browsing on woodland structure and songbirds in lowland Britain". In: *Ibis* 149.s2, pp. 119–127.

Gilliam, Frank S (2007). "The ecological significance of the herbaceous layer in temperate forest ecosystems". In: *Bioscience* 57.10, pp. 845–858.

— (2014). *The herbaceous layer in forests of eastern North America.* Oxford University Press.

Goetz, Scott and Ralph Dubayah (2011). "Advances in remote sensing technology and implications for measuring and monitoring forest carbon stocks and change". In: *Carbon Management* 2.3, pp. 231–244.

Gonzalez, Maya, Laurent Augusto, Anne Gallet-Budynek, Jianming Xue, Nathalie Yauschew-Raguenes, Dominique Guyon, Pierre Trichet, Florian Delerue, Sylvie Niollet, Frida Andreasson, et al. (2013). "Contribution of understory species to total ecosystem aboveground and belowground biomass in temperate Pinus pinaster Ait. forests". In: *Forest ecology and management* 289, pp. 38–47.

Gonzalez, Patrick, Gregory P. Asner, John J. Battles, Michael A. Lefsky, Kristen M. Waring, and Michael Palace (2010). "Forest carbon densities and uncertainties from Lidar, QuickBird, and field measurements in California". In: *Remote Sensing of Environment* 114.7, pp. 1561–1575.

Grayson, Arnold John and WB Maynard (1997). *The world's forests-Rio+ 5: international initiatives towards sustainable management*. Commonwealth Forestry Association (CFA).

Griebel, Anne, Lauren T Bennett, Darius S Culvenor, Glenn J Newnham, and Stefan K Arndt (2015). "Reliability and limitations of a novel terrestrial laser scanner for daily monitoring of forest canopy dynamics". In: *Remote Sensing of Environment* 166, pp. 205–213.

Grime, J Philip (2006). *Plant strategies, vegetation processes, and ecosystem properties*. John Wiley & Sons.

Grohmann, Carlos Henrique, Mike J Smith, and Claudio Riccomini (2011). "Multiscale analysis of topographic surface roughness in the Midland Valley, Scotland". In: *Geoscience and Remote Sensing, IEEE Transactions on* 49.4, pp. 1200–1213.

Guan, Haiyan, Jonathan Li, Yongtao Yu, Michael Chapman, and Cheng Wang (2015). "Automated Road Information Extraction From Mobile Laser Scanning Data". In: *Intelligent Transportation Systems, IEEE Transactions on* 16.1, pp. 194–205.

Guan, Haiyan, Jonathan Li, Yongtao Yu, Cheng Wang, Michael Chapman, and Bisheng Yang (2014). "Using mobile laser scanning data for automated extraction of road markings". In: {*ISPRS*} *Journal of Photogrammetry and Remote Sensing* 87, pp. 93–107.

Gupta, Vaibhav, Karin J Reinke, Simon D Jones, Luke Wallace, and Lucas Holden (2015). "Assessing metrics for estimating fire induced change in the forest understorey structure using terrestrial laser scanning". In: *Remote Sensing* 7.6, pp. 8180–8201.

Guyon, Dominique, Sylvia Dayau, Alain Kruszewski, Benoit Beguet, Jean-Charles Samalens, Jean-Pierre Wigneron, Alexis Ducousso, Jean-Marc Louvet, Sylvain Delzon, Fabrice Bonne, et al. (2014). "Near-surface remote sensing observations for monitoring deciduous broadleaf forest species phenology". In: *Geoscience and Remote Sensing Symposium (IGARSS), 2014 IEEE International*. IEEE, pp. 2379–2382.

Hackenberg, Jan, Christopher Morhart, Jonathan Sheppard, Heinrich Spiecker, and Mathias Disney (2014). "Highly Accurate Tree Models Derived from Terrestrial Laser Scan Data: A Method Description". In: *Forests* 5.5, pp. 1069–1105.

Harding, DJ, MA Lefsky, GG Parker, and JB Blair (2001). "Laser altimeter canopy height profiles: Methods and validation for closed-canopy, broadleaf forests". In: *Remote Sensing of Environment* 76.3, pp. 283–297.

Hart, Stephen A and Han YH Chen (2006). "Understory vegetation dynamics of North American boreal forests". In: *Critical Reviews in Plant Sciences* 25.4, pp. 381–397.

Hartzell, Preston, Craig Glennie, Kivanc Biber, and Shuhab Khan (2014). "Application of multispectral LiDAR to automated virtual outcrop geology". In: *ISPRS Journal of Photogrammetry and Remote Sensing* 88, pp. 147–155.

Hauglin, Marius, Vegard Lien, Erik Næsset, and Terje Gobakken (2014). "Georeferencing forest field plots by co-registration of terrestrial and airborne laser scanning data". In: *International Journal of Remote Sensing* 35.9, pp. 3135–3149.

Hedwall, Per-Ola, Jörg Brunet, Annika Nordin, and Johan Bergh (2013). "Changes in the abundance of keystone forest floor species in response to changes of forest structure". In: *Journal of vegetation science* 24.2, pp. 296–306.

Hegland, Stein J, Marte S Lilleeng, and Stein R Moe (2013). "Old-growth forest floor richness increases with red deer herbivory intensity". In: *Forest Ecology and Management* 310, pp. 267–274.

Hember, Robbie A, Werner A Kurz, Juha M Metsaranta, T Andy Black, Robert D Guy, and Nicholas C Coops (2012). "Accelerating regrowth of temperate-maritime forests due to environmental change". In: *Global Change Biology* 18.6, pp. 2026–2040.

Henning, Jason G and Philip J Radtke (2006a). "Detailed stem measurements of standing trees from ground-based scanning lidar". In: *Forest Science* 52.1, pp. 67–80.

— (2006b). "Ground-based laser imaging for assessing three-dimensional forest canopy structure". In: *Photogrammetric Engineering & Remote Sensing* 72.12, pp. 1349–1358.

Holmes, Richard T and Thomas W Sherry (2001). "Thirty-year bird population trends in an unfragmented temperate deciduous forest: importance of habitat change". In: *The Auk* 118.3, pp. 589–609.

Holopainen, Markus, Ville Kankare, Mikko Vastaranta, Xinlian Liang, Yi Lin, Matti Vaaja, Xiaowei Yu, Juha Hyyppä, Hannu Hyyppä, Harri Kaartinen, et al. (2013). "Tree mapping using airborne, terrestrial and mobile laser scanning–A case study in a heterogeneous urban forest". In: *Urban Forestry & Urban Greening* 12.4, pp. 546–553.

Hopkinson, Chris, Laura Chasmer, Colin Young-Pow, and Paul Treitz (2004). "Assessing forest metrics with a ground-based scanning lidar". en. In: *Canadian Journal of Forest Research* 34.3, pp. 573–583.

Hopkinson, Chris, Jenny Lovell, Laura Chasmer, David Jupp, Natascha Kljun, and Eva van Gorsel (2013). "Integrating terrestrial and airborne lidar to calibrate a 3D canopy model of effective leaf area index". In: *Remote Sensing of Environment* 136, pp. 301–314.

Hosoi, Fumiki, Yohei Nakai, and Kenji Omasa (2013). "3-D voxel-based solid modeling of a broad-leaved tree for accurate volume estimation using portable scanning lidar". In: *ISPRS Journal of Photogrammetry and Remote Sensing* 82, pp. 41–48.

Hosoi, Fumiki and Kenji Omasa (2006). "Voxel-based 3-D modeling of individual trees for estimating leaf area density using high-resolution portable scanning lidar". In: *Geoscience and Remote Sensing, IEEE Transactions on* 44.12, pp. 3610–3618.

Hu, Hui, Tomas M Fernandez-Steeger, Mei Dong, and Rafig Azzam (2015). "Deformation Monitoring and Recognition of Surface Mine Slope Using LiDAR". In: *Engineering Geology for Society and Territory-Volume 2*. Springer, pp. 451–454.

Huang, Huabing, Zhan Li, Peng Gong, Xiao Cheng, Nick Clinton, Chunxiang Cao, Wenjian Ni, and Lei Wang (2011). "Automated methods for measuring DBH and tree heights with a commercial scanning lidar". In: *Photogrammetric Engineering & Remote Sensing* 77.3, pp. 219–227.

Huang, Qiongyu, Anu Swatantran, Ralph Dubayah, and Scott J Goetz (2014). "The influence of vegetation height heterogeneity on forest and woodland bird species richness across the United States". In: *PloS one* 9.8, e103236.

Hunter, Malcolm L (1999). *Maintaining biodiversity in forest ecosystems.* Cambridge University Press.

Hyde, Peter, Ross Nelson, Dan Kimes, and Elissa Levine (2007). "Exploring LiDAR–RaDAR synergy?Predicting aboveground biomass in a southwestern ponderosa pine forest using LiDAR, SAR and InSAR". In: *Remote Sensing of Environment* 106.1, pp. 28–38.

Hyyppä, Juha, Markus Holopainen, and Håkan Olsson (2012). "Laser scanning in forests". en. In: *Remote Sensing* 4.10, pp. 2919–2922.

Jalonen, Johanna, Juha Järvelä, Juho-Pekka Virtanen, Matti Vaaja, Matti Kurkela, and Hannu Hyyppä (2015). "Determining Characteristic Vegetation Areas by Terrestrial Laser Scanning for Floodplain Flow Modeling". In: *Water* 7.2, pp. 420–437.

James, Mike R and John N Quinton (2014). "Ultra-rapid topographic surveying for complex environments: the hand-held mobile laser scanner (HMLS)". In: *Earth surface processes and landforms* 39.1, pp. 138–142.

Jenness, Jeff S (2004). "Calculating landscape surface area from digital elevation models". In: *Wildlife Society Bulletin* 32.3, pp. 829–839.

Jupp, David LB, DS Culvenor, JL Lovell, GJ Newnham, AH Strahler, and CE Woodcock (2009). "Estimating forest LAI profiles and structural parameters using a ground-based laser called Echidna". In: *Tree physiology* 29.2, pp. 171–181.

Kaasalainen, Sanna, Anssi Krooks, Jari Liski, Pasi Raumonen, Harri Kaartinen, Mikko Kaasalainen, Eetu Puttonen, Kati Anttila, and Raisa Mäkipää (2014). "Change Detection of Tree Biomass with Terrestrial Laser Scanning and Quantitative Structure Modelling". In: *Remote Sensing* 6.5, pp. 3906–3922.

Kalacska, M, Gerardo Arturo Sanchez-Azofeifa, Benoit Rivard, Terry Caelli, H Peter White, and Julio César Calvo-Alvarado (2007). "Ecological fingerprinting of ecosystem succession: Estimating secondary tropical dry forest structure and diversity using imaging spectroscopy". In: *Remote Sensing of Environment* 108.1, pp. 82–96.

Keersmaecker, Wanda, Stef Lhermitte, Olivier Honnay, Jamshid Farifteh, Ben Somers, and Pol Coppin (2014). "How to measure ecosystem stability? An evaluation of the reliability of stability metrics based on remote sensing time series across the major global ecosystems". In: *Global change biology* 20.7, pp. 2149–2161.

Kenk, G and S Guehne (2001). "Management of transformation in central Europe". In: *Forest Ecology and Management* 151.1, pp. 107–119.

Kerns, Becky K and Janet L Ohmann (2004). "Evaluation and prediction of shrub cover in coastal Oregon forests (USA)". In: *Ecological Indicators* 4.2, pp. 83–98.

Kint, Vincent, Noël Lust, R Ferris, and FM Olsthoorn (2008). "Quantification of forest stand structure applied to Scots pine (Pinus sylvestris L.) forests". In: *Forest Systems* 9.3, pp. 147–163.

Kint, Vincent, Marc Van Meirvenne, Lieven Nachtergale, Guy Geudens, and Noël Lust (2003). "Spatial methods for quantifying forest stand structure development: a comparison between nearest-neighbor indices and variogram analysis". In: *Forest science* 49.1, pp. 36–49.

Kraus, Karl and Norbert Pfeifer (1998). "Determination of terrain models in wooded areas with airborne laser scanner data". In: *ISPRS Journal of Photogrammetry and remote Sensing* 53.4, pp. 193–203.

Kuuluvainen, Timo, Antti Penttinen, Kari Leinonen, Markku Nygren, et al. (1996). *Statistical opportunities for comparing stand structural heterogeneity in managed and primeval forests: an example from boreal spruce forest in southern Finland.* The Finnish Society of Forest Science and The Finnish Forest Research Institute.

LaBau, Vernon J (2007). *A history of the forest survey in the United States: 1830-2004.* US Dept. of Agriculture, Forest Service.

Larrieu, Laurent, Alain Cabanettes, and Jean-Pierre Sarthou (2015). "Hoverfly (Diptera: Syrphidae) richness and abundance vary with forest stand heterogeneity: Preliminary evidence from a montane beech fir forest". In: *European Journal of Entomology* 112.4, p. 755.

Latifi, Hooman, Marco Heurich, Florian Hartig, Jörg Müller, Peter Krzystek, Hans Jehl, and Stefan Dech (2015). "Estimating over-and understorey canopy density of temperate mixed stands by airborne LiDAR data". In: *Forestry*, cpv032.

Leeuwen, Martin and Maarten Nieuwenhuis (2010). "Retrieval of forest structural parameters using LiDAR remote sensing". In: *European Journal of Forest Research* 129.4, pp. 749–770.

Lefsky, Michael A, D Harding, WB Cohen, G Parker, and HH Shugart (1999). "Surface lidar remote sensing of basal area and biomass in deciduous forests of eastern Maryland, USA". In: *Remote Sensing of Environment* 67.1, pp. 83–98.

Lehtomäki, Matti, Anttoni Jaakkola, Juha Hyyppä, Jouko Lampinen, Harri Kaartinen, Antero Kukko, Eetu Puttonen, and Hannu Hyyppä (2016). "Object Classification and Recognition From Mobile Laser Scanning Point Clouds in a Road Environment". In: *IEEE Transactions on Geoscience and Remote Sensing* 54.2, pp. 1226–1239.

Lemon, Alan M and Norman L Jones (2003). "Building solid models from boreholes and user-defined cross-sections". In: *Computers & Geosciences* 29.5, pp. 547–555.

Lesak, Adrian A, Volker C Radeloff, Todd J Hawbaker, Anna M Pidgeon, Terje Gobakken, and Kirk Contrucci (2011). "Modeling forest songbird species richness using LiDAR-derived measures of forest structure". In: *Remote Sensing of Environment* 115.11, pp. 2823–2835.

Liang, Xinlian, J Hyyppa, Antero Kukko, and Harri Kaartinen (2014a). "The use of a mobile laser scanning system for mapping large forest plots". In: *IEEE Geoscience and remote sensing letters* 11.9, pp. 1504–1508.

Liang, Xinlian and Juha Hyyppä (2013). "Automatic stem mapping by merging several terrestrial laser scans at the feature and decision levels". In: *Sensors* 13.2, pp. 1614–1634.

Liang, Xinlian, Juha Hyyppä, Harri Kaartinen, Markus Holopainen, and Timo Melkas (2012). "Detecting Changes in Forest Structure over Time with Bi-Temporal Terrestrial Laser Scanning Data". In: *ISPRS International Journal of Geo-Information* 1.3, pp. 242–255.

Liang, Xinlian, Antero Kukko, Harri Kaartinen, Juha Hyyppä, Xiaowei Yu, Anttoni Jaakkola, and Yunsheng Wang (2014b). "Possibilities of a personal laser scanning system for forest mapping and ecosystem services". In: *Sensors* 14.1, pp. 1228–1248.

Liang, Xinlian, Ville Kankare, Juha Hyyppä, Yunsheng Wang, Antero Kukko, Henrik Haggrén, Xiaowei Yu, Harri Kaartinen, Anttoni Jaakkola, Fengying Guan, et al. (2016). "Terrestrial laser scanning in forest inventories". In: *ISPRS Journal of Photogrammetry and Remote Sensing* 115, pp. 63–77.

Lichti, DD, SJ Gordon, and MP Stewart (2002). "Ground-based laser scanners: operation, systems and applications". In: *Geomatica* 56.1, pp. 21–33.

Lindenmayer, David B, Chris R Margules, and Daniel B Botkin (2000). "Indicators of biodiversity for ecologically sustainable forest management". In: *Conservation biology* 14.4, pp. 941–950.

Litvaitis, John A (2001). "Importance of early successional habitats to mammals in eastern forests". In: *Wildlife Society Bulletin* 29.2, pp. 466–473.

Liu, Lingling, Liang Liang, Mark D Schwartz, Alison Donnelly, Zhuosen Wang, Crystal B Schaaf, and Liangyun Liu (2015). "Evaluating the potential of MODIS satellite data to track temporal dynamics of autumn phenology in a temperate mixed forest". In: *Remote Sensing of Environment* 160, pp. 156–165.

Lone, Karen, Floris M van Beest, Atle Mysterud, Terje Gobakken, Jos M Milner, Hans-Petter Ruud, and Leif Egil Loe (2014). "Improving broad scale forage mapping and habitat selection analyses with airborne laser scanning: the case of moose". In: *Ecosphere* 5.11, art144.

Lovell, JL, DLB Jupp, GJ Newnham, and DS Culvenor (2011). "Measuring tree stem diameters using intensity profiles from ground-based scanning lidar from a fixed viewpoint". In: *ISPRS Journal of Photogrammetry and Remote Sensing* 66.1, pp. 46–55.

Maas, H-G, A Bienert, St Scheller, and E Keane (2008). "Automatic forest inventory parameter determination from terrestrial laser scanner data". In: *International journal of remote sensing* 29.5, pp. 1579–1593.

MacArthur, Robert H and Henry S Horn (1969). "Foliage profile by vertical measurements". In: *Ecology*, pp. 802–804.

MacFaden, Sean W and David E Capen (2002). "Avian habitat relationships at multiple scales in a New England forest". In: *Forest Science* 48.2, pp. 243–253.

Macfarlane, Craig and Gary N Ogden (2012). "Automated estimation of foliage cover in forest understorey from digital nadir images". In: *Methods in Ecology and Evolution* 3.2, pp. 405–415.

Maginnis, Stewart and Jeffrey A Sayer (2013). *Forests in landscapes: ecosystem approaches to sustainability.* Routledge.

Magney, Troy S, Spencer A Eusden, Jan UH Eitel, Barry A Logan, Jingjue Jiang, and Lee A Vierling (2014). "Assessing leaf photoprotective mechanisms using terrestrial LiDAR: towards mapping canopy photosynthetic performance in three dimensions". In: *New Phytologist* 201.1, pp. 344–356.

Maturana, Daniel and Sebastian Scherer (2015). "3D convolutional neural networks for landing zone detection from lidar". In: *2015 IEEE International Conference on Robotics and Automation (ICRA).* IEEE, pp. 3471–3478.

Maurer, KD, G Bohrer, WT Kenny, and VY Ivanov (2015). "Large-eddy simulations of surface roughness parameter sensitivity to canopy-structure characteristics". In: *Biogeosciences* 12.8, pp. 2533–2548.

Maurer, Kyle D, Brady S Hardiman, Christoph S Vogel, and Gil Bohrer (2013). "Canopy-structure effects on surface roughness parameters: Observations in a Great Lakes mixed-deciduous forest". In: *Agricultural and forest meteorology* 177, pp. 24–34.

McDaniel, Matthew W, Takayuki Nishihata, Christopher A Brooks, Phil Salesses, and Karl Iagnemma (2012). "Terrain classification and identification of tree stems using ground-based LiDAR". In: *Journal of Field Robotics* 29.6, pp. 891–910.

McElhinny, Chris, Phillip Gibbons, Cris Brack, and Juergen Bauhus (2005). "Forest and woodland stand structural complexity: its definition and measurement". In: *Forest Ecology and Management* 218.1, pp. 1–24.

McKnight, Patrick E and Julius Najab (2010). "Mann-Whitney U Test". In: *Corsini Encyclopedia of Psychology.*

McMahon, Sean M., Daniel P. Bebber, Nathalie Butt, Martha Crockatt, Keith Kirby, Geoffrey G. Parker, Terhi Riutta, and Eleanor M. Slade (2015). "Ground based LiDAR demonstrates the legacy of management history to canopy structure and composition across a fragmented temperate woodland". In: *Forest Ecology and Management* 335, pp. 255–260.

Meiggs, Russell et al. (1982). *Trees and timber in the ancient Mediterranean world.* Oxford University Press.

Méndez, Valeriano, Joan Ramon Rosell-Polo, Ricardo Sanz, Alexandre Escolà, and Heliodoro Catalán (2014). "Deciduous tree reconstruction algorithm based on cylinder fitting from mobile terrestrial laser scanned point clouds". In: *Biosystems Engineering* 124, pp. 78–88.

Messier, Christian, Sylvain Parent, and Yves Bergeron (1998). "Effects of overstory and understory vegetation on the understory light environment in mixed boreal forests". In: *Journal of Vegetation Science* 9.4, pp. 511–520.

Metz, Jérôme, Dominik Seidel, Peter Schall, Dina Scheffer, Ernst-Detlef Schulze, and Christian Ammer (2013). "Crown modeling by terrestrial laser scanning as an approach to assess the effect of aboveground intra- and interspecific competition on tree growth". In: *Forest Ecology and Management* 310, pp. 275–288.

Michel, P, J Jenkins, N Mason, KJM Dickinson, and IG Jamieson (2008). "Assessing the ecological application of lasergrammetric techniques to measure fine-scale vegetation structure". In: *Ecological Informatics* 3.4, pp. 309–320.

Mihalyi, Rãzvan-George, Kaustubh Pathak, Narunas Vaskevicius, Tobias Fromm, and Andreas Birk (2015). "Robust 3D object modeling with a low-cost RGBD-sensor and AR-markers for applications with untrained end-users". In: *Robotics and Autonomous Systems* 66, pp. 1–17.

Moorthy, Inian, John R Miller, Baoxin Hu, Jing Chen, and Qingmou Li (2008). "Retrieving crown leaf area index from an individual tree using ground-based lidar data". In: *Canadian Journal of Remote Sensing* 34.3, pp. 320–332.

Muiruri, Evalyne W, Kalle Rainio, and Julia Koricheva (2015). "Do birds see the forest for the trees? Scale-dependent effects of tree diversity on avian predation of artificial larvae". In: *Oecologia*, pp. 1–12.

Müller, Jörg, Jutta Stadler, and Roland Brandl (2010). "Composition versus physiognomy of vegetation as predictors of bird assemblages: The role of lidar". In: *Remote Sensing of Environment* 114.3, pp. 490–495.

Murphy, Stephen J and Brian C McCarthy (2014). "Temporal change in the herbaceous understory community of an old-growth forest: from seasons to decades". In: *Plant ecology* 215.2, pp. 221–232.

Murphy, WM, JP Silman, and AD Mena Barreto (1995). “A comparison of quadrat, capacitance meter, HFRO sward stick, and rising plate for estimating herbage mass in a smooth-stalked, meadowgrass-dominant white clover sward”. In: *Grass and Forage Science* 50.4, pp. 452–455.

Nagel, Thomas A, Jurij Diaci, Klemen Jerina, Milan Kobal, and Dusan Rozenbergar (2014). “Simultaneous influence of canopy decline and deer herbivory on regeneration in a conifer–broadleaf forest”. In: *Canadian Journal of Forest Research* 45.3, pp. 266–275.

Newnham, Glenn J, John D Armston, Kim Calders, Mathias I Disney, Jenny L Lovell, Crystal B Schaaf, Alan H Strahler, and F Mark Danson (2015). “Terrestrial Laser Scanning for Plot-Scale Forest Measurement”. In: *Current Forestry Reports*, pp. 1–13.

Newton, Adrian (2007). *Forest ecology and conservation: a handbook of techniques*. Oxford University Press on Demand.

Nijland, Wiebe, Scott E Nielsen, Nicholas C Coops, Michael A Wulder, and Gordon B Stenhouse (2014). “Fine-spatial scale predictions of understory species using climate-and LiDAR-derived terrain and canopy metrics”. In: *Journal of Applied Remote Sensing* 8.1, p. 083572.

Nilsson, Marie-Charlotte and David A Wardle (2005). “Understory vegetation as a forest ecosystem driver: evidence from the northern Swedish boreal forest”. In: *Frontiers in Ecology and the Environment* 3.8, pp. 421–428.

Nudds, Thomas D (1977). “Quantifying the vegetative structure of wildlife cover”. In: *Wildlife Society Bulletin*, pp. 113–117.

Olofsson, Kenneth, Johan Holmgren, and Håkan Olsson (2014). “Tree Stem and Height Measurements using Terrestrial Laser Scanning and the RANSAC Algorithm”. In: *Remote Sensing* 6.5, pp. 4323–4344.

Östlund, Lars, Olle Zackrisson, and A-L Axelsson (1997). “The history and transformation of a Scandinavian boreal forest landscape since the 19th century”. In: *Canadian journal of forest research* 27.8, pp. 1198–1206.

Othmani, Ahlem, Alexandre Piboule, Oscar Dalmau, Nicolas Lomenie, Said Mokrani, and Lew Fock Chong Lew Yan Voon (2014). “Tree Species Classification Based on 3D Bark Texture Analysis”. In: *Image and Video Technology*. Springer, pp. 279–289.

Othmani, Ahlem, Lew FC Lew Yan Voon, Christophe Stolz, and Alexandre Piboule (2013). “Single tree species classification from Terrestrial Laser Scanning data for forest inventory”. In: *Pattern Recognition Letters* 34.16, pp. 2144–2150.

Palace, Michael W, Franklin B Sullivan, Mark J Ducey, Robert N Treuhaft, Christina Herrick, Julia Z Shimbo, and Jonas Mota-E-Silva (2015). "Estimating forest structure in a tropical forest using field measurements, a synthetic model and discrete return lidar data". In: *Remote Sensing of Environment* 161, pp. 1–11.

Pan, Yude, Richard A Birdsey, Jingyun Fang, Richard Houghton, Pekka E Kauppi, Werner A Kurz, Oliver L Phillips, Anatoly Shvidenko, Simon L Lewis, Josep G Canadell, et al. (2011). "A large and persistent carbon sink in the world?s forests". In: *Science* 333.6045, pp. 988–993.

Paquette, Alain and Christian Messier (2011). "The effect of biodiversity on tree productivity: from temperate to boreal forests". In: *Global Ecology and Biogeography* 20.1, pp. 170–180.

Pathak, Kaustubh, Narunas Vaskevicius, Jann Poppinga, Max Pfingsthorn, Sören Schwertfeger, and Andreas Birk (2009). "Fast 3D mapping by matching planes extracted from range sensor point-clouds". In: *Intelligent Robots and Systems, 2009. IROS 2009. IEEE/RSJ International Conference on.* IEEE, pp. 1150–1155.

Pearman, Peter B (2002). "The scale of community structure: habitat variation and avian guilds in tropical forest understory". In: *Ecological Monographs* 72.1, pp. 19–39.

Pfeifer, Norbert and Ch Briese (2007). "Geometrical aspects of airborne laser scanning and terrestrial laser scanning". In: *International Archives of Photogrammetry, Remote Sensing and Spatial Information Sciences* 36.3/W52, pp. 311–319.

Pickett, STA, SL Collins, and JJ Armesto (1987). "A hierarchical consideration of causes and mechanisms of succession". In: *Vegetatio* 69.1-3, pp. 109–114.

Pimentel, D, C Wilson, C McCullum, and R Huang (1997). "Economic and environmental benefits of biodiversity". In: *BioScience* 47.11, pp. 747–757.

Pirotti, Francesco, Alberto Guarnieri, and Antonio Vettore (2013). "Ground filtering and vegetation mapping using multi-return terrestrial laser scanning". In: *ISPRS Journal of Photogrammetry and Remote Sensing* 76, pp. 56–63.

Pommerening, Arne (2006). "Evaluating structural indices by reversing forest structural analysis". In: *Forest Ecology and Management* 224.3, pp. 266–277.

Popescu, Sorin C, Kaiguang Zhao, Amy Neuenschwander, and Chinsu Lin (2011). "Satellite lidar vs. small footprint airborne lidar: Comparing the accuracy of aboveground biomass estimates and forest structure metrics at footprint level". In: *Remote Sensing of Environment* 115.11, pp. 2786–2797.

Pueschel, Pyare (2013). "The influence of scanner parameters on the extraction of tree metrics from FARO Photon 120 terrestrial laser scans". In: *ISPRS Journal of Photogrammetry and Remote Sensing* 78, pp. 58–68.

Pueschel, Pyare, Glenn Newnham, Gilles Rock, Thomas Udelhoven, Willy Werner, and Joachim Hill (2013). "The influence of scan mode and circle fitting on tree stem detection, stem diameter and volume extraction from terrestrial laser scans". In: *ISPRS Journal of Photogrammetry and Remote Sensing* 77, pp. 44–56.

Qiao, Yunfa, Shujie Miao, Lucas CR Silva, and William R Horwath (2014). "Understory species regulate litter decomposition and accumulation of C and N in forest soils: A long-term dual-isotope experiment". In: *Forest Ecology and Management* 329, pp. 318–327.

Raiber, Matthias, Paul A White, Christopher J Daughney, Constanze Tschritter, Peter Davidson, and Sophie E Bainbridge (2012). "Three-dimensional geological modelling and multivariate statistical analysis of water chemistry data to analyse and visualise aquifer structure and groundwater composition in the Wairau Plain, Marlborough District, New Zealand". In: *Journal of Hydrology* 436, pp. 13–34.

Raumonen, Pasi, Mikko Kaasalainen, Markku Åkerblom, Sanna Kaasalainen, Harri Kaartinen, Mikko Vastaranta, Markus Holopainen, Mathias Disney, and Philip Lewis (2013). "Fast automatic precision tree models from terrestrial laser scanner data". In: *Remote Sensing* 5.2, pp. 491–520.

Reich, Peter B, Lee E Frelich, Richard A Voldseth, Peter Bakken, and E Carol Adair (2012). "Understorey diversity in southern boreal forests is regulated by productivity and its indirect impacts on resource availability and heterogeneity". In: *Journal of Ecology* 100.2, pp. 539–545.

Réjou-Méchain, Maxime, Blaise Tymen, Lilian Blanc, Sophie Fauset, Ted R Feldpausch, Abel Monteagudo, Oliver L Phillips, Hélène Richard, and Jérôme Chave (2015). "Using repeated small-footprint LiDAR acquisitions to infer spatial and temporal variations of a high-biomass Neotropical forest". In: *Remote Sensing of Environment* 169, pp. 93–101.

Reuter, HI and A Nelson (2009). "Geomorphometry in ESRI packages". In: *Developments in Soil Science* 33, pp. 269–291.

Río, M del, G Schütze, and H Pretzsch (2014). "Temporal variation of competition and facilitation in mixed species forests in Central Europe". In: *Plant Biology* 16.1, pp. 166–176.

Ripperda, Nora and Claus Brenner (2005). “Marker-free registration of terrestrial laser scans using the normal distribution transform”. In: *Proceedings of the ISPRS working group* 4.

Roering, Joshua J, Benjamin H Mackey, Jill A Marshall, Kristin E Sweeney, Natalia I Deligne, Adam M Booth, Alexander L Handwerger, and Corina Cerovski-Darriau (2013). “Connecting the dots with airborne lidar for geomorphic fieldwork”. In: *Geomorphology* 200, pp. 172–183.

Rooney, Thomas P and Donald M Waller (2003). “Direct and indirect effects of white-tailed deer in forest ecosystems”. In: *Forest Ecology and Management* 181.1, pp. 165–176.

Ross, Michael S, Lawrence B Flanagan, and George H La Roi (1986). “Seasonal and successional changes in light quality and quantity in the understory of boreal forest ecosystems”. In: *Canadian Journal of Botany* 64.11, pp. 2792–2799.

Rosser, Nicholas J, David N Petley, Michael Lim, SA Dunning, and Robert J Allison (2005). “Terrestrial laser scanning for monitoring the process of hard rock coastal cliff erosion”. In: *Quarterly Journal of Engineering Geology and Hydrogeology* 38.4, pp. 363–375.

Royán, Manuel Jesús, Antonio Abellán, Michel Jaboyedoff, Joan Manuel Vilaplana, and Jaume Calvet (2014). “Spatio-temporal analysis of rockfall prefailure deformation using Terrestrial LiDAR”. In: *Landslides* 11.4, pp. 697–709.

Ryding, Joseph (2009). “Assessing the use of terrestrial laser scanning for woodland surveying”. Masters Thesis. United Kingdom: University of Nottingham.

Ryding, Joseph, Emily Williams, Martin J Smith, and Markus P Eichhorn (2015). “Assessing Handheld Mobile Laser Scanners for Forest Surveys”. In: *Remote Sensing* 7.1, pp. 1095–1111.

Sabatini, Francesco M, Julia I Burton, Robert M Scheller, Kathryn L Amatangelo, and David J Mladenoff (2014). “Functional diversity of ground-layer plant communities in old-growth and managed northern hardwood forests”. In: *Applied vegetation science* 17.3, pp. 398–407.

Sakai, Akiko and Masahiko Ohsawa (1994). “Topographical pattern of the forest vegetation on a river basin in a warm-temperate hilly region, central Japan”. In: *Ecological Research* 9.3, pp. 269–280.

Saout, Soizic Le, Simon Chollet, Simon Chamaillé-Jammes, Laetitia Blanc, Sophie Padié, Thibault Verchere, Anthony J Gaston, Michael P Gillingham, Olivier Gimenez, Katherine L Parker, et al. (2014). “Understanding the paradox of deer persisting at high abundance in heavily browsed habitats". In: *Wildlife Biology* 20.3, pp. 122–135.

Scheller, Robert M and David J Mladenoff (2002). "Understory species patterns and diversity in old-growth and managed northern hardwood forests". In: *Ecological Applications* 12.5, pp. 1329–1343.

Schertzer, E, AC Staver, and SA Levin (2015). "Implications of the spatial dynamics of fire spread for the bistability of savanna and forest". In: *Journal of mathematical biology* 70.1-2, pp. 329–341.

Schilling, A, A Schmidt, HG Maas, and S Wagner (2011). "Topology Extraction Using Depth First Search on Voxel Representations of Tree Point Clouds". In: *ISPRS-International Archives of the Photogrammetry, Remote Sensing and Spatial Information Sciences* 3812, pp. 85–90.

Scown, Murray W, Martin C Thoms, and Nathan R De Jager (2015). "Floodplain complexity and surface metrics: Influences of scale and geomorphology". In: *Geomorphology* 245, pp. 102–116.

Seidel, Dominik, Katja Albert, Lutz Fehrmann, and Christian Ammer (2012a). "The potential of terrestrial laser scanning for the estimation of understory biomass in coppice-with-standard systems". In: *Biomass and Bioenergy* 47, pp. 20–25.

Seidel, Dominik, Friderike Beyer, Dietrich Hertel, Stefan Fleck, and Christoph Leuschner (2011a). "3D-laser scanning: A non-destructive method for studying above- ground biomass and growth of juvenile trees". In: *Agricultural and Forest Meteorology* 151.10, pp. 1305–1311.

Seidel, Dominik, Stefan Fleck, and Christoph Leuschner (2012b). "Analyzing forest canopies with ground-based laser scanning: A comparison with hemispherical photography". In: *Agricultural and Forest Meteorology* 154, pp. 1–8.

Seidel, Dominik, Stefan Fleck, Christoph Leuschner, and Tom Hammett (2011b). "Review of ground-based methods to measure the distribution of biomass in forest canopies". In: *Annals of Forest Science* 68.2, pp. 225–244.

Seidel, Dominik, Nils Hoffmann, Martin Ehbrecht, Julia Juchheim, and Christian Ammer (2015). "How neighborhood affects tree diameter increment–New insights from terrestrial laser scanning and some methodical considerations". In: *Forest Ecology and Management* 336, pp. 119–128.

Serna, Andr?s and Beatriz Marcotegui (2013). "Urban accessibility diagnosis from mobile laser scanning data". In: {*ISPRS*} *Journal of Photogrammetry and Remote Sensing* 84, pp. 23–32.

Shugart, Herman H (1984). *A theory of forest dynamics: the ecological implications of forest succession models.* Springer-Verlag, New York, NY.

Simonse, Merlijn, Tobias Aschoff, Heinrich Spiecker, and Michael Thies (2003). "Automatic determination of forest inventory parameters using terrestrial laserscanning". In: *Proceedings of the ScandLaser Scientific Workshop on Airborne Laser Scanning of Forests.* Vol. 2003, pp. 252–258.

Simonson, William D, Harriet D Allen, and David A Coomes (2014). "Overstorey and topographic effects on understories: Evidence for linkage from cork oak (Quercus suber) forests in southern Spain". In: *Forest Ecology and Management* 328, pp. 35–44.

Singh, Kunwar K, Amy J Davis, and Ross K Meentemeyer (2015). "Detecting understory plant invasion in urban forests using LiDAR". In: *International Journal of Applied Earth Observation and Geoinformation* 38, pp. 267–279.

Sinoquet, Hervé, Sylvain Pincebourde, Boris Adam, Nicolas Donès, Jessada Phattaralerphong, Didier Combes, Stéphane Ploquin, Krissada Sangsing, Poonpipope Kasemsap, Sornprach Thanisawanyangkura, et al. (2009). "3-D maps of tree canopy geometries at leaf scale: Ecological Archives E090-019". In: *Ecology* 90.1, pp. 283–283.

Song, B, J Chen, and TM Williams (2014). "Spatial Relationships between Canopy Structure and Understory Vegetation of an Old-Growth Douglas-Fir Forest". In: *Forest Res* 3.118, p. 2.

Soni, A, S Robson, and B Gleeson (2014). "Extracting Rail Track Geometry from Static Terrestrial Laser Scans for Monitoring Purposes". In: *ISPRS-International Archives of the Photogrammetry, Remote Sensing and Spatial Information Sciences* 1, pp. 553–557.

Sotoodeh, Soheil (2006). "Outlier detection in laser scanner point clouds". In: *International Archives of Photogrammetry, Remote Sensing and Spatial Information Sciences* 36.5, pp. 297–302.

Soudarissanane, Sylvie, Roderik Lindenbergh, Massimo Menenti, and Peter Teunissen (2011). "Scanning geometry: Influencing factor on the quality of terrestrial laser scanning points". In: *ISPRS Journal of Photogrammetry and Remote Sensing* 66.4, pp. 389–399.

Spies, Thomas A and Jerry F Franklin (1991). "The structure of natural young, mature, and old-growth Douglas-fir forests in Oregon and Washington". In: *Wildlife and vegetation of unmanaged Douglas-fir forests. USDA Forest Service General Technical Report PNW-GTR-285, Portland, USA. Pacific Northwest Research Station*, pp. 91–111.

Spring, Adam P and Caradoc Peters (2014). "Developing a low cost 3D imaging solution for inscribed stone surface analysis". In: *Journal of Archaeological Science* 52, pp. 97–107.

Srinivasan, Shruthi, Sorin C Popescu, Marian Eriksson, Ryan D Sheridan, and Nian-Wei Ku (2014). "Multi-temporal terrestrial laser scanning for modeling tree biomass change". In: *Forest Ecology and Management* 318, pp. 304–317.

Stewart, KEJ, NAD Bourn, and JA Thomas (2001). "An evaluation of three quick methods commonly used to assess sward height in ecology". In: *Journal of Applied Ecology* 38.5, pp. 1148–1154.

Suárez, JC, Carlos Ontiveros, Steve Smith, and Stewart Snape (2005). "Use of airborne LiDAR and aerial photography in the estimation of individual tree heights in forestry". In: *Computers & Geosciences*, pp. 435–445.

Sumida, Akihiro, Taro Nakai, Masahito Yamada, Kiyomi Ono, Shigeru Uemura, and Toshihiko Hara (2009). "Ground-based estimation of leaf area index and vertical distribution of leaf area density in a Betula ermanii forest". In: *Silva Fennica* 43.5, pp. 799–816.

Suzuki, Maki, Tadashi Miyashita, Hajime Kabaya, Keiji Ochiai, Masahiko Asada, and Zaal Kikvidze (2013). "Deer herbivory as an important driver of divergence of ground vegetation communities in temperate forests". In: *Oikos* 122.1, pp. 104–110.

Svensson, Johan S and John K Jeglum (2001). "Structure and dynamics of an undisturbed old-growth Norway spruce forest on the rising Bothnian coastline". In: *Forest Ecology and Management* 151.1, pp. 67–79.

Tanabe, Shin-Ichi, Masanori J Toda, and Alexandra V Vinokurova (2001). "Tree shape, forest structure and diversity of drosophilid community: comparison between boreal and temperate birch forests". In: *Ecological Research* 16.3, pp. 369–385.

Tang, Pingbo, Daniel Huber, Burcu Akinci, Robert Lipman, and Alan Lytle (2010). "Automatic reconstruction of as-built building information models from laser-scanned point clouds: A review of related techniques". In: *Automation in construction* 19.7, pp. 829–843.

Tews, J, U Brose, V Grimm, K Tielbörger, MC Wichmann, M Schwager, and F Jeltsch (2004). "Animal species diversity driven by habitat heterogeneity/diversity: the importance of keystone structures". In: *Journal of biogeography* 31.1, pp. 79–92.

Thies, M and H Spiecker (2004). "Evaluation and future prospects of terrestrial laser scanning for standardized forest inventories". In: *Forest* 2.2.2, pp. 192–197.

Thomas, Sean C, Charles B Halpern, Donald A Falk, Denise A Liguori, and Kelly A Austin (1999). “Plant diversity in managed forests: understory responses to thinning and fertilization”. In: *Ecological Applications* 9.3, pp. 864–879.

Thompson, Ian D, Kimiko Okabe, John A Parrotta, Eckehard Brockerhoff, Hervé Jactel, David I Forrester, and Hisatomo Taki (2014). “Biodiversity and ecosystem services: lessons from nature to improve management of planted forests for REDD-plus”. In: *Biodiversity and conservation* 23.10, pp. 2613–2635.

Thomson, C, G Apostolopoulos, D Backes, and J Boehm (2013). “Mobile laser scanning for indoor modelling”. In: *ISPRS Ann. Photogramm. Remote Sens. Spat. Inf. Sci*, pp. 289–293.

Tichy, Lubomír (2016). “Field test of canopy cover estimation by hemispherical photographs taken with a smartphone”. In: *Journal of Vegetation Science* 27.2, pp. 427–435.

TreeMetrics (2014). *Treemetrics - Making forest management easier, sustainable & profitable.* http://www.treemetrics.com/.

Van Den Meersschaut, Diego, Kris Vandekerkhove, et al. (2000). *Development of a stand-scale forest biodiversity index based on the State Forest Inventory.* USDA, Boise, Idaho, pp. 340–349.

Vanderwel, Mark C, David A Coomes, and Drew W Purves (2013). “Quantifying variation in forest disturbance, and its effects on aboveground biomass dynamics, across the eastern United States”. In: *Global change biology* 19.5, pp. 1504–1517.

Vanegas, Carlos A., Daniel G. Aliaga, and Bedrich Benes (2012). “Automatic Extraction of Manhattan-World Building Masses from 3D Laser Range Scans”. In: *Visualization and Computer Graphics, IEEE Transactions on* 18.10, pp. 1627–1637.

Vaughn, Nicholas R, L Monika Moskal, and Eric C Turnblom (2012). “Tree species detection accuracies using discrete point lidar and airborne waveform lidar”. In: *Remote Sensing* 4.2, pp. 377–403.

Vauhkonen, Jari, Matti Maltamo, Ronald E McRoberts, and Erik Næsset (2014). “Introduction to Forestry Applications of Airborne Laser Scanning”. In: *Forestry Applications of Airborne Laser Scanning.* Springer, pp. 1–16.

Velázquez, Jorge, Robert B Allen, David A Coomes, and Markus P Eichhorn (2016). “Asymmetric competition causes multimodal size distributions in spatially structured populations”. In: *Proc. R. Soc. B.* Vol. 283. 1823. The Royal Society, p. 20152404.

Waterman, Jayson R, Andrew R Gillespie, James M Vose, and Wayne T Swank (1995). "The influence of mountain laurel on regeneration in pitch pine canopy gaps of the Coweeta Basin, North Carolina, USA". In: *Canadian Journal of Forest Research* 25.11, pp. 1756–1762.

Watt, PJ and DNM Donoghue (2005). "Measuring forest structure with terrestrial laser scanning". In: *International Journal of Remote Sensing* 26.7, pp. 1437–1446.

Weber, Christopher, Stefanie Hahmann, and Hans Hagen (2010). "Sharp feature detection in point clouds". In: *Shape Modeling International Conference (SMI), 2010*. IEEE, pp. 175–186.

Wehr, Aloysius and Uwe Lohr (1999). "Airborne laser scanning - an introduction and overview". In: *ISPRS Journal of Photogrammetry and Remote Sensing* 54.2, pp. 68–82.

Weinmann, Martin, Boris Jutzi, Stefan Hinz, and Clément Mallet (2015). "Semantic point cloud interpretation based on optimal neighborhoods, relevant features and efficient classifiers". In: *ISPRS Journal of Photogrammetry and Remote Sensing* 105, pp. 286–304.

Welsh, Elizabeth, Paul Anderson, and Paul Rea (2014). "A novel method of anatomical data acquisition using the Perception ScanWorks V5 scanner". In: *International journal on recent and innovation trends in computing and communication* 2.8, pp. 2265–2276.

West, Philip W (2009). *Tree and forest measurement*. Springer.

White, Katharine, Jennifer Pontius, and Paul Schaberg (2014). "Remote sensing of spring phenology in northeastern forests: A comparison of methods, field metrics and sources of uncertainty". In: *Remote Sensing of Environment* 148, pp. 97–107.

White, Mark A (2012). "Long-term effects of deer browsing: composition, structure and productivity in a northeastern Minnesota old-growth forest". In: *Forest Ecology and Management* 269, pp. 222–228.

White, Peter JT, Brian J McGill, and Martin J Lechowicz (2012). "Detecting changes in forest floor habitat after canopy disturbance". In: *Ecological research* 27.2, pp. 397–406.

Wilkinson, Maxwell, Gerald P Roberts, Ken McCaffrey, Patience A Cowie, Joanna P Faure Walker, Ioannis Papanikolaou, Richard J Phillips, Alessandro Maria Michetti, Eutizio Vittori, Laura Gregory, et al. (2015). "Slip distributions on active normal faults measured from LiDAR and field mapping of geomorphic offsets: an example from L'Aquila, Italy, and implications for modelling seismic moment release". In: *Geomorphology* 237, pp. 130–141.

Wing, Brian M., Martin W. Ritchie, Kevin Boston, Warren B. Cohen, Alix Gitelman, and Michael J. Olsen (2012). "Prediction of understory vegetation cover with airborne lidar in an interior ponderosa pine forest". In: *Remote Sensing of Environment* 124, pp. 730–741.

Wood, Eric M, Anna M Pidgeon, Volker C Radeloff, and Nicholas S Keuler (2012). "Image texture as a remotely sensed measure of vegetation structure". In: *Remote Sensing of Environment* 121, pp. 516–526.

Wulder, Michael A, Joanne C White, Ross F Nelson, Erik Næsset, Hans Ole Ørka, Nicholas C Coops, Thomas Hilker, Christopher W Bater, and Terje Gobakken (2012). "Lidar sampling for large-area forest characterization: A review". In: *Remote Sensing of Environment* 121, pp. 196–209.

Yang, Bisheng, Lina Fang, and Jonathan Li (2013a). "Semi-automated extraction and delineation of 3D roads of street scene from mobile laser scanning point clouds". In: {*ISPRS*} *Journal of Photogrammetry and Remote Sensing* 79, pp. 80–93.

Yang, Xiaoyuan, Crystal Schaaf, Alan Strahler, Thomas Kunz, Nathan Fuller, Margrit Betke, Zheng Wu, Zhuosen Wang, Diane Theriault, Darius Culvenor, et al. (2013b). "Study of bat flight behavior by combining thermal image analysis with a LiDAR forest reconstruction". In: *Canadian Journal of Remote Sensing* 39.sup1, S112–S125.

Yu, Xiaowei, Xinlian Liang, Juha Hyyppä, Ville Kankare, Mikko Vastaranta, and Markus Holopainen (2013). "Stem biomass estimation based on stem reconstruction from terrestrial laser scanning point clouds". In: *Remote Sensing Letters* 4.4, pp. 344–353.

Zellweger, Florian, Andri Baltensweiler, Christian Ginzler, Tobias Roth, Veronika Braunisch, Harald Bugmann, and Kurt Bollmann (2016). "Environmental predictors of species richness in forest landscapes: abiotic factors versus vegetation structure". In: *Journal of Biogeography.*

Zevenbergen, Lyle W and Colin R Thorne (1987). "Quantitative analysis of land surface topography". In: *Earth surface processes and landforms* 12.1, pp. 47–56.

Zhao, Feng, Xiaoyuan Yang, Mitchell A Schull, Miguel O Román-Colón, Tian Yao, Zhuosen Wang, Qingling Zhang, David LB Jupp, Jenny L Lovell, Darius S Culvenor, et al. (2011). "Measuring effective leaf area index, foliage profile, and stand height in New England forest stands using a full-waveform ground-based lidar". In: *Remote Sensing of Environment* 115.11, pp. 2954–2964.

Zianis, Dimitris and Maurizio Mencuccini (2004). “On simplifying allometric analyses of forest biomass”. In: *Forest Ecology and Management* 187.2, pp. 311–332.

Ziegler, Susy Svatek (2000). “A comparison of structural characteristics between old-growth and postfire second-growth hemlock–hardwood forests in Adirondack Park, New York, USA”. In: *Global Ecology and Biogeography* 9.5, pp. 373–389.